TEMPLATE SYNTHESES, COORDINATION CHEMISTRY, AND REACTIVITY OF TETRAPHOSPHORUS MACROCYCLES: TOWARD MACROCYCLIC IRON(II) COMPLEXES FOR APPLICATIONS IN NITROGEN COORDINATION

by

BRYAN P. NELL

A DISSERTATION

Presented to the Department of Chemistry and Biochemistry
and the Graduate School of the University of Oregon
in partial fulfillment of the requirements
for the degree of
Doctor of Philosophy

June 2014

DISSERTATION APPROVAL PAGE

Student: Bryan Paul Nell

Title: Template Syntheses, Coordination Chemistry, and Reactivity of Tetraphosphorus Macrocycles: Toward Macrocyclic Iron(II) Complexes for Applications in Nitrogen Coordination

This dissertation has been accepted and approved in partial fulfillment of the requirements for the Doctor of Philosophy degree in the Department of Chemistry and Biochemistry by:

Dr. Darren W. Johnson	Chairperson
Dr. David R. Tyler	Advisor
Dr. Michael M. Haley	Core Member
Dr. Eric I. Corwin	Institutional Representative

and

Kimberly Andrews Espy	Vice President for Research and Innovation; Dean of the Graduate School

Original approval signatures are on file with the University of Oregon Graduate School.

Degree awarded June 2014.

DISSERTATION ABSTRACT

Bryan Paul Nell

Doctor of Philosophy

Department of Chemistry and Biochemistry

June 2014

Title: Template Syntheses, Coordination Chemistry, and Reactivity of Tetraphosphorus Macrocycles: Toward Macrocyclic Iron(II) Complexes for Applications in Nitrogen Coordination

The preparation of tetraphosphorus macrocycles is a relatively undeveloped field of chemistry. Despite their great potential as ligands for transition metal complexes, no synthesis has been established that is both general and high yielding. One potential use for these macrocycles is with iron(II) metal complexes that can be used as robust catalysts for applications in the coordination and activation of dinitrogen, where the stability of the complex is derived from the "macrocycle effect". This dissertation describes synthetic routes based on template syntheses using copper(I), which can be removed to yield the free macrocyclic phosphine, and attempts at directly using Fe(II) as a template. Chapter I reviews the literature on the synthesis and coordination chemistry of secondary phosphines on transition metals.

Chapter II describes methods for preparing tetraphosphorus macrocycles on copper(I) using two bidentate secondary phosphines bridged with two α-ω dihalides.

Previous work with copper(I) investigated using the phosphorus Mannich reaction with 1,2-bis[(dihydroxymethyl)phosphino]ethane to form macrocycles and found that the

copper complex $Cu(DHMPE)_2Cl$ forms a dimer in the solid state. Chapter III investigates this complex using ^1H-DOSY NMR spectroscopy to find that the complex is monomeric in solution but dimeric as a solid.

Chapter IV describes a synthetic method toward tetraphosphorus macrocycles using a linear open-chain mixed tertiary/secondary phosphine on copper(I). The copper can be removed and the free ligand can be coordinated to iron(II). The complex binds dinitrogen readily at atmospheric pressures.

Chapter V investigates using iron(II) directly as a template, cutting out the need for a "surrogate" metal. The synthesis of hydrophilic tetradentate phosphines is also discussed. To conclude, an outlook for the future of this project is discussed.

This dissertation includes previously published and unpublished co-authored material.

CURRICULUM VITAE

NAME OF AUTHOR: Bryan Paul Nell

GRADUATE AND UNDERGRADUATE SCHOOLS ATTENDED:

University of Oregon, Eugene, OR
Ripon College, Ripon, WI

DEGREES AWARDED:

Doctor of Philosophy, Chemistry, 2014, University of Oregon
Master of Science, Chemistry, 2010, University of Oregon
Bachelor of Arts, Chemistry, 2009, Ripon College

AREAS OF SPECIAL INTEREST:

Organophosphorus Chemistry
Phosphine Synthesis
Nitrogen Rejection

PROFESSIONAL EXPERIENCE:

Graduate Teaching Fellow, University of Oregon, 2009-2014

Graduate Research Assistant, University of Oregon, 2010-2011

GRANTS, AWARDS, AND HONORS:

University of Oregon Travel Award, University of Oregon, 2013

Graduate Teaching Fellowship, University of Oregon, 2009-2014

Presidential Scholarship, Ripon College, 2005-2009

PUBLICATIONS:

Nell, B. P.; Tyler, D. R. *Coord. Chem. Rev.* Submitted.

Nell, B. P.; Swor, C. D.; Zakharov, L. N.; Tyler, D. R. *Polyhedron*, **2012**, *45*, 30-34.

Swor, C. D.; Nell, B. P.; Tyler, D. R.; *Acta Cryst.,* **2012**, *E68*, o2456.

ACKNOWLEDGMENTS

First, I'd like to thank my advisor, Professor David Tyler, for being a superb mentor and an ideal role model. I've grown so much as a student and as a person under his guidance. I will always remember our adventure to China and his "guide to a successful marriage". But mostly, I would thank him for his support throughout graduate school, keeping me excited and always teaching me new things.

I would also like to thank my thesis committee of Prof. Darren Johnson, Prof. Mike Haley, and Prof. Eric Corwin, for guidance and discussions and keeping me focused to progress my project forward. I'd especially like to thank Prof. Johnson for helping me find employment after graduate school, inviting me over with his lab for functions with his family, and being my golfing buddy.

I'd like to say thank you to a few special professors that I had the pleasure of working with during my undergraduate/graduate career. From Oregon, I'd like to thank Prof. Mike Koscho, Prof. Mike Pluth, and Prof. Bruce Branchaud. I've learned so much about teaching and how to be a good teacher from them. I'd like to thank Prof. Colleen Byron and Prof. Masanori Iimura from my time at Ripon College for leading me to graduate school and being some of the best mentors I've ever had.

I would also like to thank the graduate students and undergraduates who have helped me with this project, including Don Clayton, Jacob Ishibashi, Susan Cooper, Ian Doxsee (my under-undergrad), Aditya Nathan (my regular undergrad), and Adrian Henle. I'm very grateful for the help of Dr. Mike Strain and Dr. Lev Zakharov.

Graduate school wouldn't have ever been the way it was without my former and current Tyler labmates. First, I'd like to thank Charlie Swor for his mentorship when I first joined the lab and project. Secondly, I'd like to thank the former Tyler lab graduate students and undergrads, as they were a big reason why I joined the Tyler lab in the first place: Charlie, Jen Zemke, Brandy Fox, Spring Knapp, Sarah Brady, Chantal Balesdent, Toby Sherbow and Rick Saylor; and to the current members, Emma Downs, Alex Kendall, Justin Barry, and Adrian Henle. A special shoutout goes to Emma for being a great friend/companion when we went through advancement and our dissertation writing adventures. A special thanks goes out to Jen Zemke, Sarah Brady, and Chantal Balesdent for being awesome.

I'd like to thank all of my friends who've supported me through this often challenging, but rewarding, time of my life.

Finally, I'd like to thank my Mom, Dad, my brother Zachary, and my sister Jessica, Timothy, Nathan, and Allison, and my grandparents for being my biggest supporters. They've never lost any faith in me and always encouraged me to do my best. It will be hard to get used to my mom not telling me to study hard when I am finally finished with school!

Lastly, I'd like to thank my wife Kara for being my best friend and my favorite scientist. I am one lucky fellow to have her, and without with her constant love, support, and confidence, graduate school would have been much much more difficult. I am grateful and blessed to have such a wonderful, intelligent woman in my life. We have many exciting adventures ahead of us, and there's nobody else I'd have by my side.

To my family and my wife, who've always believed in me.

TABLE OF CONTENTS

LIST OF FIGURES

LIST OF TABLES

LIST OF SCHEMES

Scheme Page

CHAPTER I

Scheme Page

Scheme Page

Scheme Page

CHAPTER I

REVIEW OF THE SYNTHESIS, REACTIVITY, AND COORDINATION CHEMISTRY OF SECONDARY PHOSPHINES

1.1. Introduction

Phosphines are important compounds in chemistry, mostly because of their valuable properties as ligands in transition metal complexes. Phosphine ligands are classified as "soft", strong σ-donors, and their electronic, steric, and stereochemical properties can be varied based on the substituents attached to the phosphorus atom.[1-3] Because of this, the steric, electronic, and reaction environment of the corresponding complexes can be tuned based on the phosphine ligands.[4] This is particularly useful when the complexes are used for homogenous catalysis, such as hydrogenation, hydroformylation, hydration, hydrolysis, cross-couplings, and carbon-heteroatom bond formations, which tend to use transition metal catalysts bearing phosphine ligands.[5] Additionally, because of the sigma-donation of phosphines, transition-metal phosphine complexes are able to activate small molecules[6], such as H_2, O_2, N_2, H_2O, and CO_2, which make those complexes candidates for making some energy-intensive industrial processes more "green", such as ammonia synthesis.[7-23] The first phosphines were synthesized as early as the 1870's (a review of phosphorus chemistry up until 1970 is covered by Maier[24]) and have been extensively researched since. This review will focus on the synthesis of secondary phosphines and their uses as ligands for transition metal

complexes.

1.2. Background

Phosphines are three coordinate phosphorus compounds that have a trigonal pyramidal geometry. Tertiary phosphines **1** have three C-P bonds while secondary phosphines **2** have two C-P bonds and one P-H bond and primary phosphines **3** have one C-P bond and two P-H bonds. Phosphorus can also form compounds with halogens **4**, oxidize to form four-coordinate phosphine oxides **5**, form positively charged phosphonium cations **6**, have three and four coordinate esters/acids **7**, and form stable five-coordinate compounds **8** (Figure 1).

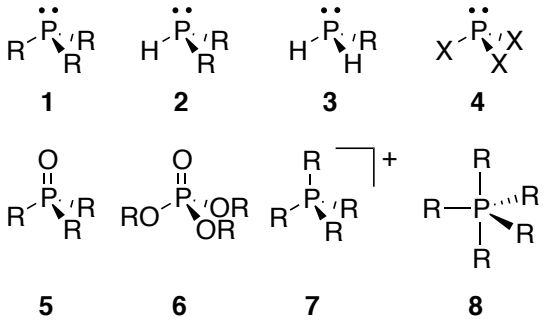

Figure 1. Examples of phosphorus compounds.

Phosphines, in general, have a pyramidal geometry, though the angle of the C-P-C bond in tertiary phosphines can change radically based on the R-group attached to phosphorus, ranging from 98.6° (trimethylphosphine **9**) to 109.9° (tri-*tert*-butylphosphine **10**) (Figure 2). The C-P-H bond angle in secondary phosphines ranges from 95-97°.[25]

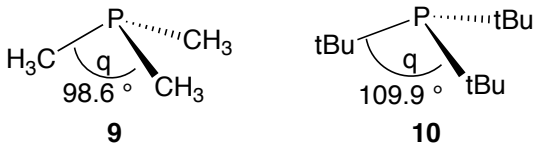

Figure 2. C-P-C bond angle comparison between trimethylphosphine **9** and tri-*tert*-butylphosphine **10**.

Phosphines tend to share characteristics with their group 15 members, the amines. Though both phosphines and amines are pyramidal, the pyramidal inversion at room temperature is rapid for amines but is extremely slow for phosphines. This is because the energy barrier for going through an sp^2 planar transition state is higher for phosphines (barrier is ~30-35 kcal/mol compared to ~5 kcal/mol for amines).[25] Because of this, a phosphine has a fixed pyramidal geometry; if the phosphine has three different substituents, the molecule can be optically active (Figure 3). The fact that phosphines can be optically active has led to many advances in organometallic asymmetric catalysis. Chirality at phosphorus has been reviewed many times and those reviews contain very valuable information on the subject.[26-28]

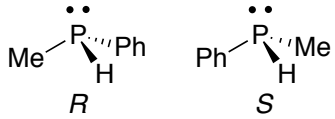

Figure 3. The two stereoisomers of methylphenylphosphine, showing the stereochemical implication of three different substituents on phosphorus.

In terms of basicity, phosphines trend well with amines, with phosphines being slightly less basic. For example, the pK_b of triethylphosphine is 5.4, similar to other simple tertiary phosphines in the range of 4.5 to 6. In comparison, triethylamine has a pK_b of 3.2. Interestingly, replacing an alkyl group with a hydrogen atom in phosphines

has a dramatic effect on basicity, with secondary phosphines having pK_b values around 9.5-10.5 and primary phosphines ranging from 13.5-14. However, when replacing alkyl groups on nitrogen, there is no appreciable effect as diethylamine has a pK_b of 2.9 and ethylamine has a pK_b of 3.2.[29]

In general, phosphines are extremely air-sensitive compounds that are characteristically malodorous and potentially toxic. These compounds also tend to be difficult to handle and pyrophoric, especially low molecular weight primary and secondary phosphines. A recent article by Stewart et al. describes computational methods to predict the air-stability of phosphines, indicating that steric bulk or incorporation of heteroatoms/conjugation is required to protect the phosphorus atom from oxidation by molecular oxygen.[30]

1.3. Secondary Phosphine Synthesis

The synthesis of secondary phosphines is well documented in the literature, but significant advances in the preparation of these molecules have not been made in many years. Essentially any procedure herein for making secondary phosphines applies to tertiary phosphines as well.[31] One appeal to synthesizing secondary phosphines is the ability to take the product onto chiral tertiary phosphines, which may be useful as ligands on transition metals for use in asymmetric catalysis.

1.3.1. Alkylation

The most basic way to make secondary phosphines is by starting with a phosphide anion derived from a primary phosphine. For example, phenylphosphine **11** can be

metallated with Na/NH_3, Li/THF, K, Ca, or deprotonated with *n*-BuLi to produce the phosphide, followed by alkylation with any number of electrophiles to yield the desired tertiary phosphine (Scheme 1).[25] This general reaction[32] is not stereospecific, and a mixture of stereoisomers should be expected. Stoichiometry is very important in these reactions, as over-alkylation is common.

Scheme 1. Alkylation of a primary phosphine to yield a secondary phosphine.

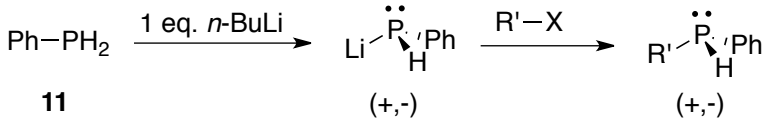

11 (+,-) (+,-)

Reaction of phosphide anions with alkylene dihalides leads to either cyclic or bis(phosphino) derivatives. The synthesis of the first phosphorus heterocycle with three members, called a phosphirane **12**, has been prepared this way as a secondary phosphine (Scheme 2).[33]

Scheme 2. Alkylation with a dihalide to form a phosphirane, **12**.

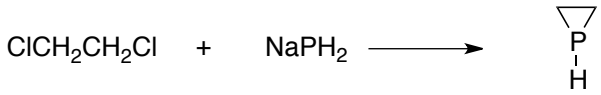

12

More recently, work investigating primary and secondary phosphine-borane adducts **13** has shown that alkylation of these compounds can be more easily controlled. A recent review on phosphine-borane adducts has described these syntheses and reactivity extensively.[34] The advantage of phosphine-boranes is the ability to work with

air-sensitive phosphines as air-stable solids. An extra deprotection step is required with a secondary amine to release the free phosphine from the adduct (Scheme 3).

Scheme 3. Alkylation of a phosphine-borane adduct **13** and subsequent deprotection with a secondary amine.

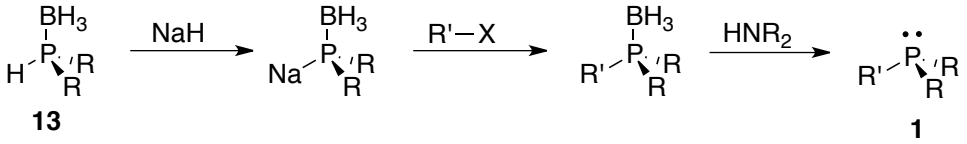

1.3.2. Reduction

Perhaps the most common method to produce secondary phosphines comes from reduction reactions. There are many phosphorus species that can be reduced to secondary phosphines: phosphinous dichlorides **14**[35,36], secondary phosphine oxides **15**[35,37], phosphonate esters and other phosphinic species **16-17**[35,38], secondary chalcogenides **18**.[39] There are also a variety of reagents and methods capable of carrying out the reduction, but traditionally, the most common reagent is use of excess lithium aluminum hydride (LAH) in an ethereal solvent (Scheme 4).

Scheme 4. Reduction to secondary phosphines with lithium aluminum hydride.

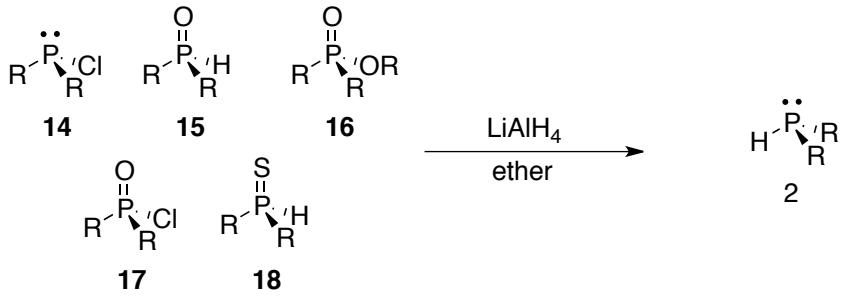

Other reagents are also capable of carrying out the reduction step to obtain phosphines. Alkali metals in inert solvents can reduce oxides to free phosphines. The silanes have been used since 1964 as a method of reducing phosphine oxides.[40] Phenylsilane,[41] trichlorosilane, and other silanes[42] have been used to reduce secondary phosphine oxides to secondary phosphines. Additionally, Busacca et al. have found that DIBAL-H and $^{i}Pr_3Al$ are capable of reducing tertiary[43] and secondary phosphine oxides[44] to the respective phosphines with very mild conditions and reaction times, achieving good yields and purities (Table 1). Engle has published a through review of the reduction chemistry of phosphorus.[45]

Table 1. Reduction of secondary phosphine oxides to secondary phosphines with DIBAL-H.

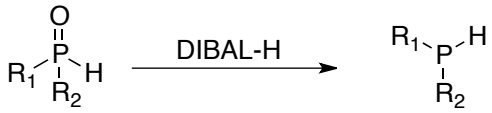

Entry	R_1	R_2	Time/T (°C)	Yield (%)
1	C_6H_5	C_6H_5	10 min/25	86
2	4-F-C_6H_4	4-F-C_6H_4	10 min/25	90
3	4-Cl-C_6H_4	4-Cl-C_6H_4	10 min/25	83
4	4-Me-C_6H_4	4-Me-C_6H_4	10 min/25	80
5	3-F-C_6H_4	3-F-C_6H_4	10 min/25	89
6	3-Cl-C_6H_4	3-Cl-C_6H_4	10 min/25	81
7	3-F,5-Me-C_6H_3	3-F,5-Me-C_6H_3	10 min/25	82
8	3,5-F_2,4-OMe-C_6H_2	3,5-F_2,4-Ome-C_6H_2	10 min/25	90
9	3,5-Cl_2-C_6H_3	3,5-Cl_2-C_6H_3	1 h/-20	90
10	3,5-F_2-C_6H_3	3,5-F_2-C_6H_3	1 h/-20	80
11	2-Me-C_6H_4	2-Me-C_6H_4	8 h/25	80
12	4-Nme_2-C_6H_4	4-Nme_2-C_6H_4	45 min/25	92
13	4-Ome-C_6H_4	4-Ome-C_6H_4	40 min/25	91
14	2-Ome-C_6H_4	2-Ome-C_6H_4	8 h/35	75
15	C_6H_5	*i*-Pr	10 min/25	90
16	C_6H_5	*t*-Bu	4 h/50	86
17	*n*-Bu	*n*-Bu	1 h/25	85
18	C_6H_{11}	C_6H_{11}	4 h/50	88
19	*t*-Bu	*t*-Bu	4 h/50	87
20	3,5-$(CF_3)_2$-C_6H_3	3,5-$(CF_3)_2$-C_6H_3	15 min/25	72

One of the most effective routes toward aryl secondary phosphines is through reductive cleavage of the P-C_{aryl} bond. The corresponding aryl tertiary phosphine can be used and treated with Li or Na/NH_3 at cold temperatures to reductively cleave a P-C_{aryl} bond, generating the metallated phosphide. Subsequent hydrolysis of the phosphide generates the desired secondary phosphine. This technique has been especially useful in the preparation of many aryl bis-bidentate secondary phosphine.[46,47] A detailed study of this reaction with Li/THF was carried out using 1,2-bis(diphenylphosphino)ethane **19** to determine a plausible mechanism of the reaction (Scheme 5).[48] The authors proposed a competitive separation of the leaving groups as the most stable anion or radical.

Scheme 5. Reductive cleavage of a bis-diaryl phosphine with lithium.

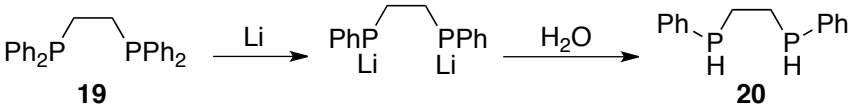

1.3.3. Addition to Unsaturated Bonds (Hydrophosphination)

Secondary and primary phosphines will readily undergo radical reactions and base-catalyzed reactions to add to unsaturated carbon-carbon bonds; this is a useful way to incorporate new P-C bonds. Reaction of a P-H bond in the presence of a radical initiator (often AIBN is used) and an olefin will lead to anti-Markovinkov addition across the double bond (Scheme 6). This is a method to incorporate multiple phosphorus atoms into a compound, but is difficult to control to stop at the secondary phosphine.[25]

Scheme 6. Radical-initiated hydrophosphination mechanism.

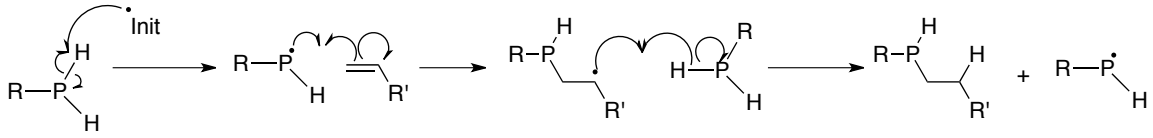

Secondary phosphines can also be prepared from phosphine gas added to α-β unsaturated nitriles and carbonyls under basic conditions.[49] This reaction is similar in nature to a Michael addition. If the reactant conditions are controlled, the reaction can be used to obtain monoalkylation, dialkylation, or trialkylation of phosphine.

1.4. Coordination Chemistry of Secondary Phosphines

In general, transition metal complexes bearing secondary phosphines are not used as catalysts in homogeneous catalysis, but often used as a methodology to generate complexes that contain tertiary phosphines, using the metal as a way to activate the secondary phosphine toward reactivity.[50] With low-valent transition metals, P-H bonds easily undergo formal oxidative additions to form metal hydrides and coordinated phosphide ligands[51-56]; this review will focus on metal complexes where the P-H bond remains intact after coordination to metals. Additionally, this review will look at more recent results (past twenty-five years) when available. A special focus of this review will be on metals that have been implemented with secondary phosphines toward the goal of preparing phosphorus macrocycles.[57,58]

1.4.1. Group 4 Transition Metals

In 2002, Ishiyama and coworkers prepared Zr(IV) and Hf(IV) complexes bearing

cyclopentadienyl (Cp) ligands with pendant secondary phosphines.[59] The authors sought to use the sidearm secondary phosphine as a method of preparing phosphide complexes due to the activation of P-H bonds upon coordination.[50] Depending on the R-group on the phosphorus atom (either 2,4,6-trimethylphenyl (Mes) **21a-b**, 2,4,6-tri-*i*-propylphenyl (Tip) **22a-b**, or 2,4,6-tri-*t*-butylphenyl (Mes*) **23a-b**), the coordination mode of the phosphine changes. When R=Mes, the pendant secondary phosphine stays coordinated to the metal center; when R=Tip, there is an equilibrium between the bound and free phosphine ligand; and when R=Mes*, there is no coordination of the phosphine to the metal (Scheme 7).

Scheme 7. Zirconium and hafnium complexes bearing pendant secondary phosphines.

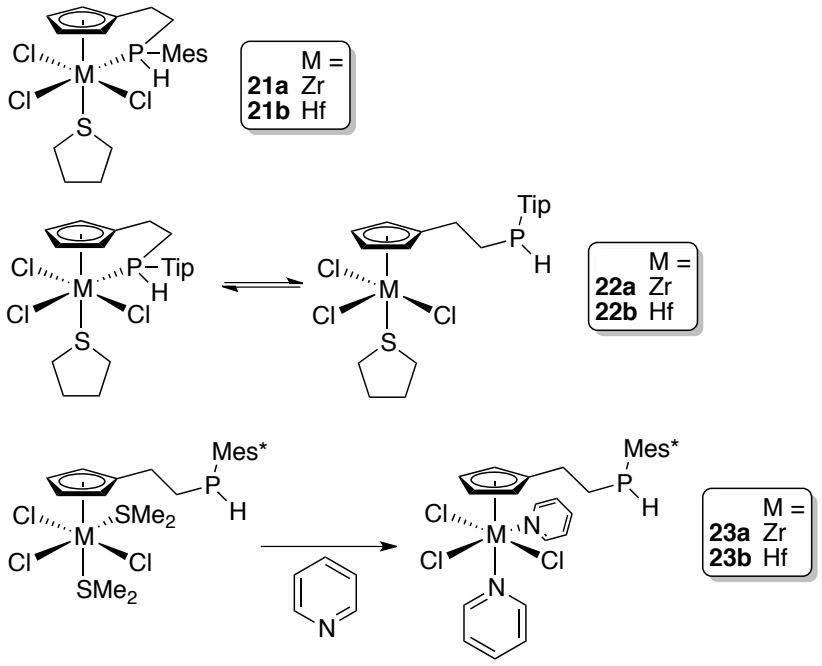

1.4.2. Group 6 Transition Metals

Norman et al. developed an elegant route to tri-phosphorus macrocycles by using

radical hydrophosphination of Mo(allylphosphine)$_3$(CO)$_3$ (Scheme 8). The resulting secondary tri-phosphine macrocycle **24a** was achieved in 85% yield and coordinates facially on the Mo(CO)$_3$ moiety. This novel metal-templated reaction utilizes three anti-Markovnikov P-H bond additions across C-C bonds of neighboring allylphosphine groups.[60] This method can also be applied to 4-phosphino-1-butene to generate a 15-membered secondary phosphine macrocyclic Mo complex **24b**. The cyclization process can be followed by ^{31}P NMR and sheds light on the mechanism of macrocycle formation.[61] Edwards et al. later used the similar routes to prepare tri-phosphorus macrocycles utilizing chromium and tungsten, **24c**[62] and **24d**[63], respectively.

Scheme 8. Tricyclization using hydrophosphination of a templated primary phosphine.

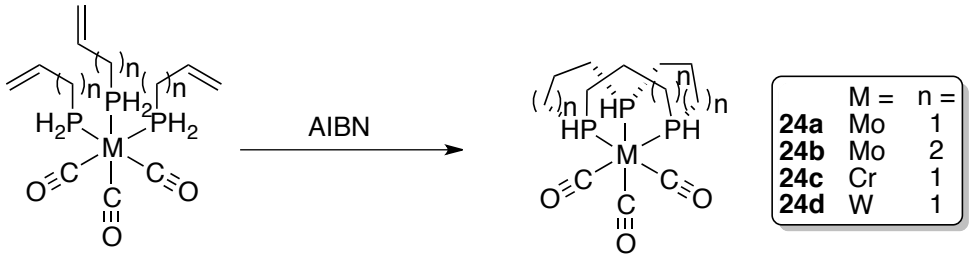

	M =	n =
24a	Mo	1
24b	Mo	2
24c	Cr	1
24d	W	1

Alkylation of the *fac*-M(P$_3$)CO$_3$ secondary phosphine macrocycles was carried out with either alkyl halides to form **25a-i**[62], or by radical-initiated hydrophosphination with various allyl compounds to yield **26a-g**[64]. Additionally, the P-H groups could be transformed to P-X bonds using CX$_4$ and NEt$_3$ (**27a-b**). The rate of this particular conversion was significantly faster than reported for free secondary phosphines, indicating that the coordination to the metal activates the P-H bond toward this reaction. After conversion to the halophosphine, **27a-b** were then changed to arylphosphines **28** using arylcopper reagents (Scheme 9).[65]

Scheme 9. Alkylated derivatives of triphosphorus macrocyclic complexes.

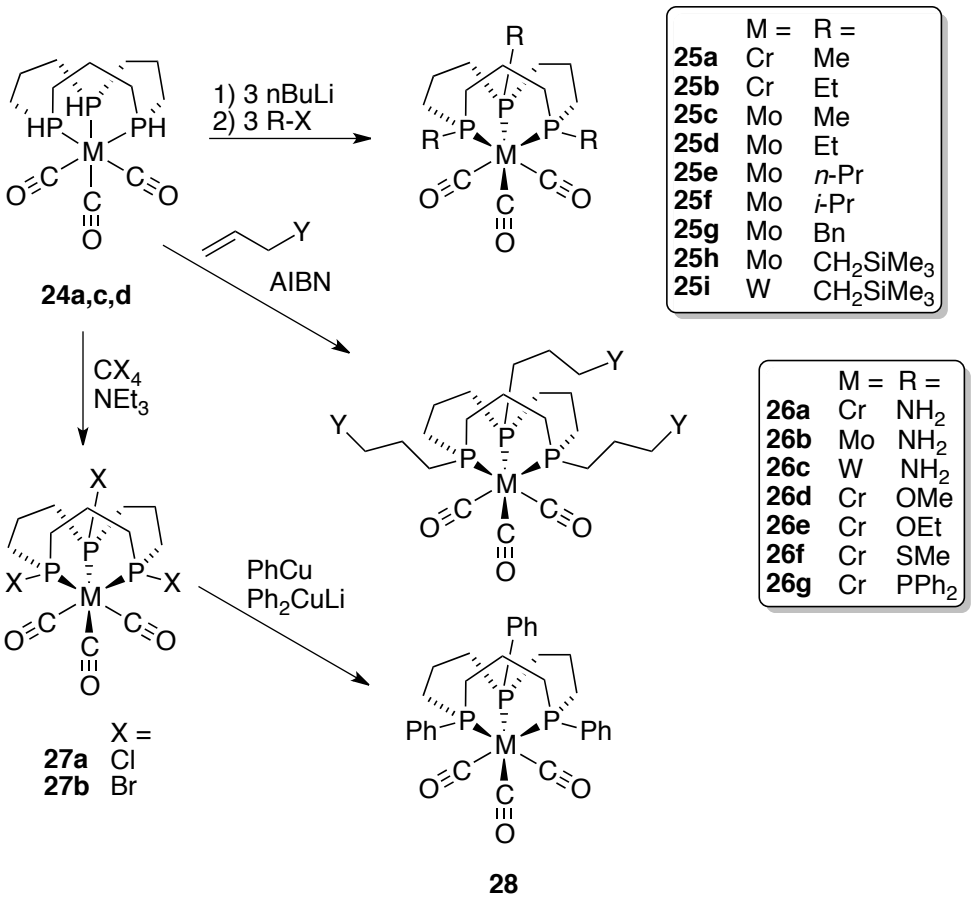

In 1997, the Morris group used diphenylphosphine to make acyl and alkyl piano-stool Mo complexes **29** (Scheme 10).[66] At low temperature (-78 °C), these complexes reacted with DBU to deprotonate the secondary phosphine, and could be alkylated with R-I (R = Me, Et) at -78 °C or RCOCl to yield alkylphosphine acyl **30a-d** and acylphosphine acyl complexes **31a-d**, respectively. Interestingly, if the deprotonation is carried out at room temperature, the anion, which is initially on phosphorus, migrates to molybdenum through an intramolecular acyl migration where the acyl group has ended on the phosphide ligand. Through this route, acylphosphine alkyl complexes **32** are accessible. A further study in the same group showed that complex **29a** can be reacted with activated alkynes to give, after deprotonation, vinylphosphines from a low-

temperature phosphorus-centered anion **33**, or acylphosphine complexes from the room-temperature molybdenum-centered anion **34**.[67]

Scheme 10. Temperature-dependent alkylation of a Mo phosphine complex.

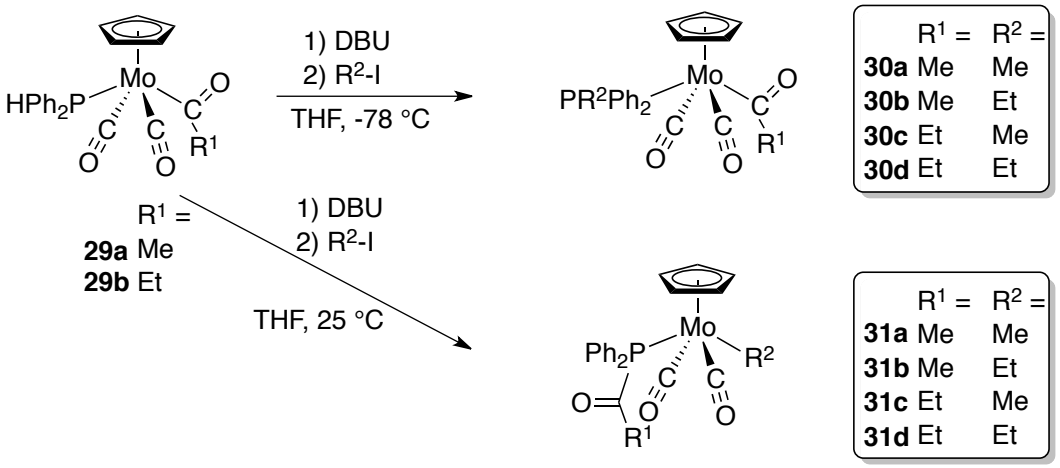

A molybdenum acetylide complex, [CpMo(CO_3)(CCR)] (R = Ph, CO_2Me) **33a-b**, was prepared and reacted with Ph_2PH to generate the secondary phosphine complex [CpMo$(CO)_2$(CCPh)(Ph_2PH)] **34**, as well as some of the hydrophosphination product, **35** (Scheme 11).[68] The P-H bond in **34** can be deprotonated with DBU and alkylated with MeI to yield the tertiary phosphine complex **36**. By changing the acetylide R group from Ph to CO_2Me, exclusive formation of the hydrophosphination product **37** can be formed as a mixture of E and Z alkenes. Presumably, the electron withdrawing nature of the CO_2Me group renders the alkene electron deficient enough to where the P-H bond reacts immediately, probably after Ph_2PH coordination via CO substitution.

Scheme 11. Direct hydrophosphination of diphenylphosphine on an acetylide complex.

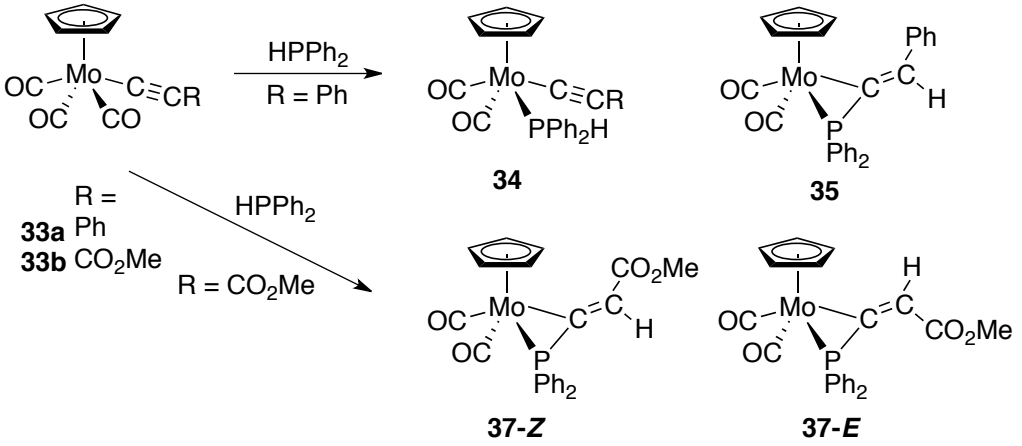

1.4.3. Group 8 Transition Metals

In 1994, Blake et al. prepared and crystallized *trans*-$Os(Ph_2PH)_4Cl_2$ **38a-b** from $[NH_4]_2[OsCl_6]$ and excess Ph_2PH or Cy_2PH, respectively (Figure 3).[69] The analogous Ru(II) complex **39** was also prepared earlier by Stephenson and co-workers.[70] Electrochemical studies of **38a** showed that oxidation potential for the Os(II)-Os(III) couple is +0.03 V (vs. ferrocene-ferrocenium), indicating that the complex oxidizes relatively easily, also seen in air by red coloration over time due to the corresponding Os(III) complex. Using this data and comparing it to analogous primary phosphine complexes, it was found that replacing a proton on each group with a phenyl group had a rather small effect on the electrochemical potentials.

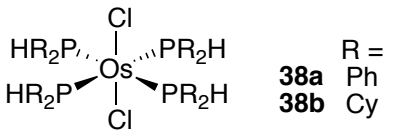

Figure 4. Blake's osmium secondary phosphine complexes.

Similar to the work previously mentioned (see section 1.4.3.), the Edwards group

continued the effort to prepare tri-phosphorus macrocycles, but using Fe(II) as a template source.[71,72] In this same way, coordination of either allylphosphine or allylphenylphosphine to an [Fe(η^5-Cp)(η^6-benzene)]PF_6 precursor led to the primary and secondary phosphine complexes **39** and **40**, respectively (Scheme 12). Cyclization then occurred using AIBN as a radical initiation to generate the tertiary and secondary triphosphorus macrocycles **41** and **42**, respectively. Interestingly, the cyclization of **40** did not occur when six equivalents of KO^{t}Bu were added, followed by three equivalents of 1,3-dibromopropane. When allylphosphine was substituted with α-methyl(vinyl)phosphine, the cyclization reaction failed to occur in a range of solvents, radical initiators, or photolysis, reaction times, and temperatures.

The secondary macrocyclic phosphine complex **42** can be reacted with ethylene with AIBN in chlorobenzene to alkylate the P-H bonds to yield the coordinated tri-tertiary phosphine macrocycle **43**. Digestion of complexes **41** and **43** with Na/NH_3 yields the corresponding free macrocycles **44a-b** as single stereoisomers (*syn-syn*).

Ruthenium and osmium porphyrin complexes **45a-g** were prepared and used for activation of P-H bonds on bound secondary and primary phosphines by Xie and coworkers.[73] A variety of substituted porphyrins of the form M(por)(CO)(L), (M = Ru(II) or Os(II) por = substituted porphyrins, L = solvent) were used as precursors. Addition of two equivalents of diphenylphosphine or phenylphosphine gave the disubstituted Ru(por)(phosphine)$_2$ **45a-d**, and in the case of Os, gave Os(por)(phosphine)(CO) **45e-g** (Scheme 13). The CO ligand in the Os(II) complexes was found to be inert to substitution by the phosphine.

Scheme 12. Syntheis of triphosphorus macrocycles on Fe-piano stool complexes.

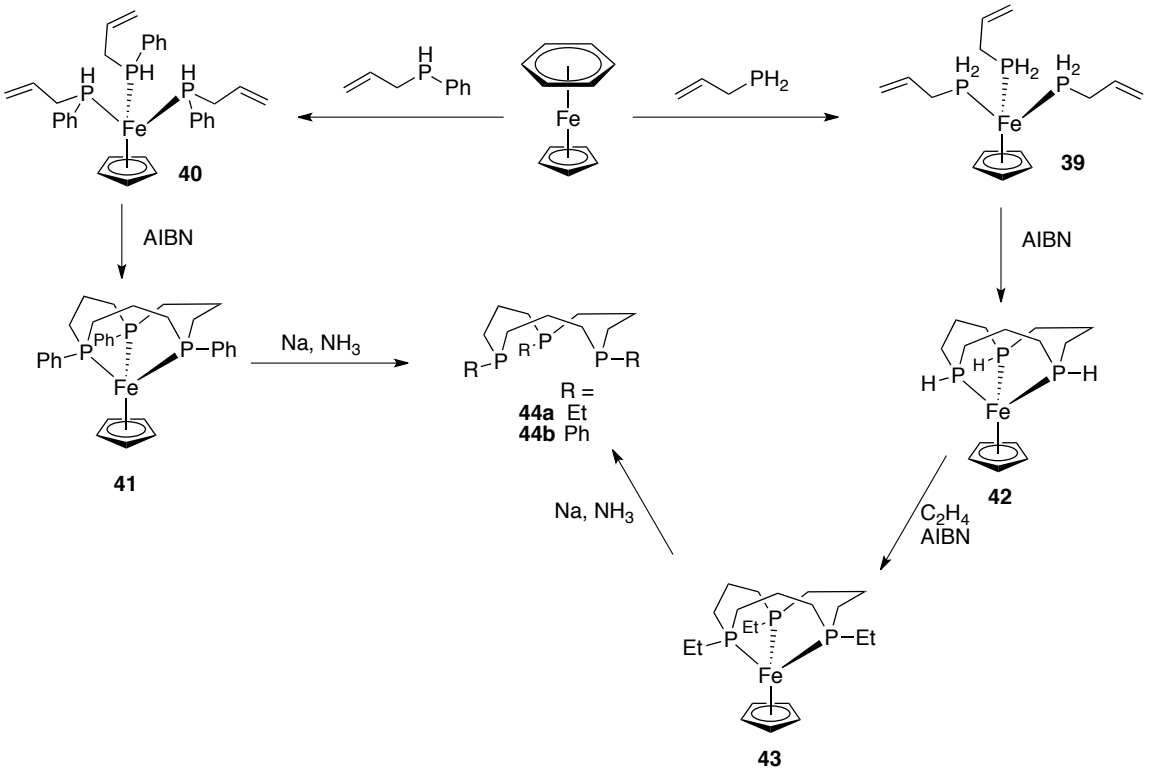

Complexes **45a-c** and **45e-f** are highly air-sensitive in the solid and solution state. Notably however, the fluorinated porphyrin complexes bearing the secondary and primary phosphines are stable in air, in both solution and in the solid state. This stability stems from the electron-withdrawing nature of the fluorinated porphyrin.

This type of chemistry was extended to Fe(II) porphyrins and Ru(II) phthalocyanine coordinating two equivalents PPh_2H to form complexes **46** and **47**, respectively (Scheme 14).[74] The Fe(II) complex was highly air-sensitive but the Ru(II) complex exhibited remarkable stability to air, in both the solid state and in solution. Complex **47**, as well as the fluorinated Ru(II) porphyrin complex mentioned previously (**45d**)[73], were taken on, and the authors showed that the P-H bond functionalization of the metal-bound phosphines in complex **47** happens easily with either

Scheme 13. Substituted Ru and Os porphyrin complexes bearing secondary phosphines.

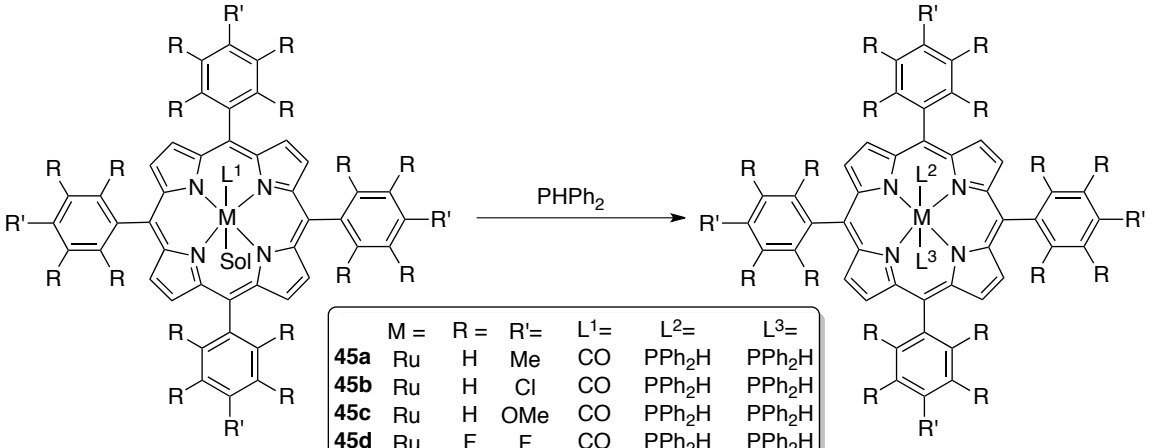

	M =	R =	R'=	L^1=	L^2=	L^3=
45a	Ru	H	Me	CO	PPh_2H	PPh_2H
45b	Ru	H	Cl	CO	PPh_2H	PPh_2H
45c	Ru	H	OMe	CO	PPh_2H	PPh_2H
45d	Ru	F	F	CO	PPh_2H	PPh_2H
45e	Os	H	Me	CO	CO	PPh_2H
45f	Os	H	Cl	CO	CO	PPh_2H
45g	Os	H	F	CO	CO	PPh_2H

deprotonation/alkylation or hydrophosphination in the presence of a base. With this chemistry, ruthenium phthalocyanine complexes of a variety of tertiary phosphines bearing alkoxycarbonyl, cyano, ketyl, alkoxyphosphonyl, sulfonyl, alkene, alkyne, and allene functional groups can be prepared (**48a-h**). The P-H bond functionalization of the Fe(II) complexes was not investigated due to their extreme air sensitivity.

Forder and Reid prepared complexes with PPh_2H of the type $[MBr_2(PPh_2H)_4]$ **51** (M = Ru or Os) and $[OsBr_2(Pcy_2H)_4]$ **52** using $RuBr_3$ or $[OsBr_6]^{2-}$, obtaining the trans-dibromide structure (confirmed by single crystal X-ray diffraction for $[OsBr_2(PPh_2H)_4]$) except for $[RuBr_2(PPh_2H)_4]$, where both *cis* and *trans* forms are seen by ^{31}P NMR spectroscopy. Electrochemical measurements were performed on these complexes and found that all of the complexes exhibit reversible $M^{II/III}$ redox couples. This study confirmed that the P-H bond remains intact on the cyclic voltammetry time scale, even on M(III) metals.[75]

Scheme 14. Substituted Fe porphyrin and Ru phalocyanine secondary phosphine complexes.

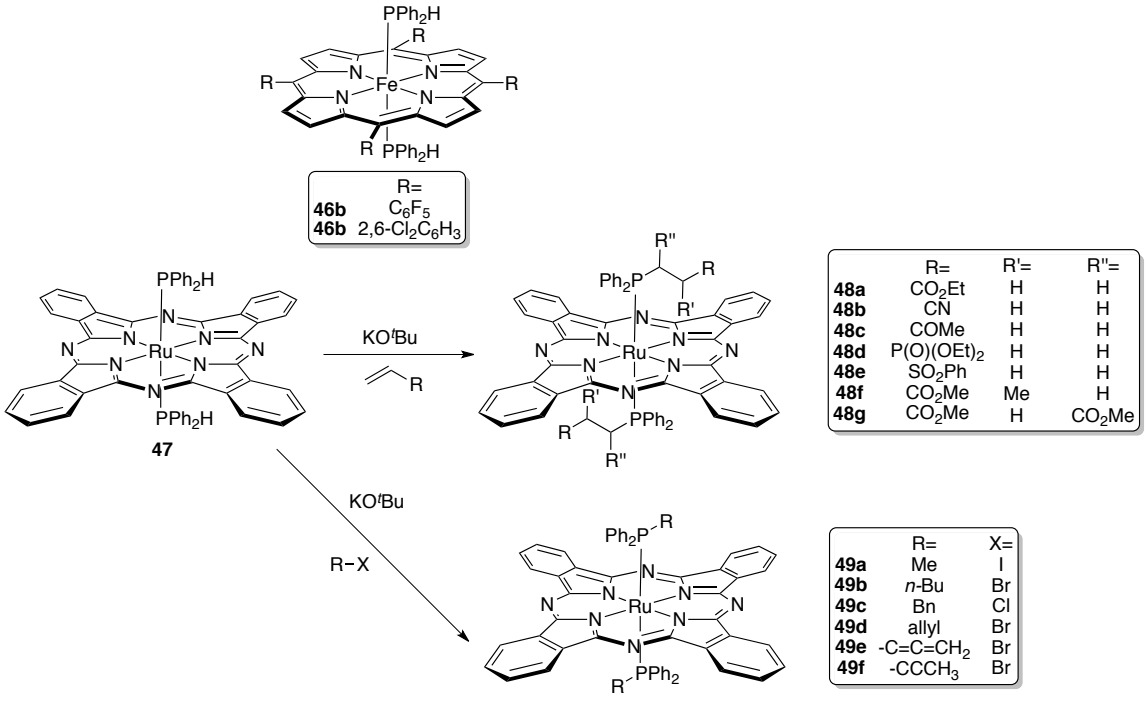

Fe(II) piano-stool complexes have been used as a method for generating coordinated chiral secondary phosphines as well as alkylation of those complexes to yield chiral tertiary phosphine complexes.[76] Coordination of phenylphosphine to (R*,R*)-(±)-(η^5-cyclopentadienyl)[1,2-phenylenebis(methylphenylphosphine)]iron(II) yields complex **53**, which can react with methyl iodide in the presence of KO^{t}Bu to produce unequal mixtures of diastereomers of the chiral secondary phosphine complex **54** (Scheme 15). Pure diastereomeric methylphenylphosphine complexes can be deprotonated at -95 °C to yield a highly reactive phosphide, which can be either be reprotonated or alkylated diastereoselectively at -95 °C. If the reaction is warmed up, the reactions give thermodynamic mixtures of chiral tertiary phosphine iron(II) complexes because of the relatively low barrier of inversion of phosphides on iron (II) (ca. 14.3 kcal/mol for

Fe(II)[76] and 11.5 kcal/mol for Ru(II)[77], calculated by dynamic NMR methods).

Scheme 15. Deprotonation and alkylation of an Fe-piano stool secondary phosphine complex. The complex can interconvert between diasteromers due to the low barrier to inversion of metal-bound phosphides.

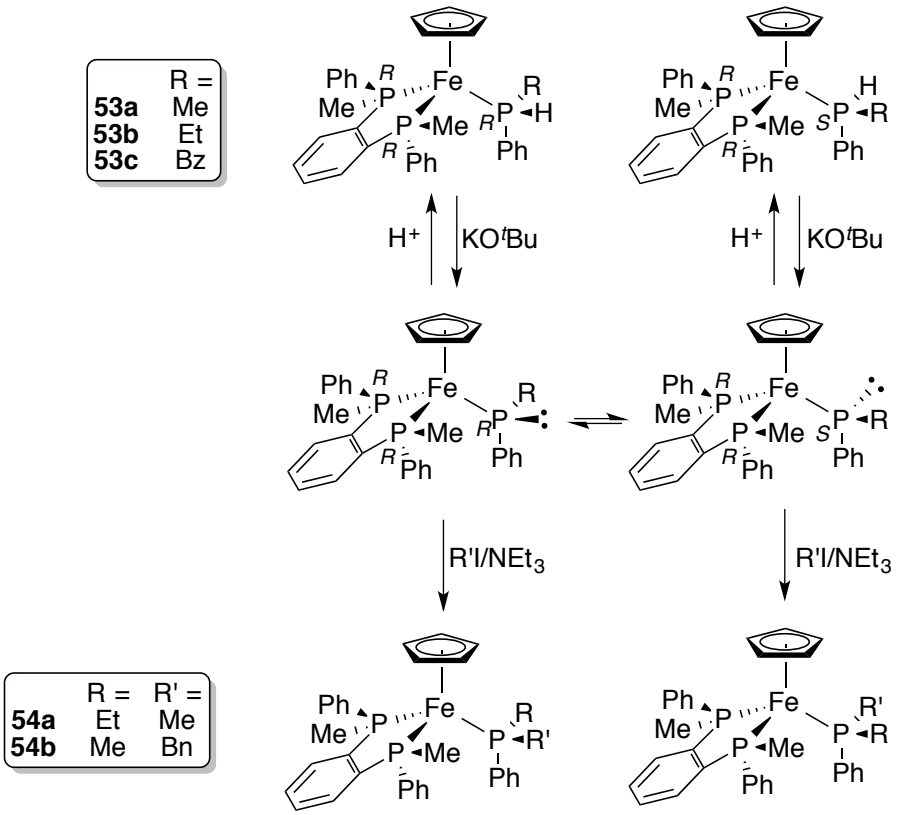

Hydridotetracarbonylferrates, $M^+[HFe(CO)_4]^-$, have been found to react with tris(amino)phosphines to form iron stabilized secondary bis(amino)phosphines (Scheme 16).[78] Two equivalents of the hydridotetracarbonylferrate **55** are needed to generate one equivalent of the secondary phosphine complex **56** and one iron tetracarbonyl salt. The reaction goes through a P-N activation-type mechanism where the hydride transfers to the phosphine and a secondary amine is eliminated.

Scheme 16. Synthesis of iron carbonyls with secondary bis(amino)phosphines.

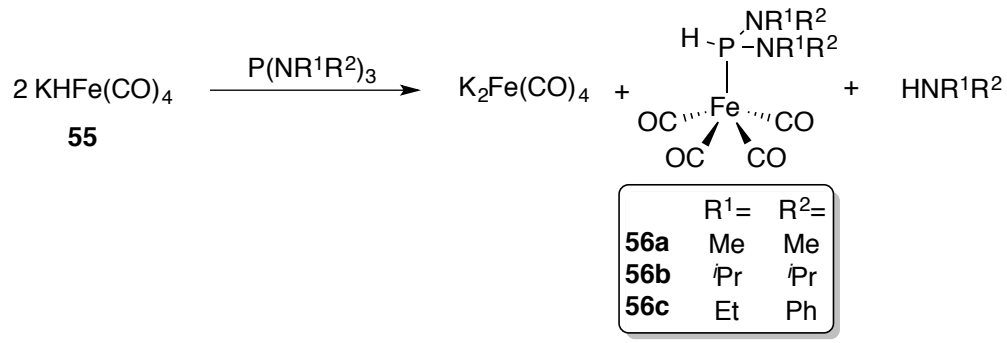

A novel route to prepare P-chiral functionalized phosphines was discovered by Malisch *et al.* by using hydrophosphination on cationic primary phosphine complexes to yield chiral secondary and tertiary phosphine complexes (Scheme 17).[79] The phosphine can be liberated from the complex in acetonitrile with 1,2-bis(diphenylphosphino)ethane added in, with yields ranging from 56 to 90%. The diastereoselectivity can be enhanced by adding chirality to the cationic iron complex in the form of an ancillary chiral phosphine ligand. This method can be tuned to be a catalytic hydrophosphination. In one example using $[\eta^5\text{-}C_5H_5(DIOP)Fe(MeCN)]BF_4$ (DIOP = 2,3-*O*-isopropylidene-2,3-dihydroxy-1,4-bis(diphenylphosphino)butane) **57**, a base catalyzed hydrophosphination of dimethyl maleate with phenyl phosphine in acetonitrile gives **58** in 97% yield with *dr*: 69:31. This method is a useful way to generate enantiomerically enriched secondary phosphines.

Scheme 17. A diasteroselective base-catalyzed hydrophosphination of dimethyl maleate with phenylphosphine using an iron-piano stool complex.

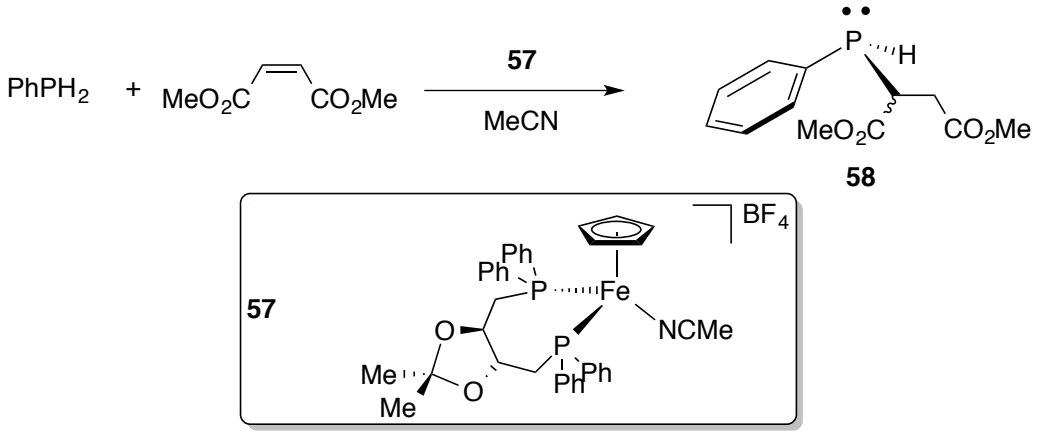

Another system looking to develop methods for enantiomeric synthesis of P-chiral phosphines investigated an assortment of five-coordinate Ru(II) catalysts. [80,81] Although these studies did not look exclusively at complexes bearing secondary phosphines as catalysts, many complexes of this type were prepared in order to study the mechanism of stereochemical enrichment and optimal base conditions for formation of the phosphide intermediate.

A Ru(II) half-sandwich complex [Ru(η^5-indenyl)Cl(P^{t}Bu(Ph)H)(PPh_3)] **60** was prepared from [Ru(η^5-indenyl)Cl(PPh_3)$_2$] **59** as a mixture of diastereomers due to the chirality of the P(Bu^t)(Ph)H ligand (Scheme 18).[82] The two diastereomers are formed in a 60:40 ratio but eventually forms all of **60a**, indicating that the two diastereomers are in equilibrium and **60a** is the more thermodynamically stable product. This complex holds promise in catalytic P-C bond forming reactions via dehydrohalogenation reactions.

Scheme 18. Synthesis of a Ru-indenyl complex as a mixture of stereoisomers.

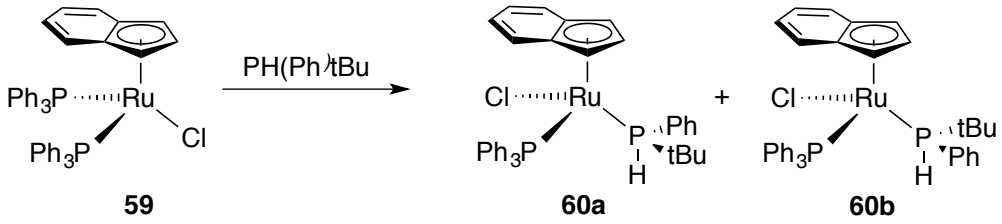

One group attempted to incorporate secondary phosphines into the first-generation Grubbs catalyst (GI) (Scheme 19).[83] Reaction of GI with dicyclohexylphosphine and di-*tert*-butylphosphine to prepare **61a** and **61b**, respectively, was examined but **61a** readily decomposed and **61b** was low yielding, most likely due to steric crowding. Instead, a modified Grubbs catalyst bearing PPh_3 instead of PCy_3 was prepared with the same secondary phosphine ligands. The use of dicyclohexylphosphine **62a** also decomposed rapidly, but di-*tert*-butylphosphine **62b** does react to replace one of the PPh_3 ligands to form the corresponding *cis* complex. This complex does act as a moderate ring-closing metathesis (RCM) catalyst, probably due to the *cis*-arrangement of the chlorides (Scheme 20). Additionally, addition of pyridine showed selective displacement of the secondary phosphine over triphenylphosphine,

Scheme 19. Ring-closing metathesis using a modified Grubbs catalyst bearing a secondary phosphine.

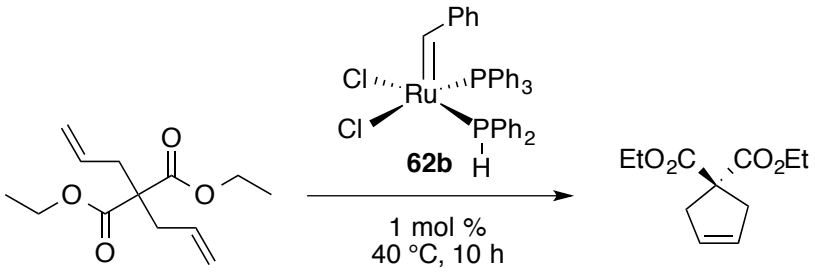

A series of mono-, bis-, and tetrakis-(phosphine) Ru(II) complexes (**63-65**) were prepared by Paris and coworkers. The group used ferrocene-based phosphines, both primary and secondary phosphines, as ligands on their scaffold (Scheme 20).[84,85]

Scheme 20. Example of mono-, bis-, and tetrakis-Ru secondary phosphine complexes.

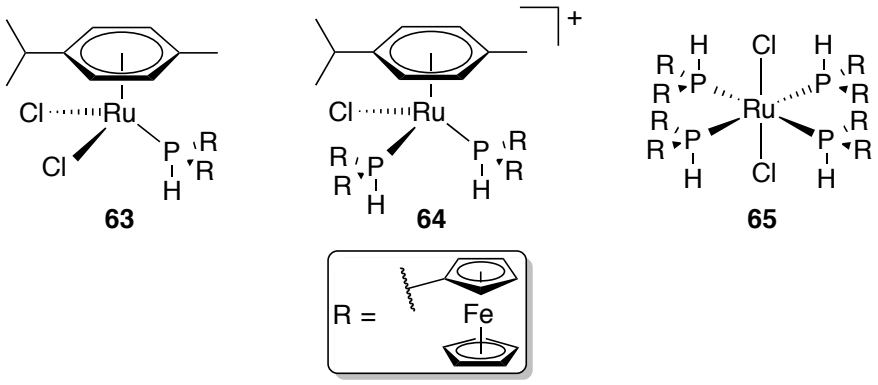

1.4.4. Group 9 Transition Metals

Some studies have looked at the reaction of secondary phosphines with di- and tri-cobalt carbonyl complexes. In one example, the trinuclear cobalt complex $[Co_3(\mu^3\text{-}CR)(CO)_9]$ (**66a**, R=Me or **66b**, R=CO_2Me) reacts with diphenylphosphine to give $[Co_3(\mu^3\text{-}CR)(CO)_8(PPh_2H)]$ **67a-b** after workup on silica in low to moderate yields (R=Me, 22%, R=CO_2Me, 56%) (Scheme 21). Additionally, $[Co_3(\mu^3\text{-}CR)(CO)_7(PPh_2H)_2]$ **68a-b** and $[Co_3(\mu^3\text{-}CR)(\mu\text{-}Ph_2POPh_2)(CO)_6(PPh_2H)]$ **69a** were isolated and characterized with mass spectrometry, IR, ^{1}H, ^{31}P, ^{13}C NMR spectroscopy. Bubbling CO gas through a solution of **68a** displaces one of the PPh_2H groups with a CO to reform **67a**, then **66a**.[86]

Scheme 21. Trinuclear cobalt complexes containing secondary phosphines.

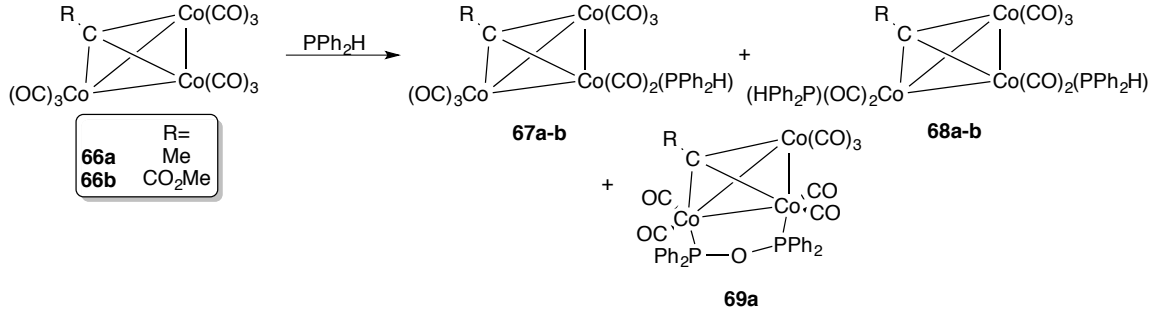

Rh(III) complexes bearing PPh_2H and PCy_2H were prepared by Reid et al. of the form *trans*-$[RhCl_2(PR_2H)_4]Cl$ **70a-b**. After attempting to grow crystals of *trans*-$[RhCl_2(PPh_2H)_4]Cl$, the crystals obtained showed that the secondary phosphines easily oxidized and the complex dimerizes to form $[(PPh_2OH)(PPh_2O)Cl(NCMe)Rh(\mu\text{-}Cl)_2Rh(PPh_2OH)(PPh_2O)Cl(NCMe)]$ **71** in MeCN/THF and $[(PPh_2OH)_2(PPh_2O)Rh(\mu\text{-}Cl_3)Rh(PPh_2OH)(PPh_2O)_2]$ **72** in ethanol (Scheme 22).[87] Other Rh(III) complexes have also been prepared with nitrite and nitro groups.[88]

Scheme 22. *trans*-Rh(III) phosphine complexes and their oxidized products.

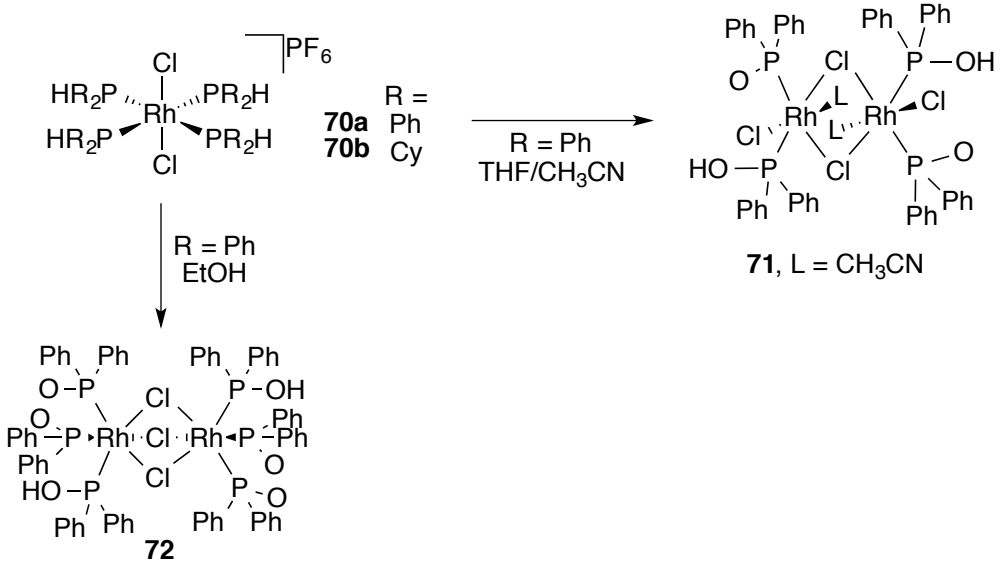

An interesting chiral secondary phosphine ligand (β-CgPH **73**, Scheme 23) based on an adamantane scaffold was coordinated to $[Rh(cod)_2]BF_4$ (cod=1,5-cyclooctadiene) **74** and used as a catalyst for asymmetric hydrogenation of dehydroamino acid derivatives.[89,90] During the catalysis, the group found that the Rh-P bond rotation is slow enough to observe rotamers using NMR spectroscopy at room temperature, indicating that the Rh-P bond rotation is restricted for this monodentate phosphine complex, and perhaps restricted bond rotation is necessary for enantioselectivity in other monodentate phosphine complexes.[90]

Scheme 23. Rh(I) complex bearing adamantane-based secondary phosphines and the two rotamers found in solution.

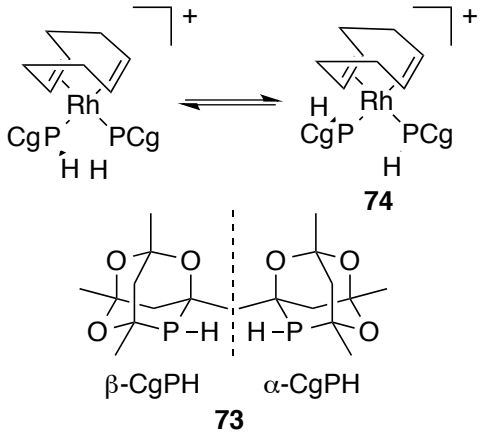

1.4.5. Group 10 Transition Metals

Secondary phosphine complexes incorporating group 10 metals is among the most studied groups of complexes. Some of the pioneering work in this areas was performed by Issleib and Hayter in the 1960's, looking at various R_2PH (R=Et, Cy, Ph) coordinated to transition metals.[91-95] This work, although not discussed in this review, provides the

initial scientific thrust for the coordination of secondary phosphines.

In 1977, DelDonno and Rosen published the seminal paper regarding a template synthesis of a tetraphosphine macrocycle.[96] This synthetic route utilized a mixed tertiary/secondary phosphine ligand and Ni(II) as the template ion. The ligand was coordinated to Ni(II) in a square-planar complex and bridged with o-dibromoxylene in the presence of K_2CO_3 to yield the macrocyclic Ni(II)-phosphine complex **75** (Scheme 24). The ligand was liberated from the Ni(II) center using NaCN. Later studies showed that the macrocyclic phosphine ligand acts as a strong field ligand, similar to phthalocyanines.[97]

Scheme 24. Ni-templated synthesis of a tetraphosphorus macrocycle.

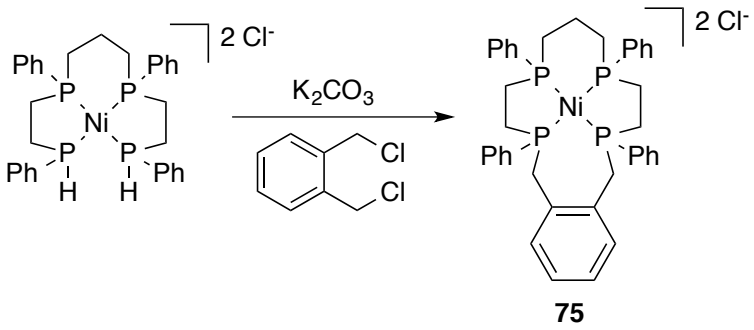

75

A lot of work looking at the preparation of tetraphosphine macrocycles from coordinated secondary phosphines on group 10 metals has been performed by the Stelzer group. A similar method to DelDonno and Rosen was used to prepare a 16-membered tetraphosphine macrocycle from $[Pd(MMPE)_2]Cl_2$ **76** (MPPE = 1,2-bis(methylphosphino)ethane) and two equivalents of o-dichloroxylene to prepare complex **77** (Scheme 25).[98] This reaction, in contrast to **75**, was complete after one hour at room temperature versus 48 hours. The structure of the macrocyclic complex was

confirmed by X-ray crystallography. Additionally, the same template was cyclized with *cis*-2-butene and isobutene linkers to form macrocyclic complexes **78** and **79**. These complexes were characterized by NMR spectroscopy and FAB mass spectrometry. Interestingly, 1,3-dichloropropane and 1,4-dichlorobutane did not react under the same reaction conditions.

Scheme 25. Stelzer's method toward Pd-tetraphosphine macrocyclic complexes.

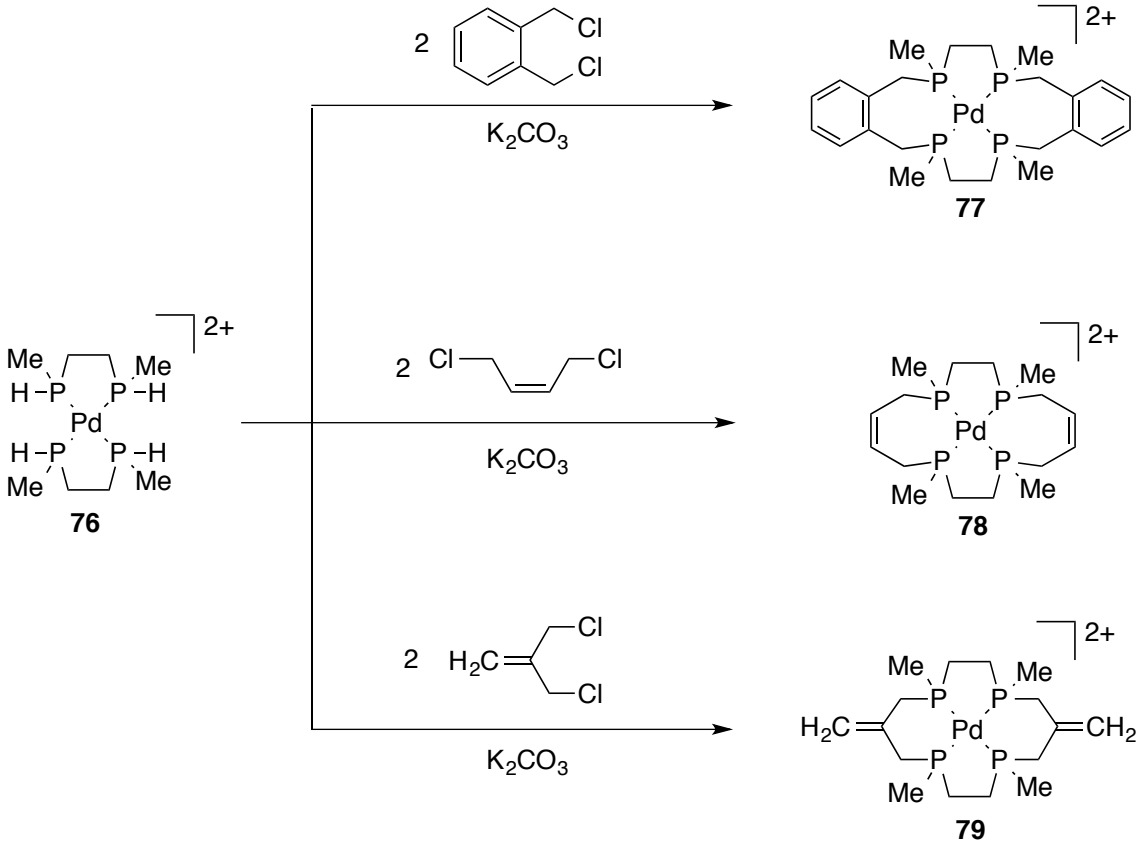

The Stelzer group also synthesized hydroxyl-functionalized tetraphosphorus macrocycles by reacting $[M(MMPE)_2]^{2+}$ (M = Ni or Pd) templates with α-ω dicarbonyl linkers to prepare 14-membered macrocycles with hydroxy groups in the backbone (Scheme 26).[99,100] Acetylacetone and malonaldehyde (added as the bis(dimethyl) acetal)

both reacted with the template to give the macrocycles **80a-c** in high yields. Macrocycles with vicinal hydroxyl groups were also prepared using$[M(MMPP)_2]^{2+}$ and 2,3-butanedione or benzil as linking agents, **81a-b**. These structures were confirmed by X-ray crystallography.

Scheme 26. Synthesis of tetraphosphorus macrocyclic complexes with pendant hydroxyl groups.

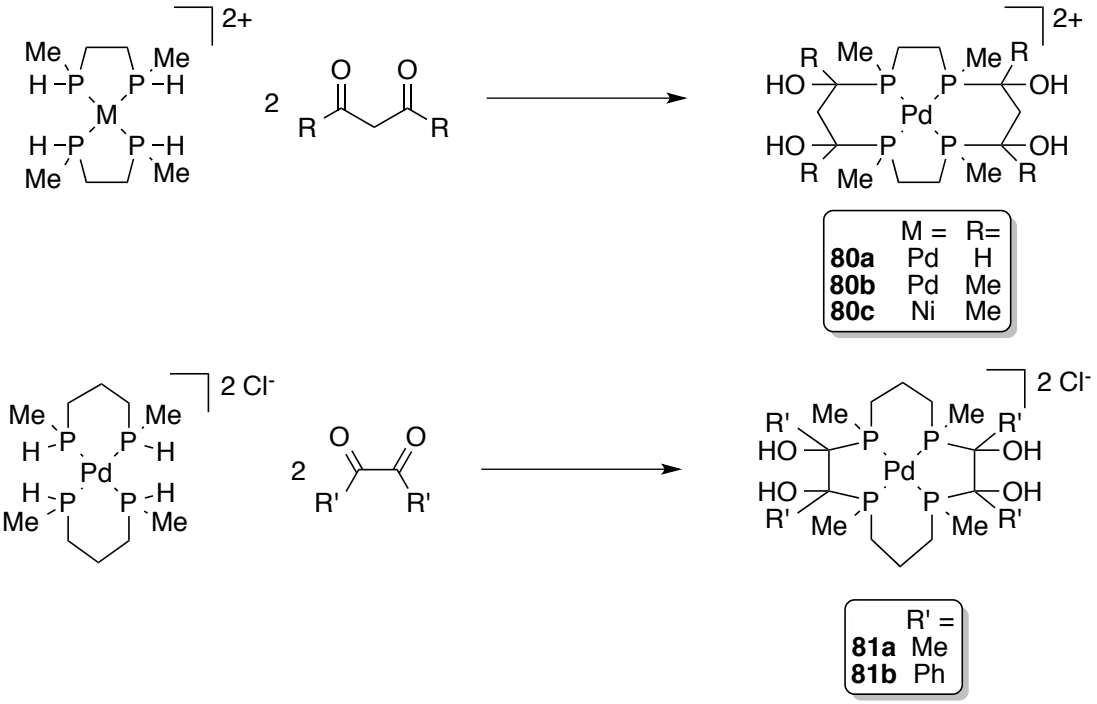

Another method by Stelzer et al. used a 1:1 template synthesis to make 14-, 15-, and 16- membered macrocyclic complexes **82a-k** by coordinating a secondary bis-phosphine (MMPE or MMPP) and one α-ω acetal-functionalized bisphosphine around a square planar metal (Scheme 27). Deprotection of the acetal with acid generates the carbonyl in situ, which then goes on to react with the secondary phosphine to form the macrocyclic product.[101,102]

Scheme 27. A route to tetraphosphorus macrocyclic complexes using acetal chemistry.

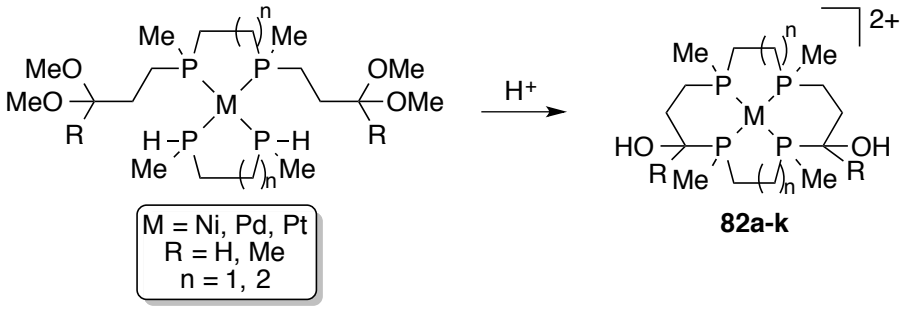

A similar method was used using a tridentate phosphine with terminal secondary phosphines and a di-vinyl functionalized phosphine.[101-103] Coordination of the two phosphines and refluxing in dichloromethane yields macrocycles **83a-e** in good yields. Two of the complexes have P-H bonds that can be further functionalized by hydrophosphination with methyl acrylate.

Scheme 28. Dihydrophosphination on Ni-templates to yield tetraphosphine macrocycles.

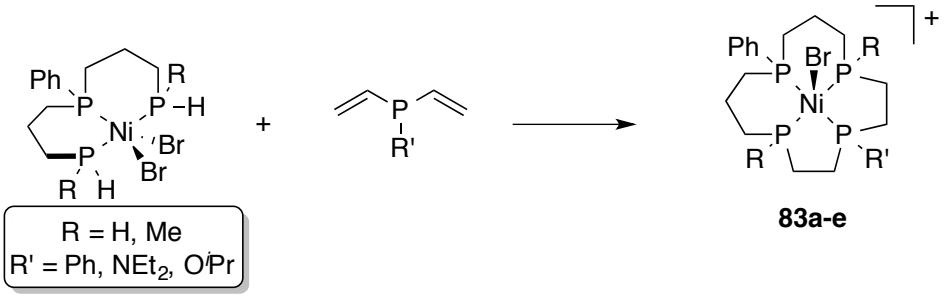

Another method for preparing tetraphosphine macrocycles was discovered in 1997 using Pt(II) and Pd(II) with two equivalents of MMPE. The resulting square planar complexes were then cyclized with 1,3-dibromopropane in the presence of K_2HPO_4 as base in low yields after HPLC with a GPC column separation (Pd(II) **84a**: 10% yield, **84b**

Pt(II): 10% yield) (Scheme 29). The macrocyclic complexes were confirmed by single crystal X-ray diffraction.[104]

Scheme 29. Mizuta's method to prepare Pt and Pd macrocyclic complexes.

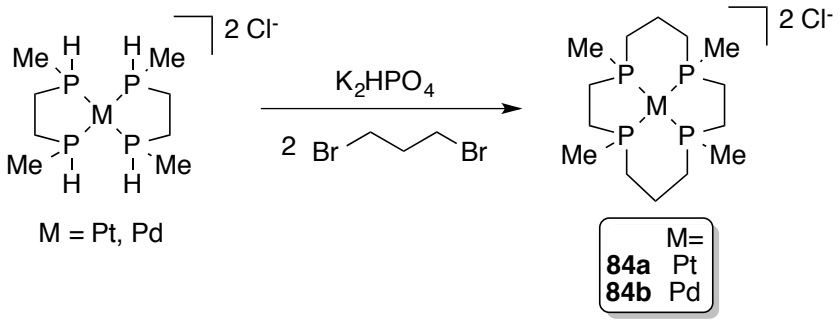

In 1993, Leoni synthesized the first mononuclear Pd(0) complex bearing only secondary phosphines as ligands.[105,106] Previously it was shown that Pd(η^5-Cp)(η^3-allyl) reacts with P^{t}Bu$_2$H to form the Pd(I) dimer [Pd(μ-P^{t}Bu$_2$)(P^{t}Bu$_2$H)]$_2$ (**85**).[107] The same precursor reacts with excess P^{t}Bu$_2$H to give Pd(P^{t}Bu$_2$H)$_3$ (**86**). This electron-rich complex can oxidatively add C-Cl bonds from dichloromethane and chloroform to give *trans*-[PdCl(CH$_2$Cl)(P^{t}Bu$_2$H)$_2$] **87** and *trans*-[PdCl(CHCl$_2$)(P^{t}Bu$_2$H)$_2$] **88**, respectively. The corresponding homoleptic Pt(0) complex was also prepared in the same fashion as **86**.[106]

The same group used similar Pd secondary phosphine dimers to synthesize the first example of an "agostic" M-H-P bond[108] (**89**, Figure 4) and investigate coordination vs. insertion reactivity with ethylene and isoprene,[109] and CO.[110] Palladium complexes bearing sulfonium ylides have also been prepared and studied.[111]

Scheme 30. The first mononuclear, homoleptic Pd-secondary phosphine complex and some of its reactions.

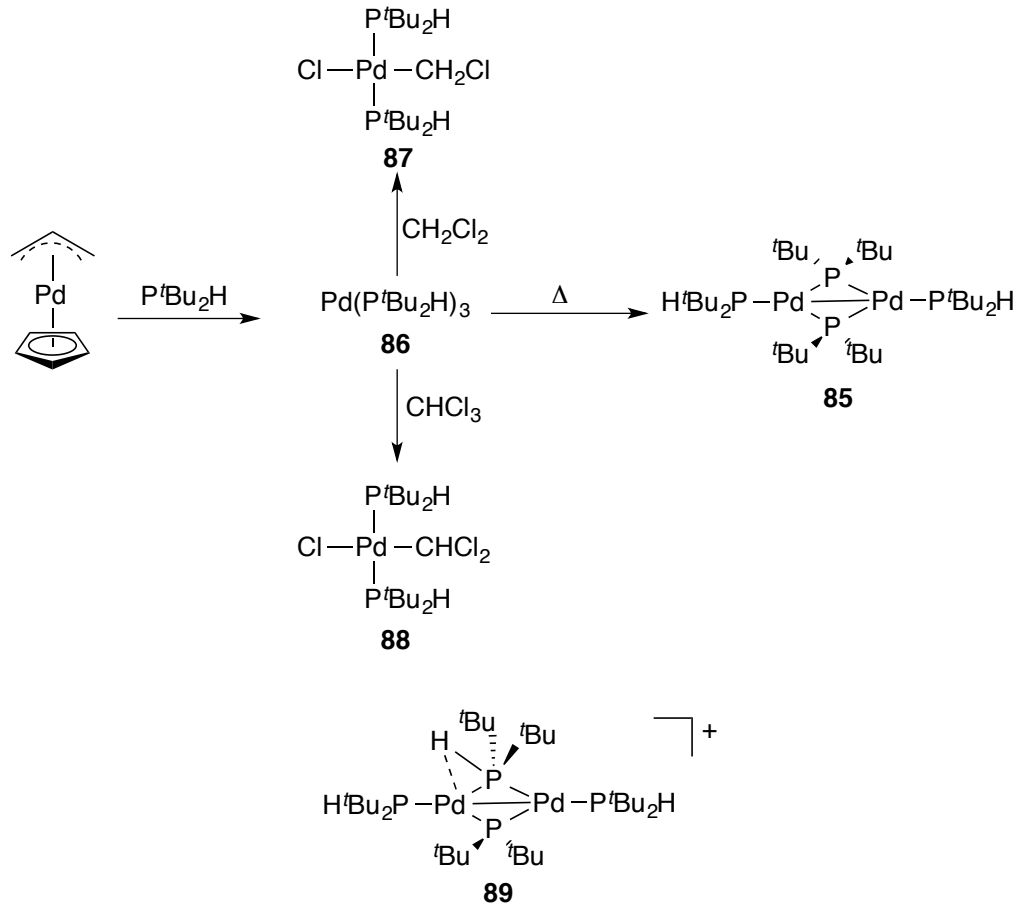

Figure 5. A Pd dimer that exhibited the first "agostic" M-H-P bond.

Coordination of secondary phosphines to Pd(II) and Pt(II) was extended to complexes bearing dicyclohexylphosphine to form $[MCl(PCy_2H)_3]X$, **90,** (M = Pt, Pd, X = Cl, BF_4^-, PF_6^-).[112] The same ligand reacting with $NiCl_2 \cdot 6H_2O$ forms the bis-secondary phosphine complex $[NiCl_2(PCy_2H)_2]$, **91**.[113] From this work, the results found that the P-H bond in these complexes is stronger than that for coordinated PPh_2H.[92,114-117] The *cis* isomer is exclusively formed in CH_2Cl_2 while the *trans* isomer is favored in benzene.

Palladium and platinum complexes with two secondary phosphine ligands have also

been prepared. Examples include *cis*-[Pt(C_6F_5)$_2$(PPh_2H)$_2$][55], **92**, and [Pd($HPPh_2$)$_2Cl_2$], **93** (which can be converted to [Pd($HPPh_2$)$_4$] with excess ligand in EtOH).[118]

Dimesitylphosphine (**94**) has also been used as a ligand with palladium and platinum to make a variety of *cis*- and *trans*-complexes **95a-g** with various other pendant groups (Table 2).[119] Dimesitylphosphine has a similar cone angle to triphenylphosphine (149° vs. 145°, respectively), and was found to act similarly to diphenylphosphine in terms of both sterics and electronics. Interestingly, complexes **95a-g** exhibited restricted rotation about the Pt-P and P-C(Mes) bonds, studied by variable temperature dynamic NMR spectroscopy.

Table 2. Reactivity of dimesitylphosphine with assorted Pt(II) and Pd(II) precursors.

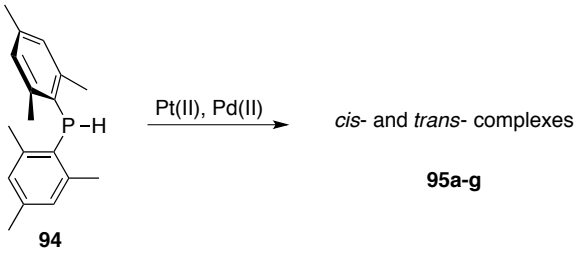

Entry	Starting Material	Product
95a	Pd(tmeda)Me_2	*cis*-Pd(L_2)Me_2
95b	$PdCl_2$/HCl Pd($NCPh)_2Cl_2$	
	Pd(cod)Cl_2	*trans*-PdL_2Cl_2
95c	K_2PtCl_4	
	$PtCl_2$	*trans*-PtL_2Cl_2
	Pt($NCPh)_2Cl_2$	
95d	Pt(cod)Cl_2	*cis*-PtL_2Cl_2
95e	*cis*-PtL_2Cl_2 + PPh_3	*cis*-Pt(L)(PPh_3)Cl_2
95f	Pt(cod)MeCl	*cis*-Pt($L)_2$(Me)(Cl)
95g	Pt(cod)(Et)(I)	*cis*-Pt($L)_2$(Et)(Cl) to *trans*-Pt($L)_2$(Et)(Cl)*

* The *cis*- complex is formed, but the isomerizes in solution to the *trans*- isomer.

Leoni and coworkers synthesized many dinuclear[109,110,120-126] and trinuclear Pt complexes that contain intact coordinated secondary phosphines. In one example, complexes of the form $[Pt_2(\mu\text{-}P^tBu_2)_2(P^tBu_2H)(L)]$ (L = P^tBu_2R (R = H, Li, *n*-heptyl), CO, η^2-CS_2) were prepared (**96-99**) (Scheme 31).[127] These complexes are very sterically congested and even slightly expanding the cone angle of the terminal phosphine has considerable effect on the Pt-P bond rotation. The terminal secondary phosphines can be lithiated and alkylated with *n*-heptyl bromide to give a terminal tertiary phosphine. Interestingly, the complex is inert to substitution by smaller cone angle phosphines, though carbonylation can take place, which allows CS_2 to add to the complex.

Scheme 31. Alkylation and substitution reactions of a Pt-dimer with terminal secondary phosphines.

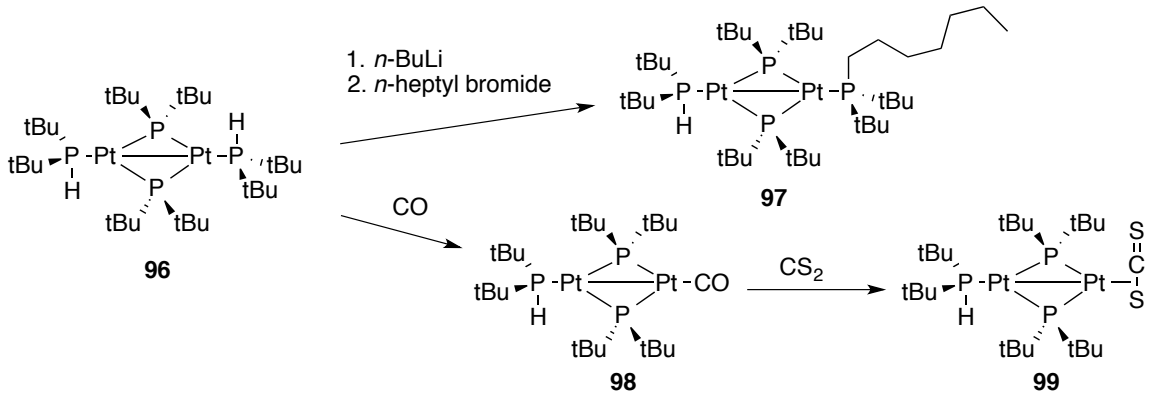

A mixed tertiary/secondary polyphosphine **100** was prepared by Green and Meek with the secondary phosphorus atom containing a phenyl group while the tertiary phosphine had two *p*-$CF_3C_6H_4$ substituents (Figure 6). The ligand coordinates to $Pt(cod)Cl_2$ (cod = 1,4-cyclooctadiene) to form complex **101**, indicated by the Pt satellites observed in the ^{31}P NMR spectrum. By comparing the chemical shifts of the complexes

to complexes that do not have the electron-withdrawing CF_3 groups, it was found that the CF_3 group does not impart much more electron withdrawing nature to the ligand.[128]

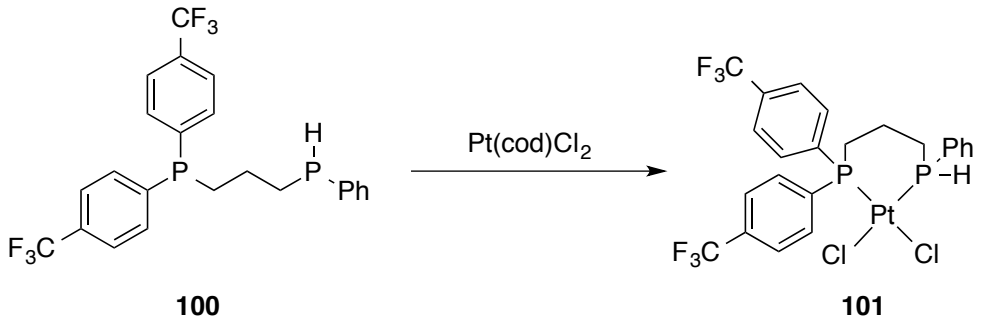

100 **101**

Figure 6. A bidentate tertiary/secondary phosphine used for Pt complex **101**.

Coordination to Pd(II) has also been used as a method of resolution of chiral secondary phosphines, with varying amounts of success. The complex [S-[(R*,R*),(R*)]]-$(+)_{589}$-[PtCl{1,2-C_6H_4(PMePh)$_2$}(PHMePh)]PF_6 **102** has been made and crystallized, but the resolved phosphine could not be displaced from the complex.[129] Albert et al. reacted methylphenylphosphine and benzylphenylphosphine with enantiomerically pure cyclopalladated dimers with pendant amines to give the mononuclear species **103a** and **103b** as a 1:1 mixture of diastereomers (Scheme 32).[130,131] The authors were able to separate the diastereomers by column chromatography. The optically pure phosphine could be released from the complex by addition of 1,2-bis(diphenylphosphino)ethane (dppe), though significant racemization of the free phosphine was observed after 3 hours in solution for benzylphenylphosphine, and in less than five minutes for methylphenylphosphine.

Scheme 32. A method of chiral phosphine resolution using Pd dimers.

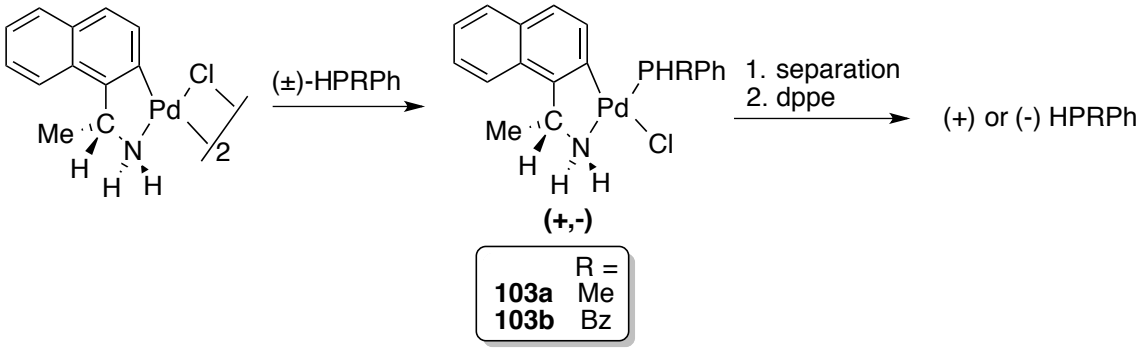

A variety of alkyl and aryl-secondary phosphine complexes of the formula *cis*-$[PtR_2(PHR'_2)_2]$ (R = Me, Ph, C_6H_4-*p*-CF_3, C_6F_5; R' = *i*-Bu, *t*-Bu, Ph) **104a-k** were prepared in good yields and characterized with NMR spectroscopy (and in some cases, single crystal X-ray diffraction) in order to prepare metallopolymers (Scheme 33).[132] These complexes were heated in a pressure-resistant NMR tube and found the formation of methane and coupling of two aryl ligands, forming multinuclear complexes with bridging phosphides.

Scheme 33. Various Pt(II)-secondary phosphine complexes and their reactivity toward metallopolymers.

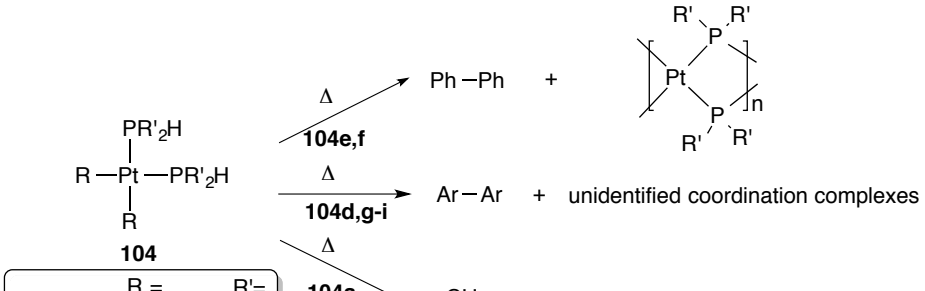

	R =	R'=
104a	Me	*i*-Bu
104b	Me	*t*-Bu
104c	Me	Ph
104d	Ph	*i*-Bu
104e	Ph	*t*-Bu
104f	Ph	Ph
104g	*p*-CF_3-C_6H_4	*i*-Bu
104h	*p*-CF_3-C_6H_4	*t*-Bu
104i	*p*-CF_3-C_6H_4	Ph
104j	C_6F_6	*i*-Bu
104k	C_6F_6	Ph

1.4.6. Group 11 Transition Metals

Gold complexes bearing secondary phosphines have generated some attraction as potentially useful complexes in medicine. In 1989, Dyson et al. prepared gold(I) complexes containing secondary phosphines in order to prepare $AuPR_2$ (where PR_2 is a phosphide) complexes from secondary phosphines.[133] It had been previously seen that addition of a thiol to [AuCl(tdg)] (tdg = thiodiglycol), will eliminate HCl and create the gold thiolate complex.[134] When investigating this reactivity with secondary phosphines, it was found that non-polar solvents will favor the $[AuX(PPh_2H_2)_n]$ **105a-c** (n = 1, 2, 4) structure instead of the phosphide polymer. Addition of base forms the polymeric phosphide as expected.

A variety of dinuclear gold(I) complexes were prepared with various bulky bis-secondary phosphines from [Au(tht)Cl] (tht = tetrahydrothiophene) to give [(AuCl)(μ-HPI~PHI)] **106a-d** as mixtures of diastereomers (Scheme 34).[135] These complexes were deprotonated to yield the phosphides, which formed a tetramer in the solid state for **106a**.

Scheme 34. Preparation of Au(I) complexes bearing bis(secondary)phosphines.

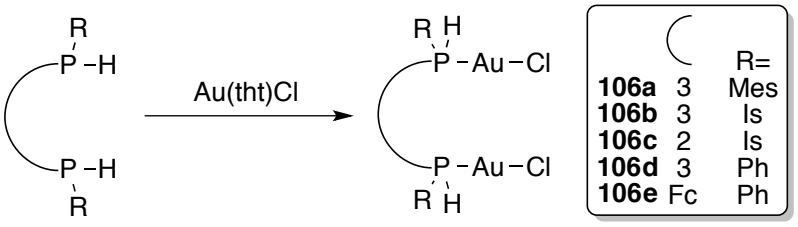

The first Au(III) complex bearing a secondary phosphine was prepared in 1998 by Blanco and coworkers. Addition of PPh_2H to $[AuR_3(tht)]$ (R = C_6F_5, tht) yielded the product $[AuR_3(PPh_2H)]$ **107** as a white solid in 37% yield. This complex was taken on

and reacted with the other coinage metals to create mixed metal phosphide complexes **108a-f** (Scheme 35).[136]

Scheme 35. Synthesis of trinuclear mixed metal phosphide complexes from Au-secondary phosphine complexes.

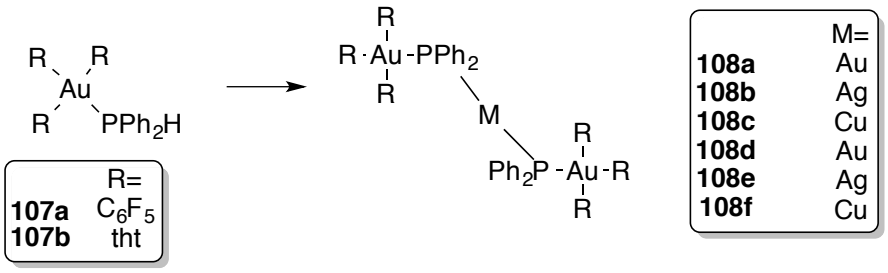

Copper(I) has been used as a template ion for the synthesis of tetraphosphine macrocycles.[137] The bis-bidentate secondary phosphine 1,2-bis(phenylphosphino)ethane (MPPE) was used to prepare $Cu(MPPE)_2OTf$ **109** as a reactive template for macrocyclization. Addition of either 1,3-dibromopropane or o-dibromoxylene in the presence of K_2CO_3 in ethanol leads to the desired macrocyclic complexes **110a** and **110b**, respectively (Scheme 36). These complexes can be demetallated using basified H_2S gas in air to yield the phosphine oxides **111a-b**.

Copper(I) can also be used as a catalyst in the alkylation of diphenylphosphine, with potential application in stereoselective alkylation catalysis.[138] This type of asymmetric catalysis was pioneered using Pt(II) for the preparation of various chiral bidentate ligands, but work toward a cheaper metal spurred the copper research.[139-144] The catalysts were effective at alkylating diphenylphosphine with various electrophiles. The proposed mechanism (Scheme 37) involved deprotonation of the secondary

Scheme 36. Template synthesis of tetraphosphine macrocycles on Cu(I).

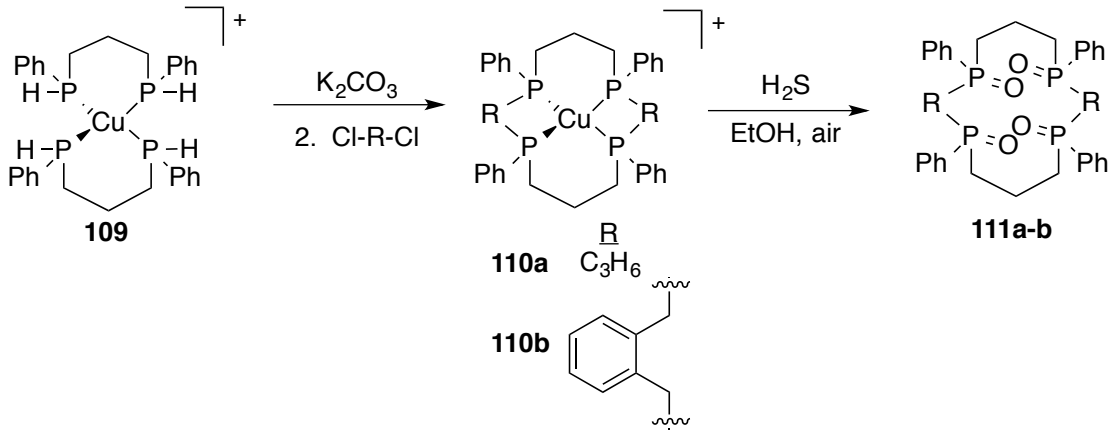

phosphine to generate a phosphide intermediate, which then performs nucleophilic attack on the substrate, followed by ligand substitution by diphenylphosphine. To investigate this, many Cu(I) complexes bearing secondary phosphines were prepared. The study found that indeed the secondary phosphine complexes do go through a phosphide intermediate that reacts with electrophiles. This was also studied with DFT calculations, which showed that the HOMO of the phosphide complex still mostly resides on phosphorus, indicating that the nucleophilic moiety is indeed the phosphorus atom. This chemistry was also used to prepare novel quinoxaline-based bidentate phosphine ligands.[145]

1.4.7. Other Metals

Some limited work has been done using Sn(IV) with secondary phosphines. Complexes of the formula $[R_2SnCl_2(PR'_2H)_2]$ (R = Ph, Me; R' = Ph, Cy) were prepared by addition of an equimolar amount of secondary phosphine to R_2SnCl_2 but not isolated. NMR studies were carried out as characterization of the complexes, and the compounds

were taken on to prepare phosphide complexes by deprotonation with base.[146]

Scheme 37. Proposed mechanism for stereoselective alkylation of secondary phosphines using Cu(I).

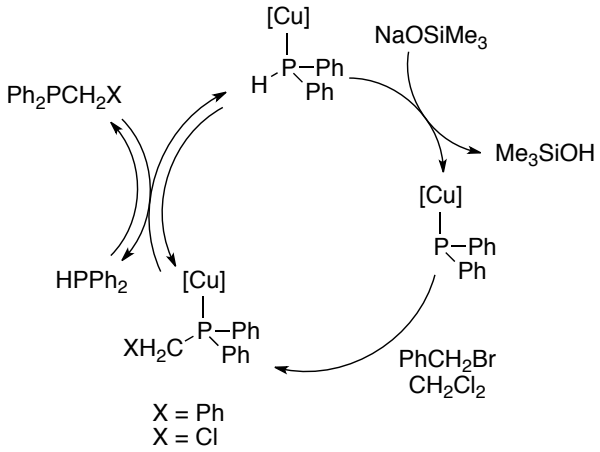

1.5. Summary

The use of secondary phosphines as ligands on transition metal complexes dates back to the 1960's. The primary use of these sorts of complexes is as precursors to metal-phosphide complexes, due to their ease of deprotonation when coordinated to a metal. A few complexes have been made bearing secondary phosphines whose intended use is as a catalyst in homogeneous catalysis methods, but these are few and far between. There are also complexes that use secondary phosphines as intermediates toward trying to make asymmetric tertiary phosphines stereoselectively. In general, secondary phosphines on metals are likely too reactive to be used in complexes made to be robust for catalysis.

One major niche use for coordinated secondary phosphines is toward macrocyclic phosphine ligands. Using a metal as a template and an activator of the secondary phosphines toward reactivity has been the bright spot in the preparation of multidentate

phosphine macrocycles in what seems a relatively slow to progress research area. The major advances in the field have stemmed from the reactivity of secondary phosphines to make P-C bonds to close the macrocycles through hydrophosphination and alkylation reactions. Overall, the field of coordinated secondary phosphines continues to grow and much is still to learn about how else the chemistry of these compounds can be used to further our knowledge of phosphines.

1.6. Bridge

Chapter I described the various synthetic methods for preparing secondary phosphines. This review also looks at the coordination chemistry and reactivity of these secondary phosphine complexes. Chapter II will detail the synthesis of bidentate secondary phosphines templated to copper(I) and their uses toward preparing tetraphosphine macrocycles.

This dissertation includes previously published and unpublished co-authored material. Chapter II contains experimental work performed by Charles D. Swor (CDS) and Aditya Nathan (AN), as well as some computational work and crystal growth performed by E. Adrian Henle. Parts of Chapter III contains experimental work by CDS, and have previously been published in Nell, B. P., Swor, C. D.; Zakharov, L. N.; Tyler, D. R. *Polyhedron* **2012**, *45*, 30-34. Parts of Chapter IV contains experimental work performed by AN, and have been prepared for Nell, B. P.; Nathan, A.; Tyler, D. R.; *manuscript in preparation*. In addition, CDS and AN performed some experimental work in Chapter V, and the crystal structures were solved by Lev N. Zakharov. The

crystal described in Appendix E was grown by CDS. The work completed in Appendix G was completed by Susan R. Cooper during a rotation in the Tyler lab.

CHAPTER II

ANALYSIS OF MACROCYCLIZATION OF $Cu(P_2)_2^+$ (P_2=A BIDENTATE SECONDARY PHOSPHINE) COMPLEXES: TOWARD IRON(II) COMPLEXES BEARING WATER-SOLUBLE MACROCYCLIC PHOSPHINES

Some of the experimental work done in this chapter was carried out by Charles D. Swor, and Aditya Nathan. Computation work and crystal growth was completed by E. Adrian Henle. Crystal structures were solved by Lev N. Zakarov. A portion of the work was written by Charles D. Swor.

2.1. Introduction

The ability of selected iron-phosphine complexes to bind N_2 makes these complexes promising candidates for use in schemes designed to separate N_2 from N_2-contaminated natural gas streams.[1-31–3] Natural gas (primarily methane) accounted for 27% of the United States' energy consumption in 2012.[4] Additionally, methane is the primary source for dihydrogen (H_2, made from steam reformation of methane), an important chemical feedstock and potential energy source in the future. Unfortunately, almost 15% of the United States' natural gas reserves are contaminated with high levels of dinitrogen (N_2). Dinitrogen acts as a dilutant in natural gas, lowering the energy density (energy output per unit volume), limiting the gas's use as a fuel. Industrially, the maximum allowed N_2 content for natural gas in the pipeline is 4%; some natural gas deposits can be made up of upwards of 86% N_2. The residual N_2 in natural gas poses a

problem from a purification standpoint; N_2 and methane are difficult to separate because of dinitrogen's chemical inertness, and the fact that both methane and dinitrogen have very similar physical properties.

Industrially, nitrogen rejection (the process of removing nitrogen from natural gas) uses the slight difference in the boiling points of methane and dinitrogen (112 K vs. 77 K, respectively), in the process of cryogenic distillation. This technique is very energy-intensive and requires large capital costs, making it only economically feasible for large gas fields.

The Tyler lab's approach to this problem is utilize dinitrogen's ability to act as a ligand on transition metals. Our laboratory previously showed[5] that complexes of the type *trans*-$Fe(P_2)_2X_2$ (where P_2 is a water-soluble bidentate phosphine) can act as "absorbents" in aqueous solution for separating N_2 from methane in a pressure-swing scheme (Scheme 1). However, in prolonged tests of the *trans*-$Fe(DMeOPrPE)_2X_2$ complex (DMeOPrPE = 1,2-bis[(dimethoxypropyl)phosphino]ethane, Scheme 2) in a pressure swing process over a continuous six-week period, the absorbent slowly became less and less effective until it eventually failed.

Scheme 1. Solution phase pressure swing process for separating N_2 from methane.

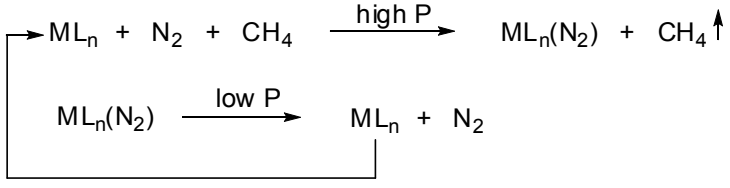

Our subsequent investigation of the failure showed that the phosphine ligands slowly dissociated from the complex, with the eventual formation of $Fe(DMeOPrPE)_3^{2+}$ (Scheme 2), which has no open coordination sites available for nitrogen coordination.[5,6] To obtain absorbent complexes that are more robust, we decided to replace the two bidentate ligands with a tetradentate phosphine macrocycle ligand. This feature should result in very slow dissociation rates of the phosphine ligand from its complex because of the kinetic macrocycle effect.[7]

Most macrocyclic phosphines have been prepared using a metal ion as a template. Our initial investigation for macrocyclization focused on using Fe(II) as a template metal, but previous results showed that Fe(II) was not an ideal metal ion, either because of a lack of electron density and/or the multiple geometries available for an octahedral metal (See Chapter V). Consequently, our research efforts focused on using a different metal ion as a template metal, using two bis-secondary phosphines that can be linked with various electrophiles to generate the desired macrocyclic product (Scheme 3). We focused our research efforts on using copper.

Cu(I) is a d^{10} metal, so it is electron-rich and has a preferred tetrahedral geometry about the metal center. This method of using copper has been used previously using Cu(I) and 1,2-bis[(phenyl)phosphino]ethane (MPPE) and bridging with 1,3-dibromopropane.[8] This chapter will describe efforts to prepare phosphine macrocycles using the same template strategy using other secondary bis-phosphines as well as novel secondary bis-phosphines bearing water-solublizing methoxypropyl groups.

Scheme 2. Degradation of $Fe(DMeOPrPE)_2Cl_2$ in water (DMeOPrPE = 1,2-bis[(dimethoxypropyl)phosphino]ethane).[6]

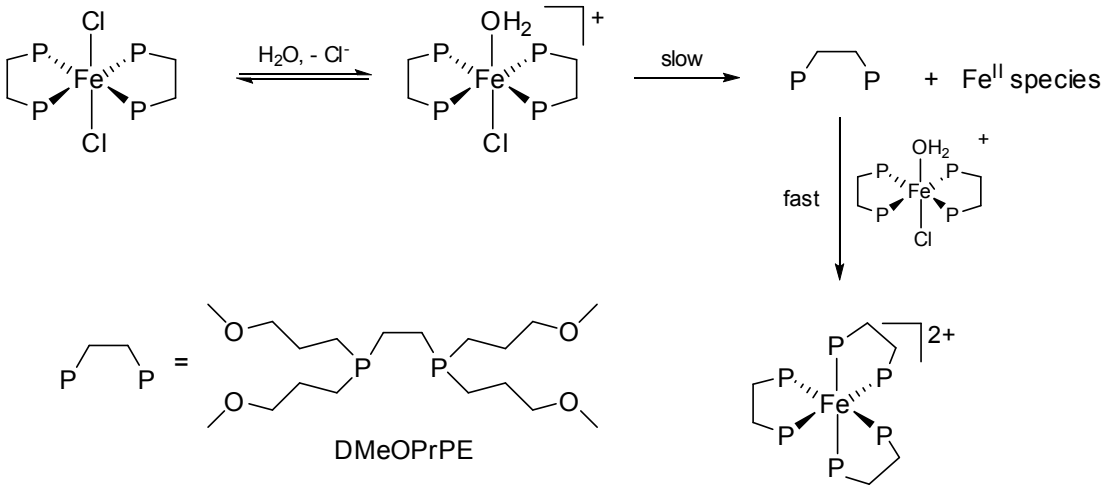

Scheme 3. General scheme for template macrocyclization with two bidentate secondary phosphines.

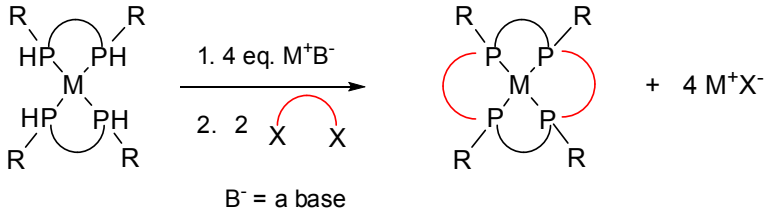

2.2. Experimental

2.2.1. Materials and Reagents

Unless otherwise noted, all experimental procedures were performed under an inert (N_2) atmosphere, using standard Schlenk and glovebox techniques. Commercially available reagents were used as received. HPLC-grade THF was dried and deoxygenated by passing through commercial columns of CuO, followed by alumina under an argon atmosphere. Deuterated solvents were obtained from Cambridge Isotope Laboratories

and degassed using three freeze-pump-thaw cycles. $[Fe(CH_3CN)_2](OTf)_2$[9] and **9**[8] were synthesized according to literature methods. $[Cu(CH_3CN)_4]OTf$ was prepared from a modified procedure.[10]

2.2.2. Instrumentation

Air-sensitive NMR samples were sealed in N_2 filled J-Young tubes. NMR spectra were obtained on either a Varian Unity/Inova 300 spectrometer at an operating frequency of 299.94 (^1H) and 121.42 (^{31}P) or a Varian Unity/Inova 500 spectrometer operating at a frequency of 500.62 MHz (^1H) or 202.45 MHz (^{31}P). The ^1H and ^{13}C NMR spectra were referenced to residual solvent peaks, and the ^{31}P NMR spectra were referenced to external 1% H_3PO_4 in D_2O. ESI mass spectra were obtained using a Thermo Finnigan LCQ Deca XP Plus ESI Mass Spectrometer using THF or CH_3CN as the solvent. Infrared spectra were recorded using a Thermo-Scientific Nicolet 6700 FT-IR spectrometer. UV-Vis spectra were collected on an Agilent 8453 spectrophotometer. Elemental analyses were performed by Complete Analysis Laboratories, Inc., Parsippany, NJ. Computations were completed using Gaussian 09, with a RHF 6-31G(d) basis set.

2.2.3. Methods

Synthesis of 1,2-bis(methoxypropylphosphino)ethane (1, MeOPrPE). To a solution of 1,2-bis(phosphino)ethane (2.26 g, 24.0 mmol) in hexane at -78 °C was added *n*-BuLi (1.6M in hexanes, 30.0 mL, 48.0 mmol) dropwise. The color of the solution turned bright yellow. This solution was stirred cold for one hour followed by the

dropwise addition of 1-chloro-3-methoxypropane (5.50 g, 50.6 mmol) in hexane. The solution was slowly warmed to room temperature over which time the yellow color faded and precipitate formed. The reaction mixture was stirred at room temperature for one hour, filtered, and the solvent removed to yield a clear oil. The oil was distilled at 85-90 °C @ 0.35 mmHg to yield the pure product. Yield: 5.02 g (88%). ^{31}P NMR ($CDCl_3$): δ -59.5 (d, $J_{P\text{-}H}$ = 202 Hz). ^{1}H NMR ($CDCl_3$): δ 1.3-1.9 (m, 12H), 3.19 (d, 2H, P*H*), 3.34 (s, 6H, OC*H*$_3$), 3.52 (t, 4H, C*H*$_2$OCH$_3$) ^{13}C{^{1}H} NMR ($CDCl_3$): δ 16.6, 19.1, 28.3, 58.6, 73.0. Anal. Calcd for $C_{10}H_{24}O_2P_2$: C, 50.41; H, 10.15; P, 26.00. Found: C, 50.36; H, 10.09; P, 25.87.

Synthesis of 1,3-bis(methoxypropylphosphino)propane (2, MeOPrPP). This synthesis was carried out in the same fashion as **1**, using 1,3-bis(phosphino)propane (2.12 g, 19.6 mmol). The oil was sufficiently pure without distillation. Yield: 4.95 g (80%). ^{31}P NMR ($CDCl_3$): δ –69.9 (d, $J_{P\text{-}H}$ = 202 Hz). ^{1}H NMR ($CDCl_3$): δ 1.4-2.0 (m, 14H), 3.13 (d, 2H, P*H*), 3.35 (s, 6H, OC*H*$_3$), 3.42 (t, 4H, C*H*$_2$OCH$_3$) ^{13}C{^{1}H} NMR ($CDCl_3$): δ 16.7, 21.8, 27.1, 28.4, 58.6, 73.2. Anal. Calcd for $C_{11}H_{26}O_2P_2$: C, 52.37; H, 10.39; P, 24.56. Found: C, 52.25; H, 10.55; P, 24.48.

[Cu(MeOPrPE)$_2$]PF$_6$ (3). A CH_3CN solution of **1** (0.0190 g, 0.080 mmol) was added to $Cu(CH_3CN)_4PF_6$ (0.0148 g, 0.040 mmol). The reaction mixture was stirred for 1 hour at RT after which the solvent was removed under reduced pressure. Yield: 0.0253 g (93.0%) of an off-white viscous oil. ^{31}P{^{1}H} NMR (THF): δ -41.1 (br). ESI-MS: 539 amu

(m^+). Anal. Calcd for $C_{20}H_{48}F_6CuO_4P_5$: C, 35.07; H, 7.06; P, 22.61. Found: C, 34.98; H, 7.13; P, 22.49.

[Cu(MeOPrPP)$_2$]OTf (4). A CH_3CN solution of **2** (0.0698 g, 0.277 mmol, 1.92 equiv) was added to a CH_3CN solution of $Cu(CH_3CN)_4OTf$ (0.0542 g, 0.144 mmol, 1 equiv) and stirred for 1 hour. The solvent was removed under reduced pressure to yield an off-white viscous oil. $^{31}P\{^1H\}$ NMR (THF): δ -50.5 (br). ESI-MS: 567 amu (m^+). Anal. Calcd for $C_{23}H_{52}F_3CuO_7P_4S$: C, 38.52; H, 7.31; P, 17.28. Found: C, 38.46; H, 7.28; P, 17.04.

[Cu(MPPE)$_2$]PF$_6$ (5). This complex was prepared in a manner similar to **3** using MPPE (0.0211 g, 0.086 mmol) and $Cu(CH_3CN)_4PF_6$ (0.0170 g, 0.046 mmol). Yield: 0.0281 g (97.3 %) of a white granular solid. $^{31}P\{^1H\}$ NMR (THF): δ -31 (br). ESI-MS: 555 amu (m^+). Anal. Calcd for $C_{28}H_{32}CuF_6P_5$: C, 47.98; H, 4.60; P, 22.09. Found: C, 47.95; H, 4.67; P, 22.01. The analogous triflate complex was also prepared, using $Cu(CH_3CN)_4OTf$ instead of $Cu(CH_3CN)_4OTf$. The spectroscopic data was identical.

[Cu(MPPP)$_2$]OTf (6). This complex was prepared in a manner similar to **4**, using MPPP (0.3830 g, 1.47 mmol) and $Cu(CH_3CN)_4OTf$ (0.2782 g, 0.74 mmol). Yield: 0.5177 g (95.9%) of a white granular solid. $^{31}P\{^1H\}$ NMR (THF): δ -42.1 (br). ESI-MS: 583 amu (m^+). Anal. Calcd for $C_{31}H_{36}F_3CuO_3P_4S$: C, 50.79; H, 4.95; P, 16.90. Found: C, 50.76; H, 4.81; P, 16.77.

General method for macrocyclization with K_2CO_3. $Cu(P_2)_2X$ (X = OTf or PF_6) was dissolved in THF and excess K_2CO_3 was added in one portion. The solution immediately turned bright yellow and was stirred at room temperature for 10 minutes. After stirring, the desired dihalide (two equivalents) was diluted in THF was added dropwise. The reaction mixture was stirred overnight, during which the reaction became lighter yellow with white precipitate. The reaction was filtered over celite and the solvent removed in vacuo. The remaining yellow residue was redissolved in dichloromethane and filtered again over celite. Removal of the solvent yielded the product was a yellow powder.

[Cu(MeOPrPE)-$P_{4\text{-DBP}}$]OTf (7). This complex was prepared following the general method above, using $[Cu(MeOPrPE)_2]PF_6$ (0.1550 g, 0.227 mmol) and 1,3-dibromopropane (0.990 g, 0.490 mmol). Yield: 0.973 g (56 %) $^{31}P\{^1H\}$ NMR ($CDCl_3$): δ -2 ppm (br). ESI-MS: 619 amu (m+).

[Cu(MeOPrPP)-$P_{4\text{-DBP}}$]OTf (8). This complex was prepared following the general method above, using $[Cu(MeOPrPP)_2]PF_6$ (0.251 g, 0.352 mmol) and 1,3-dibromopropane (0.149 g, 0.738 mmol). Yield: 0.1661 g (56 %). ESI-MS: 647 amu (m+).

[Cu(MPPP)-$P_{4\text{-DBP}}$]OTf (10). This complex was prepared following the general method above, using $[Cu(MPPP)_2]OTf$ (0.3010 g, 0.334 mmol) and 1,3-dibromopropane

(0.139 g, 0.688 mmol). Yield: 0.2140 g (65 %) $^{31}P\{^{1}H\}$ NMR ($CDCl_3$): δ -15 ppm (br). ESI-MS: 663 amu (m+).

[Cu(MPPE)-$P_{4\text{-DBB}}$]OTf (11). This complex was prepared following the general method above, using [$Cu(MPPE)_2$]OTf (03044. g, 0.432 mmol) and 1,4-dibromobutane (0.104 mL, 0.871 mmol). Yield: 0.2747 g (95.8 %) $^{31}P\{^{1}H\}$ NMR ($CDCl_3$): δ 5.83 (br). ESI-MS: 663 amu (m+). Anal. Calcd for $C_{37}H_{44}CuF_3O_3P_4S$: C, 54.6; H, 5.45. Found: C, 48.86; H, 4.92. This rather poor elemental analysis is likely due to residual KBr left over from the reaction. Anal. Calcd for $C_{37}H_{44}CuF_3O_3P_4S$•0.8 KBr: C, 48.92; H, 4.88.

General method for macrocyclization with KO^{t}Bu. $Cu(P_2)_2X$ (X = OTf or PF_6) was dissolved in THF and 4 equivalents of KO^{t}Bu was added in one portion. The solution immediately turned bright yellow and was stirred at room temperature for 10 minutes. After stirring, the desired dihalide (two equivalents) was diluted in THF was added dropwise. The reaction mixture was stirred and became cloudy and lighter yellow after a few minutes. The reaction was stirred for at least four hours. The reaction was filtered over celite and the solvent removed in vacuo. The remaining yellow residue was redissolved in dichloromethane and filtered again over celite. Removal of the solvent yielded the product was a yellow powder.

[Cu(MPPP)-$P_{4\text{-DBB}}$]OTf (12). This complex was prepared following the general method above for KO^{t}Bu, using [$Cu(MPPP)_2$]OTf (0.0535 g, 0.073 mmol), KO^{t}Bu

(0.0319 g, 0.284 mmol) and 1,4-dibromobutane (0.016 mL, 0.134 mmol). ESI-MS: 691 amu (m+). This complex can also be prepared using the general route using K_2CO_3. The spectroscopic evidence is identical.

General procedure for demetallation. In a typical procedure, the Cu-macrocyclic phosphine complex was dissolved in CH_2Cl_2 (3-5 mL) and stirred vigorously at room temperature with an aqueous solution of KCN (2 mL) overnight. The aqueous layer was removed and the organic layer was dried over $MgSO_4$ and filtered through a plug of alumina. The solvent was removed *in vacuo* to yield a waxy residue that was taken on directly to prepare metal complexes or used as a CH_2Cl_2 solution directly.

13 (Phosphine from 11): $^{31}P\{^1H\}$ NMR ($CDCl_3$): δ -20.4 ppm (s). ^1H NMR (500 MHz, $CDCl_3$) δ 8.01 – 7.03 (m, 20H), 2.77 – 0.84 (m, 29H). FAB-MS: 601 amu $[m+H]^+$.

Synthesis of Co(13)Cl_2. A solution of **13** in THF was added to a suspension of $CoCl_2$ in THF. The solution immediately turns emerald green upon addition of the ligand to the metal. Removal of the solvent yields a green powder. ^{31}P NMR (202 MHz, $CDCl_3$) δ 8.68 – -32.76 (m). ESI-MS: 694 amu $[m-Cl]^+$. UV-Vis (CH_3CN, nm): 681, 589.

2.3. Results and Discussion

2.3.1. Synthesis of the Hydrophilic Phosphines

1,2-bis[(methoxypropyl)phosphino]ethane (1) and

1,3-bis[(methoxypropyl)phosphino]propane (2)

Secondary phosphines are readily prepared by deprotonation and alkylation of primary phosphines. Thus, deprotonation of 1,2-bis(phosphino)ethane with 2 equivalents *n*-butyllithium followed by alkylation with 2 equivalents of methoxypropyl chloride (or bromide) in hexane yielded **1** as a viscous oil (Scheme 4).

Scheme 4. Synthesis of the hydrophilic secondary phosphines **1** and **2**.

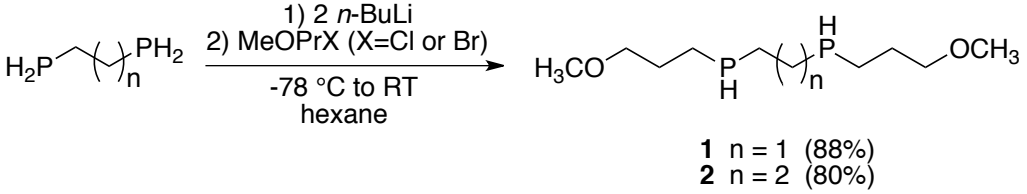

The $^{31}P\{^{1}H\}$ NMR spectrum of **1** is a singlet at -60 ppm that, when coupled to protons, splits into a doublet ($J_{P\text{-}H}$ =199 Hz), indicative of a secondary phosphine. The reaction is not stereospecific and the three expected stereoisomers (*R,R*(meso); *S,R*; and *R,S*) were not separated. The analogous phosphine 1,3-bis[(methoxypropyl)phosphino]propane (**2**) was synthesized in the same manner using 1,3-bis(phosphino)propane. Phosphine **2** also exhibits a singlet at 64 ppm in the $^{31}P\{^{1}H\}$ NMR spectrum that splits into a doublet ($J_{P\text{-}H}$=189 Hz) in the proton-coupled spectrum. Both **1** and **2** are clear, colorless, viscous oils, and the ambiphilic methoxypropyl

functional group causes these compounds to be miscible in a wide range of solvents, from water to hexanes. Over-alkylation at the phosphorus atoms can be prevented by keeping the reaction temperature at -78 °C, as indicated by ^{31}P NMR spectroscopy. Because of the extra molecular weight of the methoxypropyl group, the desired product can be separated from any under- or over-alkylated products by fractional vacuum distillation.

2.3.2. Synthesis and Characterization of $Cu(P_2)_2^+$ Complexes

In order to synthesize Cu(I) templates with water-soluble phosphines, the hydrophilic secondary phosphine ligands **1** and **2** were coordinated to Cu(I) by reaction of these ligands with $Cu(CH_3CN)_4X$ (X = $^-$OTf or $^-PF_6$) in CH_3CN to form template complexes **3** and **4** (Scheme 5). Coordination of the phosphines was confirmed by $^{31}P\{^1H\}$ NMR spectroscopy, where the chemical shifts of the coordinated phosphines moved ~20 ppm downfield from the free ligands (-41.1 ppm for **3** vs. -59.5 ppm for free **1** and -50.5 ppm for **4** vs. -69.6 ppm for **2**). The ^{31}P NMR signals are significantly broadened because of coupling with NMR-active, quadrupolar ^{63}Cu and ^{65}Cu nuclei (both spin 3/2, 69% and 31% abundance, respectively).[11,12] Cu-P coupling can be observed but generally only for highly symmetric $Cu(PR_3)_4^+$ complexes.[12-14] In some copper-phosphine complexes, this broadening can be minimized by obtaining the spectra at high temperature,[13-15] but the spectra of these complexes do not change between 25 °C and 90 °C. The $[Cu(P_2)_2]^+$structures were supported by ESI-MS analysis (**3:** m^+= 539 amu calculated and observed; **4:** m^+= 567 amu calculated and observed; see Appendix B for spectra).

Both **3** and **4** were isolated as viscous liquids. In order to obtain products that were solids instead of viscous liquids, complexes of the hydrophobic ligands MPPE and MPPP were synthesized, **5** and **6**, respectively. These complexes were also characterized by ^{31}P NMR and ESI-MS and were isolated as crystalline solids. Although previous reports[8] of such complexes state that they are air-stable, some oxidation of the copper was observed when these products were worked up in air, as evidenced by a blue coloration of the solutions. Therefore, these complexes were handled under an inert atmosphere.

Scheme 5. Synthesis of the $Cu(P_2)_2^+$ templates.

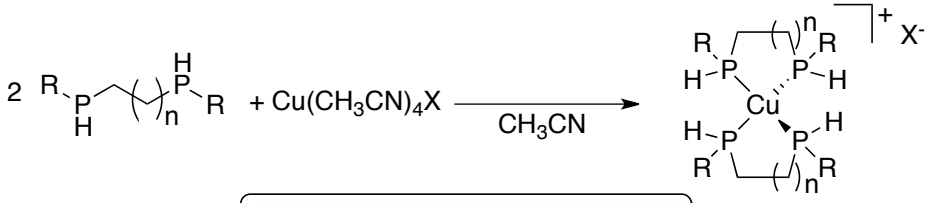

	n	R	X
3	1	$CH_3O(C_3H_6)$	PF_6
4	2	$CH_3O(C_3H_6)$	OTf
5	1	Ph	PF_6 or OTf
6	2	Ph	OTf

2.3.3. Macrocyclization of $Cu(P_2)_2^+$ Complexes

Complexes **3**-**6** reacted with 2 equivalents of 1,3-dibromopropane in the presence of K_2CO_3 in THF to form the membered macrocyclic complexes **7**-**10**, respectively (Scheme 6). Alkylation of the coordinated secondary phosphines was suggested by the downfield shifts in the ^{31}P NMR spectra (e.g., -15 ppm vs. -41 ppm for **3**). In general, it took complexes **7** and **8** longer to reach completion (2-3 days) whereas complexes **9** and **10** needed only four hours for complete alkylation. We hypothesize that the electron

withdrawing nature of the phenyl groups make the P-H bond more acidic, and thus complex **6** reacts faster with base. ESI-MS of complexes **7**-**12** all showed base peaks consistent with the masses of the macrocyclic complexes (Table 1), indicating complete alkylation with the 1,3-dibromopropane. The same procedure was carried out using 1,4-dibromopropane with complexes **5** and **6** to prepare 16- and 18-membered macrocyclic complexes **11** and **12**, respectively.

Scheme 6. Macrocyclization of $Cu(P_2)_2^+$ templates with K_2CO_3.

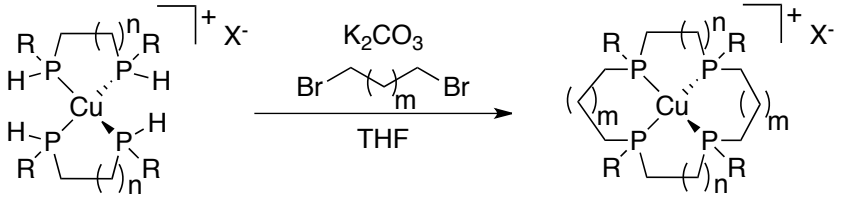

3-6

	n	m	R	X
7	1	1	$CH_3O(C_3H_6)$	PF_6
8	2	1	$CH_3O(C_3H_6)$	OTf
9	1	1	Ph	PF_6 or OTf
10	2	1	Ph	OTf
11	1	2	Ph	OTf
12	2	2	Ph	OTf

If KO^{t}Bu is used instead of K_2CO_3, the reaction progresses much faster and is done within minutes, instead of hours or days. Addition of KO^{t}Bu to any of the $Cu(P_2)_2^+$ templates generates a bright yellow solution, indicative of the phosphide in solution. After dropwise addition of the bridge, the yellow color fades to a dull yellow color with white precipitate (with MPPE and MPPP), or to colorless with white precipitate (MeOPrPE and MeOPrPP). The spectral data obtained from these experiments match those obtained when K_2CO_3 is used as a base.

If too much bridge is added or the reaction is too concentrated, multiple alkylations of the bridge are possible. For example, when complex **6** is alkylated with a slight excess of 1,3-dibromopropane or 1,4-dibromobutane, the ESI mass spectrum of the products shows the formation of a coordinated open-chain ligand with hanging propyl or butyl bromides (Figure 1, see Appendix A for ESI-MS). More stringent control of the stoichiometry of the bridge eliminates this side product from the mass spectrum. This illustrates the importance of the stoichiometry of the macrocyclization reaction.

Table 1. Mass spectral data for copper macrocyclic complexes **7-12**.

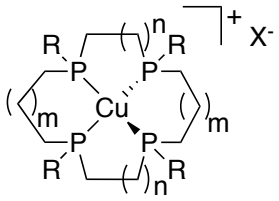

7-12

#	R	n	m	m^+ Formula	*m/z*
7	$CH_3O(C_3H_6)$	1	1	$[C_{26}H_{56}O_4P_4Cu]^+$	619
8	$CH_3O(C_3H_6)$	2	1	$[C_{28}H_{60}O_4P_4Cu]^+$	647
9	Ph	1	1	$[C_{36}H_{44}P_4Cu]^+$	635 [8]
10	Ph	2	1	$[C_{38}H_{48}P_4Cu]^+$	663
11	Ph	1	2	$[C_{38}H_{48}P_4Cu]^+$	663
12	Ph	2	2	$[C_{40}H_{52}P_4Cu]^+$	691

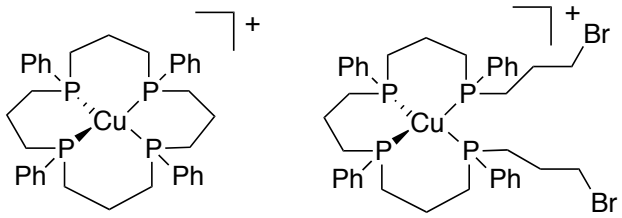

Figure 1. Macrocyclization of **4** with 1,3-dibromopropane. Double alkylation is an observed side-product in ESI-MS (right).

It should be noted that a potential problem with this synthetic route is the possibility of bridging between phosphorus atoms of the same ligand, creating a double-chelate small ring product (Scheme 7). However, no example of this reactivity has ever been observed.[16-18] To definitively determine if the small ring or macrocycle was formed, X-ray crystallography of the Cu(I) complex or free ligand is needed. Alternatively, mass spectrometry can be used to determine the mass of the free ligand (mass spectroscopy of the Cu(I) complex will give the same mass regardless of whether or not the small ring or macrocycle was formed). An X-ray quality crystal of the 16-membered macrocyclic copper(I) complex (**10**) was obtained by E. Adrian Henle, and analyzed with single crystal X-ray diffraction (Figure 2). The macrocyclic tetraphosphine had a stereochemistry of *RSRS* on copper with a disordered triflate anion.

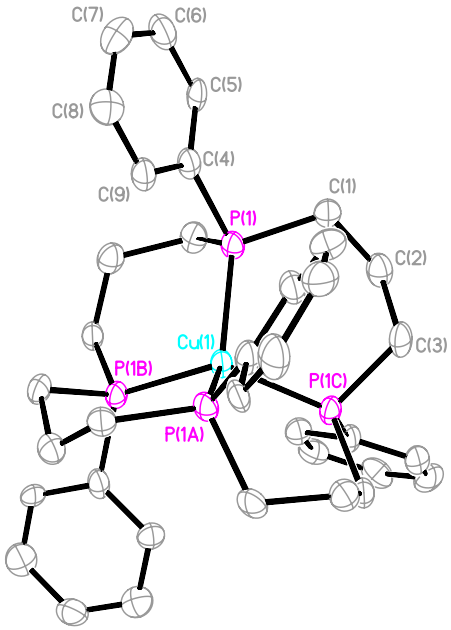

Figure 2. ORTEP drawing of the cation of **10** with thermal ellipsoids drawn at the 50% level. The H-atoms are omitted for clarity.

Scheme 7. Possible side-reaction with macrocyclization of a bis-bidentate secondary phosphine.

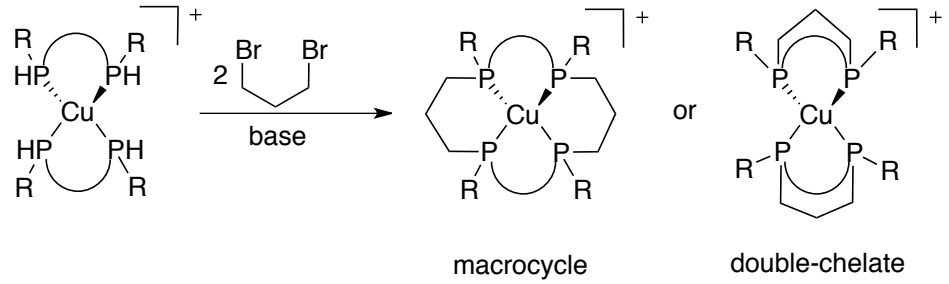

2.3.4. Demetallation with KCN

In order to examine the conditions of Cu removal, demetallation trials were first conducted with $[Cu(MPPE)_2]PF_6$ (**5**). Dissolving this complex in dichloromethane or toluene and stirring with a saturated aqueous KCN solution overnight or heating to 70 °C

for 15 minutes yielded the free ligand in the organic layer (Figure 3), as indicated by ^{31}P NMR spectroscopy.[17,19]

This route was then used to demetallate complex **11** to give the free phosphine **13** as an oily, colorless residue. The compound displayed a singlet in the $^{31}P\{^{1}H\}$ NMR spectra at -20.4 ppm. The general features of the ^{1}H NMR spectrum are broad and do not give much structural information, but the disappearance of the P-H protons support the fact that full alkylation was achieved. A FAB mass spectrum of **13** shows the expected parent mass plus a proton at 601 m/z and HR-MS gives a formula of $C_{36}H_{45}P_4$, which corresponds to $[M+H]^+$.

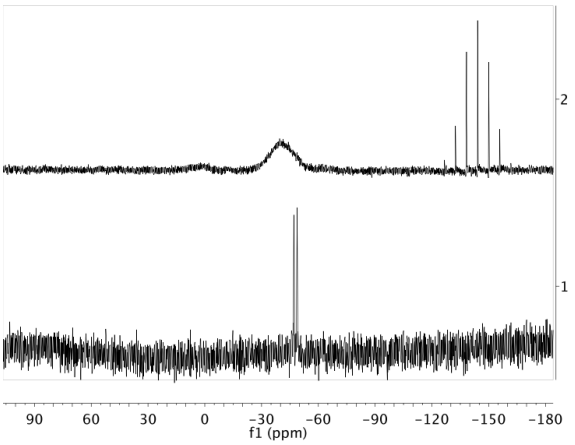

Figure 3. Top: ^{31}P NMR spectrum of $[Cu(MPPE)_2]PF_6$ (**5**). Bottom: ^{31}P NMR spectrum of $[Cu(MPPE)_2]PF_6$ after reaction with KCN. The doublet ($J_{P\text{-}H}$ = 210 Hz)* corresponds to the free MPPE ligand.

Scheme 8. Demetallation of Cu(I) complex **11** using KCN.

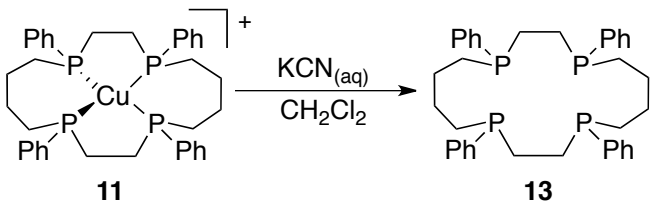

11 **13**

* $J_{P\text{-}H}$ = 210 Hz from authentic MPPE sample

2.3.5. ^{31}P-DOSY Trials

In addition to mass spectra, ^{31}P diffusion ordered spectroscopy (DOSY) was investigated as a method to differentiate between a small ring and macrocyclic product based on their diffusion rate through solution. Recently, a method of using DOSY to analyze a variety of phosphine compounds using ^{31}P NMR spectroscopy was developed.[20,21] A method for using DOSY to differentiate sizes of macrocycles has been established in conjunction with the CAMCOR NMR facility at University of Oregon and the University of Oregon Chemistry Department. The method has been developed on a 600 MHz NMR spectrometer equipped with a multichannel cryoprobe, capable of ultra-sensitive detection and enhanced signal/noise ratios.

We are interested in measuring the diffusion coefficients of a variety of phosphorus containing molecules in order to gain information about the relative size of unknown molecules. In this regard, we have altered existing pulse sequences within the Bruker TopSpin 3.2 software for ^{31}P DOSY tests (specifically, the "ledbpgp" and "stegp" pulse sequences, which are set up initially for ^{1}H DOSY experiments).

We have used these modified pulse sequences to look at a variety of phosphines. In one experiment, we looked at a different bio-related phosphines, specifically adenosine triphosphate, pyrophosphate, and inorganic phosphate in water (D_2O). In the experiment, we were able to easily distinguish each molecule based on their relative diffusion coefficient. An advantage of using ^{31}P NMR is

the fact that most ^{31}P signals are easily distinguishable from one another and do not overlap, a significant benefit for DOSY experiments.

To test this, a mixture of inorganic phosphate, pyrophosphate, and ATP was prepared in D_2O. The initial spectra showed good separation between the three species (Figure 4).

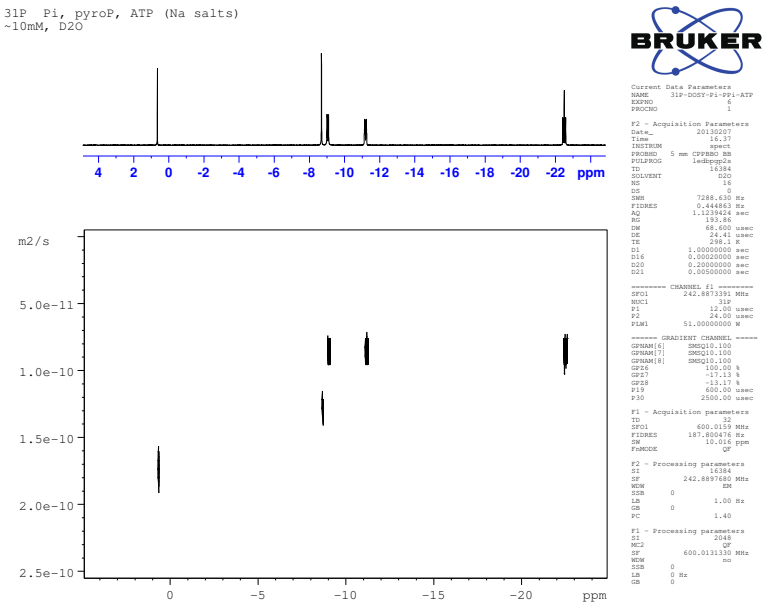

Figure 4. ^{31}P-DOSY spectrum of phosphate (0.5 ppm), pyrophosphate (-8.5 ppm), and ATP (-9.1, -11.2, -22.5 ppm).

Our goal was to use our DOSY technique to help distinguish between small ring phosphines and macrocyclic phosphines. Thus, after removal of the copper(I) metal center, DOSY can distinguish between formation of a small ring or a macrocyclic product; this method can be complimentary to mass spectrometry. To do this, a "calibration curve" was made using phosphines of varying mass and plotting the log of the diffusion coefficient (see Appendix A)

versus the log of the formula weight of the compound. With this, an unknown phosphine's formula weight (and thus, whether it is a small ring or macrocycle) can be obtained from the compound's diffusion coefficient. A calibration curve was prepared using triphenylphosphine (MW=262.29 g/mol), 1,1-bis[(diphenyl)phosphino]methane (MW=384.39 g/mol), and tris[2-(diphenylphosphino)ethyl]phosphine (TETRAPHOS-2, MW=670.62 g/mol) (Figure 5).

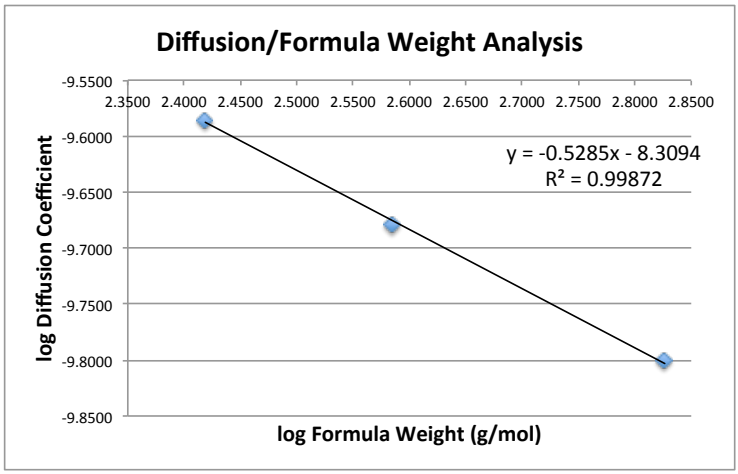

Figure 5. Calibration curve for formula weight analysis using ^{31}P-DOSY NMR spectroscopy.

The method developed was then used with a sample of phosphine **13** with a mixture of triphenylphosphine and TETRAPHOS-2 used in the calibration study (Figure 6). Phosphine **13** has a slower diffusion coefficient, indicating that it is probably a larger species in solution than TETRAPHOS-2 and triphenylphosphine. Also, all the peaks for the macrocycle trend together, which supports the fact that the other peaks are for other isomers of the macrocycle and not a small ring product.

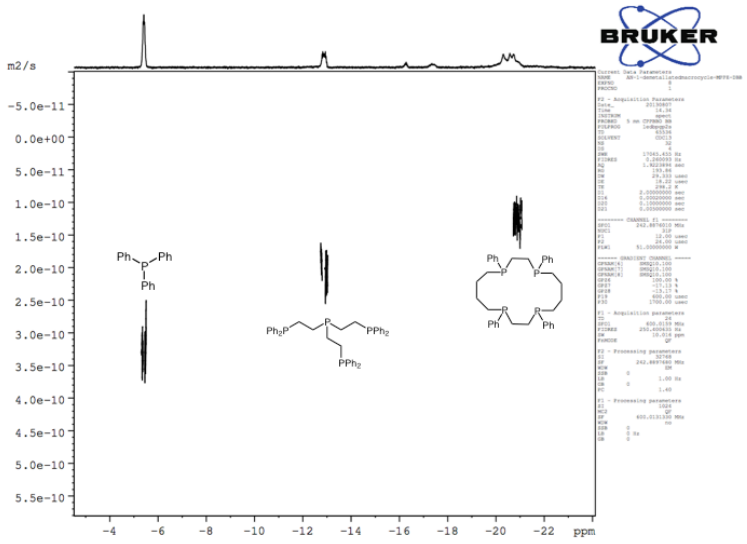

Figure 6. ^{31}P-DOSY spectrum of **13** with triphenylphosphine and TETRAPHOS-2.

2.3.6. Coordination Chemistry

A dichloromethane solution of the free ligand (**12**) was added to a suspension of anhydrous $CoCl_2$ in dichloromethane. The solution immediately turned dark green and the resulting product was obtained as a green powder, postulated to be Co(**12**)Cl_2. The green product had broad ^{1}H NMR signals and no ^{31}P NMR signal, consistent with a paramagnetic species. The product showed a single peak in the ESI-MS at a *m/z* of 694 amu, consistent with $[M\text{-}Cl]^+$; The isotope pattern of the peak at 694 is also consistent with $[M\text{-}Cl]^+$ (see Appendix A). There are no peaks in the mass spectrum corresponding to $[Co(\mathbf{12})]^{2+}$, indicating that the complex may have one bound chloride and one free chloride, giving a square pyramidal five-coordinate species. The electronic spectrum has a similar shape as other relevant $[Co(P)_4Cl]X$ (P = a phosphine) complexes with two absorption maxima at 681 and 589 nm, indicating that the complex may has a solution

structure of five-coordinate [Co(**12**)Cl]Cl (see Table 2). This type of complex is often seen with tetraphosphorus cobalt(II) complexes. Similar complexes have been found to have a five-coordinate structure with one ionic halogen.[22-26] In one example, 1,3-bis(dimethylphosphino)propane (dmpp) was added to CoI_2 and the resulting product was insoluble, crashing out of solution and characterized as $[Co(dmpp)_2I]I$.[27]

Table 2. Comparison of other $[Co(P)_4Cl]X$ complexes.

Complex	λ_{max} (ε)
[Co(**12**)Cl]Cl	589 (78), 681 (117)
$[Co[QP]_2Cl]Cl$*[27]	588 (sh), 685 (sh)
$[Co(PPh(OEt)_2)_4Cl]BPh_4$ [22]	588 (570), 630 (490)
$[Co(dmpp)_2Cl]BPh_4$ [28]	610 (419), 690 (319)
$[Co(MC)_2Cl][CoCl_4]$ [23]	575 (240), 675 (400)
$[Co(dppp)_2Cl]Cl$ [29]	600 (600), 680 (730)

* Trigonal pyramidal geometry
QP = tris-(o-diphenylphosphinophenyl) phosphine
dmpp = 1,3-bis(dimethylphosphino)propane
MC = Macrocycles with two phosphorus atoms, acting as a bidentate ligand

2.3.7. Computational Work

In addition to the experimental observations, initial calculations were run by E. Adrian Henle to determine whether or not the double chelate small ring or the macrocycle would be more favored energetically on copper(I), as well as the relative energies of the possible isomers of a macrocyclic phosphine complex (Scheme 9). A copper(I) complex bearing two 1,2-bis(phosphino)ethane ligands was chosen as a model complex (**14**). The calculations showed that it is more energetically favorable by 5.23 kcal/mol to have the

first alkylation form an open-chain tetradentate ligand coordinated to copper (**16**) versus a coordinated eight-membered bidentate ring (**15**). The calculations also found that the *RSRS* (**17e**) stereochemistry of the macrocyclic ligand on copper is favored by a over 10 kcal/mol over any other ones (**17a-d**), consistent with the X-ray structure obtained (see Figure 2 above). A more detailed discussion of the possible stereochemistries of a coordinated macrocycle is included in Chapter IV.

Scheme 9. A model macrocyclic copper(I) complex used for calculations of the relative energies for a double-chelate vs. macrocycle reaction, and the stereochemistries of possible macrocyclic complexes.

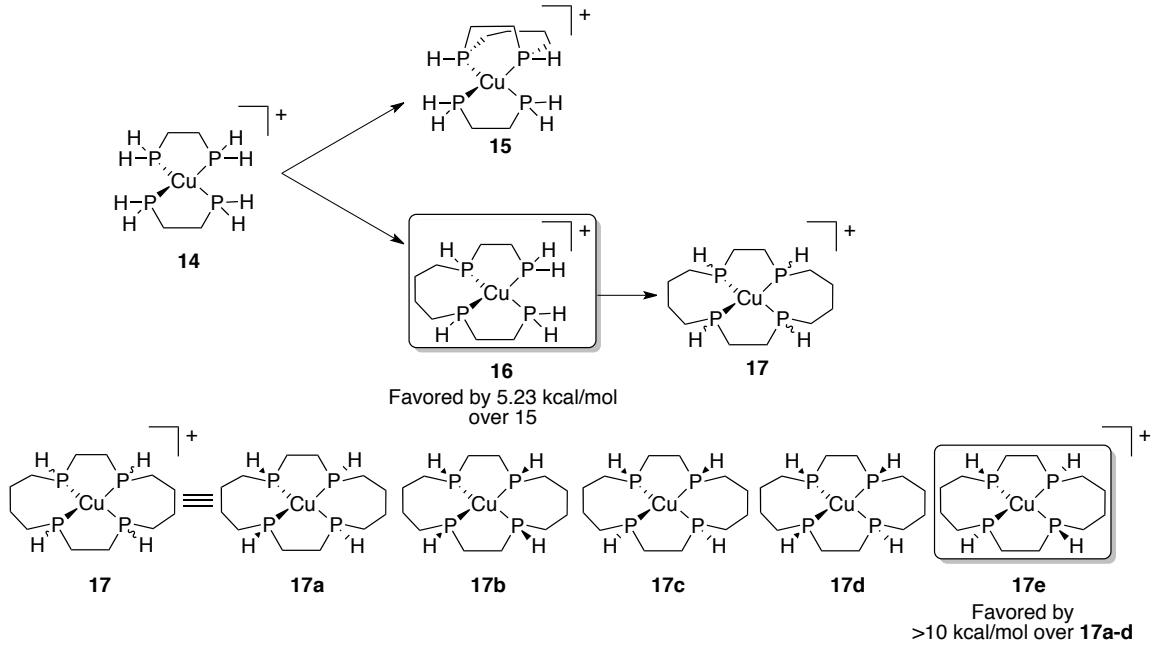

2.4. Conclusions

Tetraphosphine macrocycles may be considered one of the most difficult classes of compounds to synthesize. A solution to this is to use Cu(I) as a template metal using two bis-bidentate secondary phosphines as a precursor to macrocyclic phosphines.

$Cu(P_2)_2^+$ templates can be bridged with various dihalides in the presence of a base to yield macrocyclic Cu(I) complexes. Reaction with aqueous cyanide affords the free phosphine. This ligand can be used with other transition metals of interest, which can potentially be useful in a pressure-swing absorption nitrogen rejection scheme.

2.5. Bridge

Chapter II described how $Cu(P_2)_2^+$ complexes are a viable route toward tetraphosphine macrocycles. Chapter III describes how $Cu(DHMPE)_2^+$ (DHMPE = 1,2-bis[(dihydroxymethyl)phosphino]ethane), a complex that was thought to be a potential starting material for preparing tetraphosphine macrocycles through a phosphorus Mannich reaction, crystallizes as a dimer in the solid state but ^1H DOSY experiments show the complex is monomeric in solution.

CHAPTER III

SYNTHESIS OF THE HYDROPHILIC PHOSPHINE COMPLEX $Cu(DHMPE)_2^+$ FROM COPPER(I) CHLORIDE (DHMPE = 1,2-BIS[(DIHYDROXYMETHYL)PHOSPHINO]ETHANE, A WATER-SOLUBLE BIDENTATE PHOSPHINE)

Some of this work has been previously published and is reproduced with permission from: Nell, B. P.; Swor, C. D.; Zakharov, L. N.; Tyler, D. R. *Polyhedron*, **2012**, *45*, 30-34.

3.1. Introduction

Copper(I) phosphine complexes have potential biomedical applications as anti-cancer drugs[1-5] and as PET imaging reagents.[6,7] Especially attractive for these purposes are Cu(I) complexes containing water-soluble phosphine ligands. When researchers synthesize such complexes, they typically begin with halide-free copper starting materials, such as $CuOTf{\cdot}C_6H_6$ or $Cu(MeCN)_4PF_6$. For example, the water-soluble copper phosphine complex $[Cu(DHMPE)_2]^+$ (DHMPE = 1,2-bis[(dihydroxymethyl)phosphino]ethane) was prepared by the reaction of $[Cu(CH_3CN)_4]PF_6$ and DHMPE (The complex possesses antitumor activity comparable to cisplatin[5]). CuCl would be a cheaper and more easily obtained starting material but the problem is that terminal or bridging halide ligands complicate the coordination chemistry of bidentate phosphines with Cu(I). Examples of the types of products that can form with

bidentate ligands and halides are shown in Figure 1.[8-13] The main disadvantage of the halide-free starting materials is their high cost compared to simple copper salts, being up to 100 times more expensive than copper(I) chloride.

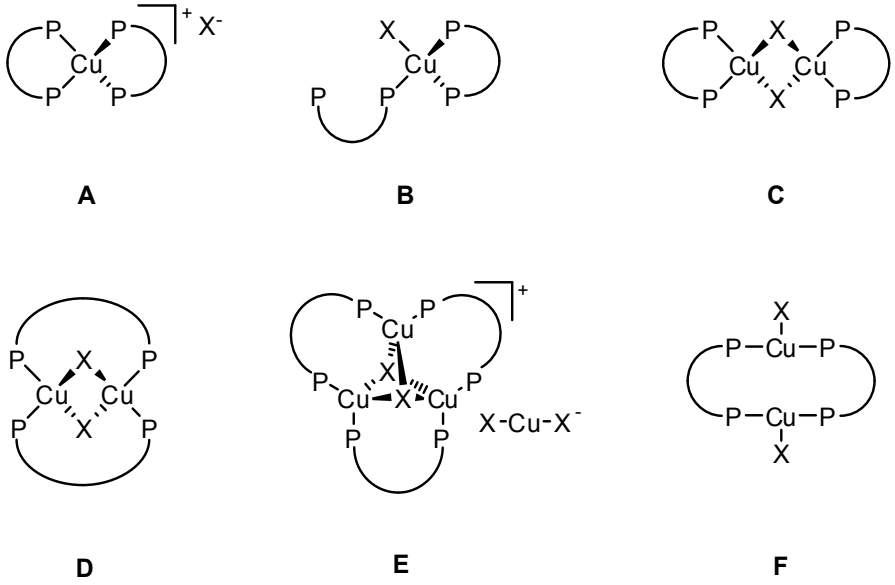

Figure 1. Structures of copper(I) halide complexes with bidentate phosphine ligands.

In this chapter, we report a convenient synthesis of $Cu(DHMPE)_2^+$, with either halide or PF_6^- counteranions, from CuCl in methanol. The ability to use a cheap source of Cu(I) as the starting material should help to spur development of water-soluble Cu-phosphine complexes. It is noted that CuCl has been used previously for the generation of $Cu(DHMPE)_2Cl$; however, the complex was obtained only as an oil and limited spectroscopic data were reported.[3]

3.2. Experimental

3.2.1. Materials and Reagents

Unless otherwise noted, all experimental procedures were performed under an N_2 atmosphere using standard Schlenk and glovebox techniques. Commercially available reagents were used as received. HPLC-grade THF was dried and deoxygenated by passing through commercial columns of CuO, followed by alumina under an argon atmosphere. Deuterated solvents were obtained from Cambridge Isotope Laboratories and degassed using three freeze-pump-thaw cycles.

1,2-bis[(dihydroxymethyl)phosphino]ethane (DHMPE)[14], tris(hydroxymethyl)phosphine (thp)[15], and $Cu(thp)_4PF_6$[5] were synthesized according to literature methods. The complex $Cu(DHMPE)_2Cl$ was prepared by a modified literature synthesis.[3]

3.2.2. Instrumentation

NMR spectra were obtained on a Varian Unity/Inova 500 spectrometer operating at a frequency of 500.62 MHz (^1H) or 202.45 MHz (^{31}P). The ^1H and ^{13}C NMR spectra were referenced to residual solvent peaks, and the ^{31}P NMR spectra were referenced to external 1% H_3PO_4 in D_2O. ESI mass spectra were obtained using a Thermo Finnigan LCQ Deca XP Plus ESI Mass Spectrometer using CH_3OH as the solvent. Infrared spectra were recorded using a Thermo-Scientific Nicolet 6700 FT-IR spectrometer.

3.2.3. X-ray Crystallography

Diffraction intensities for $[Cu_2(DHMPE)_4]Cl_2$ were collected at 173(2) K on a Bruker Apex CCD diffractometer using MoKα radiation λ=0.71073 Å. Space groups were determined based on systematic absences. Absorption corrections were applied by SADABS. The structure was solved by direct methods and Fourier techniques and refined on F^2 using full matrix least-squares procedures. All non-H atoms were refined with anisotropic thermal parameters. The H atoms were treated in calculated positions and refined in a rigid group model, except the H atoms in terminal –OH groups involved in H-bonds which were found on the residual density map and refined with isotropic thermal parameters and with restrictions; the O-H distance of 0.97 Å was used in the refinement as a target for the corresponding O-H bonds. One of the CH_2OH groups in $[Cu_2(DHMPE)_4]Cl_2$ is disordered over two positions in the ratio 0.77/0.23. The H atom at the O atom in the disordered CH_2OH group was refined in the calculated position in a rigid group model. The H atom at the O atom in the solvent CH_3OH molecule was not found and has not been taken into consideration in the refinement. All OH groups in the cation together with the solvent methanol molecule and the Cl anion form in the crystal structure of $[Cu_2(DHMPE)_4]Cl_2$ a network of H-bonds. All calculations were performed by the Bruker SHELXTL (v. 6.10) package.

3.2.4. Methods

Synthesis of $Cu_2(DHMPE)_4Cl_2$. CuCl (0.128 g, 2.34 mmol) was added to a solution of DHMPE (0.551 g, 4.67 mmol) in 30 mL MeOH. The reaction was stirred for

1.5 h at room temperature, and the solvent was removed *in vacuo* yielding $Cu_2(DHMPE)_4Cl_2$, a white, air-stable solid. Yield: 0.584 g (86%). $^{31}P\{^1H\}$ NMR (D_2O): δ +10.6 ppm (brd). ^1H NMR (D_2O): δ 1.99 (s, 8H, -C*H*$_2$OH), 4.16 (m, 16H, -C*H*$_2$C*H*$_2$-). ^{13}C NMR (D_2O): δ 19.74, 59.32. ESI-MS: 491 amu (m+). IR (ATR, cm^{-1}): 3350-3000 (s), 2897 (m), 2831 (w). Single crystals suitable for X-ray diffraction were grown by slow evaporation of a methanol solution. Anal. Calcd for $C_{12}H_{32}ClCuO_8P_4$: C, 27.33; H, 6.12; P, 23.50. Found: C, 27.31; H, 6.19; P, 23.43.

Synthesis of $Cu(DHMPE)_2PF_6$. CuCl (0.065 g, 0.66 mmol) was added to a suspension of DHMPE (0.270 g, 1.26 mmol) in 30 mL THF. To this suspension was added $NaPF_6$ (0.111 g, 0.66 mmol). The reaction was stirred for 1.5 h at room temperature, and the solvent was removed *in vacuo,* yielding an inseparable mixture of $Cu(DHMPE)_2PF_6$ and NaCl as a white, air-stable solid. $^{31}P\{^1H\}$ NMR (D_2O): δ +10.0 ppm (brd), -145 ppm (septet, PF_6). ^1H NMR (D_2O): δ 1.99 (s, 8H, -C*H*$_2$OH), 4.16 (m, 16H, -C*H*$_2$C*H*$_2$-). ^{13}C NMR (D_2O): δ 13.74, 59.32. ESI-MS: 491 amu (m+).

3.3. Results and Discussion

Our initial aim was to prepare $Cu(DHMPE)_2^+$ using CuCl. Copper(I) chloride and DHMPE reacted in methanol within minutes at room temperature (Eq. 1). The ^{31}P NMR spectrum of the product showed a broad doublet at +12 ppm, consistent with coordination of the phosphine to Cu(I).[16-18] The signal was broadened due to coupling of the phosphorus nuclei with the quadrupolar copper nuclei (^{63}Cu and ^{65}Cu).[19,20] In some

copper(I)-phosphine complexes, the ^{31}P-^{63}Cu coupling can be fully resolved into a quartet by raising the temperature;[16,18,20,21] however, in this case the signal for the product (shown below to be $Cu(DHMPE)_2^+$) remained a broad peak in D_2O, even at 90° C. Thus, ^{31}P NMR spectroscopy was not an effective method for structurally characterizing the product.

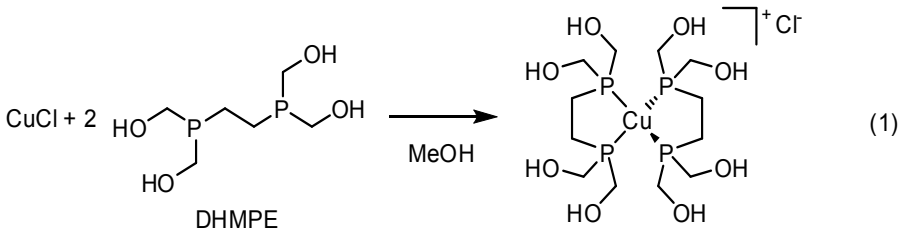

(1)

Slow evaporation of a methanol solution containing the product gave single crystals suitable for X-ray diffraction. The product was a phosphine-bridged dimer, $[Cu_2(DHMPE)_4]Cl_2$ (Figure 2). The molecule is centrosymmetric (C_i symmetry), with each copper atom bearing one terminal bidentate phosphine ligand. Two bidentate phosphine ligands bridge between the two copper atoms, forming a 10-membered ring. The bridging ligands are in an extended conformation (P-C-C-P torsion = 166.5(2)°), in contrast to the *gauche* conformation of the terminal phosphine ligands (P-C-C-P torsion = 51.3(3)°). The copper coordination sphere is distorted tetrahedral, with the P1-Cu-P2 (terminal phosphine) plane intersecting the P3-Cu-P4 (bridging phosphines) plane at 87.3°. One of the hydroxymethyl groups in each asymmetric unit (2 per molecule) is disordered. Two molecules of methanol per Cu dimer are present as solvents-of-crystallization. A three-dimensional hydrogen-bonding network exists among molecules of the complex, methanol, and the chloride counterions (See appendix). A phosphine-bridged Cu(I) dimer of this type has only been observed once before, with the

hydrophobic ligand dimethylphosphinoethane (DMPE).[21] In this case, the counteranion was the weakly-coordinating BF_4^-. (The $Cu(DMPE)_2^+$ monomer has also been synthesized and structurally characterized by X-ray crystallography with $[Cu(CoCO_4)_2]^-$ and $[CpTi(SCH_2CH_2S)_2]^-$ as the counterions.[22,23])

The ^{31}P NMR spectrum of the $Cu_2(DHMPE)_4Cl_2$ crystals dissolved in D_2O is a broad singlet, similar to that of the reaction solution described above. The spectrum did not have sufficient resolution to determine whether the species in solution was a dimer or the monomer.

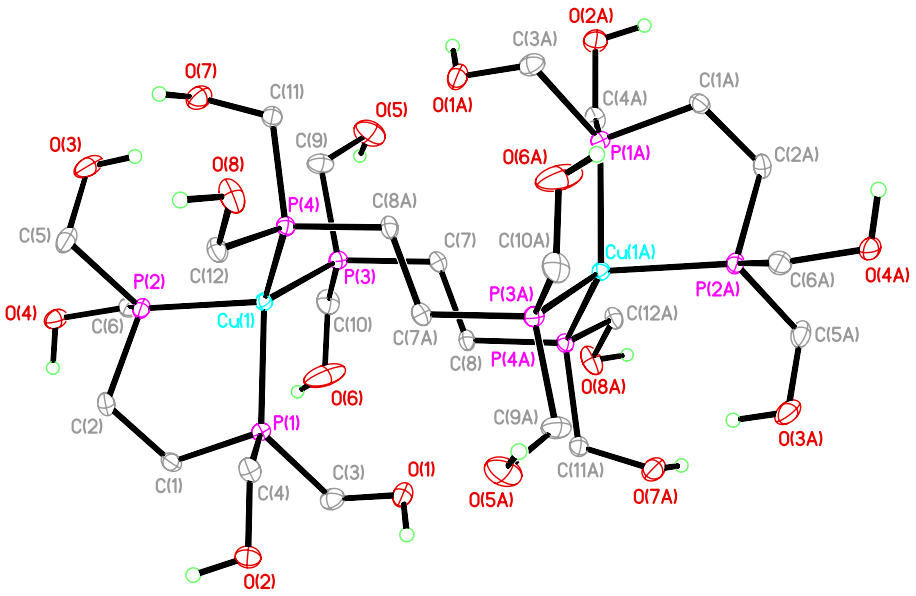

Figure 2. An ORTEP view of the cation in $Cu_2(DHMPE)_4Cl_2$ with thermal ellipsoids at the 30% level. Only H atoms in -OH groups and only one position for the disordered -O(6)H atom are shown for clarity. Symmetry code (A): -x,-y,-z.

It is interesting to compare the crystal structures of $[Cu_2(DHMPE)_4]Cl_2$ and $[Cu_2(DMPE)_4](BF_4)_2$. (Figure 3). Both structures display very similar conformations in

terms of bite angles, orientation of the 10-membered Cu_2(bisphosphine)$_2$ ring, etc. Table 1 shows a comparison of selected bond lengths, angles, and torsions in the two complexes. A few slight differences are noticeable between the two complexes: all Cu-P bond lengths are slightly shorter in the DHMPE complex; most P-C bond lengths are shorter with DHMPE (with the exception of the backbone P-C bonds of the bridging phosphines); and the backbone C-C bonds are longer in the DHMPE complex.

The bite angle of the terminal DHMPE ligand (88.59°) is slightly less than DMPE (89.2°), as is the P-Cu-P angle between the bridging phosphines (108.29° vs. 110.7°). All other P-Cu-P angles are slightly larger for the DHMPE complex than for the DMPE complex. Thus, the tetrahedral geometry of the Cu(I) ions in $[Cu_2(DHMPE)_4]Cl_2$ is more distorted than in $[Cu_2(DMPE)_4](BF_4)_2$.

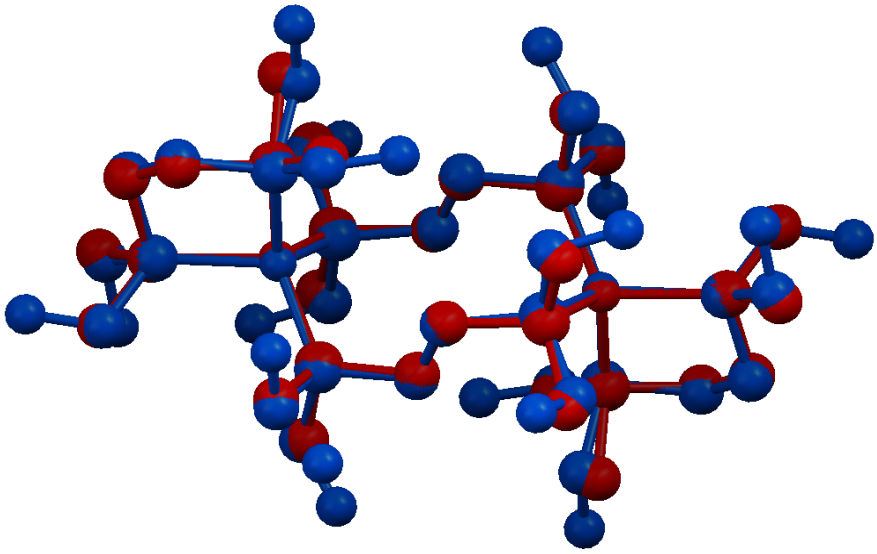

Figure 3. Overlaid structures (ball and stick models) of $[Cu_2(DHMPE)_4]^{2+}$ (blue) and $[Cu_2(DMPE)_4]^{2+}$ (red).

Table 1. Comparison of crystal data, bond lengths (Å) and angles (°) for $Cu_2(DHMPE)_4Cl_2$ and $[Cu_2(DMPE)_4](BF_4)_2$.

				$[Cu_2(DHMPE)_4]Cl_2$	$[Cu_2(DMPE)_4](BF_4)_2$[21]	Diff.
Counterion				Cl^-	BF_4^-	
Crystal System				Monoclinic	Triclinic	
Space Group				C2/c	P	
Solvent of Crystallization				MeOH	(none)	
Cu-P Bonds		Terminal	Cu-P1	2.279 (1)	2.289 (1)	0.009
			Cu-P2	2.265 (2)	2.293 (1)	0.028
		Bridging	Cu-P3	2.248 (1)	2.267 (1)	0.018
			Cu-P4	2.259 (1)	2.263 (1)	0.004
P-C Bonds	Terminal	PCCP	P1-C1	1.837 (4)	1.833 (3)	-0.004
			P2-C2	1.832 (4)	1.831 (3)	-0.001
		$P-CH_2X$ (X = H, OH)	P1-C3	1.845 (4)	1.817 (3)	-0.028
			P1-C4	1.839 (4)	1.819 (4)	-0.020
			P2-C5	1.834 (4)	1.822 (4)	-0.012
			P2-C6	1.834 (4)	1.813 (4)	-0.021
	Bridging	PCCP	P3-C7	1.827 (4)	1.835 (2)	0.008
			P4-C8	1.832 (4)	1.839 (2)	0.007
		$P-CH_2X$ (X = H, OH)	P3-C9	1.835 (4)	1.819 (3)	-0.016
			P3-C10	1.845 (4)	1.812 (3)	-0.033
			P4-C11	1.844 (4)	1.813 (4)	-0.031
			P4-C12	1.823 (4)	1.815 (4)	-0.008
C-C Bonds		Terminal	C1-C2	1.537 (5)	1.525 (4)	-0.012
		Bridging	C7-C8	1.527 (5)	1.521 (4)	-0.006
Bond Angles			P1-Cu-P2†	88.59 (4)	89.2 (1)	0.59
			P3-Cu-P4‡	108.29 (4)	110.7 (1)	2.44
			P1-Cu-P3	118.08 (5)	116.9 (1)	-1.21
			P1-Cu-P4	114.03 (4)	113.2 (1)	-0.85
			P2-Cu-P3	112.14 (4)	110.3 (1)	-1.86
			P2-Cu-P4	114.83 (4)	115.1 (1)	0.32
P-C-C-P Torsions		Terminal	P1-C1-C2-P2	51.3 (3)	54.8	3.51
		Bridging	P3-C7-C8-P4	166.5 (2)	168.9	2.39

†Terminal ligand bite angle. ‡Bridging ligand "bite angle".

Because only one other phosphine-bridged Cu(I) dimer of this type has been structurally characterized, the reasons for formation of a dimer instead of a CuP_4^+ monomer are not understood. It is conceivable that formation of the dimer may have something to do with crystallization conditions or the properties of the anion; however, because $[Cu_2(DHMPE)_4]Cl_2$ contains a different type of anion than $[Cu_2(DMPE)_4](BF_4)_2$, as well as a hydrophilic, hydrogen-bonded environment instead of a hydrophobic one, this explanation seems doubtful. The explanation may lie instead in the relative stabilities of the rings and their conformations. Clearly, the formation of a flexible ten-membered ring (formed in this case by the two Cu^+ ions and the two bridging phosphines) is entropically disfavored, in contrast to the more stable five-membered chelate rings that would be present in a monomeric structure. However, inspection of the dimer structure reveals two conformational advantages of the dimeric form over a CuP_4^+ monomer. First, the terminal phosphines have a small (<90°) bite angle, which is significantly less than the 109.5° P-Cu-P angle of an ideal tetrahedral complex. Formation of the phosphine-bridged dimer removes one of these strained chelate rings, allowing for less distortion of the tetrahedral coordination geometry. Second, the bridging phosphine ligands are in a fully extended conformation, with favorable *anti* P-C-C-P torsion angles, as opposed to the energetically disfavored *gauche* conformation of a terminal bridging ligand. These factors, along with possible intermolecular and crystal packing interactions (such as the extended hydrogen-bonding network), might accumulate to favor crystallization of the dimer over the monomer.

To fully characterize the solution-state structure of the complex, a ^{1}H DOSY experiment was carried out to determine the size of the complex in solution relative to the model complex $Cu(thp)_4^+$ complex (thp = tris(hydroxymethyl)phosphine). This latter complex is monomeric and is expected to have a similar hydrogen-bonding environment to the $Cu(DHMPE)^+$ complex.[5] (The ^{1}H DOSY experiment yields diffusion coefficients so the comparison is able to distinguish between a monomeric or dimeric solution structure for the $Cu(DHMPE)^+$ complex.) The ^{1}H DOSY experiment of a mixture of both CuP_4^+ complexes in D_2O showed that the diffusion coefficients for both complexes were very similar, which strongly suggests that the $Cu(DHMPE)^+$ complex has a similar hydrodynamic radius as the model complex and is monomeric in D_2O. In addition, methanol solutions of the $Cu(DHMPE)^+$ complex were analyzed by ESI mass spectrometry. Positive-mode ESI-MS showed a single ion at m/z = 491. This may correspond to either the monomeric $Cu(DHMPE)_2^+$ ion (structure A in Figure 1) or the dimeric $Cu_2(DHMPE)_4^{2+}$ ion. Both of these ions correspond to m/z = 491, but the isotope pattern allows a distinction. As shown in Figure 4, the isotope pattern corresponds to that of the monomer, $Cu(DHMPE)_2^+$. Moreover, the absence of the half mass peaks shown in the theoretical dimer spectrum is evidence that the complex can exist as a monomer in the gas phase.

In contrast to the synthesis of $Cu(DHMPE)_2^+$ in methanol, the synthesis of the complex in THF did not proceed when CuCl and DHMPE were reacted (Eq. 2). However, addition of a halide abstractor such as $NaPF_6$ or NaOTf resulted in complete conversion to $Cu(DHMPE)_2^+$ (Eq. 3), as indicated by ^{31}P NMR. The reaction in this case

presumably occurs by initial chloride abstraction, generating solvated Cu^{+} ions, which are then easily coordinated by the phosphine. The reaction is driven to completion by precipitation of NaCl. Unfortunately, it was experimentally impossible to separate the NaCl from the $[Cu(DHMPE)_2]PF_6$ due to similar solubilities, and so THF is not recommended as the reaction solvent.

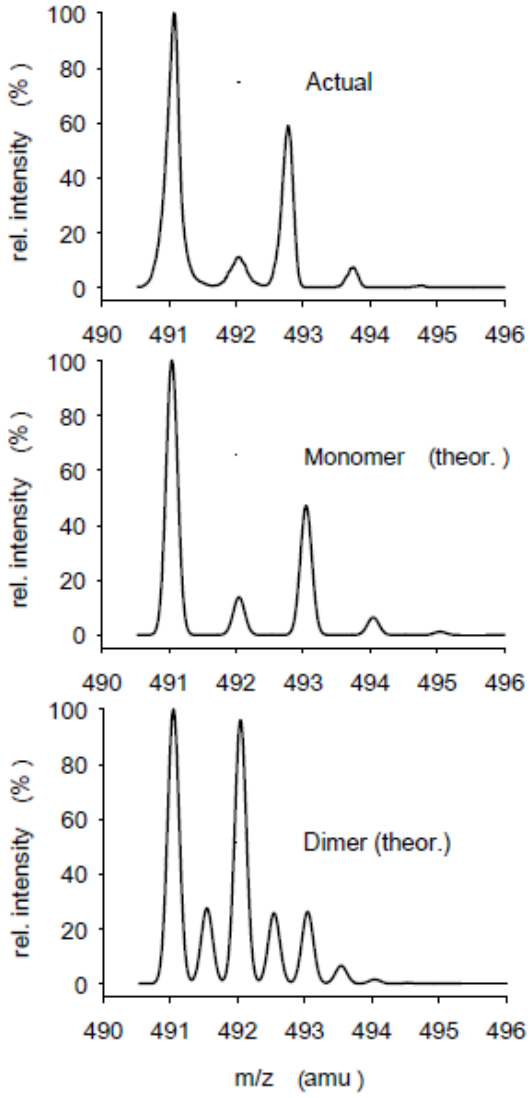

Figure 4. ESI-MS of $Cu(DHMPE)_2Cl$.

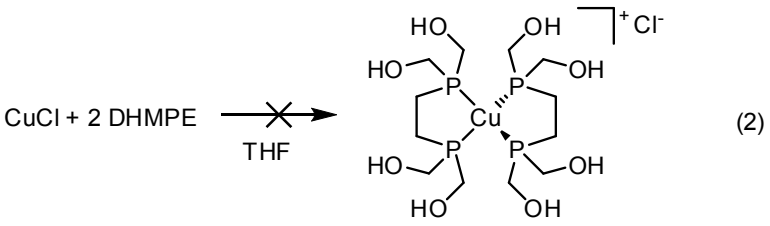

(2)

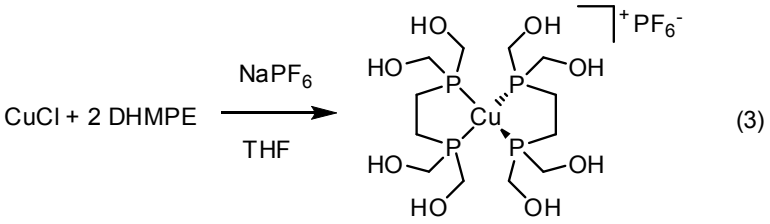

(3)

3.4. Conclusions

The reaction of CuCl with DHMPE in methanol is an efficient synthetic route to the water-soluble copper(I) phosphine complex $Cu(DHMPE)_2Cl$. The advantage of the synthetic method is that relative cheap CuCl is used as the starting material rather than higher priced Cu(I) salts. The $Cu(DHMPE)_2Cl$ complex crystallizes as a phosphine-bridged dimer but ^1H DOSY experiments suggest the complex is a monomer in solution. The crystal structure of the dimer shows a striking resemblance to the one other phosphine-bridged dimer, $[Cu_2(DMPE)_4](BF_4)_2$, even though the $Cu(DHMPE)_2^+$ unit is hydrophilic instead of hydrophobic. In a general sense, phosphine-bridged dimers need to be considered when attempting to characterize copper(I)-bisphosphine complexes.

3.5. Bridge

Chapter III described an interesting duality between a Cu(I) phosphine complex that is monomeric in solution and dimeric in the solid-state. Chapter IV continues to use

Cu(I) and will describe a method using a Cu(I) tetradentate phosphine complex as a template for generating tetra-phosphorus macrocycles.

CHAPTER IV

SYNTHESIS OF TETRAPHOSPHINE MACROCYCLES USING A COPPER(I) TEMPLATE WITH A TETRADENTATE PHOSPHINE

Parts of Chapter IV contains experimental work performed by AN, and have been prepared for Nell, B. P.; Nathan, A.; Tyler, D. R.; *manuscript in preparation*.

4.1. Introduction

Chapter II focused on using copper(I) as a template metal with two bidentate secondary phosphines to prepare tetraphosphine macrocycles. The main drawback to that approach is the possibility of synthesizing a bidentate small ring phosphine as opposed to the large ring macrocycle that is desired (Scheme 1, top). This possible product can be avoided completely by using an open chain tetradentate ligand that has two reactive P-H bonds at the end of the chain that, after coordination to a template metal ion, can be bridged by some bifunctional moiety to selectively give a macrocycle; there is no possible way to make a small ring product (Scheme 1, bottom).

Scheme 1. Template syntheses for preparing tetraphosphorus macrocycles.

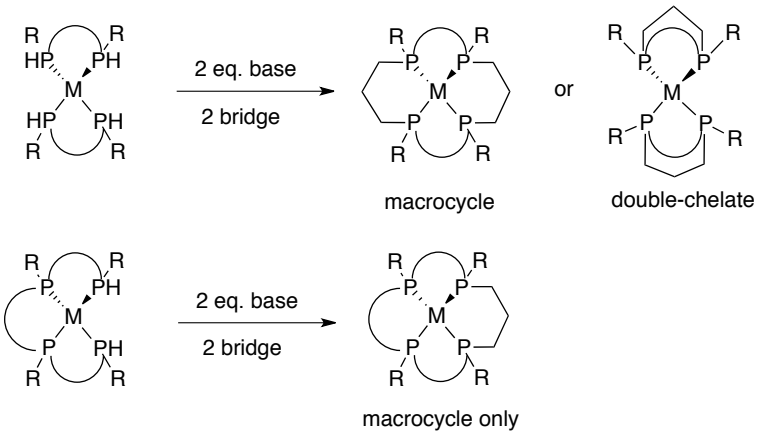

In this chapter, we report a general method for preparing tetraphosphine macrocycles from an open-chain tetradentate phosphine ligand using Cu(I) as a template. The method is a combination of prior reports that show i) Ni(II) can template the formation of a macrocyclic tetradentate phosphine from an open-chain tetradentate phosphine (Scheme 2),[1,2] and ii) Cu(I) templates can be removed facilely using cyanide or H_2S (Scheme 3).[3,4]

Scheme 2. DelDonno's method for preparing tetraphosphine macrocycles.[1]

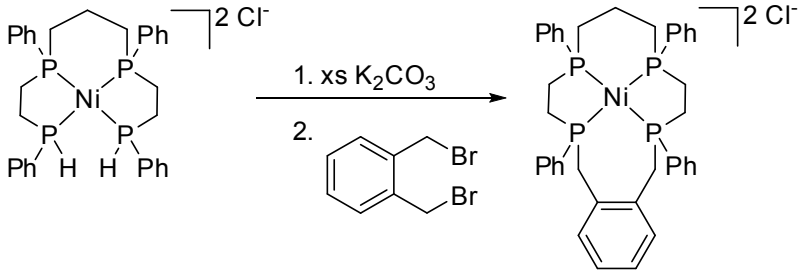

Scheme 3. Examples of template syntheses using Cu(I).[3,4]

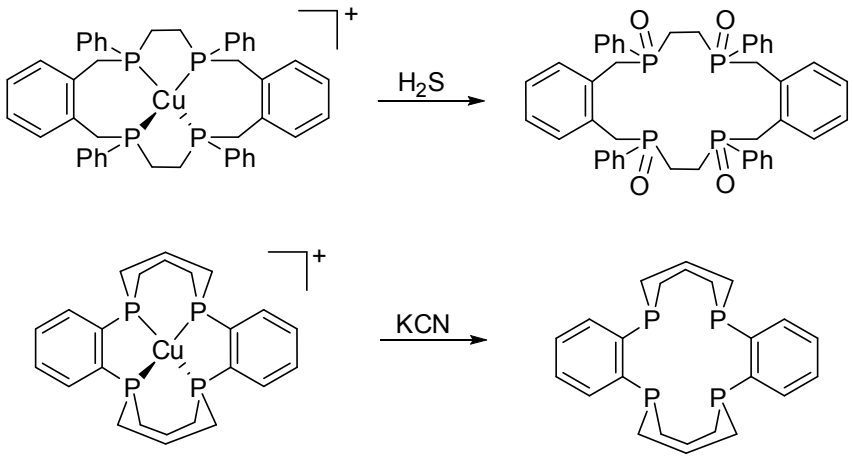

4.2. Experimental

4.2.1. Materials and Reagents

Unless otherwise noted, all experimental procedures were performed under an inert (N_2) atmosphere, using standard Schlenk and glovebox techniques. Commercially available reagents were used as received. HPLC-grade THF was dried and deoxygenated by passing through commercial columns of CuO, followed by alumina under an argon atmosphere. Deuterated solvents were obtained from Cambridge Isotope Laboratories and degassed using three freeze-pump-thaw cycles. The ligand MPPP and **3**[5] were synthesized according to literature methods. $[Cu(CH_3CN)_4]OTf$ was prepared from a modified procedure.[6]

4.2.2. Instrumentation

Air-sensitive NMR samples were sealed in N_2 filled J-Young tubes. NMR spectra were obtained on either a Varian Unity/Inova 300 spectrometer at an operating frequency

of 299.94 (^{1}H) and 121.42 (^{31}P) or a Varian Unity/Inova 500 spectrometer operating at a frequency of 500.62 MHz (^{1}H) or 202.45 MHz (^{31}P). The ^{1}H and ^{13}C NMR spectra were referenced to residual solvent peaks, and the ^{31}P NMR spectra were referenced to external 1% H_3PO_4 in D_2O. ESI mass spectra were obtained using a Thermo Finnigan LCQ Deca XP Plus ESI Mass Spectrometer using THF or CH_3CN as the solvent. Infrared spectra were recorded using a Thermo-Scientific Nicolet 6700 FT-IR spectrometer. UV-Vis spectra were collected on an Agilent 8453 spectrophotometer. Elemental analyses were performed by Complete Analysis Laboratories, Inc., Parsippany, NJ.

4.2.3. Methods

Synthesis of isopropyl allyl(phenyl)phosphinate (1). Allyl bromide (6.0132 g, mmol) was added to a 50 mL Schlenk flask containing diisopropyl phenylphosphonite (5.0193 g, mmol) and the mixture heated to 70 °C for 12 hr. After heating, the product was distilled under reduced pressure (85-90 °C @ 250 mTorr) to yield a clear oil. Yield: 4.9094 g (96.7 %). ^{31}P NMR ($CDCl_3$): δ -38.8 (s). ^{1}H NMR ($CDCl_3$): δ 7.77 (m, 2H), 7.47 (m, 2H), 5.72 (m, -C*H*CH2, 1H), 5.06 (m, 2H), 4.61 (m, 1H), 2.73 (m, 2H), 1.36 (dd, 3H), 1.19 (dd, 3H). ^{13}C NMR ($CDCl_3$): 132.23 (d, J = 2.6 Hz), 131.90 (d, J = 9.6 Hz), 128.44 (d, J = 12.5 Hz), 127.51 (d, J = 9.1 Hz), 120.28 (d, J = 13.0 Hz), 69.88 (d, J = 6.8 Hz), 36.57 (d, J = 97.6 Hz), 26.79 – 21.46 (m).

Synthesis of 2 and 3. Phosphinate **1** (1.5081 g, 6.73 mmol, 2.01 equiv) was added in a 50 mL Schlenk flask with MPPP (0.8731 g, 3.35 mmol, 1.00 equiv). A spatula

tip full of AIBN was added to the reaction mixture. The flask was heated to 80 °C overnight. After heating, all volatiles were removed in vacuo at 100 °C. The product (**2**) was an extremely viscous, clear oil. $^{31}P\{^{1}H\}$ NMR ($CDCl_3$): δ 42.4 (s), -27.2 (d). ^{1}H NMR (300 MHz, $CDCl_3$) δ 7.76 (dt, J = 12.3, 6.7 Hz, 4H), 7.62 – 7.17 (m, 11H), 4.70 – 4.37 (m, 2H), 1.96 (s, 4H), 1.36 (t, J = 6.3 Hz, 6H), 1.16 (dd, J = 6.2, 2.1 Hz, 5H). The product of this reaction was directly carried on to reduction.

Compound **2** was dissolved in diethyl ether and added dropwise to an ice-cooled suspension of $LiAlH_4$ (0.4120 g, 10.86 mmol, 3.24 equiv) in ether. After addition, the reaction mixture was warmed to room temperature and stirred for 12 hr. The reaction was cooled again with an ice-bath and carefully quenched with 0.5 mL H_2O, followed by 0.5 mL 10% NaOH, finally followed by 1.5 mL H_2O. The resulting white precipitate was filtered and the solvent removed *in vacuo* to yield ligand **3** as a clear, viscous oil. Yield: 1.1532 g (61.4 % over two steps). $^{31}P\{^{1}H\}$ NMR ($CDCl_3$): δ -26.7 (s), -53.3 (s), -53.7 (s) ($^{1}J_{P\text{-}H}$ = 210 Hz). ^{1}H NMR ($CDCl_3$): δ 7.79 (m, 8H), 7.66 (m, 12H), 4.46 (d, $^{1}J_{P\text{-}H}$ = 210 Hz, -P*H*, 2H), 1.2-2.4 (m, 20H).

Synthesis of [Cu(3)]OTf (4). Ligand **3** (0.2020 g, 0.360 mmol, 1 equiv) was dissolved in CH_3CN and added dropwise to a stirred solution of $[Cu(CH_3CN)_4]OTf$ (0.1373 g, 0.364 mmol, 1.01 equiv) in CH_3CN. The solution was stirred for 20 minutes at room temperature and the solvent removed *in vacuo* to yield a waxy white solid. The solid was triturated with ether to yield an off-white powder. Yield: 0.2750 g (98.7%).

$^{31}P\{^{1}H\}$ NMR ($CDCl_3$): δ -15 (br), -45 (br). ESI-MS: 623 amu (m+). Anal. Calcd for $C_{34}H_{40}CuF_3O_3P_4S$: C, 52.82; H, 5.21; P, 16.02. Found: C, 52.80; H, 5.18; P, 15.57.

General Method for Macrocyclization of 4. A THF solution of KO^{t}Bu was added dropwise to **4** dissolved in THF and the solution turned a bright yellow color. After stirring for 15 minutes, a THF solution of the corresponding α-ω dihalide was added dropwise. The yellow color faded to a dull yellow color with KBr precipitate. The solution was filtered through a 0.25 micron syringe filter or a celite plug and the solvent removed. The yellow residue was redissolved in CH_2Cl_2 and filtered again. Removal of the solvent yielded a waxy yellow solid that was triturated with ether to yield a yellow powder.

5a: (**4:** (0.6016 g, 0.778 mmol, 1.0 equiv), KO^{t}Bu: (0.1871 g, 1.667 mmol, 2.14 equiv), 1,3-dibromoproane: (0.1571 g, 0.778 mmol, 1.0 equiv)) Yield: 0.3279 g (51.8%). $^{31}P\{^{1}H\}$ NMR ($CDCl_3$): δ -24 (br). ESI-MS: 663 amu ($[m\text{-}OTf]^+$). Anal. Calcd for $C_{37}H_{44}CuF_3O_3P_4S$: C, 54.64; H, 5.45; P, 15.23. Found: C, 54.46; H, 5.52; P, 15.07.

5b: (**4**: 0.0583 g, 0.075 mmol, 1 equiv), KO^{t}Bu: (0.0169 g, 0.151 mmol, 2.01 equiv), 1,4-dibromobutane: (0.0164 g, 0.076 mmol, 1.01 equiv)) Yield: 0.0489 g (78.4%). $^{31}P\{^{1}H\}$ NMR ($CDCl_3$): δ -24 (br). ESI-MS: 677 amu (m+). Anal. Calcd for $C_{38}H_{46}CuF_3O_3P_4S$: C, 55.17; H, 5.60; P, 14.98. Found: C, 54.89; H, 5.63; P, 14.60.

5c: (**4:** 0.0330 g, 0.043 mmol, 1.0 equiv), KO^{t}Bu: (0.0111 g, 0.099 mmol, 2.3 equiv) (*o*-dibromoxylene: 0.0113 g, 0.043 mmol, 1.0 equiv) Yield: 0.0156 g (41.8 %).

$^{31}P\{^{1}H\}$ NMR ($CDCl_3$): δ -21 (br). ESI-MS: 725 amu (m+). Anal. Calcd for $C_{42}H_{46}CuF_3O_3P_4S$: C, 57.63; H, 5.30; P, 14.15. Found: C, 57.65; H, 5.22; P, 14.27.

Synthesis of 6a-c (described for 6b). In a typical procedure, complex **5a** was dissolved in CH_2Cl_2 (3-5 mL) and stirred vigorously at room temperature with an aqueous solution of KCN (2 mL) overnight. The aqueous layer was removed and the organic layer was dried over $MgSO_4$ and filtered through a plug of alumina. The solvent was removed *in vacuo* to yield a waxy solid or residue that was taken on directly to prepare metal complexes or used as a CH_2Cl_2 solution directly.

6a: $^{31}P\{^{1}H\}$ NMR ($CDCl_3$): δ -26.8 (s). ^{1}H NMR ($CDCl_3$): δ 1.07-2.53 (m, 24H), 6.78-8.05 (m, 20H, aromatic).

6b: $^{31}P\{^{1}H\}$ NMR ($CDCl_3$): δ -26.4 (s), -27.4 (s). ^{1}H NMR ($CDCl_3$): δ 1.5-2.3 (m, 26H), 7.2-7.6 (m, 20H, aromatic).

6c: $^{31}P\{^{1}H\}$ NMR ($CDCl_3$): δ -23.2 (s), -26.7 (s). ^{1}H NMR ($CDCl_3$): δ 1.5-2.3 (m, 22H), 7.2-7.6 (m, 24H, aromatic).

Synthesis of $[Fe(6b)(CH_3CN)_2](BPh_4)_2$. To a suspension of $FeCl_2 \cdot 4H_2O$ (0.0013 g, 0.007 mmol, 1.0 equiv) and $NaBPh_4$ (0.0045 g, 0.013 mmol, 1.9 equiv.) in CH_3CN was added **6b** as a CH_2Cl_2 solution (0.0040 g, 0.007 mmol, 1.0 equiv.). The solution immediately turned light orange and was then stirred for 1 h; the solution was filtered through celite and the solvent was then removed *in vacuo*. The orange residue was washed with ether to yield an orange powder. ESI-MS: 670 $[m\text{-}2(BPh_4)]^+$, 335

[m-2(BPh_4)]$^{2+}$. Anal. Calcd for $C_{89}H_{94}FeB_2P_4N_2$: C, 76.84; H, 6.67; N, 2.01; P, 8.91. Found: C, 65.60; H, 6.07; N, 3.40; P, 6.86. (with 2.4 CH_3CN and 3.4 CH_2Cl_2 as solvents of crystallization, Calcd: C, 65.57; H, 6.11; N, 3.46; P, 6.96.)

Synthesis of [Co(6b)]Cl_2·4 H_2O. To a suspension of $CoCl_2$ (0.0211 g, 0.162 mmol) in CH_2Cl_2 was added **6a** (prepared from 0.0855 g **5a**, 0.103 mmol) in CH_2Cl_2. The solution turned from a bright blue suspension to an emerald green solution. The reaction mixture was filtered and the solvent removed *in vacuo*. The resulting residue was washed with ether to yield a dark green powder. Yield: 0.0595 g (77.3%). ESI-MS: 708 [m-Cl]$^+$ Anal. Calcd. for $C_{37}H_{46}CoP_4Cl_2$: C, 59.67; H, 6.23. Found: C, 54.39; H, 6.83. (with four water of hydration, Calcd: C, 54.42; H, 6.67). UV-Vis (CH_2Cl_2): 611, 660 nm. μ_{eff} = 1.57 B.M.

4.3. Results and Discussion

4.3.1. Synthesis of the Linear Tetradentate Ligand (3)

The mixed tertiary-secondary tetradentate phosphine ligand **3** (Scheme 4) was prepared according to literature methods as a mixture of stereoisomers by $LiAlH_4$ reduction of the corresponding bis-phosphinate (**2**).[5] Phenyl groups were chosen as demonstration substituents on the phosphine for ease of synthesis and solubility in organic solvents.

Scheme 4. Preparation of a tetradentate mixed tertiary/secondary phosphine ligand (**3**).

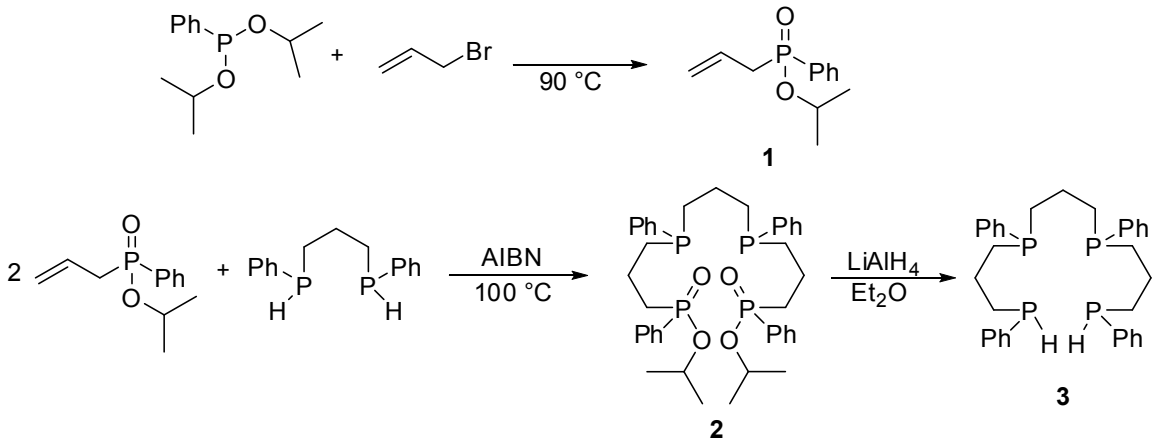

4.3.2. Preparation of [Cu(3)]OTf

Ligand **3** reacted with one equivalent of $[Cu(CH_3CN)_4]OTf$ in CH_3CN to yield a white solid product characterized as [Cu(**3**)]OTf (**4**) (Scheme 5). The $^{31}P\{^1H\}$ NMR spectrum of **5** exhibited two broad peaks centered at -15 and -40 ppm, corresponding to the tertiary and secondary phosphorus atoms of the ligand, respectively. The broadness is consistent with coordination of **3** to Cu(I); the ^{31}P NMR signals are significantly broadened because of coupling with NMR-active, quadrupolar ^{63}Cu and ^{65}Cu nuclei (as discussed previously, see Chapter II). As reported for related Cu(I)-phosphine complexes, the tetrahedral geometry about Cu(I) in **4** is likely distorted by the propylene bridges between the phosphorus atoms, resulting in a tetrahedral bite angle less than ≈ 109.5°. Thus, because of the distortion, ^{31}P NMR spectroscopy does not reveal much structural information except for the type of phosphine coordinated to copper (e.g. tertiary vs. secondary). However, the ESI-MS of the complex displayed the anticipated *m/z* at 623 ($C_{33}H_{40}CuP_4^+$, $[m\text{-}OTf]^+$) with the expected isotope pattern (See Appendix C).

The elemental analysis of the complex is also consistent with the proposed molecular formula.

Scheme 5. Preparation of the Cu(I)-tetradentate phosphine complex **4**.

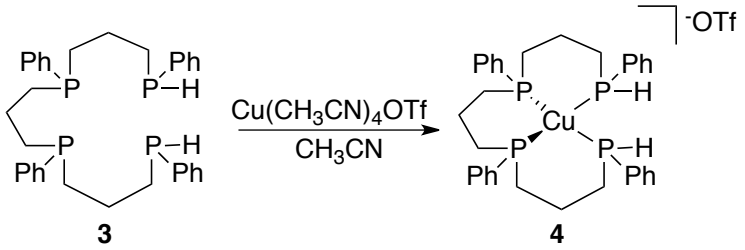

3 **4**

4.3.3. Macrocyclization of [Cu(3)]OTf (4)

Complex **4** was converted to a macrocyclic complex using the general route depicted for the Ni complex in Scheme 2. Deprotonation of complex **4** with two equivalents of KO^{t}Bu in THF immediately gave a bright yellow solution. Attempts to bridge the two phosphide anions with various α-ω dibromides gave varied results. When 1,2-dibromoethane was used a linking reagent, there was no conclusive evidence for clean formation of the macrocyclic Cu(I) phosphine complex. However, with either 1,3-dibromopropane, 1,4-dibromobutane, or *o*-dibromoxylene, the macrocyclic complexes **6a-c**, respectively, were obtained (Scheme 6). All complexes were isolated as yellow powders that displayed broad peaks in the $^{31}P\{^1H\}$ NMR spectra (see Table 1), consistent with alkylation of the two secondary phosphines to give an all-tertiary phosphine product. Because no Cu-P coupling is observed in the ^{31}P NMR spectrum, the complex likely has a distorted tetrahedral geometry about Cu.[7-9,18–20]

Scheme 6. Macrocyclization of **4**.

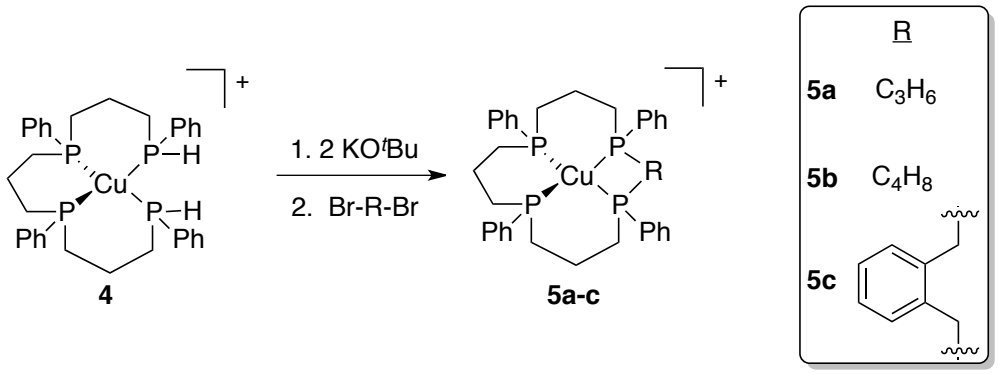

Table 1. Data for copper(I) complexes **4** and **5a-c**.

Compound	$^{31}P\{^1H\}$ NMR (ppm)	ESI-MS: m/z (expected)	Elemental Analysis Actual (Calc'd)		
			C	H	P
Cu(3)OTf (4)	-15, -40	623 (623)	52.80 (52.82)	5.18 (5.21)	15.87 (16.02)
5a	-14.7, -21.4	663 (663)	54.46 (54.60)	5.52 (5.45)	15.07 (15.23)
5b	-18.4	677 (677)	54.89 (55.17)	5.60 (5.63)	14.60 (14.98)
5c	-13.6, -21.4	725 (725)	57.65 (57.63)	5.22 (5.30)	14.27 (14.15)

4.3.4. Demetallation of Complexes 5a-c

Removal of the Cu(I) center in complexes **5a-c** is necessary to prepare macrocyclic phosphine complexes with other metals. The demetallation procedure is described in Chapter II. The same procedure was then carried out with complexes **5a-c** (Scheme 7). The products resulting after removal of the solvent were colorless, oily residues (**6a**) or semi-solids (**6b-c**). In general, phosphines **6a-c** displayed sharp peaks in their $^{31}P\{^1H\}$ NMR spectra (see Table 2 for NMR data). These peaks, indicative of tertiary phosphines, are much sharper than those in complexes **5a-c**, indicating the absence of Cu coordination. In the ^1H NMR spectra, the aromatic protons of the phenyl

rings give rise to a group of signals at 7.3 ppm and the aliphatic protons have a broad signals from 1.2 to 2.1 ppm. In addition, the P-H signals present in **3** were not in the ^{1}H NMR spectrum of **6a-c**, indicating full alkylation of the phosphines.

Scheme 7. Demetallation of complexes **5a-c** using KCN.

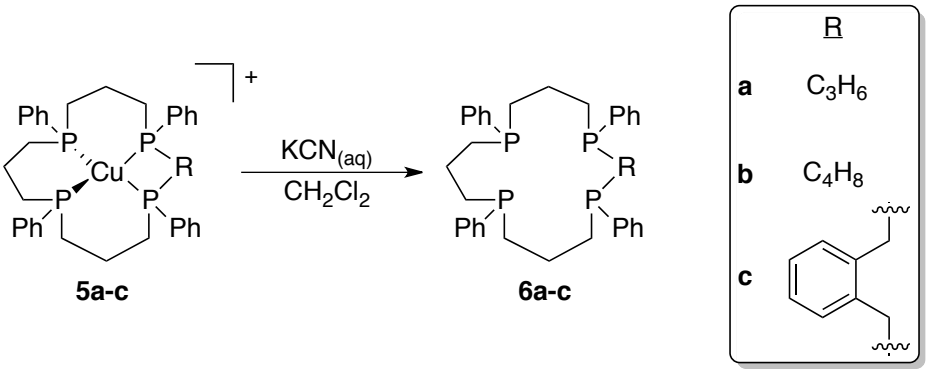

Table 2. NMR data for phosphines **6a-c**.

Compound	$^{31}P\{^{1}H\}$ NMR (ppm)	Integrals from ^{1}H NMR: actual (expected)	
		Aromatic	Aliphatic
6a	-26.8	20 (20)	23.7 (24)
6b	-25.6, -26.8	20 (20)	27.4 (26)
6c	-23.2, -26.7	24 (24)	25.3 (22)

It is interesting to note that a singlet is observed for phosphine **6a**. Because of the many stereoisomers possible from the open-chain ligand **3** (see Chapter V for discussion of the stereochemistry of the ligand), a simple NMR spectrum may not be expected. The phosphine is capable of exhibiting four isomers (Figure 1), with two isomers with a geometry lending a singlet in the ^{31}P NMR spectrum (Figure 1, **A**, **D**). However, other

phosphine macrocycles, both coordinated and free, have been prepared where a singlet has been observed for isomers other isomers **A** and **D**.[10-12] It is possible that the singlet for phosphine **6a** can arise from one of the other two isomers (B-C), with coincidentally all the peaks for the phosphorus atoms are at the same frequency with no P-P coupling . The possibility of a symmetric A_4 spin-system could be a result of stereoselective inversion of the coordinated phosphide anions to form a preferred geometry.[13,14]

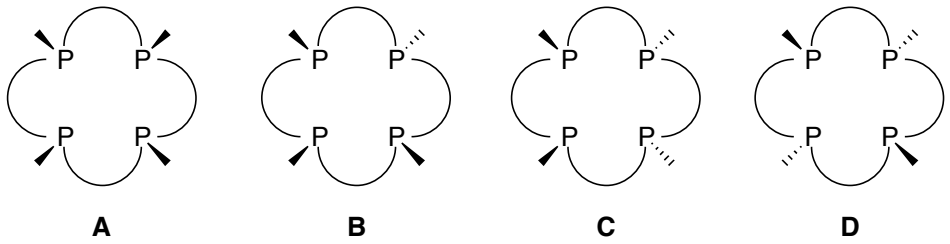

Figure 1. Possible stereoisomers of tetraphosphine **6b**.

Phosphine **6b** displays two equally intense singlets at -25.6 ppm and -26.8 ppm. Two peaks are expected as there are two different phosphorus environments. could be from two isomers of **6b**. Because **6b** is less symmetric, there are 7 possible diastereomeric pairs (two meso forms and five pair of enantiomers, see Appendix C).

The product resulting from **5c** displayed sharp peaks in the expected region in the ^{31}P NMR spectrum, but the number of peaks indicated some degradation of the phosphine during demetallation.

Because the oily nature of the free ligands prevented their more detailed characterization, derivatives of the ligand and metal complexes containing the ligands

were synthesized as a way to help confirm the identities of the ligands. The coordination complexes of **6b** with Co(II) and Fe(II) are described.

4.3.5. Attempts to Derivatize Free Phosphines 6a-c

In order to further the characterization of the free ligand **6b**, derivatives were sought that would lend air-stable and potentially crystalline products. A variety of methods were used, including alkylation to phosphonium salts, protection with borane, and oxidation with peroxide and elemental sulfur (Figure 2). Unfortunately, none of the products obtained were useful in determining the structure of the free ligand. For example, phosphine **6b** does react with BH_3THF in THF to yield a white solid. This solid, however, is notoriously insoluble in most solvents except warm DMSO. The ^{31}P NMR spectrum of this product shifts from -25.6 and -26.8 ppm to a broadened peak at +15.0 ppm, in the range of phosphine-borane adducts.[15]

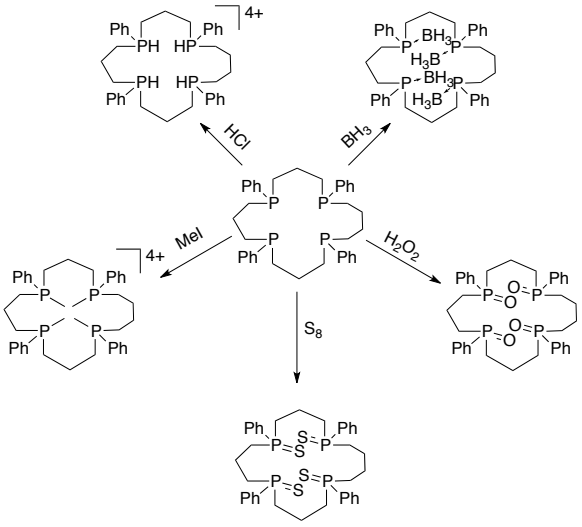

Figure 2. Attempted routes to derivatize ligand **6b**

4.3.6 Coordination Chemistry of 6b with Co(II) and Fe(II)

Reaction of **6b** with anhydrous $CoCl_2$ in CH_2Cl_2 gave an emerald green solution from which a dark green powder was isolated (Scheme 5). The product showed a single peak in the ESI-MS at 708 *m/z*, corresponding to the calculated value for $[Co(\mathbf{6b})Cl]^+$; the expected isotope pattern for this structure was also observed (see Appendix C), indicating that the species in solution may have only one coordinated chloride. An analogous complex, $[Co(dppp)_2Cl]Cl$, was proposed to be five-coordinate with one ionic halogen due to the sterics of the phenyl groups on the phosphine ligands, from which analogies could be drawn for the $Co(\mathbf{6b})Cl_2$.[16]

The green product had broad NMR signals, consistent with a paramagnetic species, which could be expected for an d^7 Co(II) complex. The complex has a μ_{eff} of 1.54 B.M. (Bohr Magnetons), consistent with 1 unpaired electron[17]; this effective magnetic moment is congruous with Co(II) tetraphosphorus complexes.[18-21] Additionally, the electronic spectrum has a similar shape as other relevant five-coordinate $[Co(P)_4Cl]Cl$ (P = a phosphine) complexes with two absorption maxima at 611 and 660 nm (extinction coefficients of 397 and 372, respectively), indicating that the complex is likely five-coordinate $[Co(\mathbf{6b})Cl]Cl$. The elemental analysis of the green powder gave a formula of $[Co(\mathbf{6b})]Cl_2 \bullet 4H_2O$, consistent with the proposed formula for $Co(\mathbf{6b})Cl_2$ and not $[Co(\mathbf{6a})][CoCl_4]$, which is a common structure for Co(II) complexes (see Chapter II).

Reaction of **6b** with $FeCl_2 \bullet 4H_2O$ and two equivalents of $NaBPh_4$ in CH_3CN, gave an orange solid identified as $[Fe(\mathbf{6b})(CH_3CN)_2](BPh_4)_2$ (Scheme 8). The ESI-MS showed peaks at 670 and 335 *m/z*, corresponding to $[m\text{-}2(BPh_4)]^+$ and $[m\text{-}2(BPh_4)]^{2+}$,

respectively (see Appendix C). Elemental analysis of the orange product indicated a formula of [Fe(**6b**)(CH_3CN)$_2$](BPh_4)$_2$·2CH_3CN·3.5CH_2Cl_2. The solvent molecules could not be removed by heating and pumping on the sample *in vacuo* for 12 hours. The IR spectrum of the orange powder has weak stretches around 2251 and 2284 cm^{-1} and a strong stretch at 2091 cm^{-1}, which could correspond to $\nu_{N\text{-}N}$, indicating that the complex binds dinitrogen relatively easily, strongly enough to displace an acetonitrile ligand.

The same complex was then prepared in an argon-filled glovebox in the absence of dinitrogen. An IR spectrum of the resulting orange powder showed a 64% reduction the intensity of the stretch at 2091 cm^{-1}. Passing N_2 over the solid and taking another IR spectrum showed no change. The complex was then put under vacuum and backfilled with N_2. A small amount of CH_3CN was added and N_2 bubbled through the solution to remove the solvent. An IR of the resulting complex showed a slight increase in intensity (12%) of the N-N stretch. It is possible that the complex binds N_2 slowly over time, as the complex with a strong N-N stretch was in an N_2-filled glovebox for weeks.

Scheme 8. Reactions of **6b** with $CoCl_2$ and $FeCl_2$·4H_2O.

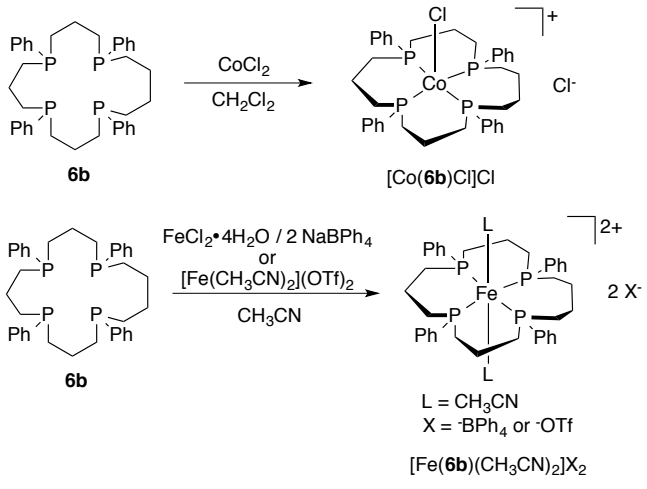

Phosphine **6b** also seemed to react with $NiCl_2$ to give the corresponding $[Ni(\mathbf{6b})]^{2+}$ by ESI-MS (See Appendix C). Investigation into optimizing the coordination of ligands **6a-c** to other transition metals is ongoing.

4.4. Conclusions

Tetradentate, macrocyclic ligands **6a-c** can be successfully synthesized from the linear, tetradentate, secondary phosphine ligand **3** using a Cu(I) metal center as a template. After alkylation, the Cu(I) template is easily removed with cyanide. The uncoordinated macrocycle ligands thus obtained can be used to form complexes with other metals, as was demonstrated here using $CoCl_2$ and $FeCl_2$ to form macrocyclic complexes $Co(\mathbf{6b})Cl_2$ and $[Fe(\mathbf{6b})(CH_3CN)_2]^{2+}$, respectively. The ability to form tetradentate, macrocyclic phosphine complexes of Fe is important because a long-term goal is to use water-soluble versions of these complexes in a pressure-swing purification of natural gas contaminated by N_2 (Scheme 1, Chapter II).

In summary, a straightforward route to tetradentate, macrocyclic phosphine ligands and their complexes with various metals was demonstrated. The route is, in principle, general and should be applicable to the synthesis of macrocyclic phosphine ligands with various R groups bonded to the P atoms. Work in our laboratory is continuing with the preparation of water-soluble phosphine macrocycle ligands for use in the pressure-swing purification of natural gas.

4.5. Bridge

Chapter IV described the use of a mixed secondary/tertiary tetraphosphine as a ligand to make tetraphosphine macrocycles. This synthetic strategy works well to produce the desired macrocyclic ligands which can be coordinated to other metals of interest, but requires many synthetic steps, which is problematic for scaling up the synthesis. Chapter V details attempts to uses Fe(II) as a template metal to directly prepare Fe(II) macrocyclic tetraphosphine complexes.

CHAPTER V

SYNTHESIS AND REACTIVITY OF COORDINATED BIDENTATE, TETRADENTATE, AND MACROCYCLIC PHOSPHINES ON IRON(II): TOWARD REVERSIBLE DINITROGEN BINDING

Charles D. Swor and Aditya Nathan performed some experimental work in this chapter, and the crystal structures were solved by Lev N. Zakharov.

5.1. Introduction

As mentioned previously in Chapter II, the ability of selected iron-phosphine complexes to bind N_2 makes these complexes promising candidates for use in schemes designed to separate N_2 from N_2-contaminated natural gas streams.

Previous chapters have shown that copper(I) can be used as a template to prepare tetraphosphine macrocyclic ligands, but the ligand must be liberated from copper and re-coordinated to iron(II) in order to obtain the desired final product. Ideally, iron(II) could be used directly as a template, eliminating the need for multiple steps involved from needing a separate metal template.

The Tyler lab has previously used iron(II) phosphine complexes to access reactivity with the inert dinitrogen. Our lab has synthesized water-soluble iron(II) phosphine complexes that are capable of reversibly binding N_2 in a pressure-swing absorption scheme (see Chapter II)[1,2], as well as activating N_2 toward reduction to NH_3 at ambient temperature and pressure.[3-5]

Our hypothesis with iron(II) was that a *trans*-octahedral complex would act similarly toward macrocyclization as the more ubiquitous square-planar d^8 metals that are used as templates (Scheme 1). Our lab has prepared many *trans*-$Fe(P_2)_2X_2$ (P_2 = a bidentate phosphine, X = Cl, Br, H) complexes in the past, so the idea for the planned synthetic route stemmed from these initial *trans*- complexes.[1,2,4,6]

Scheme 1. General route to Fe(II) macrocycles using *trans*-$Fe(P_2)_2X_2$ complexes (P_2 = a bis-bidentate secondary phosphine.

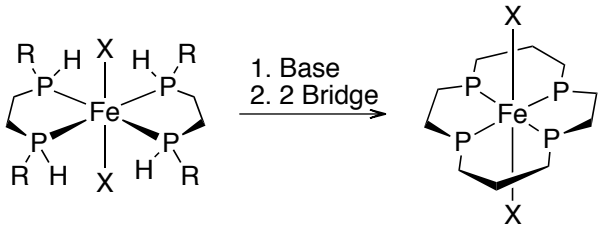

This chapter illustrates our attempts to prepare phosphine macrocycles directly on iron(II) without the use of another template metal. This route was attempted with both secondary and tetradentate secondary phosphines of both hydrophobic and hydrophilic natures. The syntheses of the novel secondary and tetradentate phosphine ligands and complexes are described as well as the preparation of macrocyclic phosphine complexes directly on iron(II) with a variety of bridges. Finally, nitrogen binding studies were carried out with a range of iron(II) phosphine complexes.

5.2. Experimental

5.2.1. Materials and Reagents

Unless otherwise noted, all experimental procedures were performed under an inert (N_2) atmosphere, using standard Schlenk and glovebox techniques. Commercially

available reagents were used as received. HPLC-grade THF was dried and deoxygenated by passing through commercial columns of CuO, followed by alumina under an argon atmosphere. Deuterated solvents were obtained from Cambridge Isotope Laboratories and degassed using three freeze-pump-thaw cycles. $[Fe(CH_3CN)_2](OTf)_2$,[7] was synthesized according to literature methods. Ligand **9** was prepared from literature methods[8] and described in Chapter IV. Compound **21** was commercially available.

5.2.2. Instrumentation

Air-sensitive NMR samples were sealed in N_2 filled J-Young tubes. NMR spectra were obtained on either a Varian Unity/Inova 300 spectrometer at an operating frequency of 299.94 (^{1}H) and 121.42 (^{31}P) or a Varian Unity/Inova 500 spectrometer operating at a frequency of 500.62 MHz (^{1}H) or 202.45 MHz (^{31}P). The ^{1}H and ^{13}C NMR spectra were referenced to residual solvent peaks, and the ^{31}P NMR spectra were referenced to external 1% H_3PO_4 in D_2O. ESI mass spectra were obtained using a Thermo Finnigan LCQ Deca XP Plus ESI Mass Spectrometer using THF or CH_3CN as the solvent. Infrared spectra were recorded using a Thermo-Scientific Nicolet 6700 FT-IR spectrometer. UV-Vis spectra were collected on an Agilent 8453 spectrophotometer. Elemental analyses were performed by Complete Analysis Laboratories, Inc., Parsippany, NJ.

5.2.3. Methods

Synthesis of *cis*-Fe(MeOPrPE)$_2$Cl$_2$ (1). A THF solution of MeOPrPE (see Chapter II) (0.593 g, 2.48 mmol) was added to a THF suspension of $FeCl_2 \cdot 4H_2O$ (0.2500

g, 1.25 mmol). The color of the solution immediately turned a red/purple color and eventually a dark purple color with a purple precipitate. The solvent was removed to yield a purple powder. Yield: 0.6060 g (81%). $^{31}P\{^{1}H\}$ NMR ($CDCl_3$): δ 54.0 (br), 60.6 (br), 66.8 (br), 77.6 (br). ESI-MS: 567 amu ($[m\text{-}Cl]^+$). Anal. Calcd for $C_{20}H_{48}Cl_2FeO_4P_4$: C, 39.82; H, 8.02; P, 20.54. Found: C, 39.82; H, 8.14; P, 20.36.

Synthesis of *cis*-Fe(MeOPrPP)$_2$Cl$_2$ (2). Complex **2** was prepared in an analogous manner to complex **1**, using MeOPrPP (Chapter II) (0.6040 g, 2.39 mmol) and $FeCl_2 \cdot 4H_2O$ (0.2433 g, 1.22 mmol). Yield: 0.6400 g (85%) of a purple powder. $^{31}P\{^{1}H\}$ NMR ($CDCl_3$): δ 11.0 (br), 24.8 (br), 36.3 (br), 49.4 (br). ESI-MS: 595 amu ($[m\text{-}Cl]^+$). Anal. Calcd for $C_{22}H_{52}Cl_2FeO_4P_4$: C, 41.86; H, 8.30; P, 19.63. Found: C, 41.99; H, 8.15; P, 19.43.

Synthesis of *cis*-Fe(MPPE)$_2$Cl$_2$ (3). Complex **3** was prepared in an analogous manner to complex **1**, using 1,2-bis(phenylphosphino)ethane (MPPE) (0.5890 g, 2.39 mmol) and $FeCl_2 \cdot 4H_2O$ (0.2380 g, 1.20 mmol). Yield: 0.5320 g (72%) of a purple powder. $^{31}P\{^{1}H\}$ NMR ($CDCl_3$): δ +40 to +120 (br). ESI-MS: 583 amu ($[m\text{-}Cl]^+$). IR (ATR, cm^{-1}): 2319 (m, P-H). Anal. Calcd for $C_{28}H_{32}Cl_2FeO_4P_4$: C, 54.31; H, 5.21; P, 20.01. Found: C, 54.39; H, 5.20; P, 19.95.

Synthesis of *cis*-Fe(MPPP)$_2$Cl$_2$ (4). Complex **4** was prepared in an analogous manner to complex **1**, using 1,3-bis(phenylphosphino)propane (MPPP) (0.5700 g, 2.19

mmol) and $FeCl_2 \cdot 4H_2O$ (0.2180 g, 1.10 mmol). Yield: 0.5249 g (74%) of a purple powder. $^{31}P\{^1H\}$ NMR ($CDCl_3$): δ +26 to +50 (m). ESI-MS: 611 amu ($[m\text{-}Cl]^+$). IR (ATR, cm^{-1}): 2310 (s, P-H). Anal. Calcd for $C_{30}H_{36}Cl_2FeO_4P_4$: C, 55.67; H, 5.61; P, 19.14. Found: C, 55.68; H, 5.71; P, 19.05. Single crystals suitable for X-ray diffraction were grown by vapor diffusion of hexanes into a THF solution over the course of 1 month.

Synthesis of *trans*-[Fe(MeOPrPE)$_2$(CH$_3$CN)$_2$](OTf)$_2$ (5). A CH_3CN solution of MeOPrPE (0.0378 g, 0.159 mmol) was added to a CH_3CN solution of $[Fe(CH_3CN)_2](OTf)_2$ (0.0252 g, 0.058 mmol) to give a bright orange solution. After stirring for 12 hours, the solvent was removed to yield an orange, viscous oil. Yield: 0.0390 g (95.4%). $^{31}P\{^1H\}$ NMR (CD_3CN): δ +40 to +70 (m). Anal. Calcd for $C_{26}H_{54}F_6FeN_2O_{10}P_4S_2$: C, 34.22; H, 5.96; N, 3.07; P, 13.58. Found: C, 34.29; H, 5.88; N, 2.94; P, 13.46.

Synthesis of *trans*-[Fe(MeOPrPP)$_2$(CH$_3$CN)$_2$](OTf)$_2$ (6). A CH_3CN solution of MeOPrPP (0.0770 g, 0.305 mmol) was added to a CH_3CN solution of $[Fe(CH_3CN)_2](OTf)_2$ (0.0672 g, 0.154 mmol) to give a bright orange solution. After stirring for 12 hours, the solvent was removed to yield an orange, viscous oil. $^{31}P\{^1H\}$ NMR (CD_3CN): δ +30 to +80 (m). Anal. Calcd for $C_{28}H_{58}F_6FeN_2O_{10}P_4S_2$: C, 35.75; H, 6.22; N, 2.98; P, 13.17. Found: C, 35.73; H, 6.26; N, 3.06; P, 13.06.

Synthesis of *trans*-[Fe(MPPE)$_2$(CH$_3$CN)$_2$](OTf)$_2$ (7). A CH_3CN solution of MPPE (0.1016 g, 0.413 mmol) was added to a CH_3CN solution of $[Fe(CH_3CN)_2](OTf)_2$ (0.0910 g, 0.209 mmol) to give a bright orange solution. After stirring for 12 hours, the solvent was removed. The resulting orange gel was triturated with hexanes and ether to yield an orange powder. Yield: 0.1186 g (84.2 %). $^{31}P\{^1H\}$ NMR (CD_3CN): δ +30 to +80 (m). IR (ATR, cm^{-1}): 2303 (m, P-H), 2260 (w, CN). Anal. Calcd for $C_{34}H_{38}F_6FeN_2O_6P_4S_2$: C, 43.98; H, 4.13; N, 3.02; P, 13.34. Found: C, 43.89; H, 4.03; N, 2.86; P, 13.22.

Synthesis of *trans*-[Fe(MPPP)$_2$(CH$_3$CN)$_2$](OTf)$_2$ (8). A CH_3CN solution of MPPP (0.1095 g, 0.420 mmol) was added to a CH_3CN solution of $[Fe(CH_3CN)_2](OTf)_2$ (0.0929 g, 0.213 mmol) to give a bright orange solution. After stirring for 12 hours, the solvent was removed. The resulting orange gel was triturated with hexanes and ether to yield an orange powder. Yield: 0.1308 g (89.4 %). $^{31}P\{^1H\}$ NMR (CD_3CN): δ +25 to +47 (m). IR (ATR, cm^{-1}): 2319 (m, P-H). Anal. Calcd for $C_{36}H_{42}F_6FeN_2O_6P_6S_2$: C, 45.20; H, 4.43; N, 2.93; P, 12.95. Found: C, 45.20; H, 4.43; N, 2.93; P, 12.95. Single crystals of the triflate salt suitable for X-ray diffraction could not be obtained so crystals of the PF_6^- salt were grown (see below).

Synthesis of *trans*-[Fe(MPPP)$_2$(MeCN)$_2$](PF$_6$)$_2$ (8-PF$_6$). $NaPF_6$ (0.1550 g, 0.922 mmol) was added to a CH_3CN solution of **4** (0.2920 g, 0.451 mmol). The initial purple solution faded to a bright orange color with a white precipitate. The reaction

mixture stirred for 12 hours and was then filtered. The solvent was removed *in vacuo* to yield an orange, crystalline solid. Yield: 0.3990 g (93%). $^{31}P\{^{1}H\}$ NMR (CD_3CN): δ +25 to +47 (m). Single crystals suitable for X-ray diffraction were grown by slow evaporation of an acetonitrile solution over the course of three months.

Synthesis of Fe(9)X_2 (X = Cl (10a), Br (10b)). A THF solution of tetradentate ligand **9** was added dropwise to a suspension of $FeCl_2{\cdot}4H_2O$ or $FeBr_2$ in THF. The color of the solution immediately turned dark purple. The reaction was stirred for 12 hours after which the solvent was removed under vacuum to yield a purple solid.

10a: **9** (0.1968 g, 0.351 mmol), $FeCl_24H_2O$ (0.0701 g, 0.353 mmol) Yield: 0.1492 g (61.6 %) $^{31}P\{^{1}H\}$ NMR ($CDCl_3$): δ 47.28 (ddd, *J* = 68.8, 54.0, 40.5 Hz), 43.57 (ddd, *J* = 71.1, 61.7, 40.0 Hz), 39.45 (t, *J* = 60.4 Hz), 30.78 (t, *J* = 60.4 Hz), 28.40 (ddd, *J* = 159.1, 71.0, 54.0 Hz), 15.22 (ddd, *J* = 158.6, 69.1, 61.9 Hz). IR (ATR, cm^{-1}): 2305 (m, P-H). Anal. Calcd for $C_{33}H_{40}FeCl_2P_4$: C, 57.67; H, 5.87; P, 18.03. Found: C, 57.65; H, 5.99; P, 17.83.

10b: **9** (0.2145 g, 0.383 mmol), $FeBr_2$ (0.0863 g, 0.400 mmol). $^{31}P\{^{1}H\}$ NMR ($CDCl_3$): δ 52.44 (ddd, *J* = 66.9, 53.1, 41.2 Hz), 47.04 (ddd, *J* = 71.1, 59.7, 40.9 Hz), 42.32 (t, *J* = 59.4 Hz), 26.32 (t, *J* = 58.7 Hz), 24.23 (ddd, *J* = 143.3, 71.4, 53.6 Hz), 10.34 (ddd, *J* = 143.7, 67.9, 60.2 Hz).

Synthesis of [Fe(9)$(CH_3CN)_2$]$(BPh_4)_2$ (11). Complex **10a** (0.0095 g, 0.014 mmol) was dissolved in CH_3CN and the solution turned orange. Two equivalents of

$NaBPh_4$ (0.0100 g, 0.029 mmol) in CH_3CN were added and stirred for 24 hours. After stirring, the reaction mixture was filtered over celite to remove the precipitated NaCl and the solvent was removed in vacuo. The residue was triturated with ether to yield an orange solid. IR (ATR, cm^{-1}): 2315 (m, P-H). Anal. Calcd for $C_{85}H_{86}B_2FeN_2P_4$: C, 76.36; H, 6.48; P, 9.27. Found: C, 76.35; H, 6.72; P, 9.19.

Synthesis of ethyl allyl(methoxypropyl)phosphinate (13a). Methoxypropyl bromide (0.42 mL, 3.76 mmol) was added to diethyl allylphosphonite (0.6255 g, 3.74 mmol) neat under N_2. The reaction mixture was heated to 80 °C overnight. After heating, the reaction was cooled to room temperature and all volatiles were removed *in vacuo*. The remaining oil was distilled under reduced pressure to yield the desired product. Yield: 0.4851 g (63 %). $^{31}P\{^1H\}$ NMR ($CDCl_3$): δ 53.1. ^1H NMR ($CDCl_3$): δ 5.79 (ddtd, J = 12.9, 9.8, 7.5, 5.4 Hz, 1H), 5.23 – 5.14 (m, 2H), 4.05 (ddtd, J = 17.2, 10.1, 7.2, 2.9 Hz, 2H), 3.39 (t, J = 6.0 Hz, 2H), 3.30 (s, 3H), 2.58 (dd, J = 17.0, 7.4 Hz, 2H), 1.89 – 1.69 (m, 4H), 1.29 (t, J = 7.0 Hz, 3H). ^{13}C NMR ($CDCl_3$): δ 128.04 (d, J = 8.7 Hz), 120.08 (d, J = 12.5 Hz), 72.49 (d, J = 15.5 Hz), 60.42 (d, J = 6.7 Hz), 58.58 , 34.56 (d, $J_{C\text{-}P}$ = 86.3 Hz), 24.23 (d, $J_{C\text{-}P}$ = 94.5 Hz), 22.02 (d, J = 4.0 Hz), 16.73 (d, J = 5.6 Hz). Anal. Calcd for $C_{10}H_{24}O_2P_2$: C, 50.41; H, 10.15; P, 26.00. Found: C, 50.36; H, 10.09; P, 25.87.

Synthesis of ethyl allyl(3-((triisopropyl)oxy)propyl)phosphinate (13b). (3-bromopropoxy)triisopropylsilane (**19**, 1.5048 g, 5.11 mmol) was added to diethyl

allylphosphonite (**18**) (0.8538 g, 5.11 mmol) neat under N_2. The reaction mixture was heated to 80 °C overnight. After heating, the reaction was cooled to room temperature and all volatiles were removed *in vacuo*. The remaining oil was sufficiently pure by ^{1}H NMR. Yield: 0.3835 g (28 %). $^{31}P\{^1H\}$ NMR: δ 53.41. ^{1}H NMR (300 MHz, $CDCl_3$) δ 5.82 (ddtd, *J* = 17.2, 10.0, 7.4, 5.2 Hz, 1H), 5.31 – 5.08 (m, 2H), 4.08 (ddq, *J* = 10.7, 6.8, 3.6 Hz, 2H), 3.73 (dt, *J* = 8.4, 5.6 Hz, 2H), 3.52 (dq, *J* = 10.2, 6.6 Hz, 3H), 2.61 (dd, *J* = 17.2, 7.5 Hz, 2H), 2.06 (dq, *J* = 12.2, 6.0 Hz, 2H), 1.94 – 1.69 (m, 4H), 1.31 (t, *J* = 7.0 Hz, 3H), 1.05 (t, *J* = 4.0 Hz, 21H).

Synthesis of ethyl allyl(2-(benzyloxy))phosphinate (13c). ((3-bromopropoxy)methyl)benzene (**20**) (0.18 mL, 1.14 mmol) was added to diethyl allylphosphonite **18** (0.1794 g, 1.10 mmol) neat under N_2. The reaction mixture was heated to 80 °C overnight. After heating, the reaction was cooled to room temperature and all volatiles were removed *in vacuo*. $^{31}P\{^1H\}$ NMR: δ 50.59. ^{1}H NMR (300 MHz, $CDCl_3$) δ 7.33 (qd, *J* = 6.4, 5.5, 2.5 Hz, 5H), 5.94 – 5.62 (m, 1H), 5.37 – 4.97 (m, 2H), 4.58 (d, *J* = 2.0 Hz, 2H), 4.07 (ddd, *J* = 9.3, 7.2, 3.5 Hz, 2H), 3.78 (td, *J* = 6.2, 2.0 Hz, 3H), 3.48 (td, *J* = 6.2, 2.0 Hz, 2H), 2.65 (dd, *J* = 17.7, 7.9 Hz, 2H), 2.10 (ddd, *J* = 14.6, 7.1, 3.6 Hz, 2H), 1.28 (ddt, *J* = 11.3, 8.9, 6.4 Hz, 3H).

Synthesis of 14 and 15. Phosphinate **13a** (0.1379 g, 0.669 mmol) was added in a 50 mL Schlenk flask with MeOPrPE (0.0787 g, 0.330 mmol). A spatula tip full of AIBN was added to the reaction mixture. The flask was heated to 80 °C overnight. After

heating, all volatiles were removed in vacuo at 100 °C. The product (**14**) was an extremely viscous, clear oil. $^{31}P\{^{1}H\}$ NMR (202 MHz, $CDCl_3$) δ -26.63, -70.53.^{1}H NMR (300 MHz, $CDCl_3$) δ 4.03 (p, J = 7.1 Hz, 4H), 3.39 (q, J = 6.1, 5.6 Hz, 8H), 3.31 (s, 12H), 1.98 – 1.59 (m, 17H), 1.57 – 1.36 (m, 11H), 1.37 – 1.22 (m, 6H). The product of this reaction was directly carried on to reduction.

Compound **14** was dissolved in diethyl ether and added dropwise to an ice-cooled suspension of $LiAlH_4$ in ether. After addition, the reaction mixture was warmed to room temperature and stirred for 12 hr. The reaction was cooled again with an ice-bath and carefully quenched with 0.5 mL H_2O, followed by 0.5 mL 10% NaOH, finally followed by 1.5 mL H_2O. The resulting white precipitate was filtered and the solvent removed *in vacuo* to yield ligand **3** as a clear, viscous oil. Yield: 0.0588 g (34 % over two steps). ^{31}P NMR (202 MHz, $CDCl_3$) δ -26.63 , -70.53 (d, J = 199.3 Hz). ^{1}H NMR (300 MHz, $CDCl_3$) δ 3.40 (t, J = 6.3 Hz, 7H), 3.33 (s, 12H), 1.95 – 0.94 (m, 18H).

Synthesis of 16 and 17. Diethyl allylphosphonate (0.6795 g, 3.81 mmol) was added in a 50 mL Schlenk flask with MeOPrPE (0.4277 g, 1.80 mmol). A spatula tip full of AIBN was added to the reaction mixture. The flask was heated to 80 °C overnight. After heating, all volatiles were removed in vacuo at 100 °C. The product (**16**) was an extremely viscous, clear oil. $^{31}P\{^{1}H\}$ NMR ($CDCl_3$): δ 31.3 (s), 27.0 (s). ^{1}H NMR (300 MHz, $CDCl_3$) δ 4.07 (pdd, J = 7.1, 4.9, 3.0 Hz, 2H), 3.37 (t, J = 6.4 Hz, 1H), 3.30 (s, 2H), 1.95 – 1.59 (m, 2H), 1.55 – 1.35 (m, 3H), 1.29 (t, J = 7.0 Hz, 4H). The product of this reaction was directly carried on to reduction.

Compound **16** was dissolved in diethyl ether and added dropwise to an ice-cooled suspension of $LiAlH_4$ (4 equivalents) in ether. After addition, the reaction mixture was warmed to room temperature and stirred for 12 hr. The reaction was cooled again with an ice-bath and carefully quenched with 0.5 mL H_2O, followed by 0.5 mL 10% NaOH, finally followed by 1.5 mL H_2O. The resulting white precipitate was filtered and the solvent removed *in vacuo* to yield ligand **17** as a clear, viscous oil. ^{31}P NMR (121 MHz, $CDCl_3$) δ -26.98, -138.72 (t, J = 194.7 Hz). ^{1}H NMR (300 MHz, $CDCl_3$) δ 3.42 (t, J = 6.4 Hz, 5H), 3.34 (s, 7H), 3.02 (t, J = 7.0 Hz, 2H), 2.36 (s, 10H), 1.90 – 1.52 (m, 16H), 1.47 (dq, J = 11.6, 7.4, 6.0 Hz, 11H). ^{13}C NMR (75 MHz, $CDCl_3$) δ 73.70 (d, J = 5.8 Hz), 58.73, 29.49, 28.10, 26.66 – 25.78 (m), 23.44, 22.78, 21.64, 15.87.

Synthesis of diethyl allylphosphonite (19). An ether solution of allylmagnesium bromide (1 M, 35 mL, mmol, equiv.) was added dropwise to an ether solution of diethyl chlorophosphonite (5.0 mL, mmol, equiv.) at 0 C. The reaction was warmed to RT and stirred for 12 hours. After stirring, the the reaction was filtered and the solvent removed by distillation to yield the product as an extremely air-sensitive, clear oil. Yield: 1.1531 g (20%) ^{31}P NMR (121 MHz, Chloroform-*d*) δ 175.83. ^{1}H NMR (300 MHz, $CDCl_3$) δ 5.86 – 5.63 (m, 1H), 5.23 – 5.00 (m, 2H), 4.02 – 3.71 (m, 4H), 2.41 (ddt, J = 7.6, 4.1, 1.2 Hz, 2H), 1.24 (t, J = 7.0 Hz, 6H).

Synthesis of (3-bromopropoxy)triisopropylsilane (20).

Imidazole (1.2991 g, 18.05 mmol) was added to a solution of 1-bromopropanol (1.70 mL, 18.80 mmol) in dichloromethane. Triisopropylsilyl chloride (4.0 mL, 18.70 mmol) was added dropwise via syringe. White precipitate formed and the reaction mixture was stirred for 12 hours. The reaction was then filtered over celite, and the solvent was removed *in vacuo*. Yield: 4.4216 g (79.6 %). ^{1}H NMR (300 MHz, $CDCl_3$) δ 3.82 (t, *J* = 5.7 Hz, 2H), 3.55 (t, *J* = 6.5 Hz, 2H, -C**H**$_2$-), 2.07 (h, *J* = 6.1, 5.5 Hz, 2H, -C**H**$_2$-), 1.06 (d, *J* = 4.4 Hz, 21H, -CH(C**H**$_3$)$_2$ (x 3), -C**H**(CH$_3$)$_2$ (x 3)).

Dinitrogen Binding Experiments: In a typical experiment, the complex of interest was put in a Fischer-Porter tube with one equivalent of $NaBPh_4$. The tube was sealed and pressurized to 40 psi N_2 and stirred for at least 24 hours. After the reaction, the tube was vented and the reaction mixture filtered over celite to yield the product.

5.3. Previous Work with $Fe(P_2)_2X_2$ Complexes

5.3.1. Reaction of the Secondary Phosphines with $FeCl_2{\cdot}4H_2O$

The majority of templates for the synthesis of macrocyclic phosphines are square-planar d^8 metals, coordinated by two bidentate secondary phosphines.[9-13] However, can octahedral iron-phosphine complexes be used as templates for macrocyclic iron-phosphine complexes? Iron(II) would be the ideal template because it is the metal of choice for the reversible N_2-binding chemistry described in the introduction. To answer this question, ligands MeOPrPE and MeOPrPP were each reacted with $FeCl_2{\cdot}4H_2O$ (Scheme 2).

Scheme 2. Preparation of *cis*-$Fe(P_2)_2Cl_2$ complexes

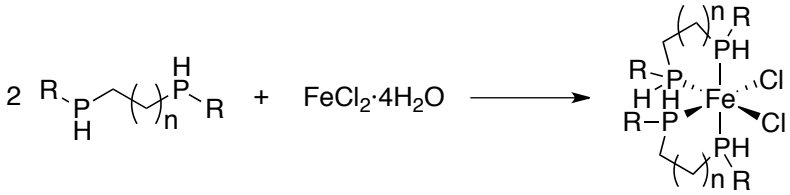

	n	R
1	1	$CH_3O(C_3H_6)$
2	2	$CH_3O(C_3H_6)$
3	1	Ph
4	2	Ph

Addition of 2 equivalents of MeOPrPE or MeOPrPP to $FeCl_2 \cdot 4H_2O$ in THF immediately gave complexes identified by elemental analysis and mass spectrometry as **1** and **2**, respectively, as deep reddish-purple products. The $^{31}P\{^1H\}$ NMR spectra of these complexes showed a complicated series of peaks (see Appendix D), which made the spectra difficult to interpret definitively. However, the sharp singlets in some of the spectra may indicate the presence of symmetric *trans*-isomers. A number of both *cis*- and *trans*-$Fe(P)_4Cl_2$-type complexes (where P represents a phosphine ligand) have been synthesized previously by us and others.[1,14-244,24–34] In all cases, the *trans* complexes are green or yellow in color, while the *cis* complexes are red or purple (Table 1). Based on this simple rule-of-thumb, it is suggested that the geometries of the product complexes in Scheme 2 are *cis*-octahedral. Because of the flexible methoxypropyl substituents on these complexes, both **1** and **2** are viscous oils at room temperature.

Table 1. Selected FeP_4Cl_2 complexes and their respective colors.

Complex	Color of Complex	Reference
trans-Fe(1,2-bis[(dihydroxybutyl)phosphino]ethane)$_2$Cl$_2$	Green	1
trans-Fe(1,2-bis[(methoxypropyl)phosphino]ethane)$_2$Cl$_2$	Green	1
trans-Fe(*cis*-1,2-bis[(diphenyl)phosphino]ethylene)$_2$Cl$_2$	Yellow	14
trans-Fe(*o*-phenylenebisdiethylphosphine)$_2$Cl$_2$	Green	15
trans-Fe(1,2-bis[(diethyl)phosphino]ethane)$_2$Cl$_2$	Green	15, 16
trans-Fe(1,2-bis[(dimethyl)phosphino]ethane)$_2$Cl$_2$	Green	18
trans-Fe(1,2-bis[(dipropyl)phosphino]ethane)$_2$Cl$_2$	Green	20
cis-Fe{(HOCH$_2$)P{CH$_2$N(CH$_2$P(CH$_2$OH)$_2$)-CH$_2$}$_2$P(CH$_2$OH)}Cl$_2$	Violet	21
cis-Fe(1,2-diphospholanoethane)$_2$Cl$_2$	Violet	22
cis-Fe(Ph$_2$PCH$_2$CH$_2$PPhCH$_2$PPhCH$_2$- CH$_2$PPh$_2$)Cl$_2$	Violet	23

In order to obtain further evidence consistent with the proposed *cis*-octahedral geometry, $FeCl_2 \cdot 4H_2O$ was reacted with the hydrophobic secondary phosphines 1,2-bis-(phenylphosphino)ethane (MPPE) and 1,3-bis(phenylphosphino)propane (MPPP), which are more likely to crystallize than the products obtained with MeOPrPE and MeOPrPP. (The assumption in making the complexes with these ligands is that they would form complexes with geometries identical to those with ligands MeOPrPE and MeOPrPP.) Reddish-purple solids **3** and **4** were obtained from the MPPE and MPPP reactions, respectively. Single crystals of **4** were grown and analyzed by X-ray crystallography (Figure 1). Note the *cis*-octahedral geometry of the complex. Also note the phosphorus atoms in the MPPP ligands are of *R,R* and *S,S* stereochemistry and are coordinated to the iron in a Λ (left-handed twist) fashion. The space group is P21, meaning that the crystal is enantiopure. Each six-membered metallacycle has a chair conformation. The bite angles for the MPPP ligands are 91.09(5)° (*R,R*) and 88.81(5)° (*S,S*). The chloro ligands and the phosphorus atoms *trans* to them are almost exactly coplanar with the central iron

atom (sum of L-M-L angles = 359.9(1)°), and thus can be considered an equatorial plane. One of the axial phosphines (P2) is nearly orthogonal to the equatorial plane, while the other (P3) is tilted about 10° toward the chloro ligands.

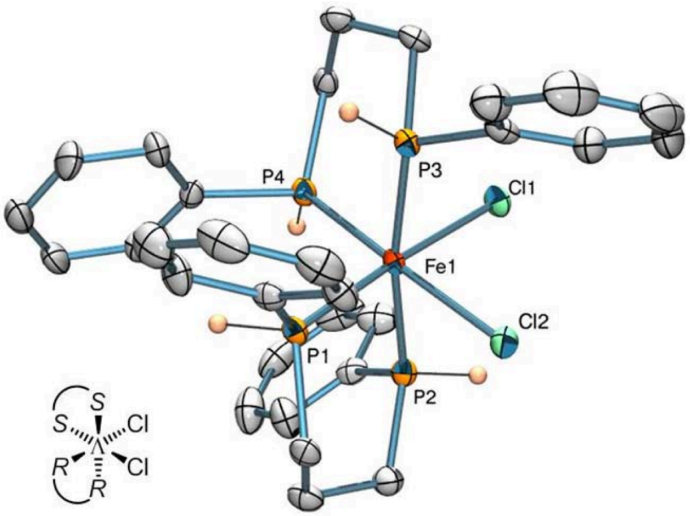

Figure 1. ORTEP plot (ellipsoids at 50% probability) of *cis*-Fe(MPPP)$_2$Cl$_2$ (**4**). Only the hydrogen atoms bonded to P are shown; the other hydrogen atoms have been omitted for clarity.

Because of the chirality of the secondary phosphine groups on these complexes, as well as the twist chirality of the *cis*-octahedral metal center, these complexes can exist as a mixture of up to 7 diastereomeric pairs of enantiomers. Only three of these pairs are sufficiently symmetric to give rise to a simple A_2B_2 pattern (two triplets) in the ^{31}P NMR spectrum. The rest of the isomers are of such low symmetry that all phosphorus atoms are magnetically inequivalent and couple as four-spin systems, resulting in a complicated ^{31}P NMR spectrum for each of these complexes. Thus, as was the case with **1** and **2**, the ^{31}P NMR spectra of **3** and **4** exhibited multiple peaks that cannot be definitively

interpreted. It is noted that, in a few attempts to prepare **3** in THF, a bright green precipitate was observed as the major product and isolated. The $^{31}P\{^{1}H\}$ NMR spectrum of a freshly prepared $CDCl_3$ solution revealed a sharp singlet at +71.2 ppm as the major peak ($J_{P\text{-}H}$ = 325 Hz in the proton-coupled spectrum), which indicates that the major product is a highly-symmetric isomer of *trans*-$Fe(MPPE)_2Cl_2$. This product was only soluble in dichloromethane and chloroform, and it isomerized rapidly to the *cis*-octahedral products in both solvents (see Appendix D). None of these spectra change upon heating or cooling, indicating that these isomers are diamagnetic at room temperature, i.e., there is no spin crossover.

5.3.2. Conversion of cis-$Fe(P_2)_2X_2$ to trans-$[Fe(P_2)_2(CH_3CN)_2]^{2+}$

In order to convert the *cis*-FeP_4Cl_2 complexes to *trans*-octahedral complexes suitable for use as templates, the chloro ligands were substituted by less π–donating ligands so they would be less likely to coordinate *trans* to the secondary phosphines. Acetonitrile was used as the new ligand because of its slightly π–accepting nature, ease of substitution, and weak coordination such that it could potentially be replaced by other ligands later in the synthesis. The *trans* complexes **5**-**8** were prepared directly using $[Fe(CH_3CN)_2](OTf)_2$ and the appropriate ligand (Scheme 3).* As with the *cis*-$Fe(P_2)_2Cl_2$ complexes, the lack of stereospecificity in the ligands resulted in multiple isomers of the [*trans*-$Fe(P_2)_2(CH_3CN)_2]^{2+}$ complexes **5**-**8**, as indicated by the multitude of peaks in the

* This synthesis gave pure products by elemental analysis and is therefore the recommended method for preparing the *trans*-$Fe(P_2)_2(CH_3CN)_2^{2+}$ complexes. Attempts to prepare **13**-**16** by reacting *cis*-FeP_4Cl_2 with CH_3CN did not give pure products.)

$^{31}P\{^{1}H\}$ NMR spectra. The observed ^{31}P NMR spectra were complicated and consequently no structural information could be obtained (Appendix D).

Scheme 3. Synthesis of the *trans*-$[Fe(P_2)_2(CH_3CN)_2]^{2+}$ complexes, **5-8**.

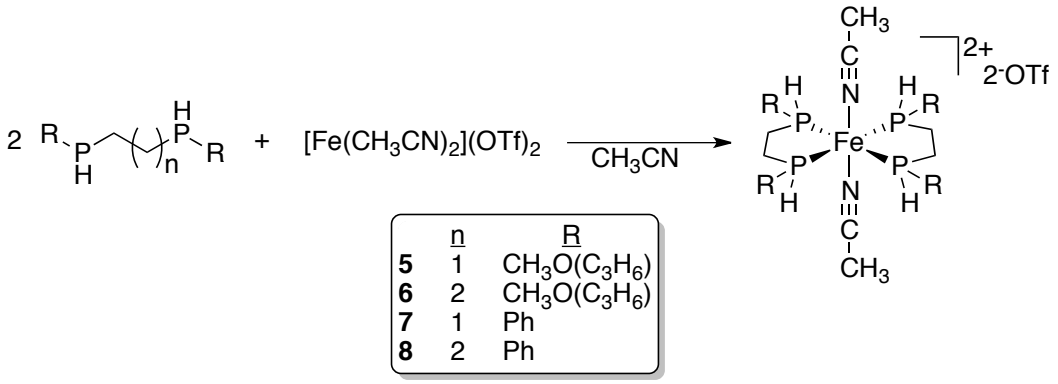

	n	R
5	1	$CH_3O(C_3H_6)$
6	2	$CH_3O(C_3H_6)$
7	1	Ph
8	2	Ph

In order to confirm the *trans* geometry of complexes **5-8**, single crystals of *trans*-$[Fe(MPPP)_2(CH_3CN)_2](PF_6)_2$ (**8-PF$_6$**) were grown and analyzed by X-ray diffraction (Figure 2). (The PF_6^- salt of the complex was used because the $^-$OTf salt did not give X-ray quality crystals.) The complex is indeed *trans*-octahedral and is C*i* symmetric, with both MPPP ligands lying in the equatorial plane. The stereochemistry of both MPPP ligands is *R*,*R*. Each six-membered metallacycle has a chair conformation. The bite angles for the MPPP ligands are 87.83(2)°. The axially coordinated acetonitrile ligands are nearly orthogonal to the equatorial plane (bond angles: P(1)-Fe-N 89.31°; P(2)-Fe-N 88.46°). One non-coordinated, disordered acetonitrile molecule is present as a solvent of crystallization.

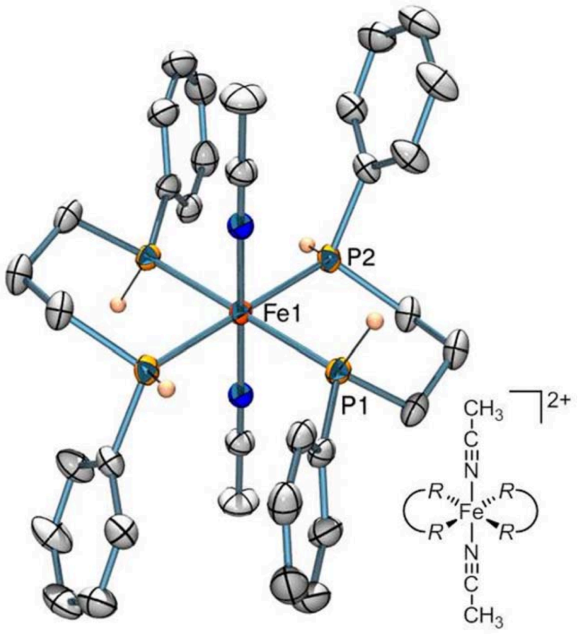

Figure 2. ORTEP plot (ellipsoids at 50% probability) of the cation of *trans*-$[Fe(MPPP)_2(CH_3CN)_2](PF_6)_2$ (**8-PF$_6$**). Only the hydrogen atoms bonded to P are shown; the other hydrogen atoms have been omitted for clarity.

5.3.3. Macrocyclization Reactions Using the $[Fe(P_2)_2(CH_3CN)_2]^{2+}$ Complexes.

Macrocyclic tetraphosphine ligands have previously been synthesized with secondary phosphines bonded to square-planar d^8 (Ni(II), Pd(II), or Pt(II)), or more rarely, tetrahedral d^{10} (Cu(I)) templates.[9-12,25] With both d^8 and d^{10} templates, not only does the metal act as a collection point, placing the phosphines in the correct stoichiometry and geometry for macrocyclization, but the metal also activates the phosphines toward alkylation.[12,26] This activation is two-fold: 1) coordination to the metal lowers the pK_a of the ligand, making deprotonation easier, and 2) back-donation from the electron-rich metal center destabilizes the lone pair on the deprotonated ligand, increasing its nucleophilicity.[26]

Experiments using a variety of conditions (different bases, various electrophiles, a

range of temperatures) showed that the P-H bonds in the *cis*-$Fe(P_2)_2Cl_2$ and *trans*-$[Fe(P_2)_2(CH_3CN)_2]^{2+}$ complexes were not alkylated under normal macrocyclization conditions. It is suggested that the absence of reactivity is caused by decreased electron density in the d^6 iron(II) atom in comparison to the more electron-rich d^8 and d^{10} metals normally used for templates. The decreased electron density of Fe(II) results in reduced nucleophilicity of the phosphido ligands after deprotonation.

5.4. Analysis of Coordination Chemistry and Macrocyclization of $Fe(P_4)X_2$ Complexes (P_4 = a Linear Tetradentate Phosphine)

5.4.1. Preparation of $Fe(P_4)X_2$ and $[Fe(P_4)(CH_3CN)_2](OTf)_2$ Complexes (P_4 = a Linear Tetradentate Phosphine).

Initial work focused on using an open-chain tetradentate mixed tertiary/secondary phosphine (see Chapter IV). The ligand (**9**) reacts with one equivalent of $FeCl_2 \cdot 4H_2O$ in THF to yield a purple solid product, proposed to be *cis*-Fe(**9**)Cl_2 (**10a**). There are three possible bonding motifs for a tetradentate ligand binding octahdedrally on a metal (cis-α, cis-β, and trans) (Figure 3). Because there are 10 possible stereoisomers, two meso forms and four possible pairs of enantiomers) and three possible geometries, it seemed likely and unfortunate that the ^{31}P NMR spectrum will be complicated (see Appendix D).

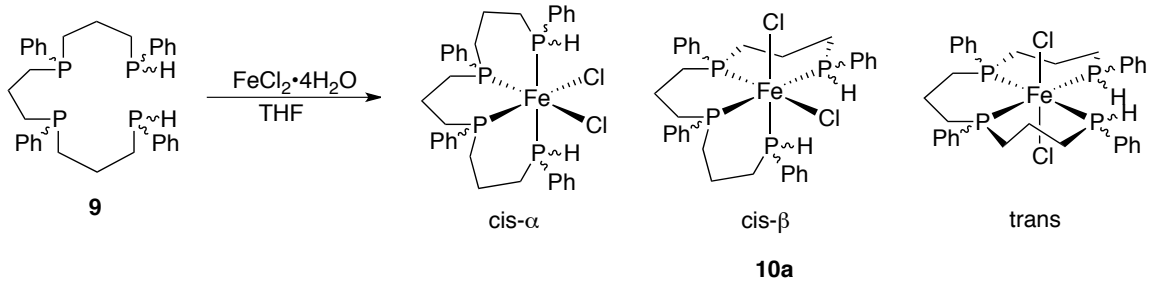

Figure 3. The three binding motifs in which tetradentate ligand **9** can coordinate to Fe(II) in an octahedral geometry to form **10a**.

The $^{31}P\{^{1}H\}$ NMR spectrum of **10a** in $CDCl_3$ shows three groups of peaks (Figure 5). The largest two peaks are triplets at 30.8 and 39.4 ppm, indicative of a A_2B_2 spin system with a single *cis* P-P coupling ($J_{P\text{-}P}$ = 60.4 Hz). If a *cis*-α geometry is assumed (*cis*-β will give four inequivalent phosphorus atoms regardless of the phosphine stereochemistry, so two triplets is not likely. Also, most *trans*-tetraphosphine iron(II) dichloride complexes are "typically" green in color, so it seems likely that a bulk of the species in solution adopts the *cis*-α geometry (see Table 1 above), there are only two stereochemistries where the terminal phosphorus atoms and the internal phosphorus atoms are equivalent, *RRRR/SSSS* and *SRRS/RSSR* (See appendix D); these combinations of geometry and stereochemistry gives rise to a simple A_2B_2 pattern but the *SRRS/RSSR* geometry is more sterically strained, so most likely the triplets arise form *RRRR/SSSS* in solution. Simulation of the spectrum with the coupling constants in Table 2 (Figure 4) is in good agreement with the experimental spectrum.

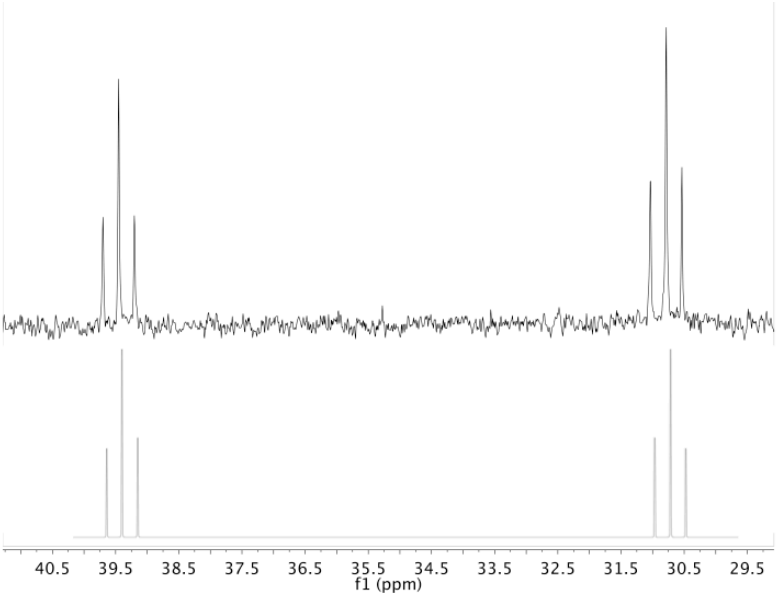

Figure 4. $^{31}P\{^{1}H\}$ NMR spectrum of the triplets of **10a** (top) and the simulated data for the triplets as an A_2B_2 spin system (bottom). The spectrum was simulated with *WinDNMR-Pro*.[27]

Table 2. The coupling constants for the doublet of doublet of doublets in the $^{31}P\{^{1}H\}$ NMR spectrum of **10a**.

Coupling constant	Value (in Hz)
J_{AB}	159.1
J_{AC}	54.0
J_{AD}	71.1
J_{BC}	68.9
J_{BD}	71.7
J_{CD}	40.5

The four other groups of peaks in the $^{31}P\{^{1}H\}$ NMR spectrum are doublets of doublets of doublets, indicating another species in solution where all four phosphorus atoms are inequivalent. The peaks at 15.2 and 28.4 ppm are attributed to the terminal

secondary phosphines and the peaks at 43.6 and 47.3 ppm are assigned to the internal tertiary phosphorus atoms. The coupling constants (Table 2) indicated that the system was coupling as an ABCD spin system. The coupling between the two secondary phosphorus atoms is 158.9 Hz, indicating that they are *trans* to each other in the complex, eliminating the possibility of both a *trans* or a *cis*-β geometry where the two P-H bonds would be *cis* to each other. In this case, the four-spin system arises from the *RSSS/SRRR* pair of enantiomers (see Appendix D). Simulation of the spectrum with the coupling constants in Table 3 (Figure 5) are in good agreement with the experimental spectrum. The data is consistent with **10b** being in a *cis*-α geometry, with at least two isomers in solution. The analogous bromide complex (**10b**) was prepared likewise and exhibited an analogous $^{31}P\{^{1}H\}$ NMR spectrum with similar coupling constants.

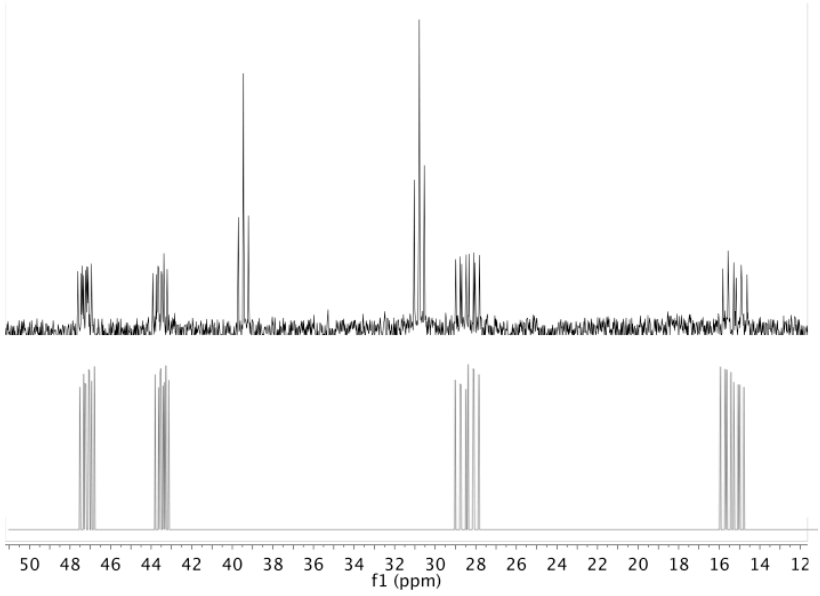

Figure 5. $^{31}P\{^{1}H\}$ NMR Spectrum of **10a** (top) and the simulated data for the doublet of doublet of doublets as an ABCD spin system (bottom). The spectrum was simulated with *WinDNMR-Pro*.[27]

In order to try and induce a *trans*-octahedral complex, complex **10a** was reacted with two equivalents of $NaBPh_4$ in CH_3CN to yield the bis(acetonitrile) complex (**11**) as an orange powder. The $^{31}P\{^1H\}$ NMR of this complex was too complicated to interpret accurately. This complex had comparable reactivity toward macrocyclization to the dichloride and dibromide species.

5.4.2. Macrocyclization Attempts using Fe(9)X_2

The goal of using iron as a template is to eliminate the use of a "surrogate" metal ion, streamlining the synthesis of iron(II)-tetraphosphine macrocyclic complexes. Macrocyclization of complex **10a** does not work using K_2CO_3 as a base as no evidence of any alkylation was observed using ESI-MS of the product obtained. When a stronger base, KO^{t}Bu, was used, the initially purple solution of complex **10a** turns a dark yellow color. Dropwise addition of 1,3-dibromopropane, 1,4-dibromobutane, or *o*-dibromoxylene leads to a color change from dark yellow to tan/brown with precipitate. After workup, some of the peaks in the ESI-MS indicated masses corresponding to the desired macrocyclic compounds with scrambling of the halides (typically, masses of $[M-Cl]^+$ and $[M-2Cl+Br]^+$ are both observed), but isolating a pure compound was not possible. If the iron(II) complex is prepared using $FeBr_2$ instead of $FeCl_2•4H_2O$, only $[M-Br]^+$ is observed in the ESI-MS for the macrocyclic complex, making the spectrum cleaner and easier to interpret (See Appendix D for ESI-MS).

Instead of adding a base to deprotonate the coordinated phosphine and adding an α-ω dihalide to bridge, there is literature precedent for adding α-ω dialdehydes and

diketones to act as bridges instead to form hydroxymethylphosphine linkages, without the need for a potentially detrimental base. In this vein, complexes **10a** and **10b** were treated with excess acetylacetone in THF and a color change from purple to red occurred. The solid powders (**12a** and **12b**, respectively) that were collected after removal of the solvent were analyzed with ESI-MS. Both reactions gave the same m/z of 715, corresponding to $[m\text{-}2X\text{-}H]^+$ (See Appendix D). This route may be a useful technique when coupled with water-solublizing ligands to help lend more hydrophilicity.

5.5. Synthesis of Hydrophilic Secondary Tetradentate Phosphine Ligands

Because of the success of macrocyclization of hydrophobic tetradentate ligands templated with both copper(I) (see Chapter IV) and iron(II), novel hydrophilic tetradentate phosphine ligands were envisioned. These ligand would be able to follow the same synthetic pathway as their hydrophobic counterparts, but impart water-solubility so that the complexes could be utilized in a pressure-swing absorption scheme to achieve the ultimate goal of removing N_2 from contaminated natural gas streams.

The synthetic strategy toward hydrophilic secondary tetradentate phosphines was to follow the same route as the hydrophobic ligand: 1) prepare a bis-secondary phosphine and a phosphinate bearing a water-solubilizng group 2) couple the two together using radical-activated hydrophosphination and 3) reduction to the phosphine. Since secondary bis-phosphines bearing methoxypropyl groups had already been synthesized, this seemed the logical point to start.

To prepare the desired phosphinate containing a methoxypropyl group, allyl diethyl phosphonite (**19**) was reacted neat with methoxypropyl bromide in an Arbuzov reaction to give the desired product (**13a**) as a colorless oil after distillation (Scheme 4). The phosphinate displayed a singlet in the $^{31}P\{^{1}H\}$ NMR spectrum at +53.1 ppm.

The same method was used to prepare other phosphinates bearing pro-hydrophilic groups (protected alcohols or amines, which upon either deprotection (alcohols) or alkylation (amines), give water-soluble groups). The amines that were investigated, dimethylaminoethyl chloride and dimethylaminopropyl chloride, posed problems because of the volatile nature of the amines and the relatively high temperatures needed for the Arbuzov reaction. These reactions could potentially work better with a much larger excess of the amine than used in these experiments to ensure enough amine stays around long enough to react. The protected alcohols investigated (3-bromopropanol protected with triisopropylsilyl chloride (**20**) and benzyl bromide (**21**)) proceeded smoothly to give the corresponding phosphinates **13b** and **13c**, respectively.

Scheme 4. Synthesis of **19** and Arbuzov reaction to form phosphinates **13a-e.**

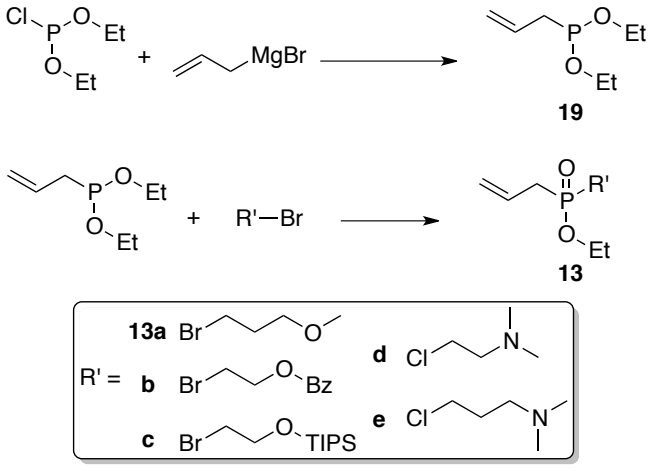

Phosphinate **13a** was taken on and reacted with MeOPrPE (Chapter II) with AIBN to give the mixed tertiary phosphine/phosphinate **14** as clear, colorless, viscous oil (Scheme 5). Bis-phosphonate **14** displays two resonances in the $^{31}P\{^{1}H\}$ NMR spectrum at +56.3 and -27.0 ppm, corresponding to the phosphinate and tertiary phosphine phosphorus atoms, respectively. **14** is then reduced with $LiAlH_4$ in ether to afford the mixed tertiary/secondary phosphine **15** as a colorless, viscous oil that has two resonances in the $^{31}P\{^{1}H\}$ NMR spectrum at -26.6 and -70.5 ppm, for the tertiary and secondary phosphorus atoms, respectively. In the proton-coupled ^{31}P NMR spectrum, the peak at -70.5 ppm splits into a doublet ($J_{P\text{-}H}$ = 199 Hz), which is expected for a secondary phosphine. Unfortunately, the phosphine is not appreciably water soluble.

Scheme 5. AIBN-mediated reaction to form **14**, followed by reduction to form **15**.

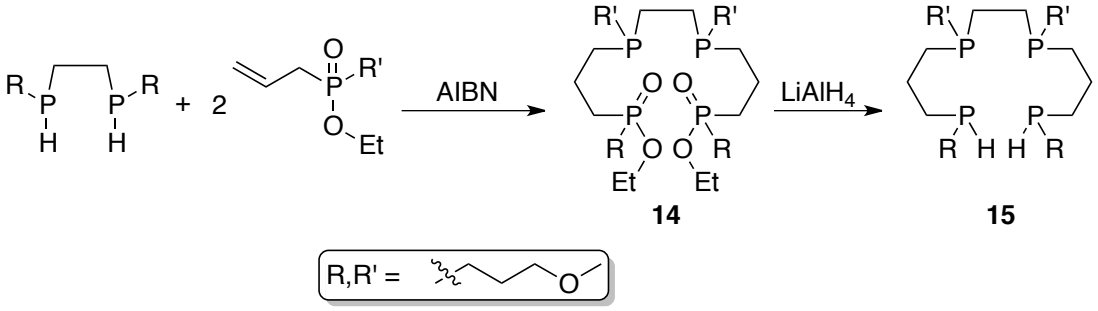

We proposed that perhaps four methoxy groups on a large ligand like **15** were not enough to lend appreciable water solubility. To address this, a ligand was envisioned that could encompass more methoxy groups on phosphorus. In order to do this, the ligand could not be macrocyclic in nature, but an open-chain tetradenate ligand where all the substituents on phosphorus were methoxypropyl groups. The same synthetic route as Scheme 5 was used, but instead using diethyl allylphosphonate instead of a substituted

phosphinate (Scheme 6). This compound, **16**, was prepared in near quantitative yield. The $^{31}P\{^{1}H\}$ NMR spectrum shows two resonances at -27.3 and +30.9 ppm, indicative of the internal tertiary phosphorus atoms and the terminal phosphonates. After reduction with $LiAlH_4$ in ether to give the phosphine ligand **17**, the phosphonate peak shifts to -138.7 ppm in the $^{31}P\{^{1}H\}$ NMR and is a triplet in the proton coupled spectrum ($J_{P\text{-}H}$=194.8 Hz), indicative of the tertiary/primary phosphine. Phosphine **17** then underwent hydrophosphination with allyl methyl ether in the presence of AIBN to yield phosphine **18** as a viscous oil. The $^{31}P\{^{1}H\}$ NMR of **18** showed peaks at -27.1, -31.5, and 32.0 ppm, with no peaks corresponding to primary phosphine, indicating that alkylation had occurred. This procedure works well to alkylate the phosphine, but optimization is needed in the future.

Scheme 6. Preparation of tetradentate ligand **18**.

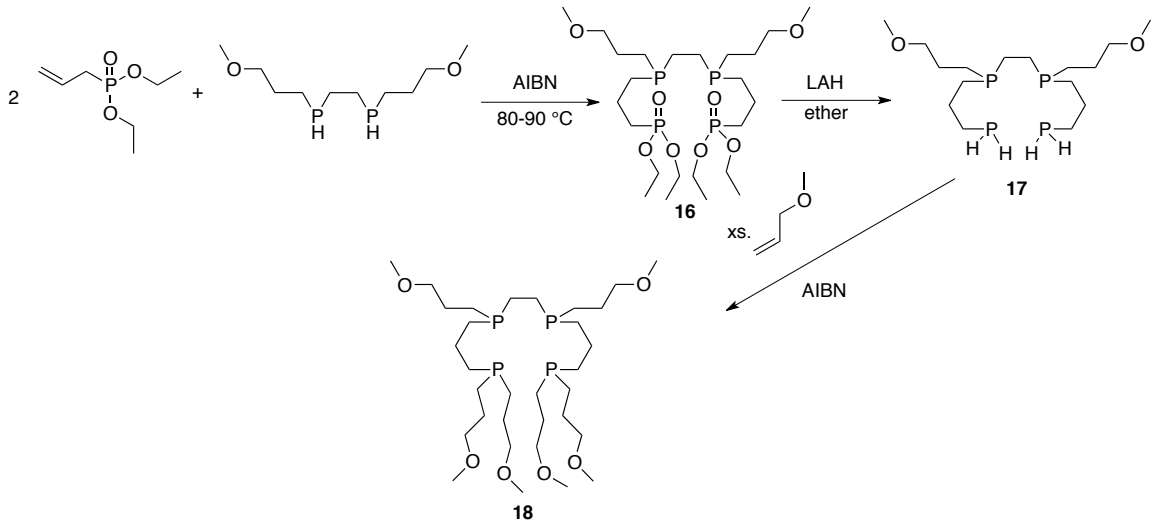

5.6. N_2-Binding Experiments

The use of transition metal complexes to coordinate dinitrogen and activate the rather inert molecule toward further reactivity has been investigated extensively though the years. In our particular application, we envision finding a suitable iron(II) complex that can reversibly bind dinitrogen for uses in nitrogen rejection.

A variety of iron(II) complexes bearing secondary phosphines or macrocyclic phosphines were investigated for their ability to bind N_2 (Table 4). The complex was dissolved in THF and pressurized to 40 psi N_2 in a Fischer-Porter tube and stirred rapidly for at least 24 hours. If the complex had a halogen, a halogen abstractor was also added to open a coordination site for N_2 (Scheme 7).†

Scheme 7. N_2-binding experiments with $Fe(P)_4Cl_2$ complexes.

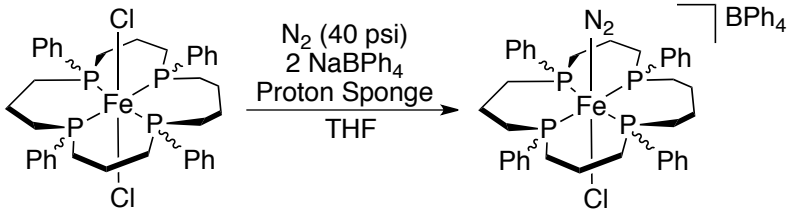

In order to determine if there was any coordinated N_2, liquid-cell IR or ATR measurements were taken of the complex before and after reaction with N_2 to look for the coordinated N_2 stretch. This stretch typically falls between 2008-2145 cm^{-1} for monomeric Fe(II)-N_2 complexes.[28] The results obtained for the Fe(II) complexes investigated in this study are summarized in Table 3.

† This method is not what would be used in an actual pressure-swing absorption application, where the halogens would not be removed so that when then N_2 pressure was released, the displaced halide could re-coordinate to regenerate the starting complex.

Table 3. IR N_2 binding data for selected iron(II)-phosphine complexes (all data taken with ATR attachment unless noted otherwise.

Complex	ν_{N-N} observed (cm^{-1})	ν_{C-N} observed (cm^{-1})	ν_{P-H} observed (cm^{-1})
$Fe(MPPE)_2Cl_2$ (**3**)	-	N/A	2319
$Fe(MPPP)_2Cl_2$ (**4**)	-	N/A	2310
$[Fe(MPPE)_2(CH_3CN)_2](OTf)_2$ (**7**)	-	2260	2303
$[Fe(MPPP)_2(CH_3CN)_2](OTf)_2$ (**8**)	-	not observable	2319
Fe(**9**)Cl_2 (**10**)	-	N/A	2305
$[Fe(\mathbf{9})(CH_3CN)_2](OTf)_2$ (**11**)	-	not observable	2315
$[Fe(P_{4\text{-}DBB})(CH_3CN)_2](OTf)_2$*	2096	2251, 2285	-
$Fe(MPPP)_2Cl_2$ (**4**) + $N_2/NaBPh_4$	-	N/A	2319
$[Fe(P_{4\text{-}DBB})(CH_3CN)_2](OTf)_2$* + N_2	2063§	not observable	-

§ Taken with a liquid IR cell. *Macrocyclic iron(II) complex $[(Fe(\mathbf{6b})(CH_3CN)_2](OTf)_2$ from Chapter IV

Even though Fe(II) tetraphosphine complexes normally bind dinitrogen readily, complexes bearing secondary phosphines do not, in these cases, bind N_2, even under 40 psi of N_2 pressure. The reason for this lack of reactivity may stem from an electronic effect. It is unlikely a steric effect as $[Fe(dppe)_2(H)]X$ ($X = BPh_4^-$, ClO_4^-) binds N_2 out of ambient air.[29] No iron(II) secondary phosphine complexes (see Chapter I) have been found to bind dinitrogen. One example, in particular, where complexes of the form $[Fe(PR_2H)_4X]Y$ (R_2 = Me(Ph), Et(Ph), $(Et)_2$; X = Cl, Br, I; Y = BF_4, PF_6) are formed, no N_2 binds to the five-coordinate species, even in an N_2 atmosphere.[30] Perhaps the lack of another alkyl group limits the donation from the phosphine to the metal, rendering it unreactive toward N_2. Additionally, the P-H bond antibonding orbital can accept

appreciable electron density from the metal. This may also have an effect on the electronics needed to coordinate N_2.

One particularly interesting result was for one of the macrocyclic Fe(II) complexes, $[Fe(P_{4\text{-}DBB})(CH_3CN)_2](OTf)_2$. This complex, prepared in a nitrogen-filled glovebox, displays a strong peak at 2096 cm^{-1}, assigned to coordinated N_2. This $\nu_{N\text{-}N}$ is lower than for free N_2 ($\nu_{N\text{-}N}$ = 2331 cm^{-1}), and is on the level of "typical" divalent iron complexes. This may indicate that the binding is relatively weak, which could be advantageous for a pressure-swing absorption process. As mentioned in Chapter IV, preparing the same complex in an argon-filled glovebox leads to a decrease in intensity of the N_2 stretch. Redissolving the complex and bubbling N_2 through the solution leads to a small increase in intensity (See appendix C for IR spectra).

5.7. Conclusions

Both bidentate and tetradentate phosphines bearing secondary phosphines coordinate to Fe(II) to yield *cis*-complexes. In the case of tetradentate ligand **9**, the ligand coordinates in a *cis*-α fashion to yield complexes **10a-b**. Iron complexes **3-6** do not alkylate cleanly to give macrocycles. However, **10a-b** do alkylate to give macrocyclic complexes by ESI-MS, but more work needs to done to determine the right conditions and workup to cleanly obtain iron(II) macrocyclic complexes directly.

Initial syntheses were completed to append water-solublizing methoxypropyl groups to the tetradentate phosphine scaffold. Unfortunately, it does not seem that these ligands are appreciably water-soluble, so other water-solublizing are likely needed.

Dinitrogen binding experiments show that iron complexes bearing secondary phosphines do not seem to coordinate dinitrogen, even under 40 psi of N_2; this lack of reactivity could stem from a lack of electron density at iron because the secondary phosphine doesn't donate as much electron density to the iron(II) center.(tolman) However, iron complexes bearing a tetraphosphine macrocycle bind N_2 from a N_2 filled glovebox, as shown by the $\nu_{N\text{-}N}$ at 2096 cm^{-1}.

In summary, direct alkylation to prepare tetraphosphine macrocycles directly on iron(II) seems promising. If this method can be developed, initial studies show that complexes bearing macrocyclic phosphines might be able to bind dinitrogen readily, which could hold promise for N_2-activation chemistry on iron.

5.8. Bridge

Chapter V described our efforts to prepare tetraphosphine macrocycles directly on iron(II), without the use of a "surrogate" metal. The ultimate goal is to take the iron(II) complexes bearing macrocyclic phosphine ligands and analyze their behavior in nitrogen binding and in a pressure-swing absorption model. Chapter VI describes the outlook of the project and some ideas for future directions.

CHAPTER VI

SUMMARY/OUTLOOK

6.1. Introduction

Macrocyclic phosphine ligands hold promise to be excellent ligands to provide extremely robust complexes because of the macrocyclic effect. However, their incorporation into complexes and catalysts have been hampered due to their extremely difficult syntheses. The syntheses that do exist are either lengthy, which makes the preparation extremely expensive, or low yielding, or both. The best routes utilize template syntheses, but only certain metals can be used effectively for tetraphosphine macrocycles.

The previous chapters have described our lab's work toward preparing tetraphosphine macrocycles using copper(I) as a template, and later, investigating the coordination chemistry and reactivity toward macrocyclization of iron(II). Chapter I summarized previous work done with the coordination chemistry and reactivity of secondary phosphines on transition metals. Chapter II looks at using copper(I) as a template for macrocyclization with two bidentate secondary phosphines. The phosphines on the templates are readily alkylated to give an all-tertiary phosphine product after demetallation with cyanide. The problem with this approach lies in the fact that it is difficult to determine if two small ring bidentate phosphines or one tetraphosphine

macrocycle is formed. Mass spectral evidence indicates that the macrocyclic product is formed, but better evidence in the form of a X-ray quality crystal would be quite beneficial. Additionally, theoretical work suggests that the macrocyclic product is energetically favored.

As mentioned, alkylation of secondary phosphines is one useful way to prepare higher order phosphines. One alternative way is to implement the phosphorus Mannich reaction between a hydroxymethylphosphine and an amine. Previous work in our lab discovered that the lone pair of the phosphine is integral to the phosphorus Mannich reaction, so coordinated hydromethylphosphines coordinated to metals can not react. Chapter III describes work with copper(I) as a template using 1,2-[bis(dihydroxymethyl)phosphino]ethane (DHMPE) as the hydroxymethylphosphine. An X-ray crystal structure of the complex shows that it crystallizes as a dimer in the solid state. To ascertain if the same behavior occurs in solution, ^{1}H-DOSY experiments were carried out and determined that the complex remains monomeric in solution.

Chapter IV investigates the same concept as Chapter II, but uses a tetradentate mixed tertiary/secondary phosphine coordinated to copper(I). With this synthetic modification, there is no possibility of a small ring double chelate product. Indeed this method works well to prepare macrocyclic Cu(I) complexes with a variety of bridging agents. The complexes can be demetallated with cyanide and the free phosphine can be used as a ligand on other metals of interest, specifically Fe(II).

Ideally, the macrocyclization reaction would be carried out on Fe(II), without using Cu(I) as a sort of "surrogate" metal; Chapter V looks at this particular synthetic

route. Unfortunately, secondary bidentate phosphines do not seem to be reactive towards macrocyclization on Fe(II). Curiously, the tetradentate phosphine used in Chapter IV does alkylate to give the expected macrocyclic product according to ESI-MS. However, the products from this reaction are difficult to purify and definitively characterize.

A modular synthetic method for preparing tetraphosphine ligands bearing water-solubilizing groups was devised. A variety of alkyl halides can be used to append hydrophilic groups to the scaffold via an Arbuzov reaction with phosphonites.

The N_2 binding capabilities of the iron(II) complexes that were prepared was also investigated. Interestingly, the iron complexes bearing secondary phosphines did not coordinate N_2, even at 40 psi of N_2. However, an iron complex with a coordinated macrocyclic tetraphosphine prepared from $Fe(CH_3CN)_2(OTf)_2$ seemed to spontaneously bind N2 under ambient pressures in a nitrogen-filled glovebox, as indicated by the $\nu_{N\text{-}N}$ at 2091 cm^{-1} in the IR spectrum.

6.2. Outlook

In light of our most recent FAB-MS mass spectrum of the 16-membered free macrocyclic P_4 ligand (made from bridging MPPE with 1,4-dibromobutane), indicating that two bidentate secondary phosphines do indeed close to make a macrocycle and not a double chelate small ring, it makes synthetic sense to stay with this route to macrocycles. Additionally, an X-ray crystal structure was obtained of the 16-membered P_4 macrocycle made from bridging MPPP with 1,3-dibromopropane, which matches the theoretically predicted stereochemistry, giving even more credence to the bis-bidentate route.

With this synthetic scheme sorted out, reactions can be scaled up to obtain a usable amount of macrocyclic ligand to investigate coordination to other metals, specifically Fe(II). The initial results outlined in Chapter IV indicate that Fe(II) complexes bearing tetraphosphine macrocycles could be outstanding for binding dinitrogen for uses in separation techniques or activation of N_2 toward reduction to ammonia.

Additionally, more time can be spent investigating how to make these complexes appreciably water-soluble. It may be that four pendant methoxypropyl groups on a macrocyclic phosphine might not be enough hydrophilicity, so a new method for adding water-solubility is needed. A promising route is to use pendant amino groups that could be protonated/alkylated to provide a cationic moiety, which should be appreciably water-soluble.

Another advantage of the route established for macrocycles is to prepare different size macrocycles so a systematic study can be done to establish the thermodynamic and kinetic parameters for the phosphine macrocycle effect, which has not be accomplished to date because of the lack of a practical synthesis for macrocycles. Now that a route has been established, this should be relatively straightforward to complete.

APPENDIX A

SUPPORTING INFORMATION FOR CHAPTER II

A.1. Spectra

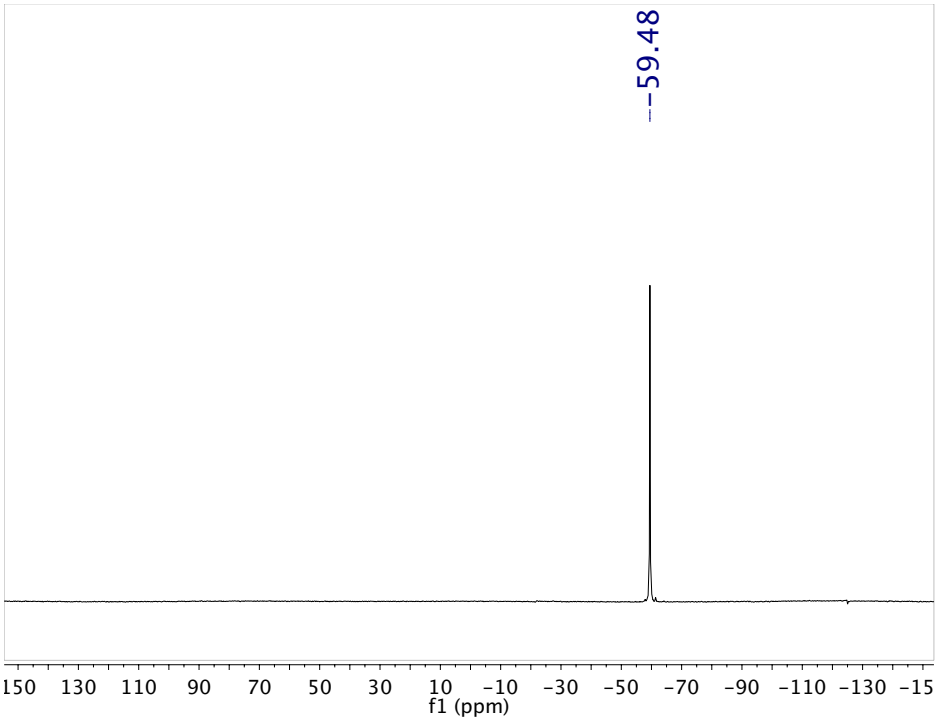

Figure A.1.1. $^{31}P\{^{1}H\}$ NMR Spectrum of MeOPrPE (**1**)

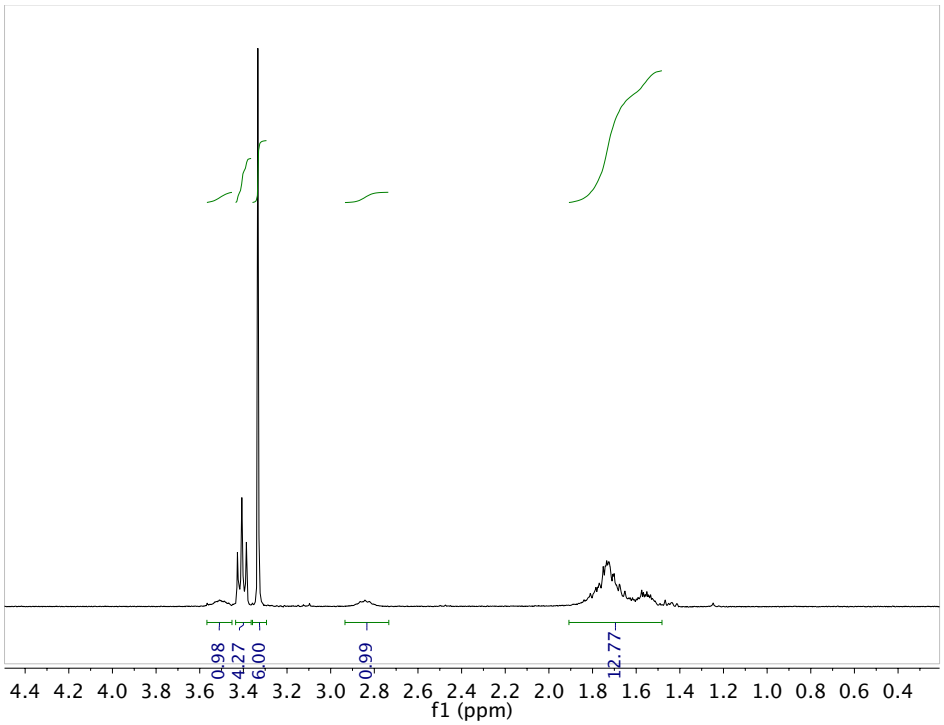

Figure A.1.2. ^{1}H NMR Spectrum of MeOPrPE (**1**)

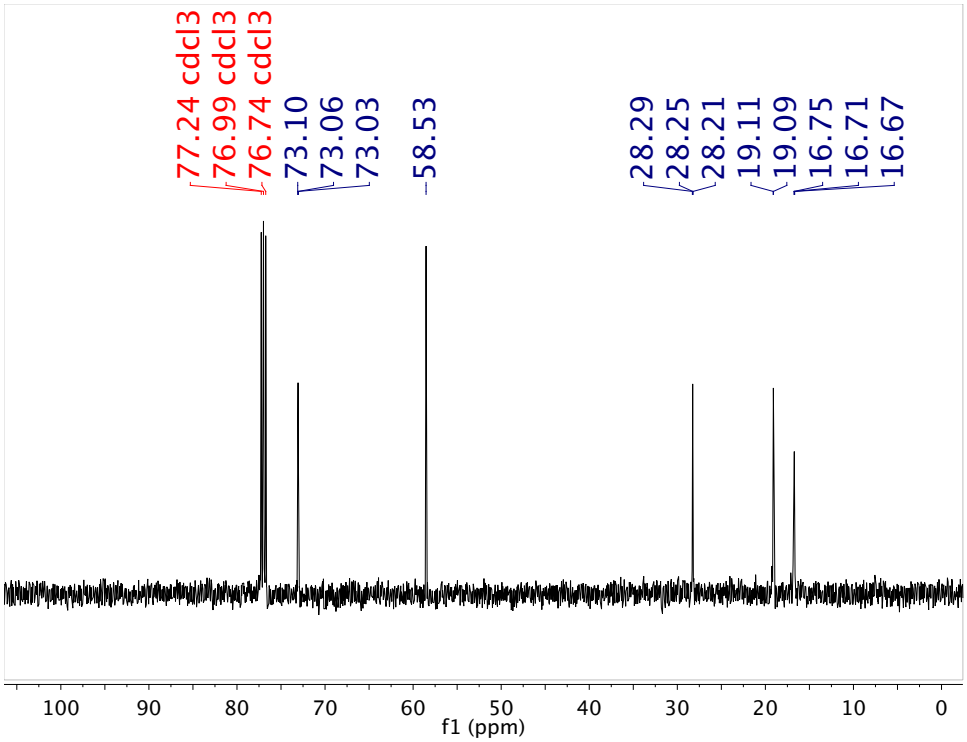

Figure A.1.3. ^{13}C NMR Spectrum of MeOPrPE (**1**)

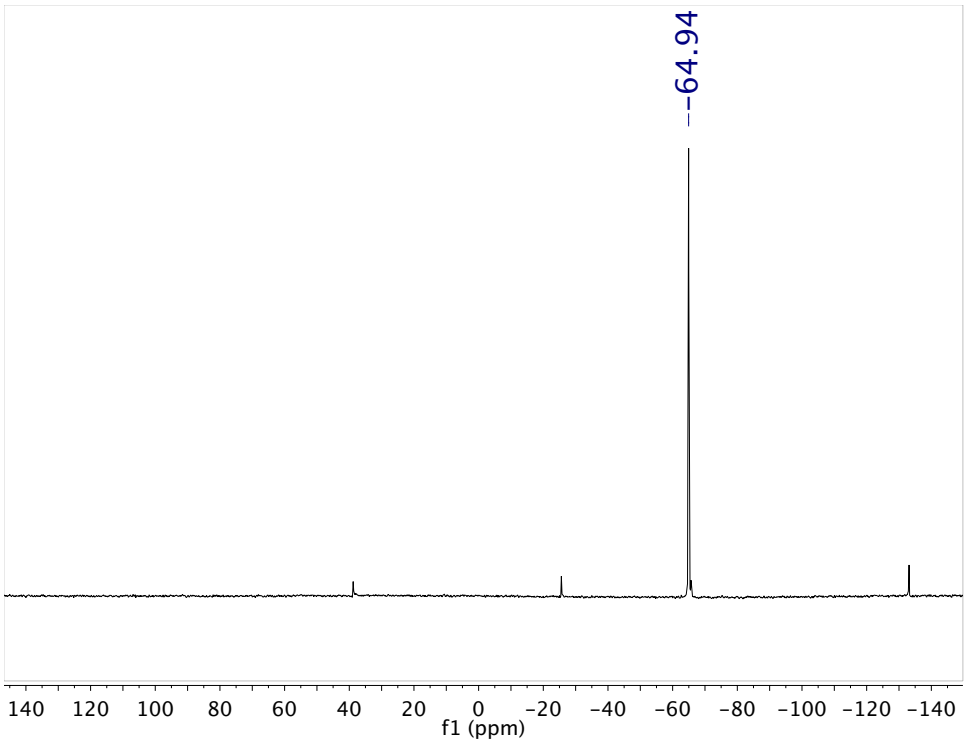

Figure A.1.4. $^{31}P\{^{1}H\}$ NMR Spectrum of MeOPrPP (**2**)

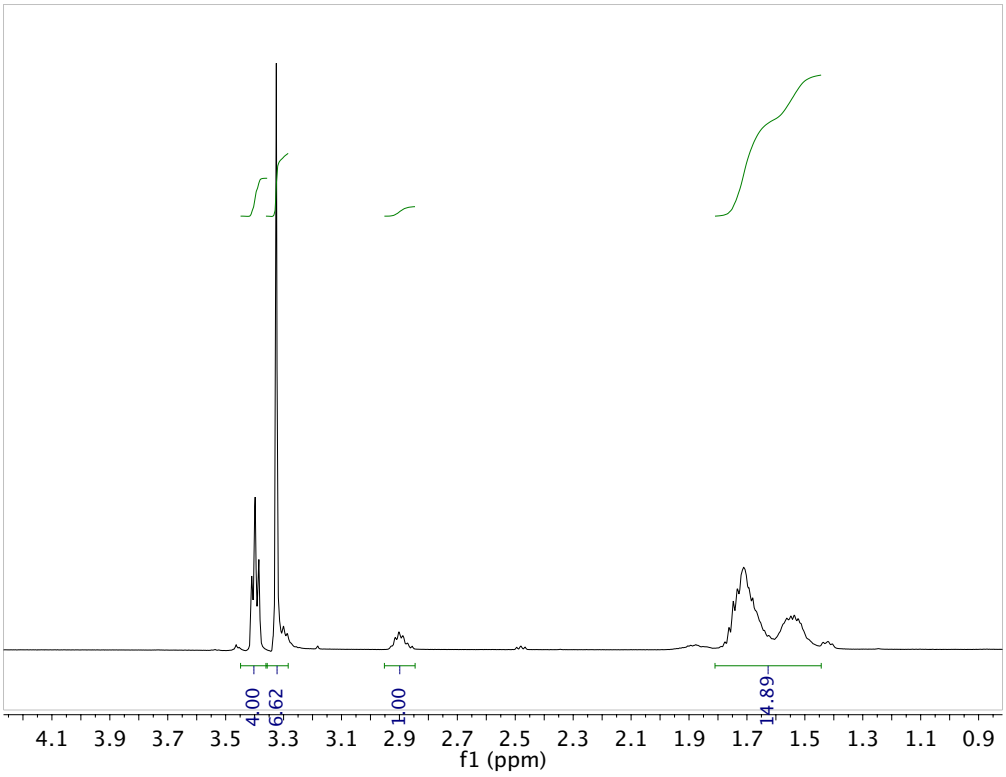

Figure A.1.5. ^{1}H NMR Spectrum of MeOPrPP (**2**)

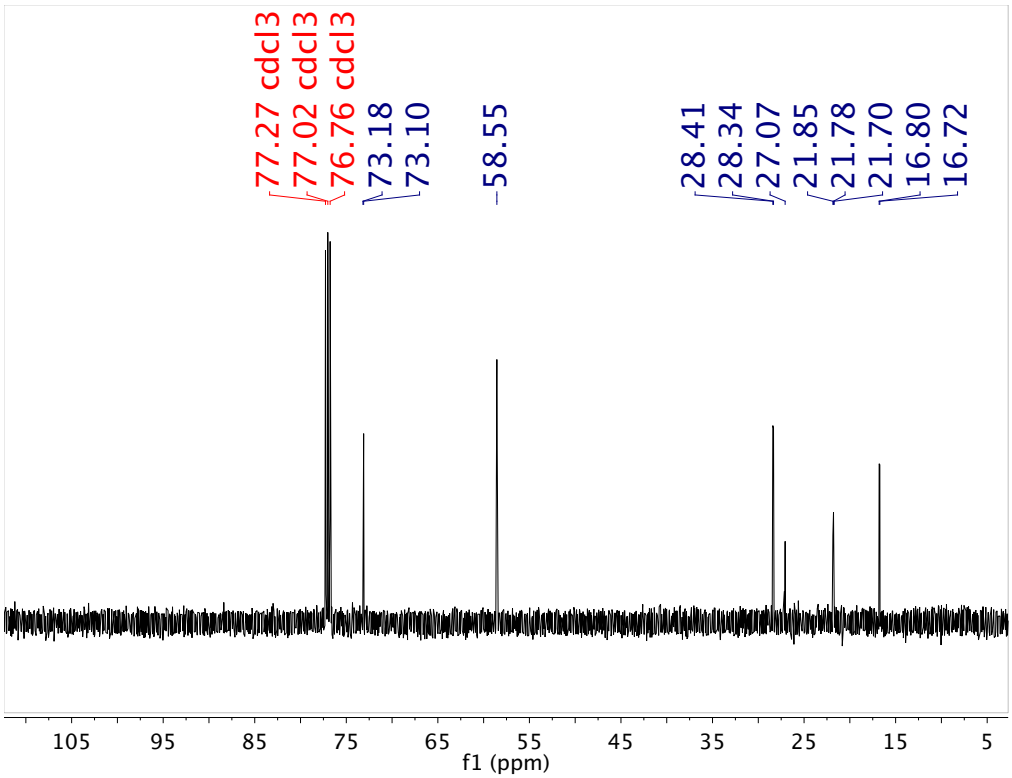

Figure A.1.6. ^{13}C NMR Spectrum of MeOPrPP (**2**)

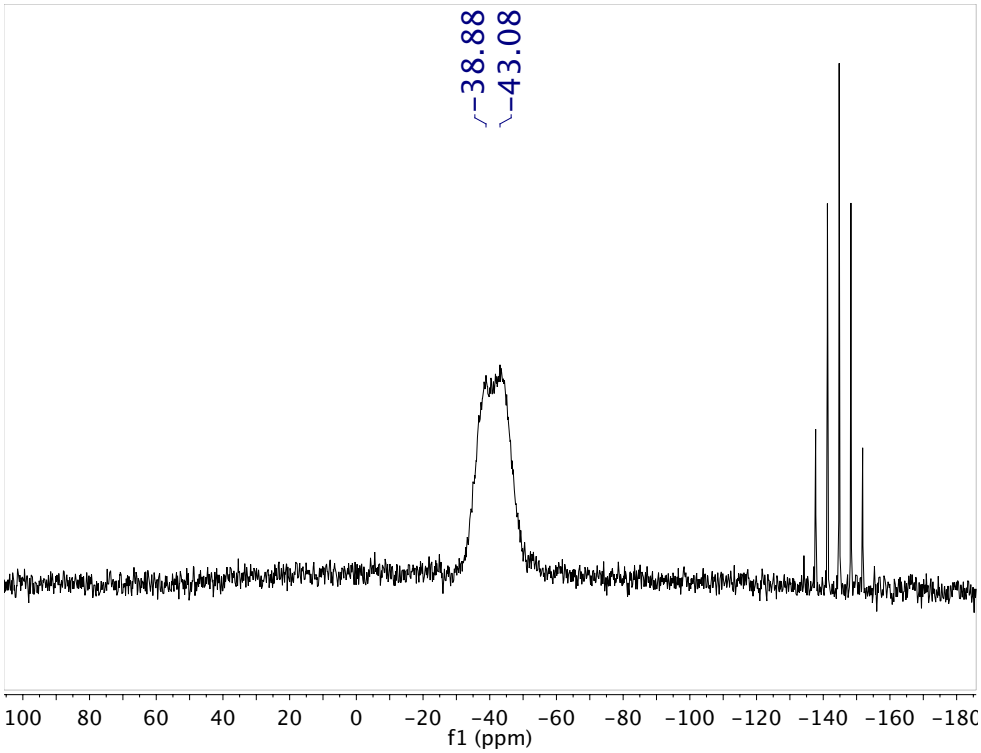

Figure A.1.7. $^{31}P\{^{1}H\}$ NMR Spectrum of (**3**)

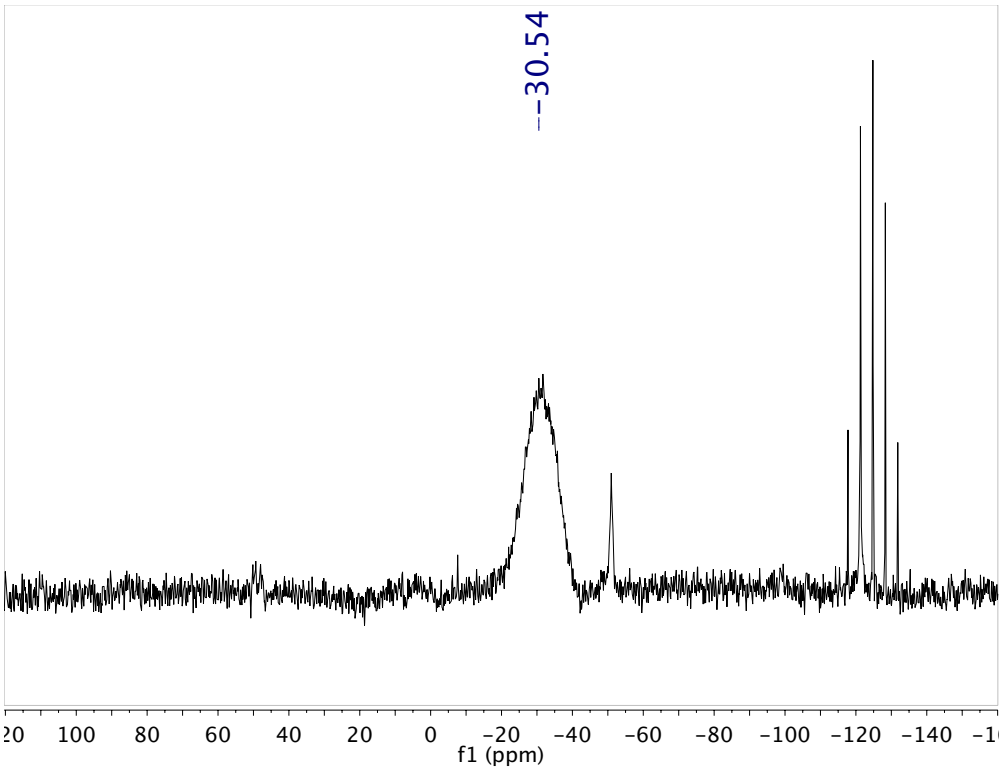

Figure A.1.8. $^{31}P\{^{1}H\}$ NMR Spectrum of (**4**)

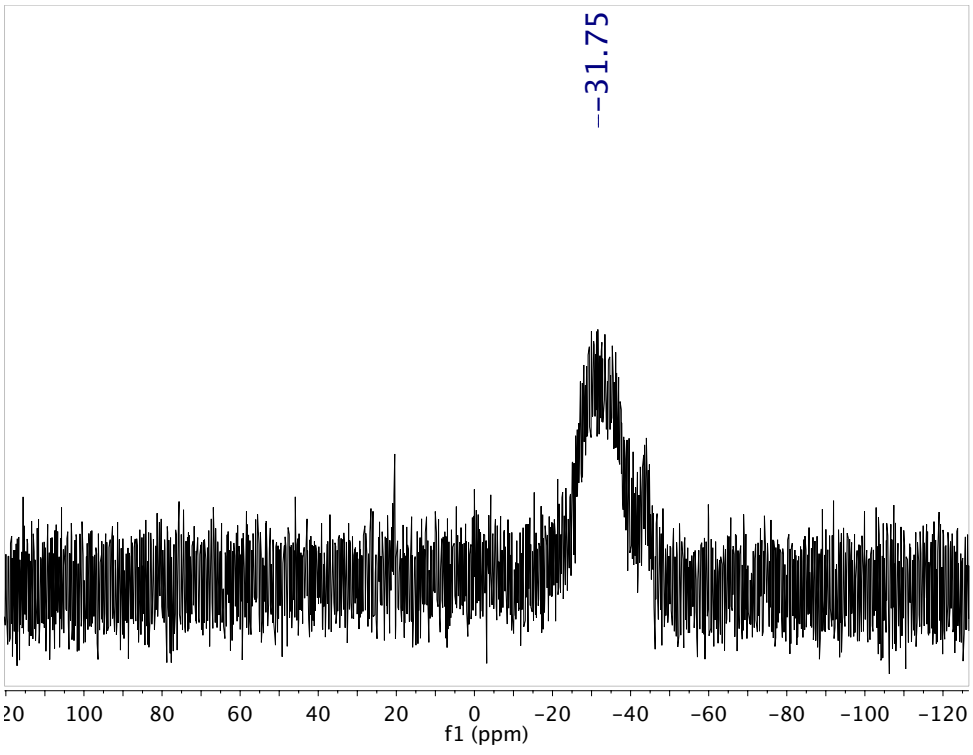

Figure A.1.9. $^{31}P\{^{1}H\}$ NMR Spectrum of (**5**)

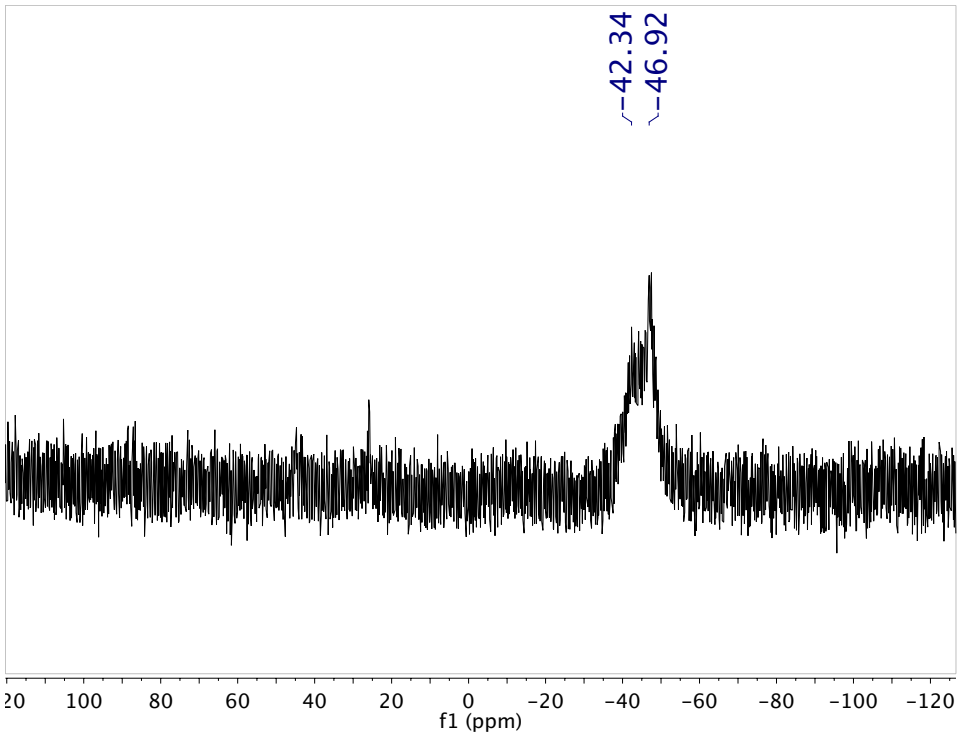

Figure A.1.10. $^{31}P\{^{1}H\}$ NMR Spectrum of (**6**)

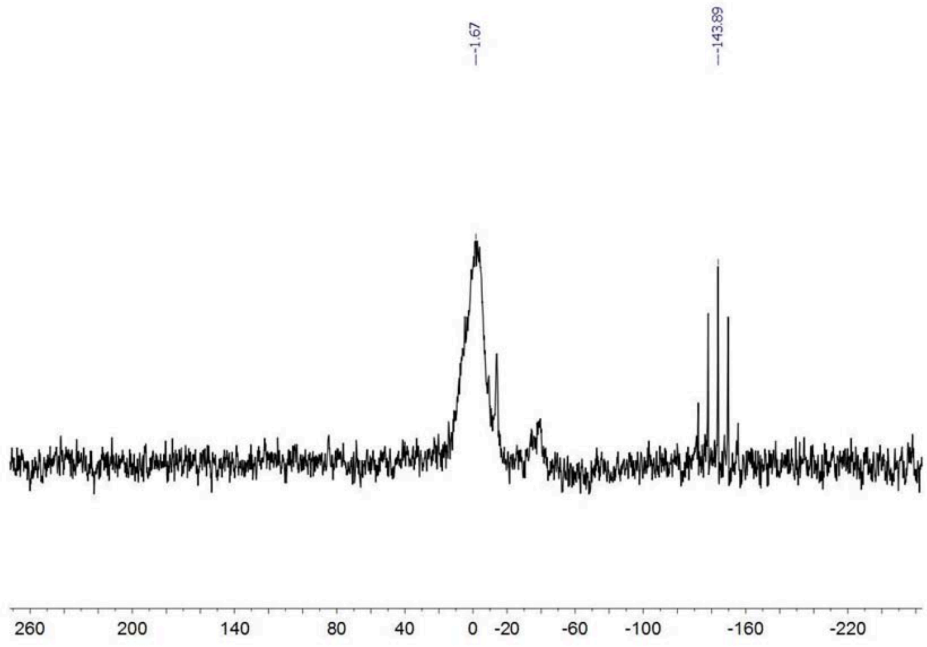

Figure A.1.11. $^{31}P\{^{1}H\}$ NMR Spectrum of [Cu(MeOPrPE)-P4$_{DBP}$]OTf (**7**)

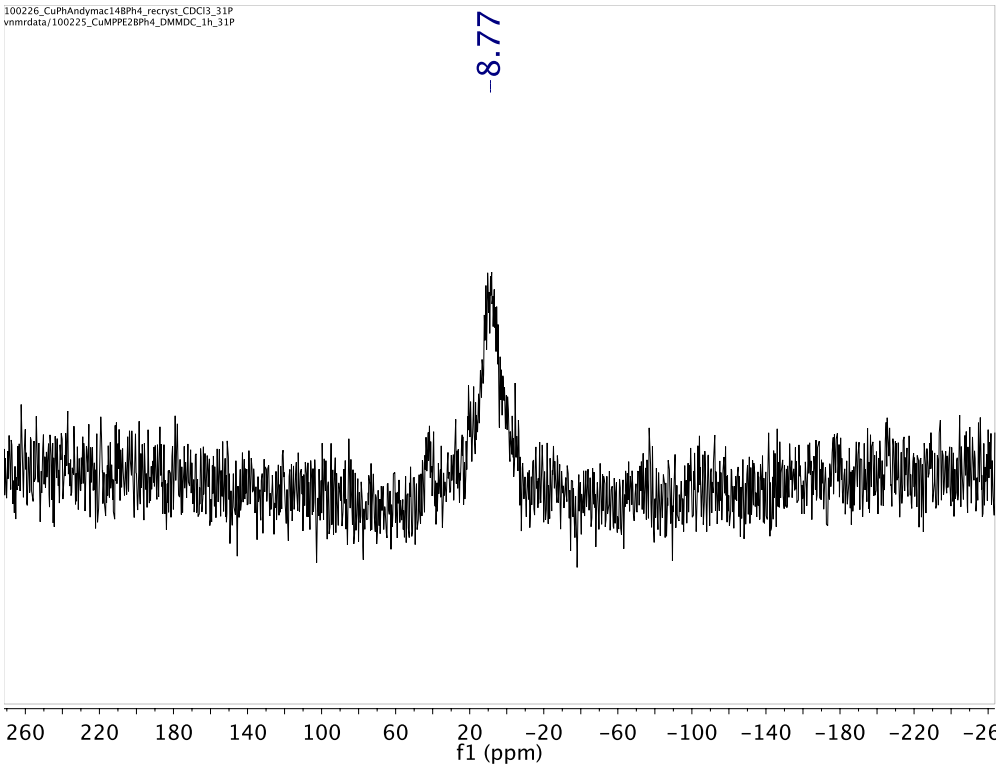

Figure A.1.12 $^{31}P\{^{1}H\}$ NMR Spectrum of [Cu(MPPE)-P4$_{DBP}$]OTf (**9**)

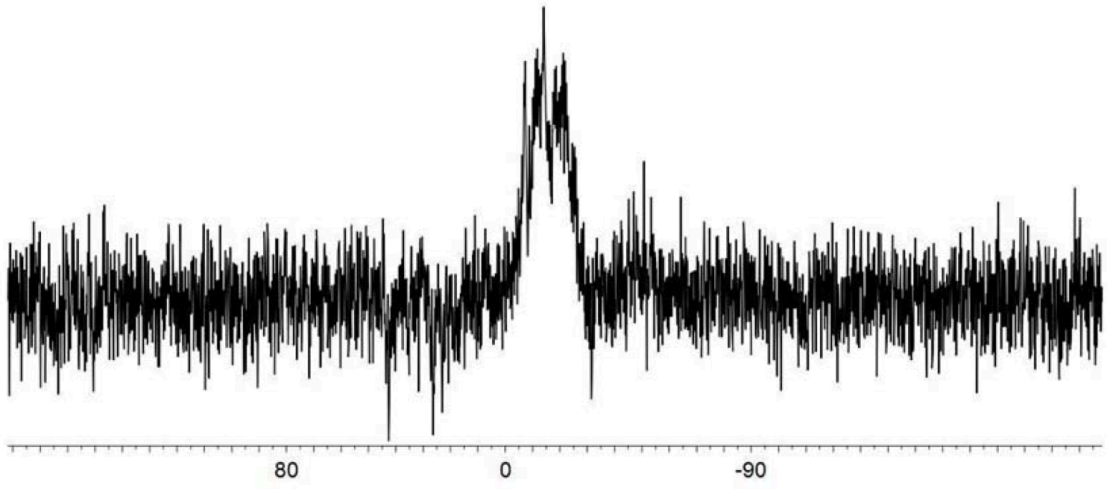

Figure A.1.13. $^{31}P\{^{1}H\}$ NMR Spectrum of [Cu(MPPP)-P4$_{DBP}$]OTf (**10**)

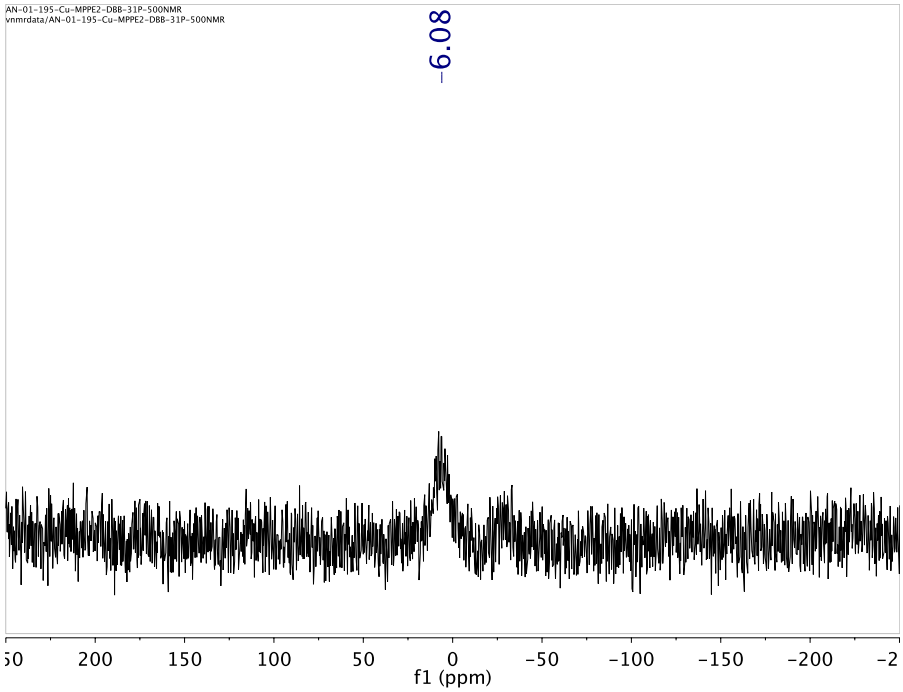

Figure A.1.14. $^{31}P\{^{1}H\}$ NMR Spectrum of [Cu(MPPE)-P4$_{DBB}$]OTf (**11**)

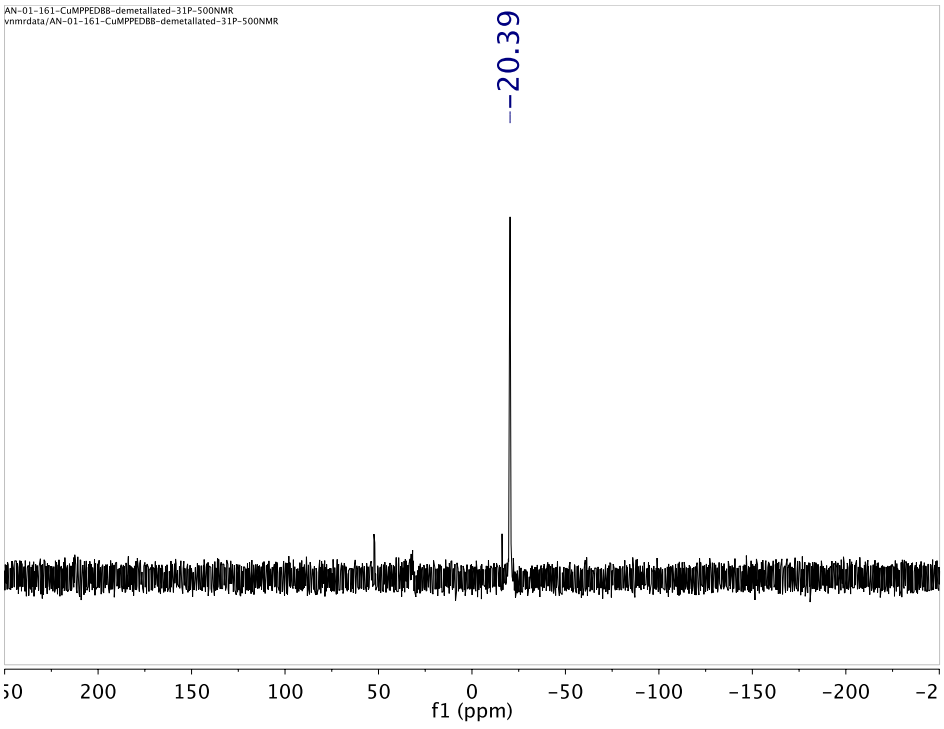

Figure A.1.15. $^{31}P\{^{1}H\}$ NMR Spectrum of **13.**

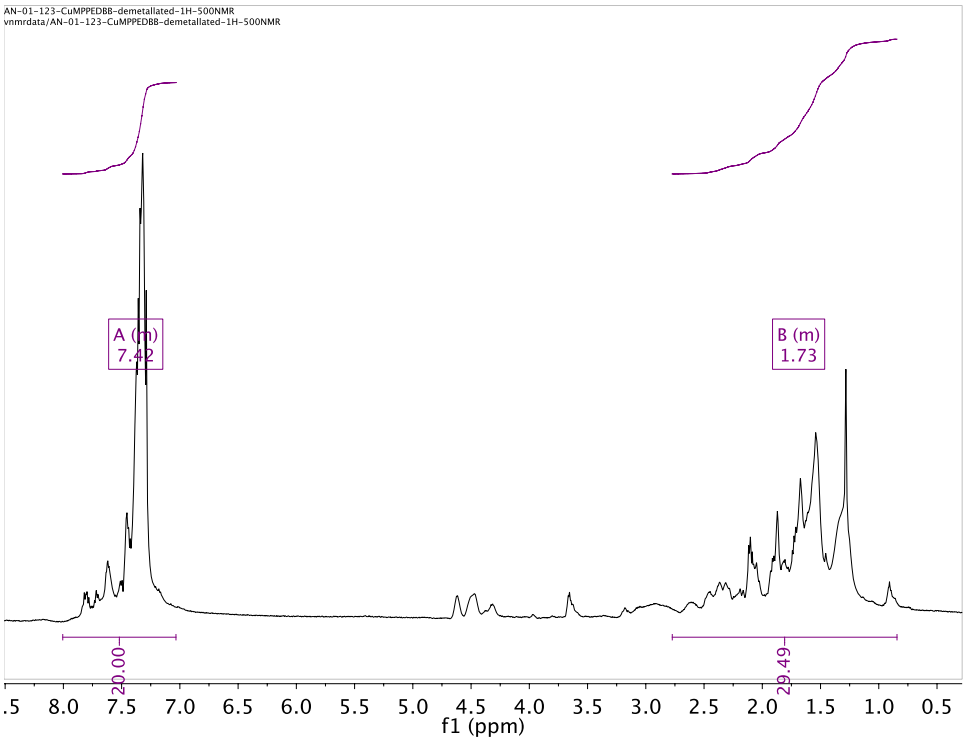

Figure A.1.16. ^{1}H NMR Spectrum of **13.**

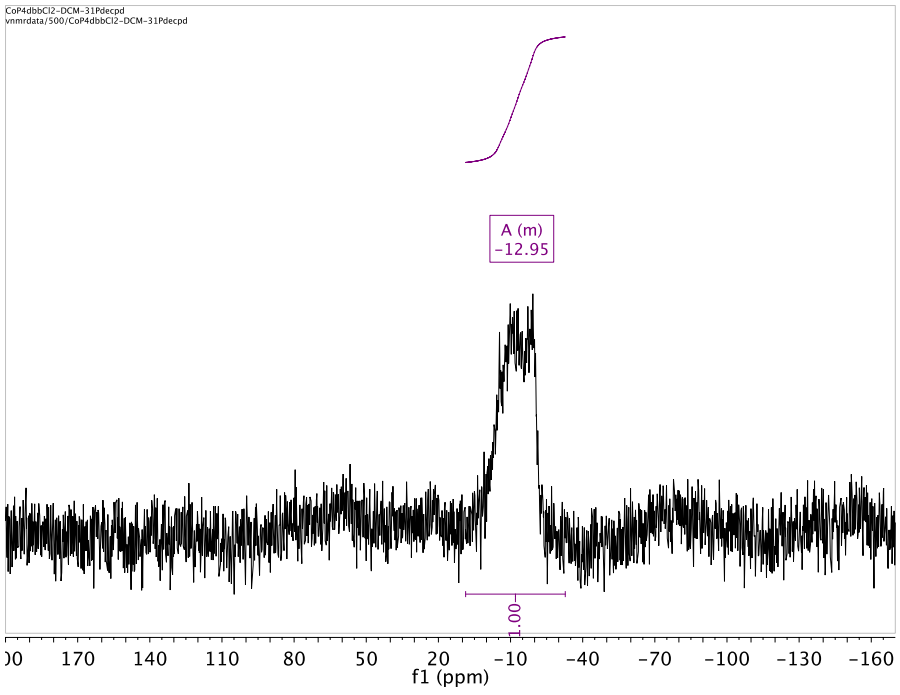

Figure A.1.17. $^{31}P\{^{1}H\}$ NMR Spectrum of Co(**13**)Cl_2.

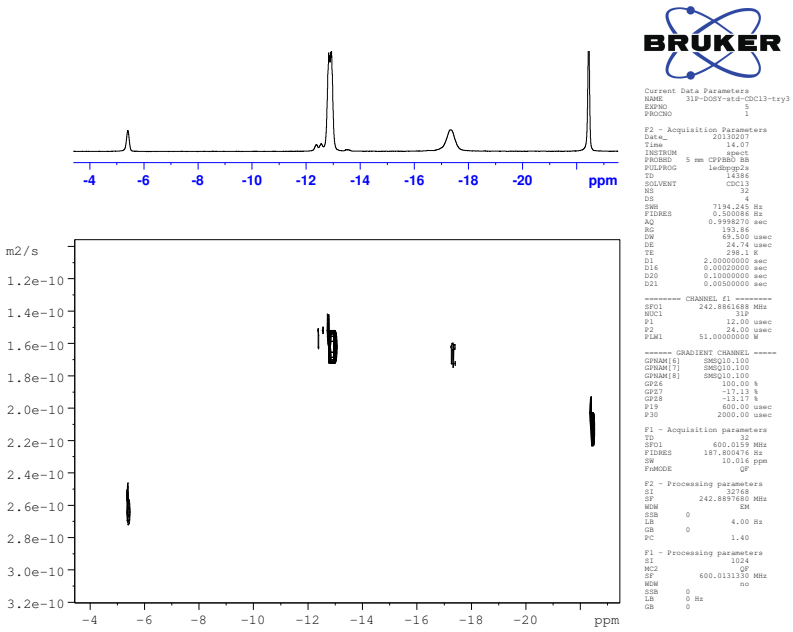

Figure A.1.18. ^{31}P-DOSY spectrum of triphenylphosphine, 1,1-bis(diphenylphosphino)methane, and TETRAPHOS-2.

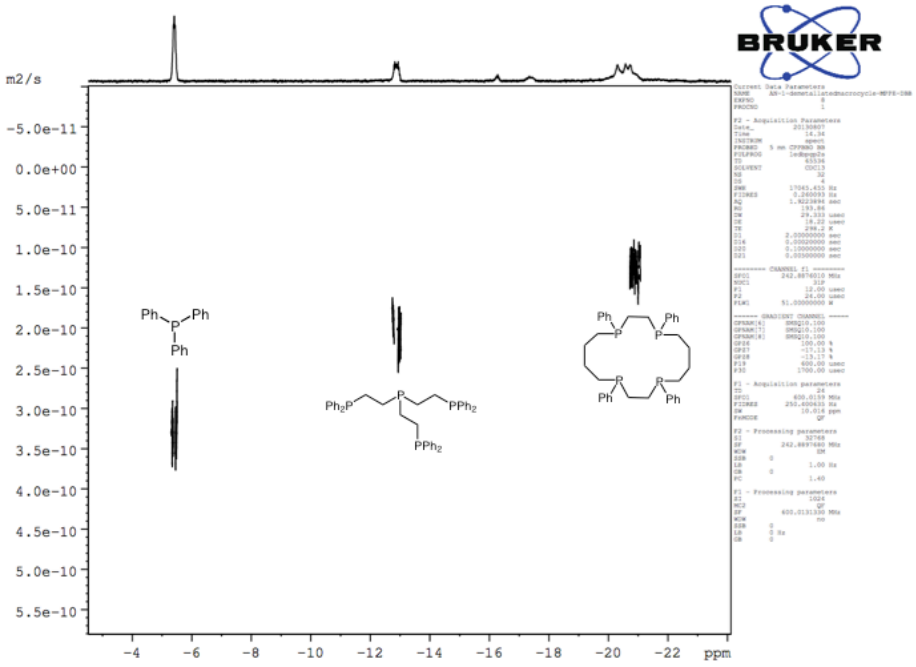

Figure A.1.19. ^{31}P-DOSY spectrum of triphenylphosphine, TETRAPHOS-2, and **13**.

A.2. Mass Spectra

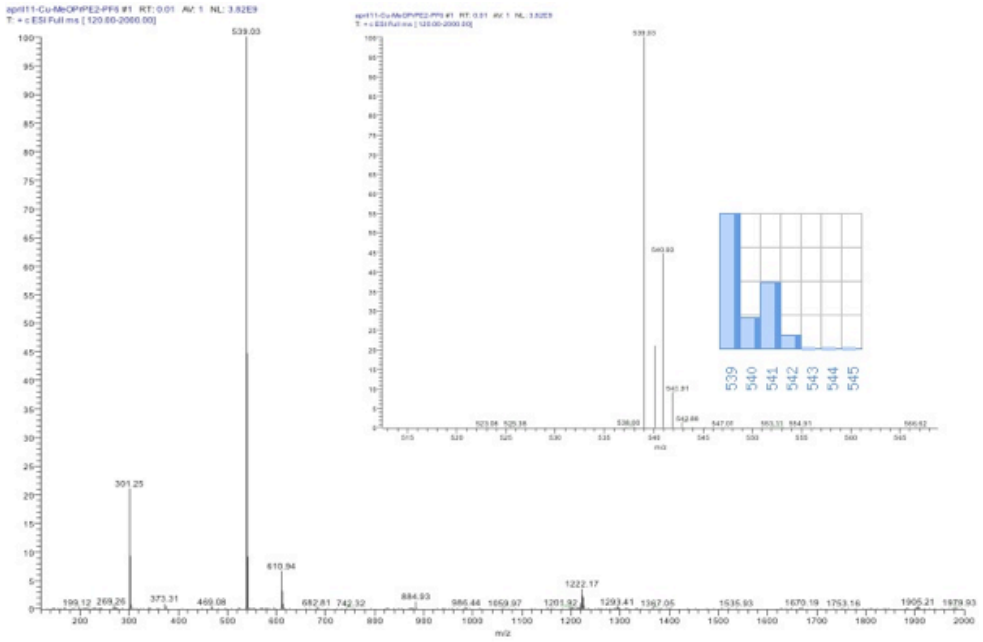

Figure A.2.1. ESI mass spectrum of $[Cu(MeOPrPE)_2]PF_6$ (**3**).

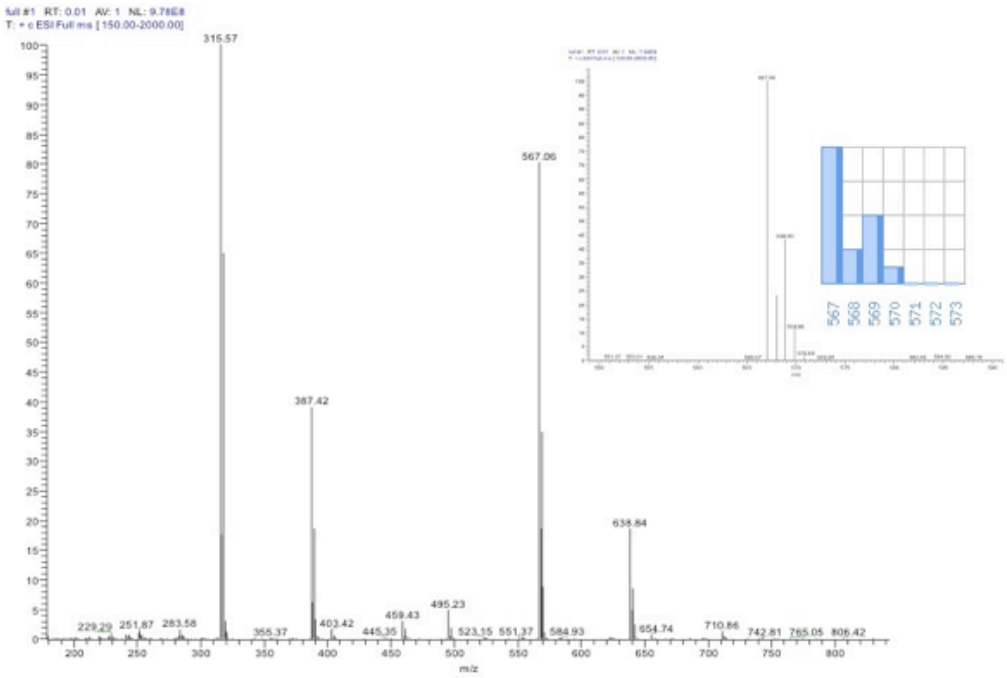

Figure A.2.2. ESI mass spectrum of $[Cu(MeOPrPP)_2]OTf$ (**4**).

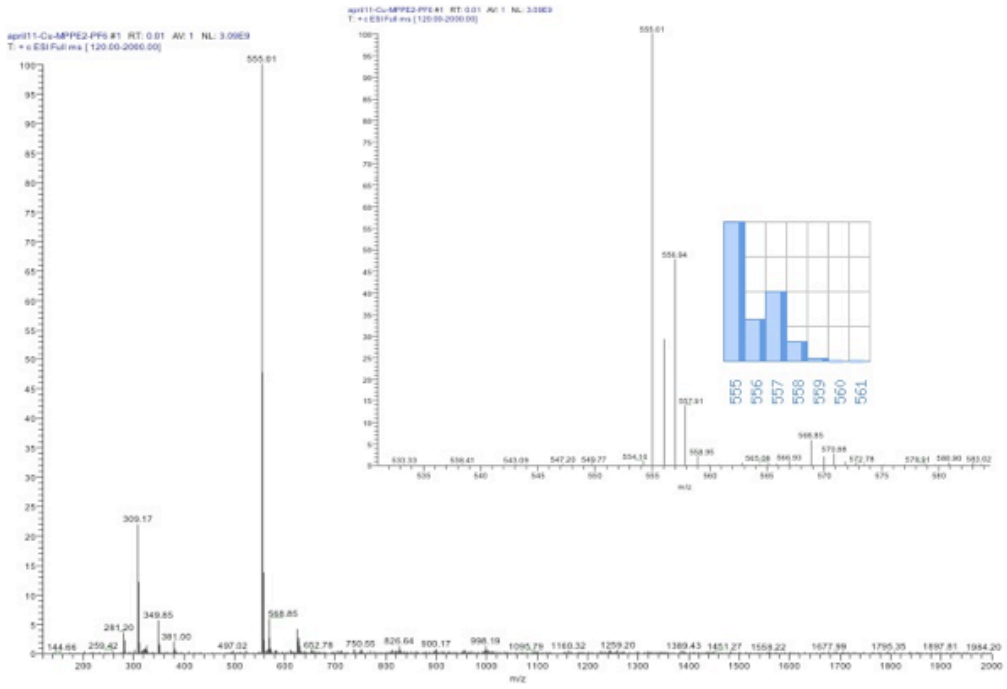

Figure A.2.3. ESI mass spectrum of $[Cu(MPPE)_2]PF_6$ (**5**).

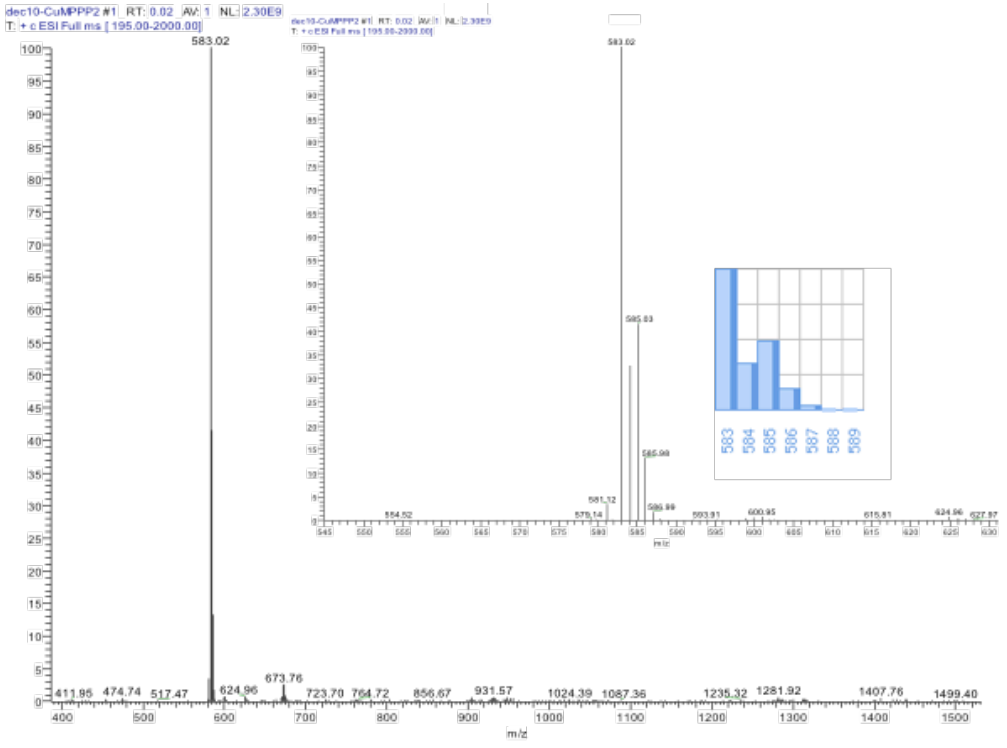

Figure A.2.4. ESI mass spectrum of $[Cu(MPPP)_2]OTf$ (**6**).

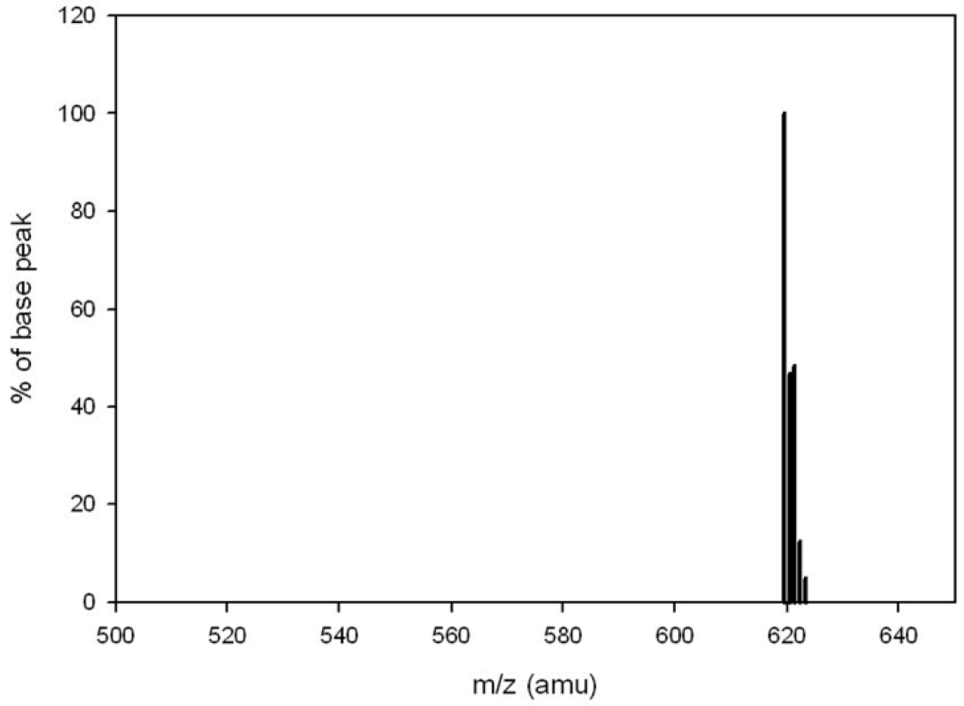

Figure A.2.5. ESI mass spectrum of [Cu(MeOPrPE)-P4$_{DBP}$]OTf (**7**).

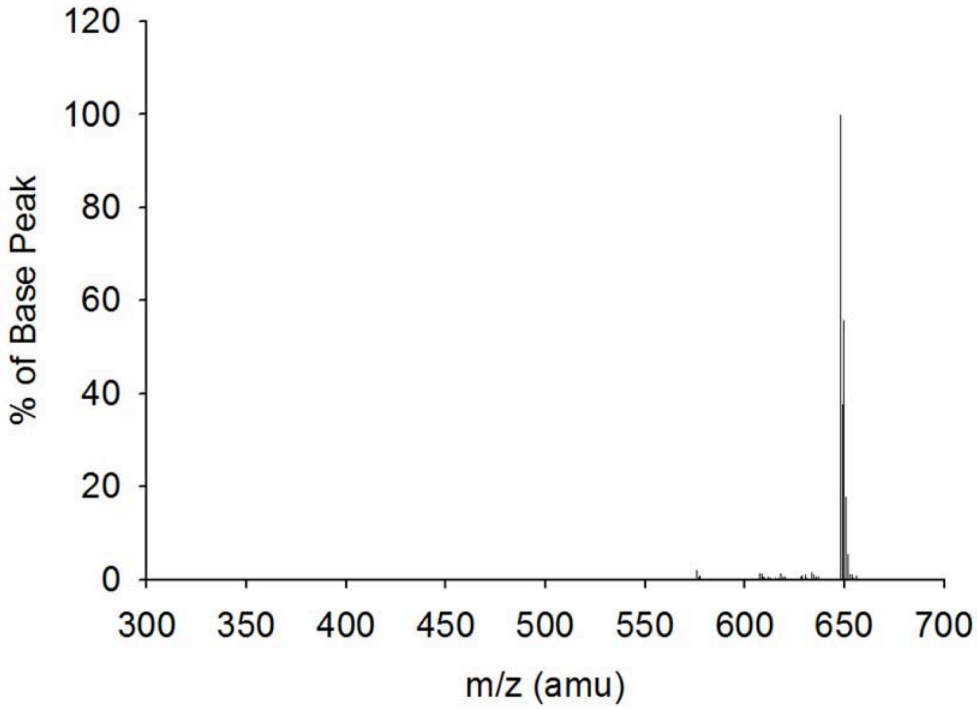

Figure A.2.6. ESI mass spectrum of [Cu(MeOPrPP)-P4$_{DBP}$]OTf (**8**).

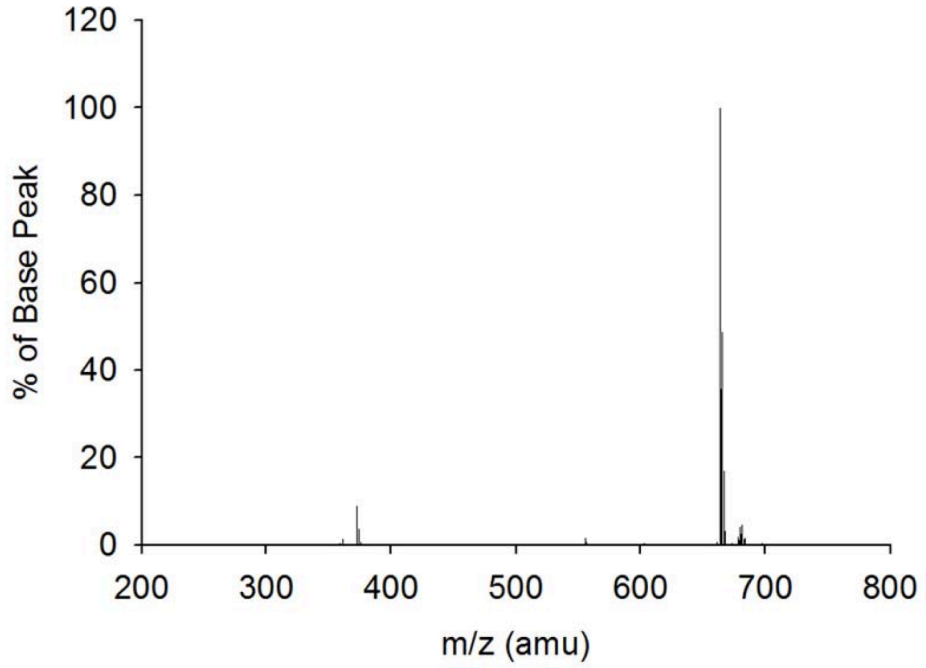

Figure A.2.7. ESI mass spectrum of [Cu(MPPP)-P4$_{DBP}$]OTf (**10**).

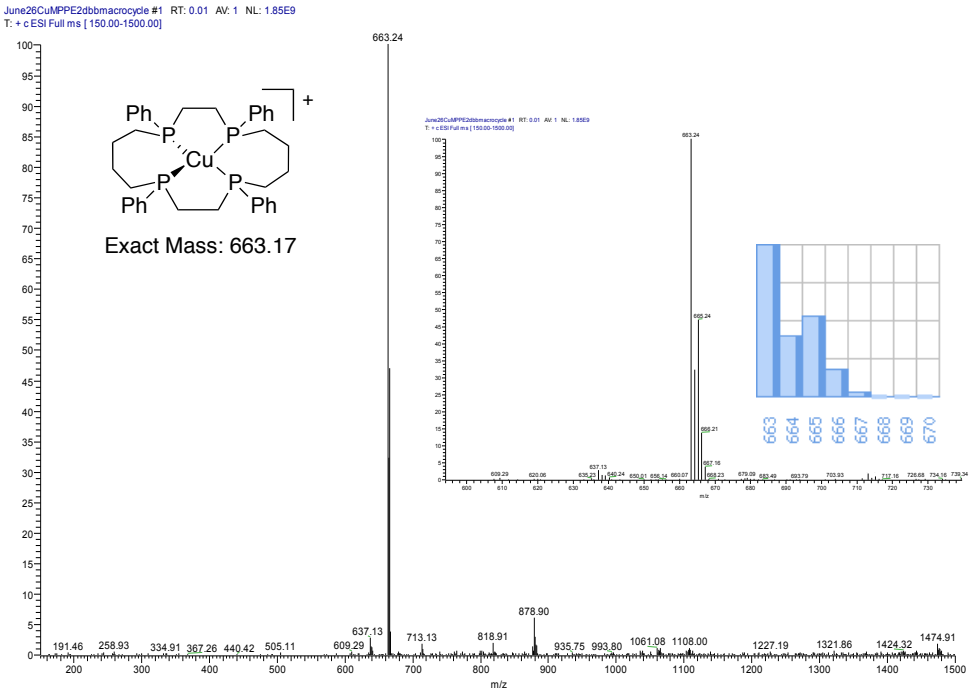

Figure A.2.8. ESI mass spectrum of [Cu(MPPE)-P4$_{DBB}$]OTf (**11**).

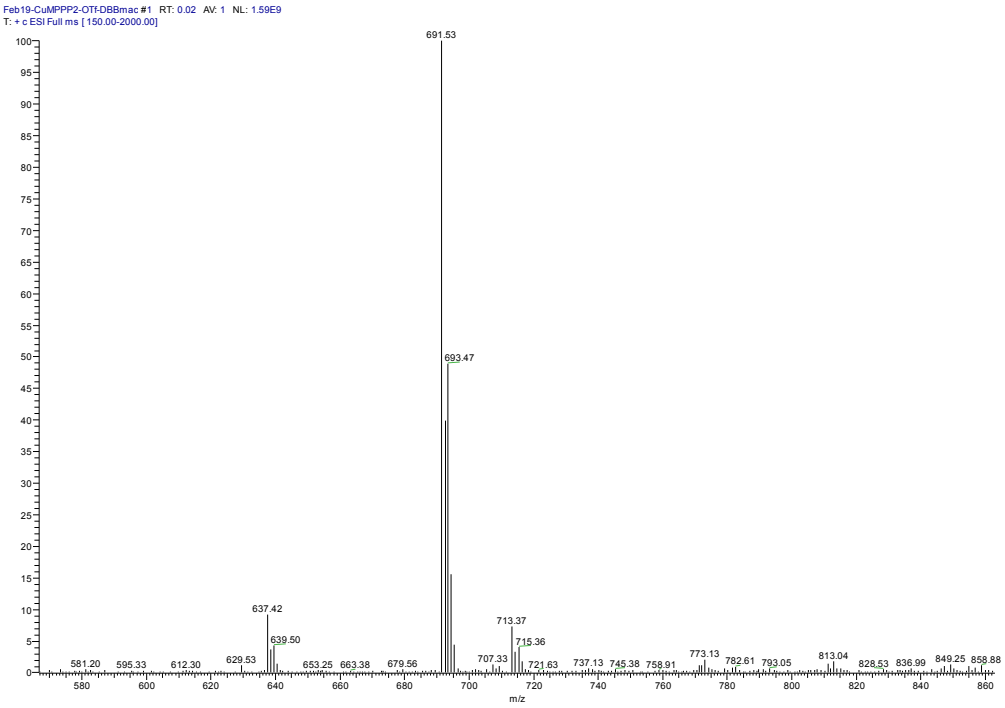

Figure A.2.9. ESI mass spectrum of [Cu(MPPP)-P4$_{DBB}$]OTf (**12**).

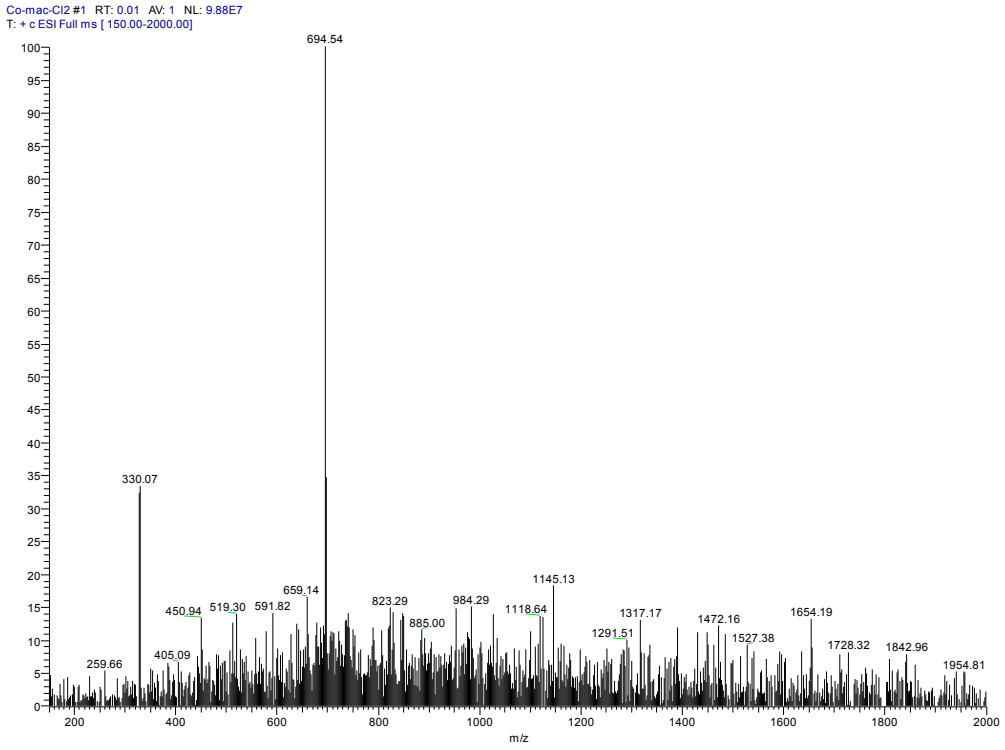

Figure A.2.10. ESI mass spectrum of Co(**14**)Cl$_2$.

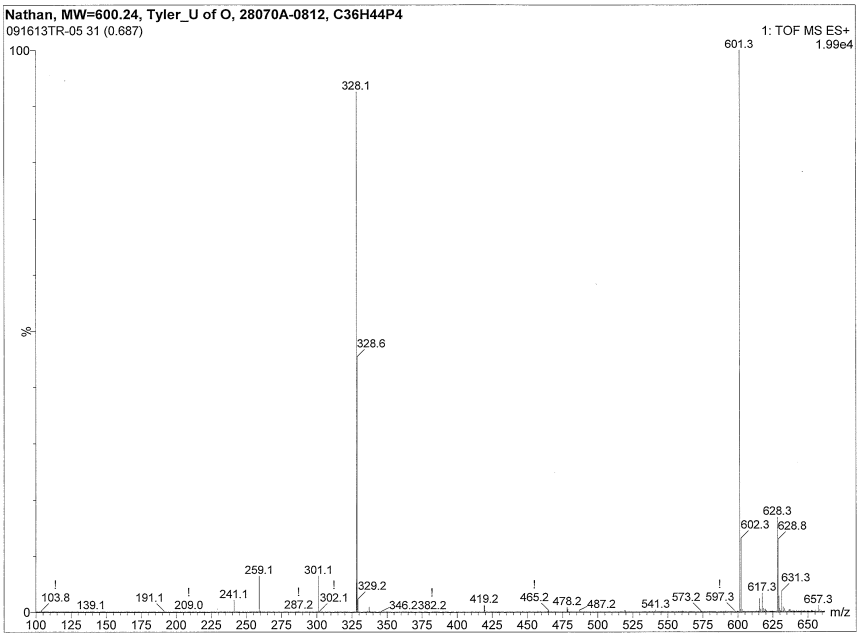

Figure A.2.11. FAB mass spectrum of **14**.

Elemental Composition Report **Page 1**

Single Mass Analysis
Tolerance = 50.0 PPM / DBE: min = -1.5, max = 50.0
Selected filters: None

Monoisotopic Mass, Even Electron Ions
8 formula(e) evaluated with 1 results within limits (up to 50 best isotopic matches for each mass)
Elements Used:
C: 0-36 H: 0-45 Na: 0-1 P: 0-4

Nathan, MW=600.24, Tyler_U of O, 28070A-0812, C36H44P4
091613TR-05 36 (0.793) Cm (36:48)

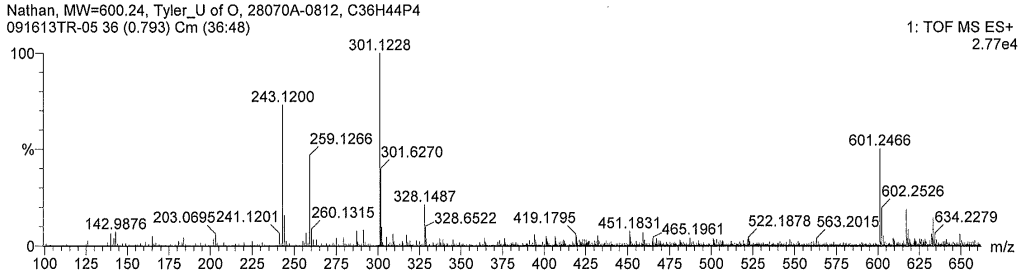

Minimum:				-1.5		
Maximum:		5.0	50.0	50.0		
Mass	Calc. Mass	mDa	PPM	DBE	i-FIT	Formula
601.2466	601.2472	-0.6	-1.0	16.5	43.1	C36 H45 P4

Figure A.2.12. Hi-Res FAB-MS of **14**.

A.3. UV-Vis Spectra

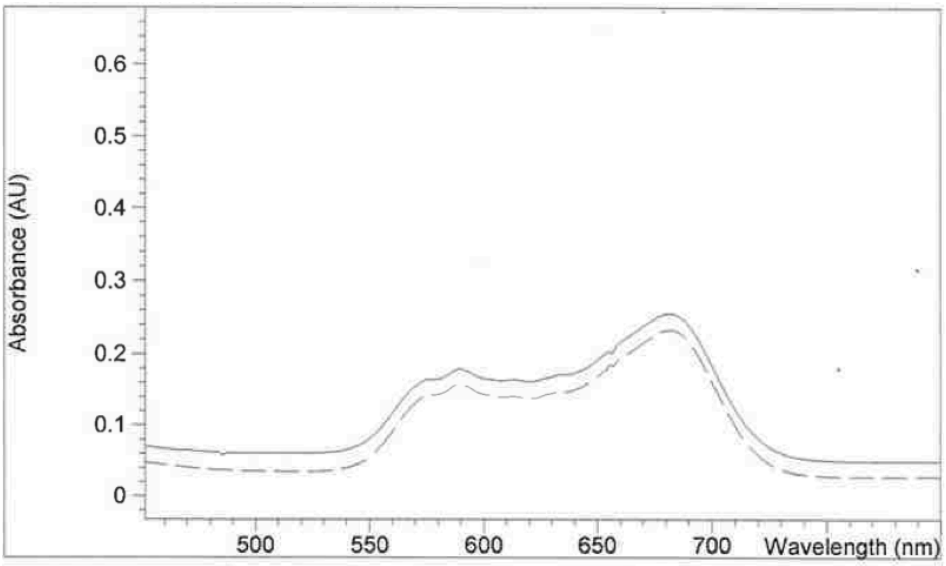

Figure A.3.1. UV-Vis spectrum of Co(**13**)Cl_2 in dichloromethane.

APPENDIX B

SUPPORTING INFORMATION FOR CHAPTER III

B.1. NMR Spectra

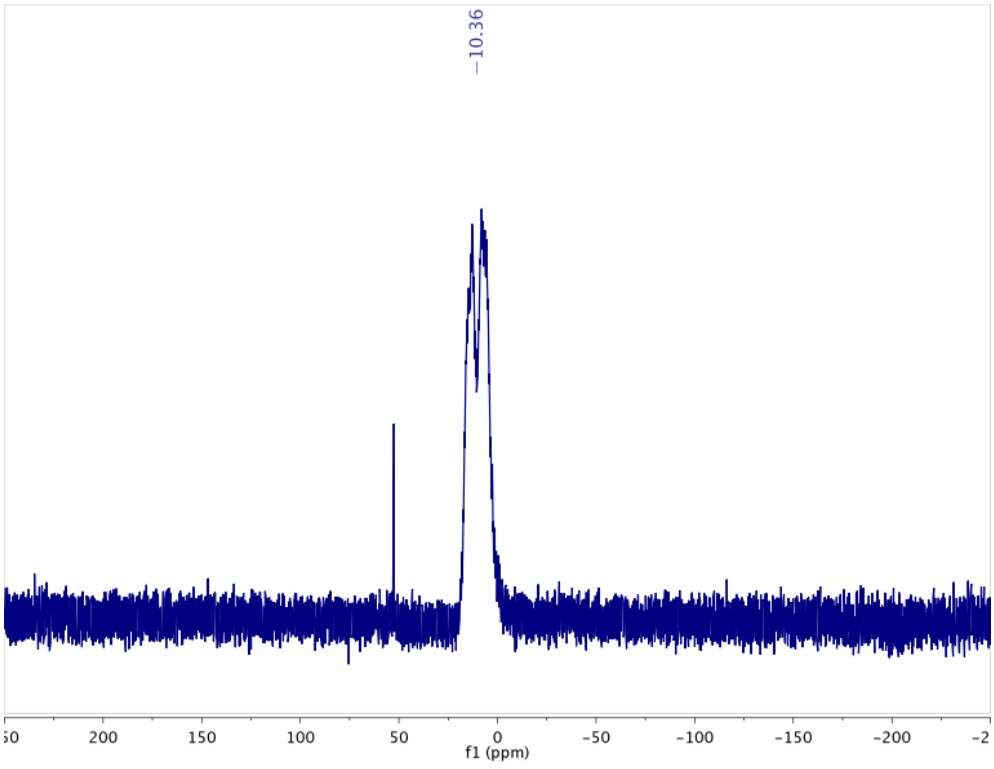

Figure B.1.1. $^{31}P\{^{1}H\}$ NMR Spectrum of $Cu(DHMPE)_2Cl$ with small oxidized phosphine impurity

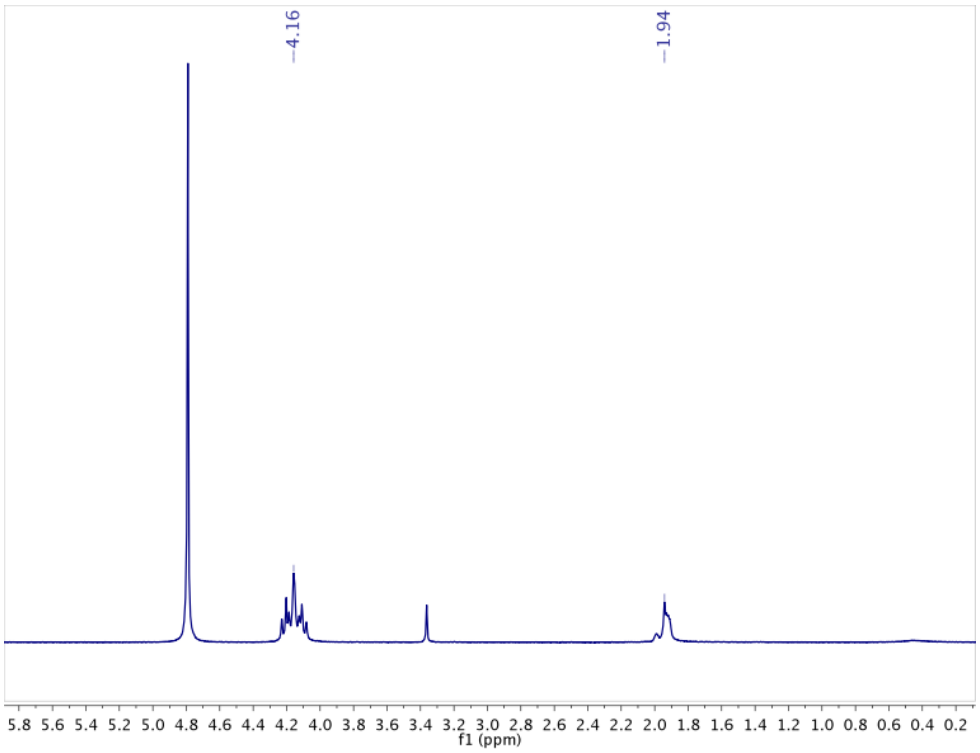

Figure B.1.2. ^{1}H NMR Spectrum of $Cu(DHMPE)_2Cl$ (small peaks are trace water from D_2O and methanol)

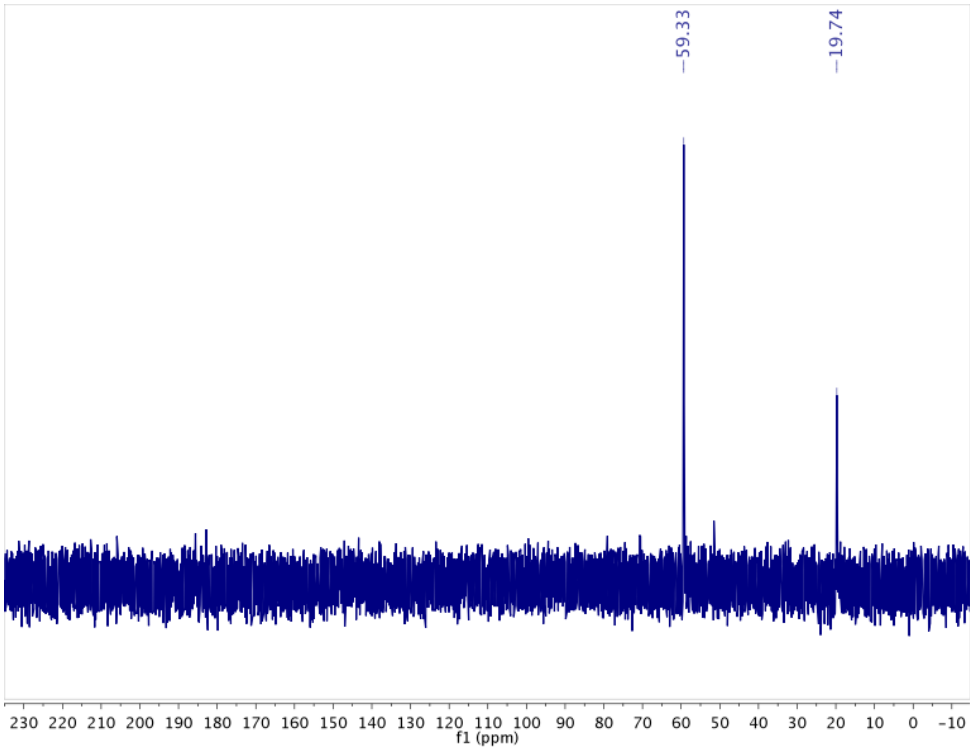

Figure B.1.3. ^{13}C NMR Spectrum of $Cu(DHMPE)_2Cl$

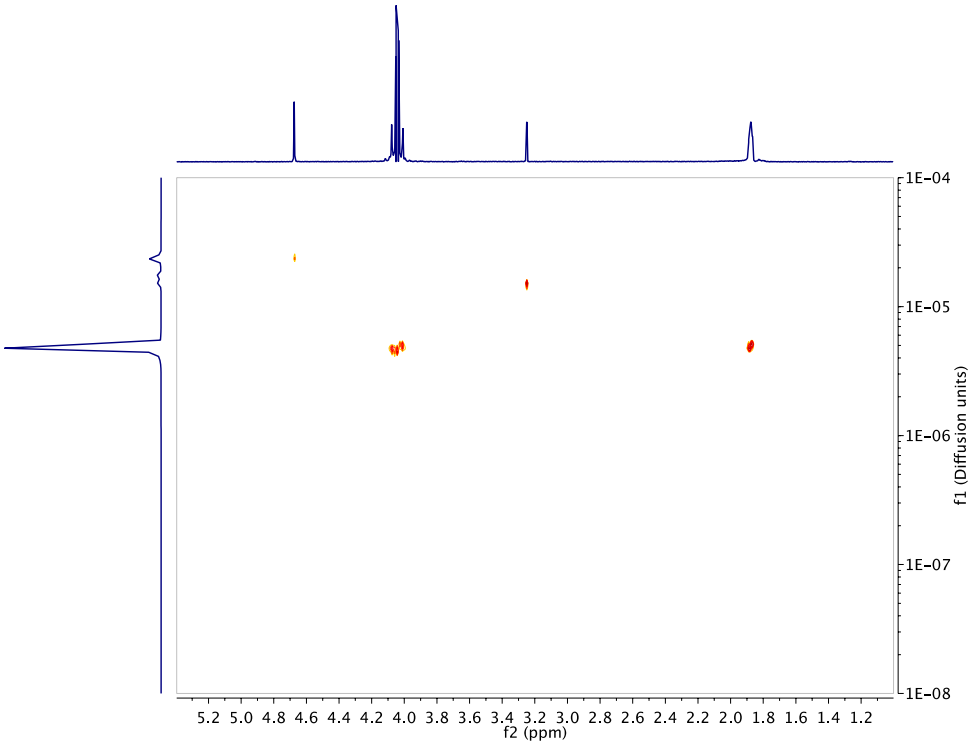

Figure B.1.4. ^{1}H DOSY Spectrum of Cu(DHMPE)$_2$Cl (small crosspeaks are trace water from D_2O and methanol)

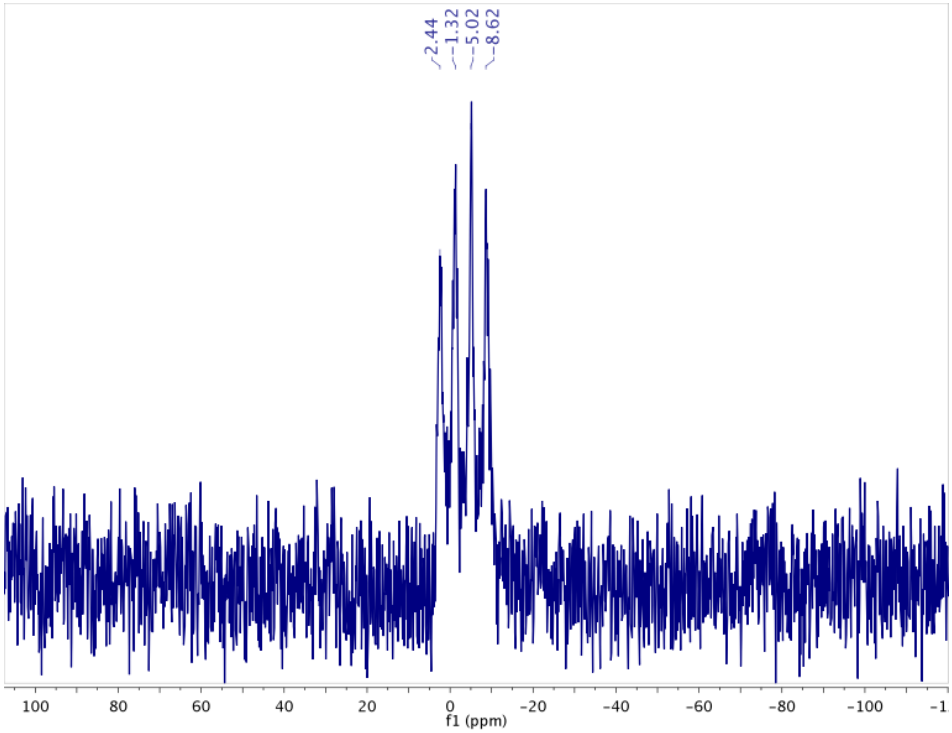

Figure B.1.5. ^{31}P NMR of Cu(thp)$_4$PF$_6$

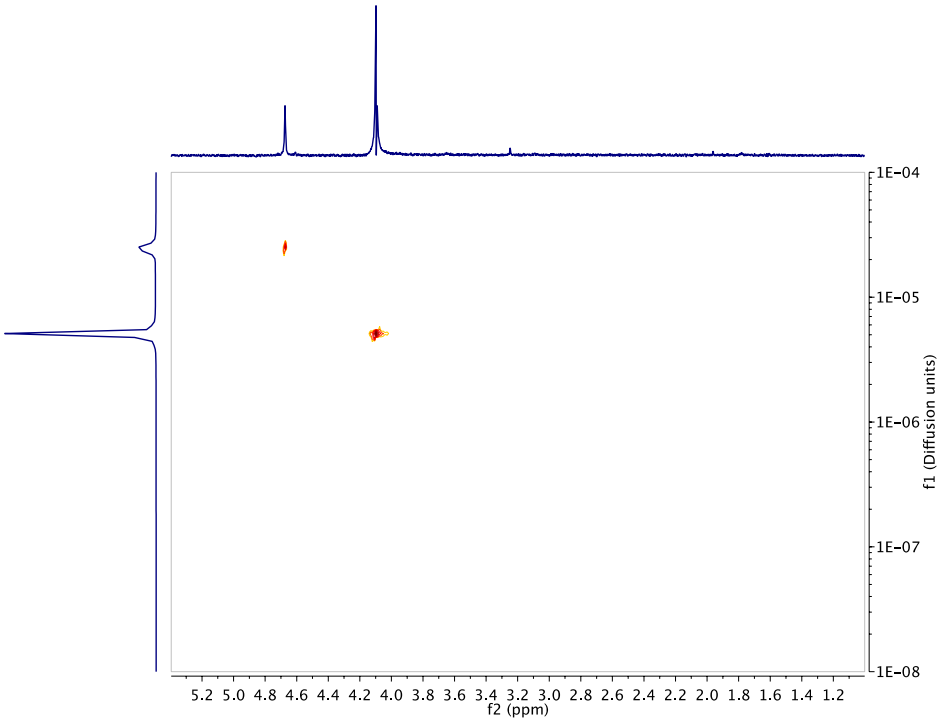

Figure B.1.6. ^{1}H DOSY Spectrum of $Cu(thp)_4PF_6$ (small crosspeak is trace water from D_2O)

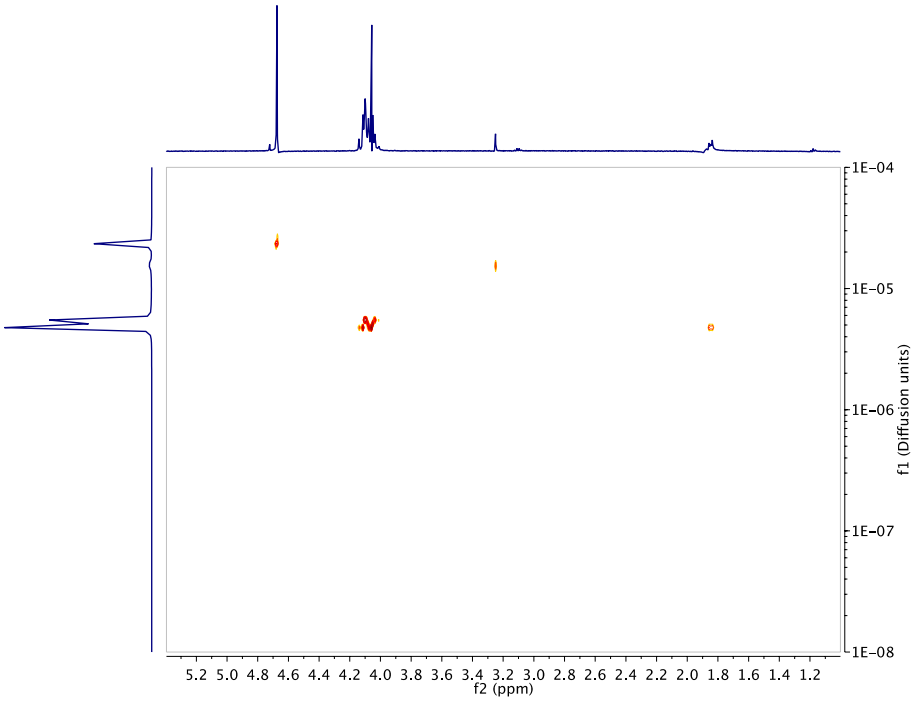

Figure B.1.7. ^{1}H DOSY Spectrum of a mixture of $Cu(DHMPE)_2Cl$ and $Cu(thp)_4PF_6$ (small crosspeaks are trace water from D_2O and methanol)

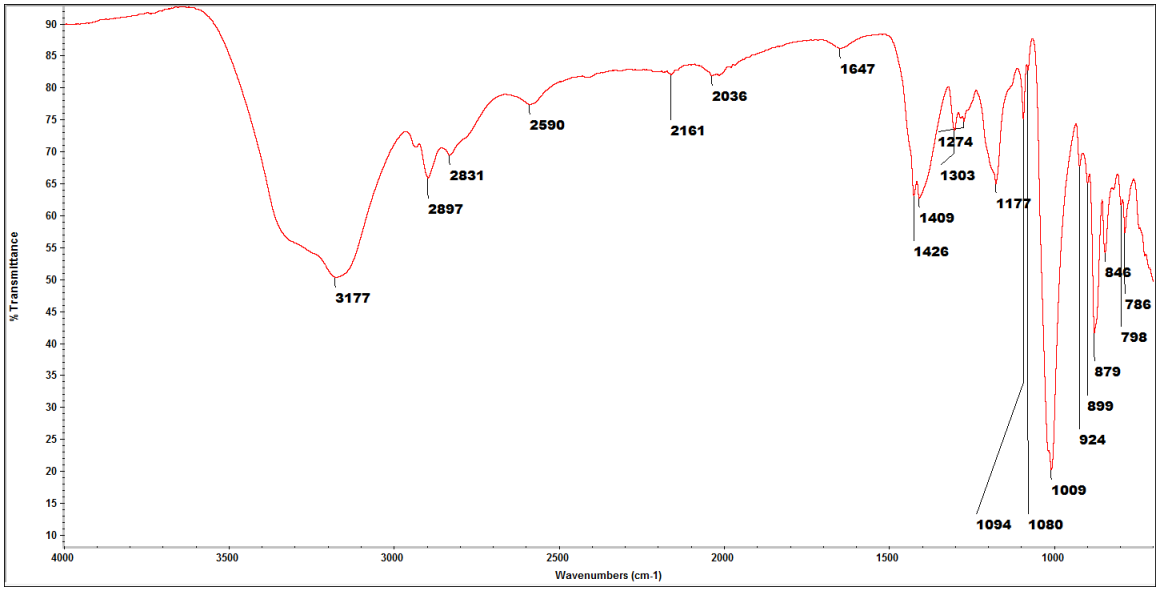

Figure B.1.8. Infrared spectrum of $Cu(DHMPE)_2Cl$ (ATR)

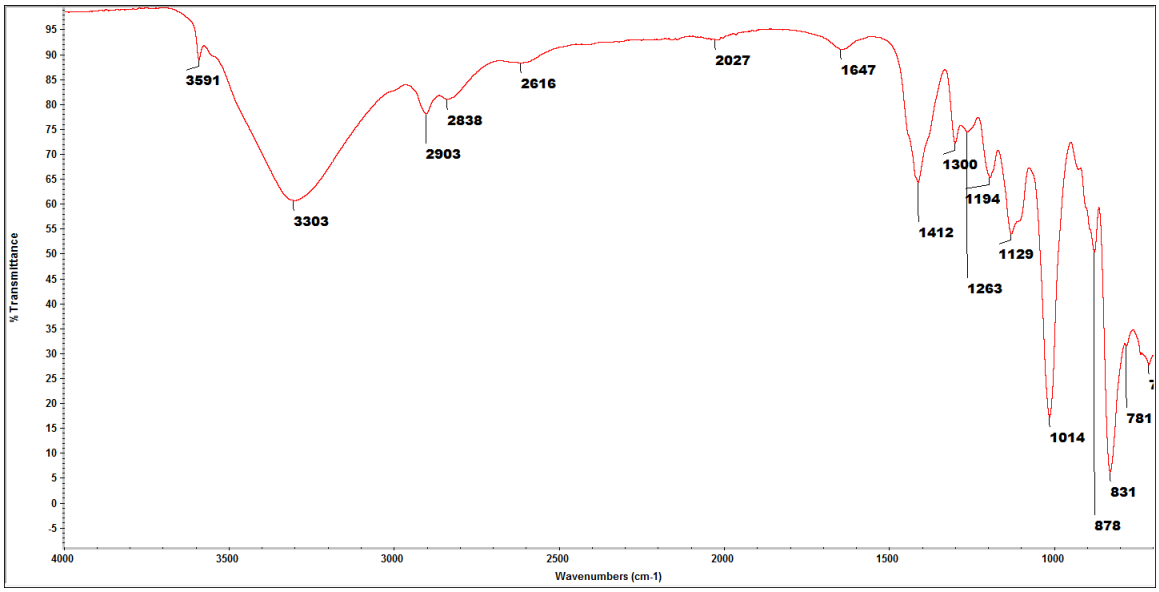

Figure B.1.9. Infrared spectrum of $Cu(DHMPE)_2PF_6$ (ATR)

APPENDIX C

SUPPORTING INFORMATION FOR CHAPTER IV

C.1. NMR Spectra

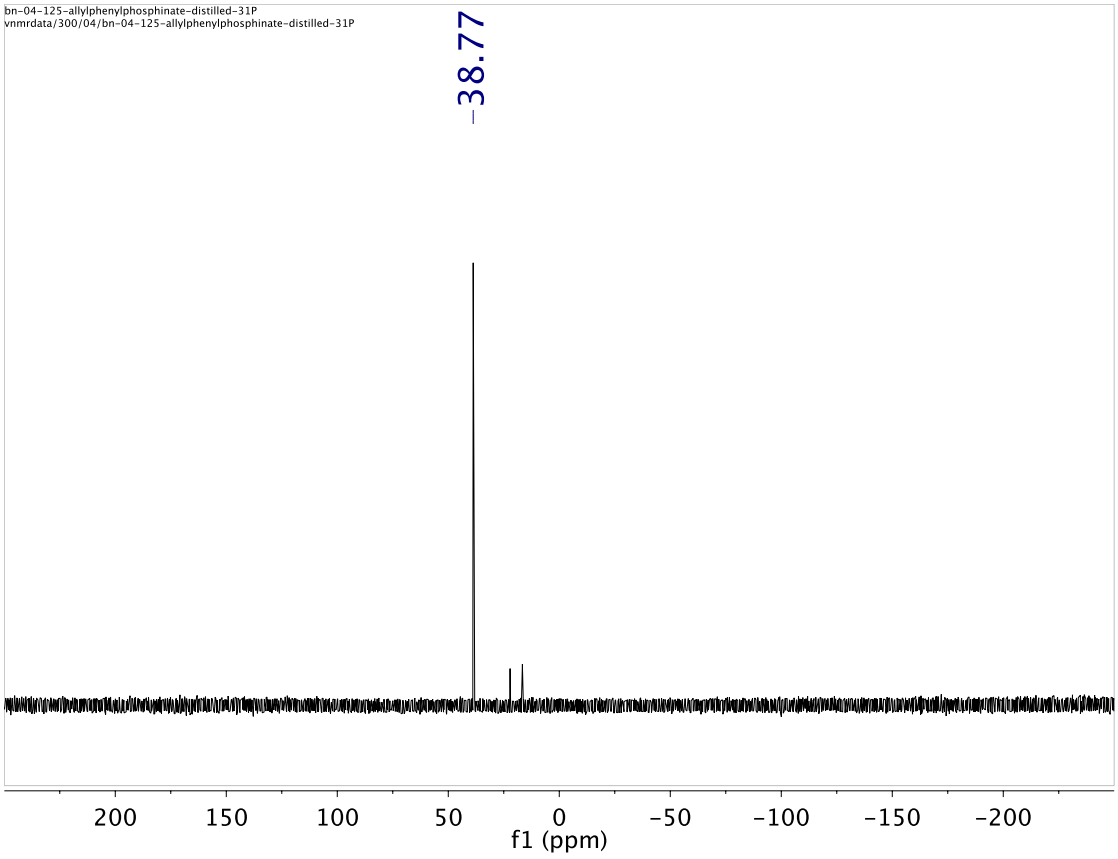

Figure C.1.1. $^{31}P\{^{1}H\}$ NMR spectrum of **1**.

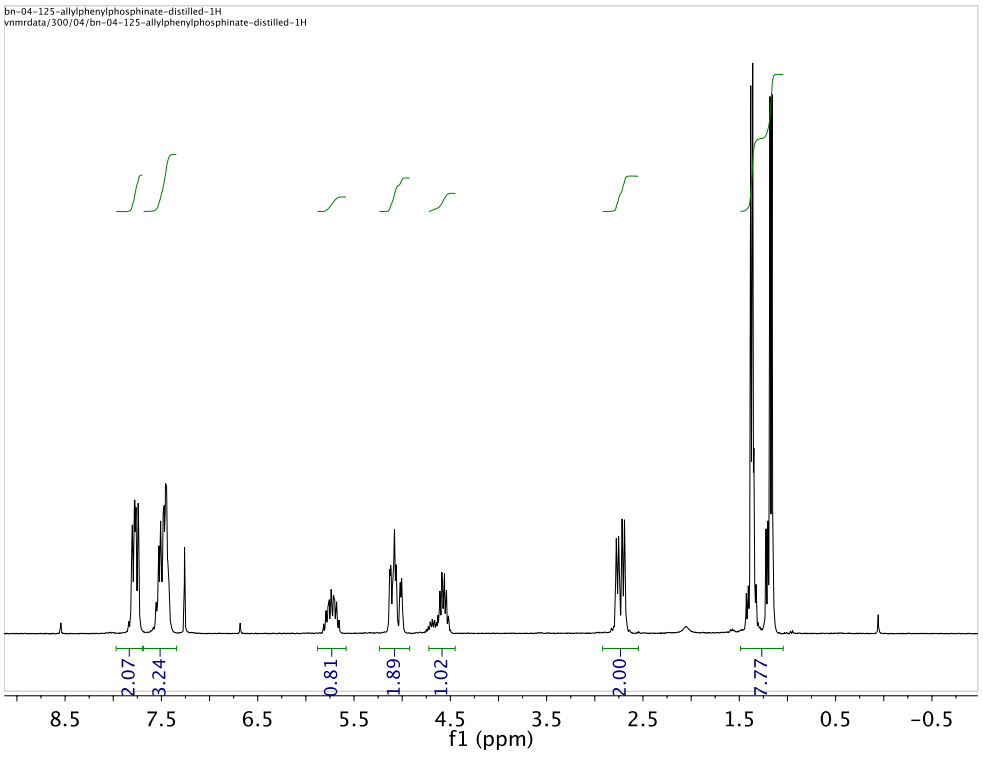

Figure C.1.2. ^{1}H NMR spectrum of **1**.

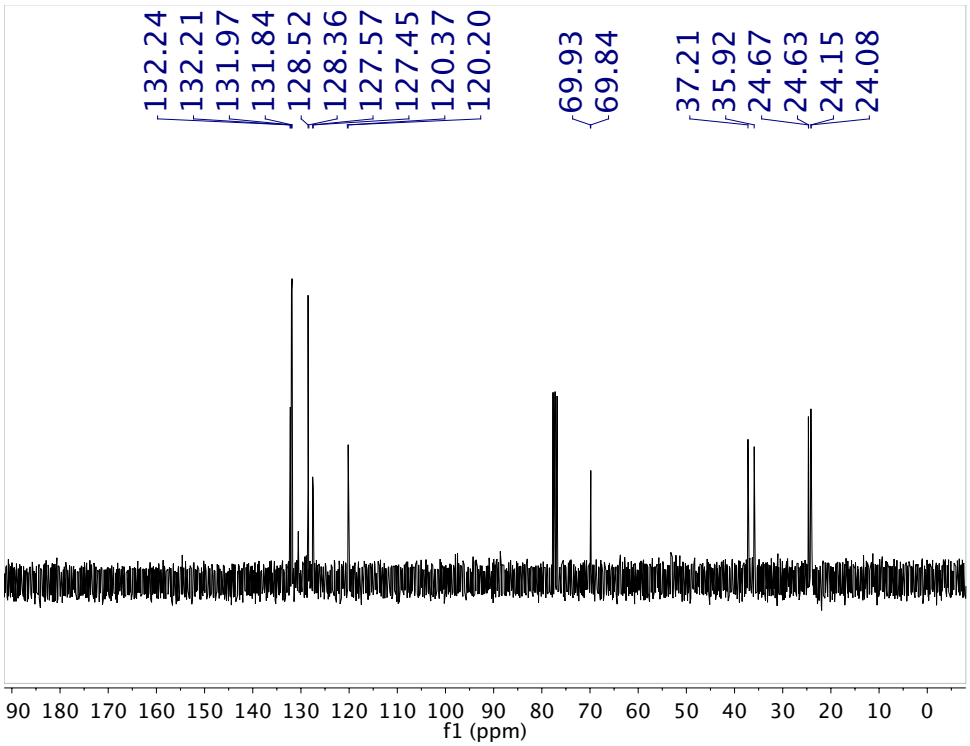

Figure C.1.3. ^{13}C NMR spectrum of **1**.

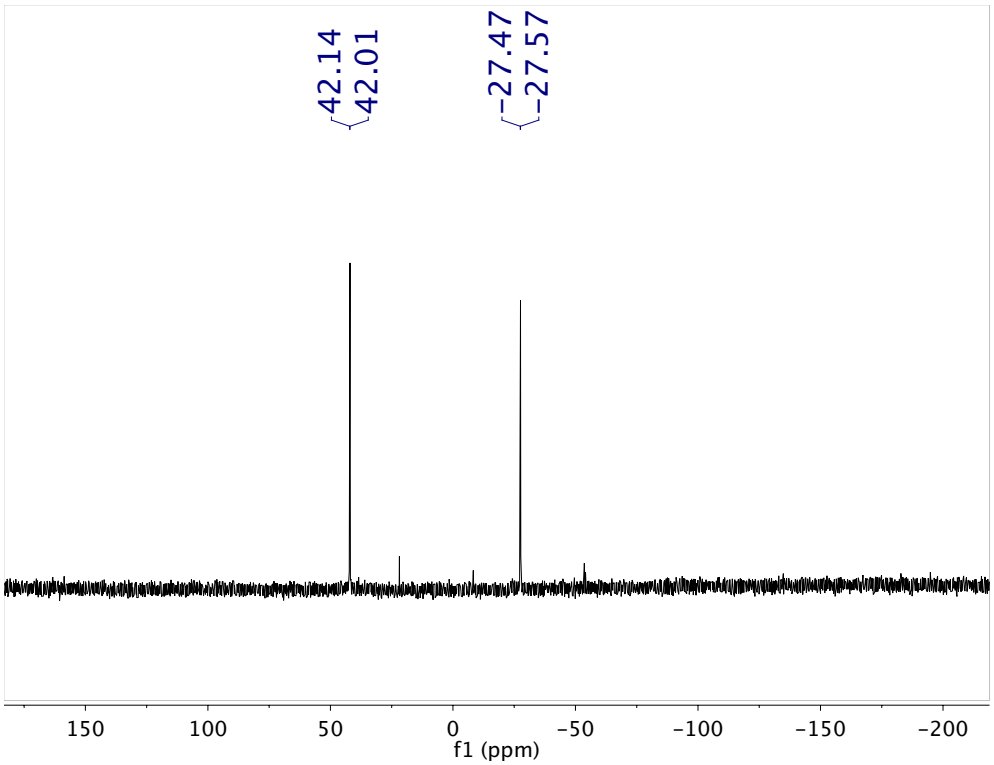

Figure C.1.4. $^{31}P\{^{1}H\}$ NMR spectrum of **2**.

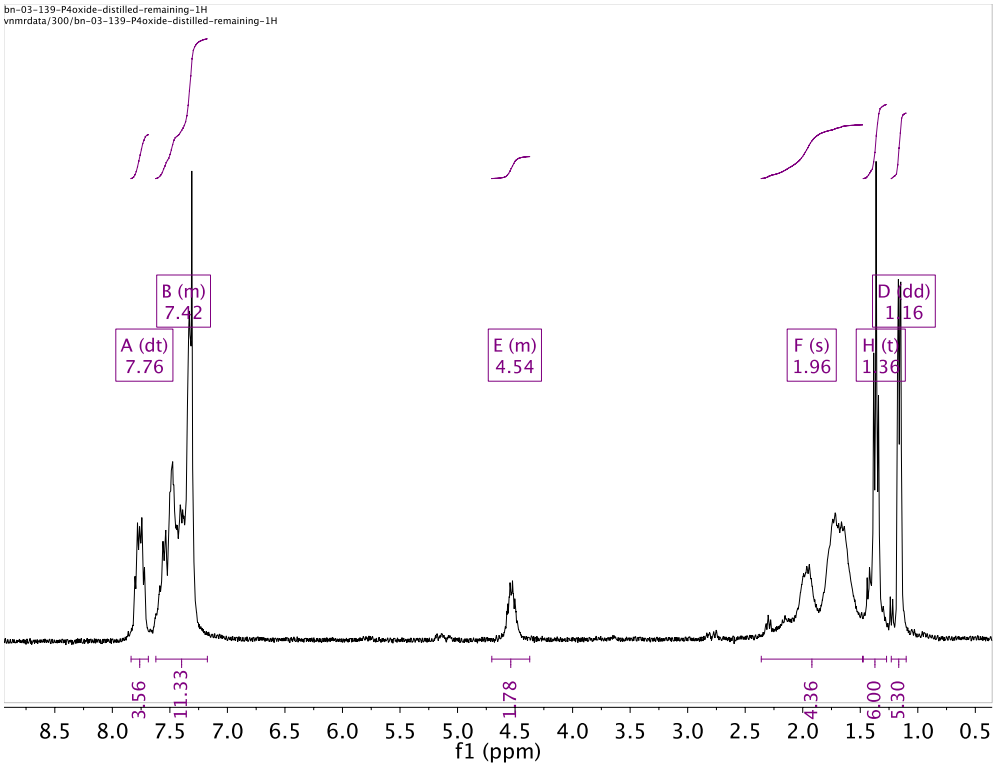

Figure C.1.5. ^{1}H NMR spectrum of **2**.

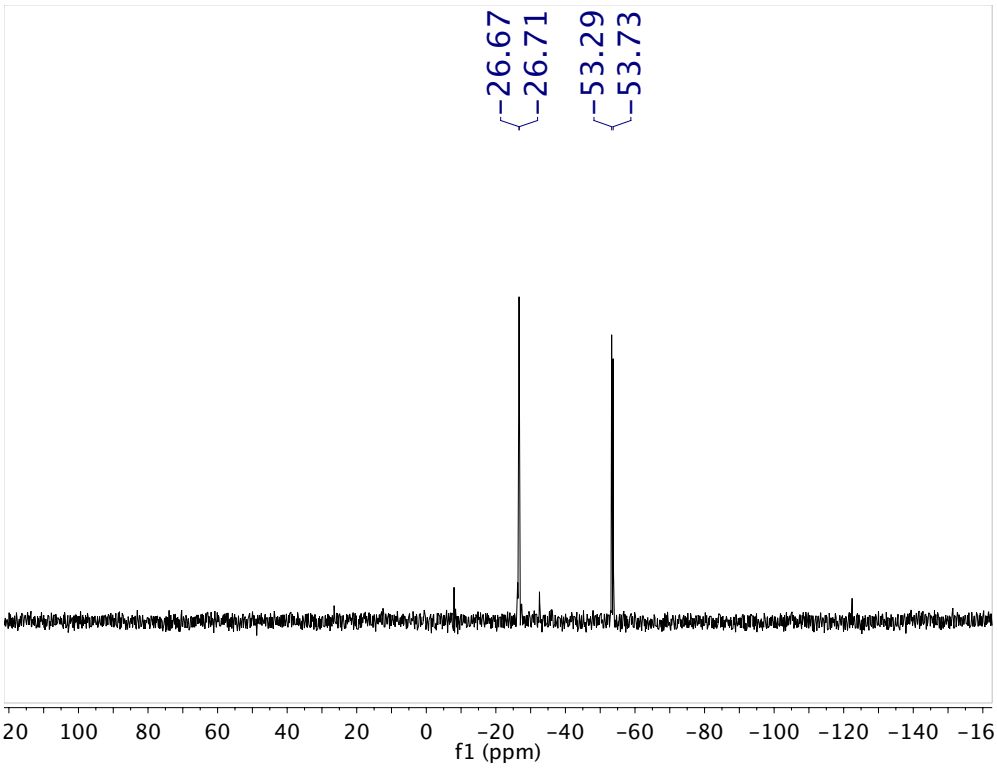

Figure C.1.6. $^{31}P\{^{1}H\}$ NMR spectrum of **3**.

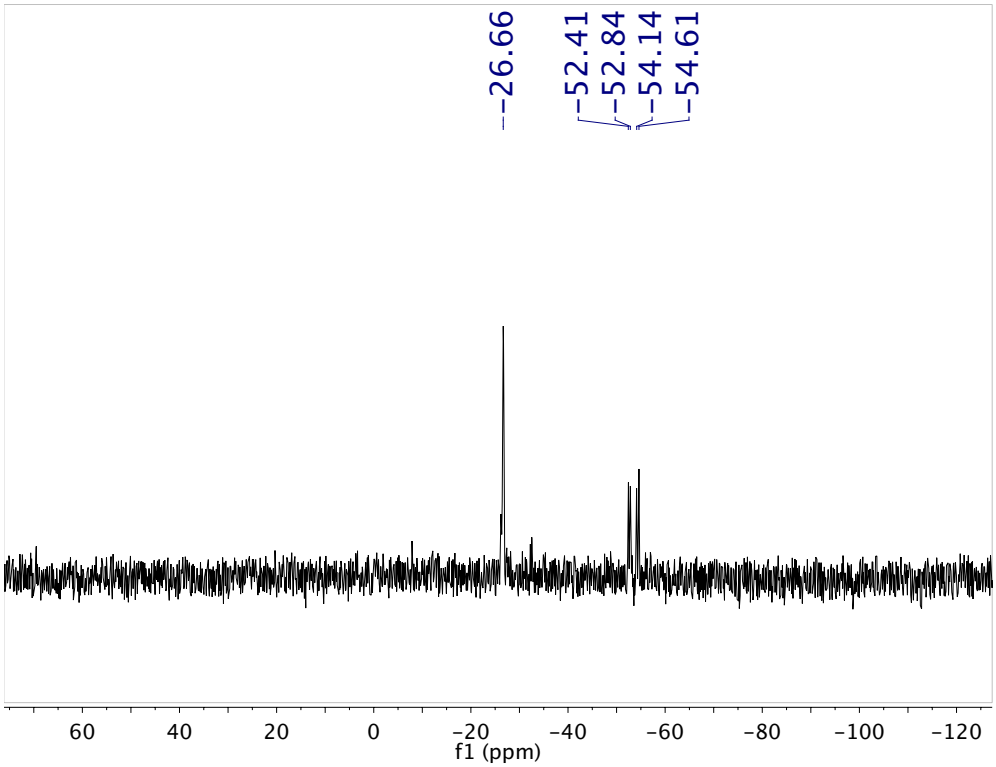

Figure C.1.7. ^{31}P NMR spectrum of **3**.

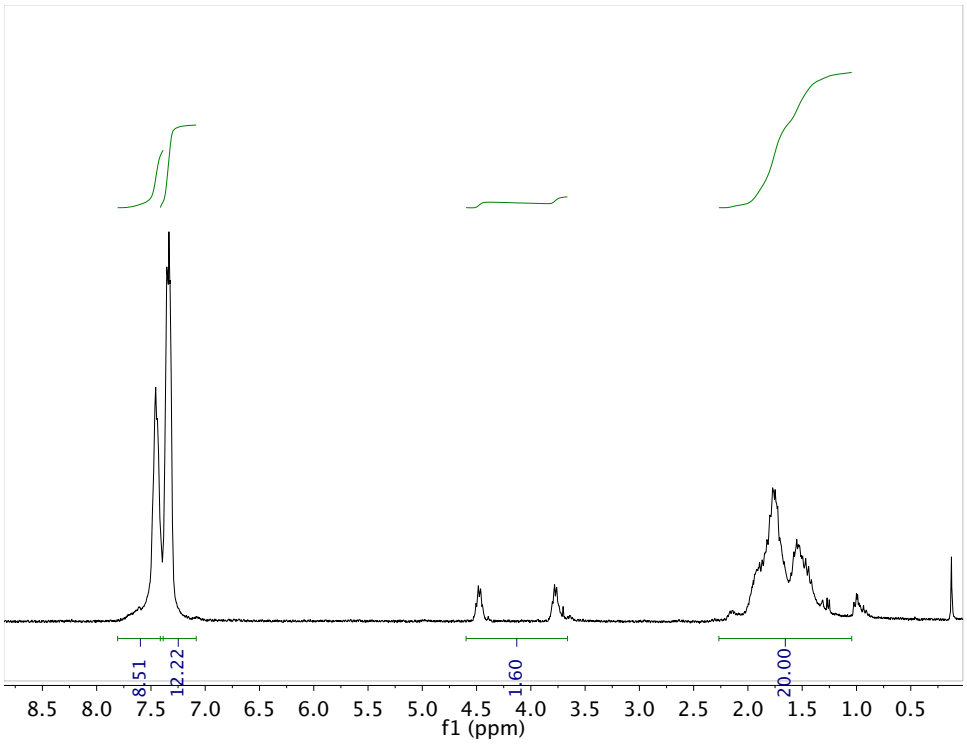

Figure C.1.8. ^{1}H NMR spectrum of **3**.

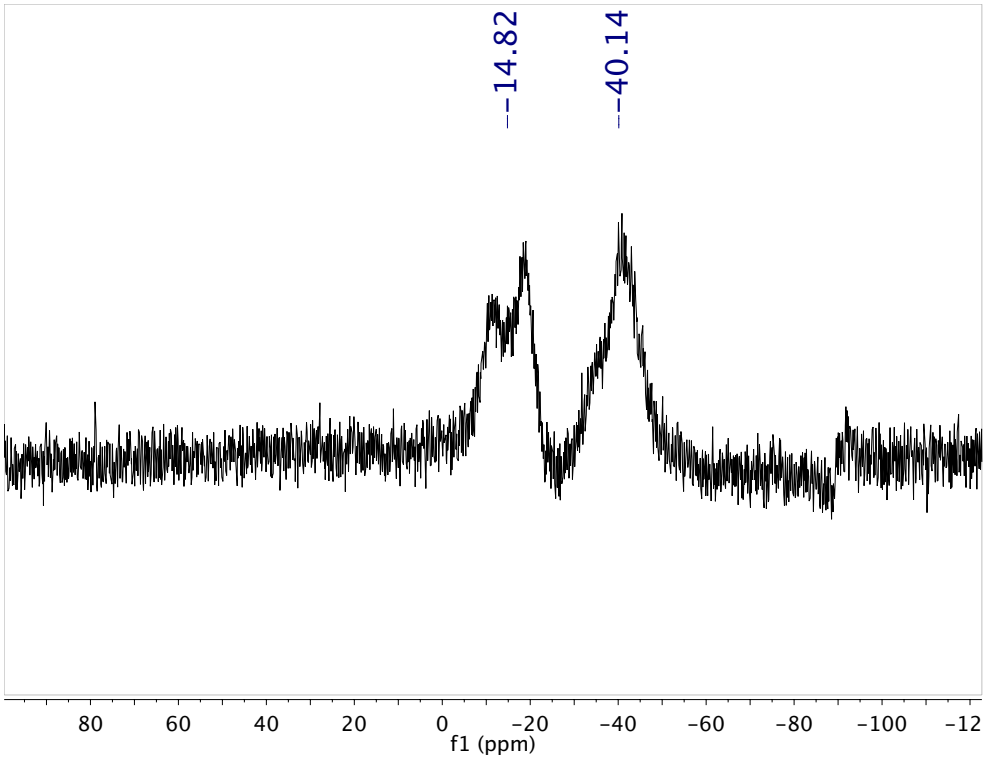

Figure C.1.9. $^{31}P\{^{1}H\}$ NMR spectrum of **4**.

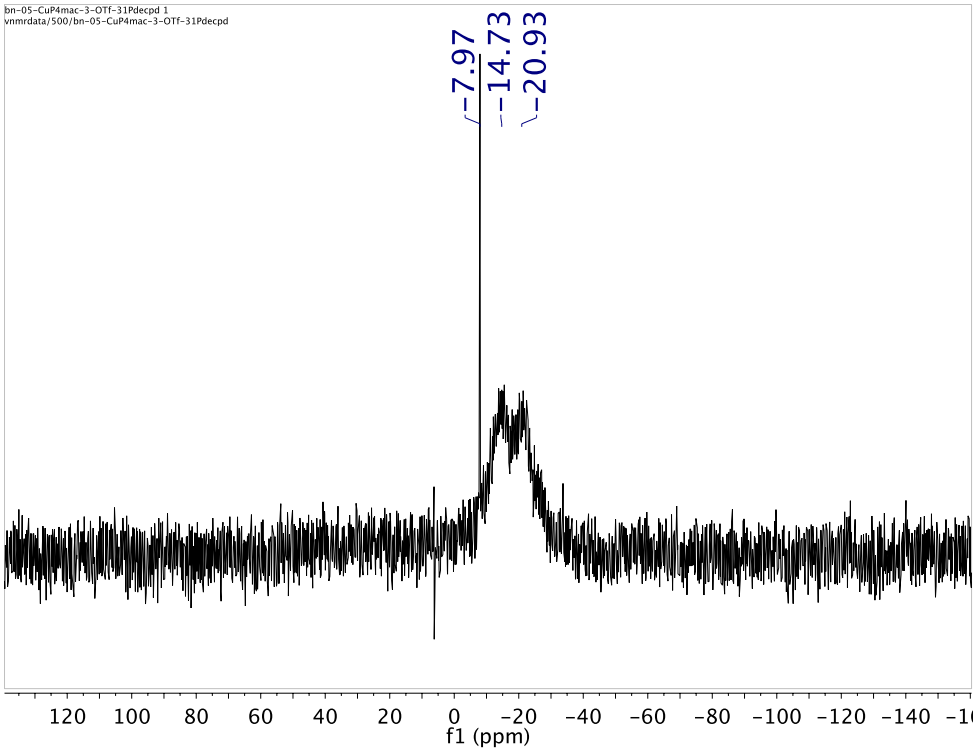

Figure C.1.10. $^{31}P\{^{1}H\}$ NMR spectrum of **5a**.

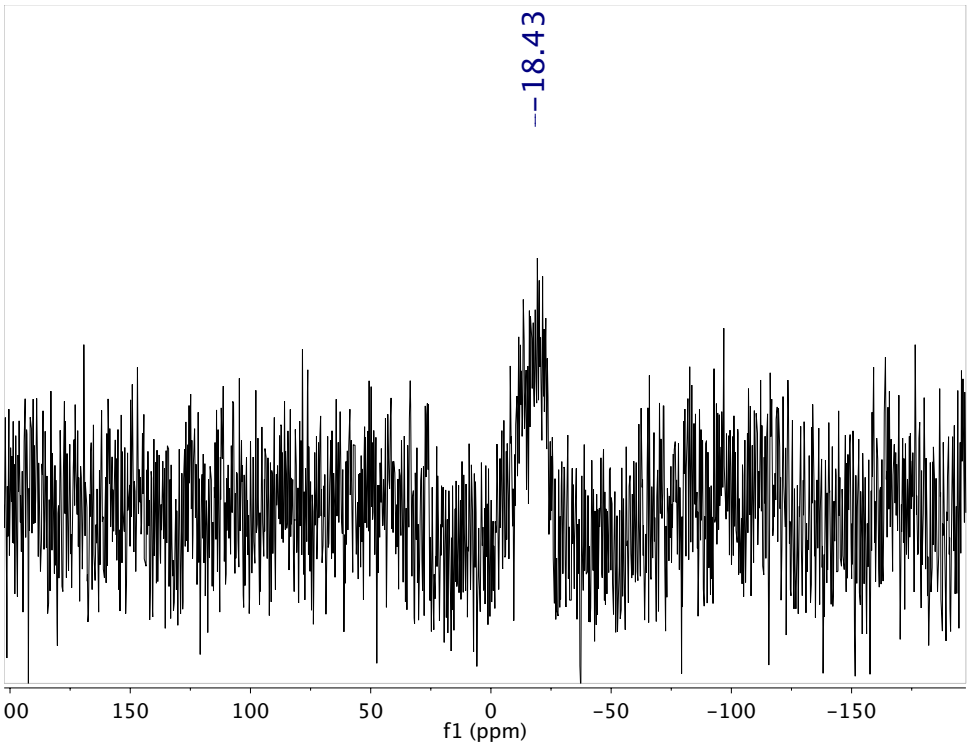

Figure C.1.11. $^{31}P\{^{1}H\}$ NMR spectrum of **5b**.

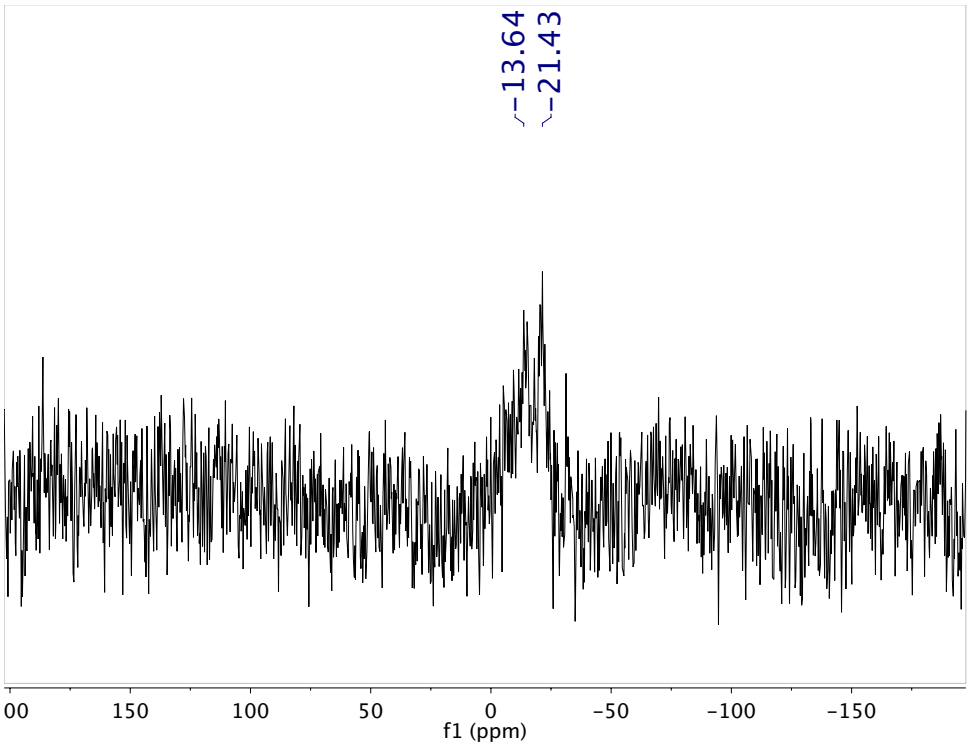

Figure C.1.12. $^{31}P\{^{1}H\}$ NMR spectrum of **5c**.

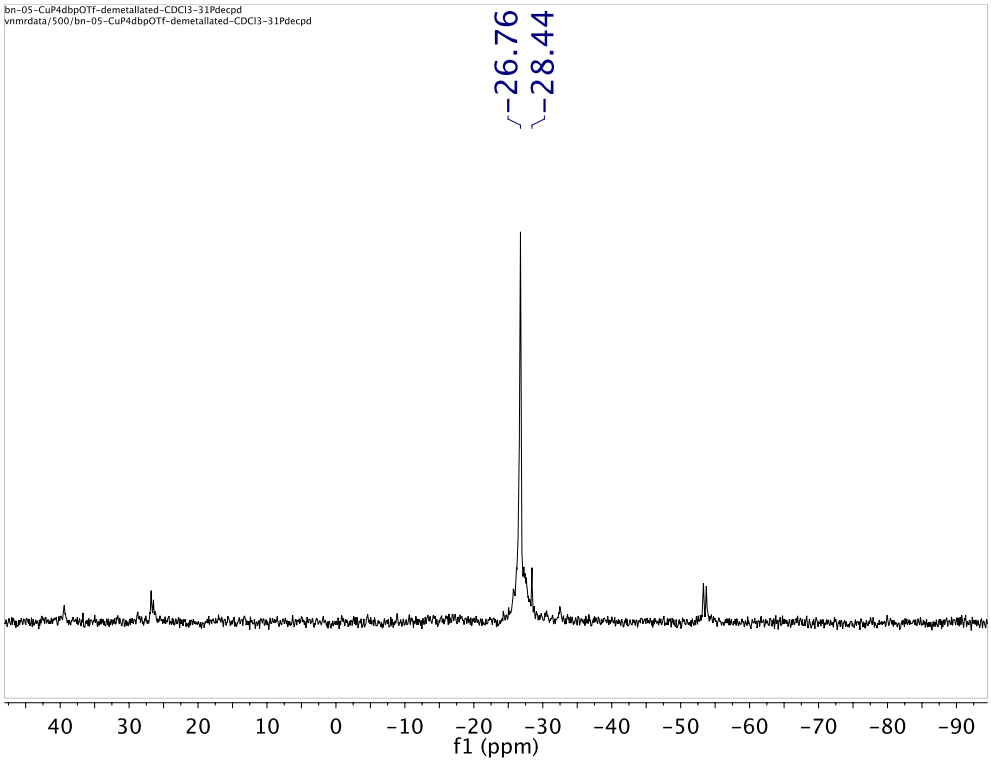

Figure C.1.13. $^{31}P\{^{1}H\}$ NMR spectrum of **6a**.

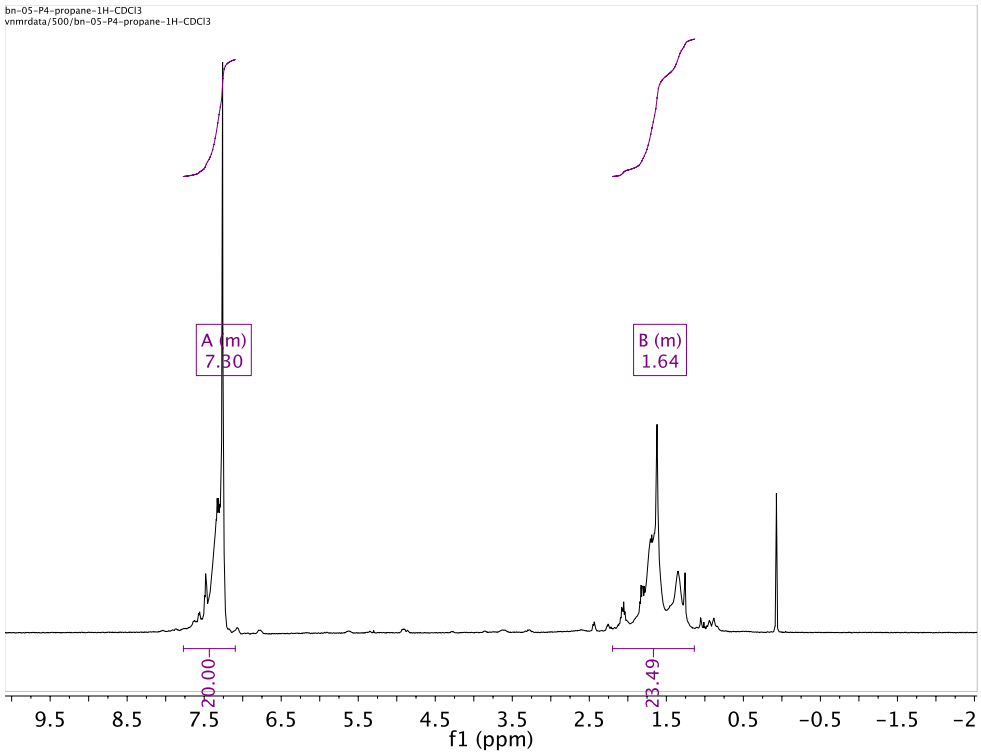

Figure C.1.14. ^{1}H NMR spectrum of **6a**.

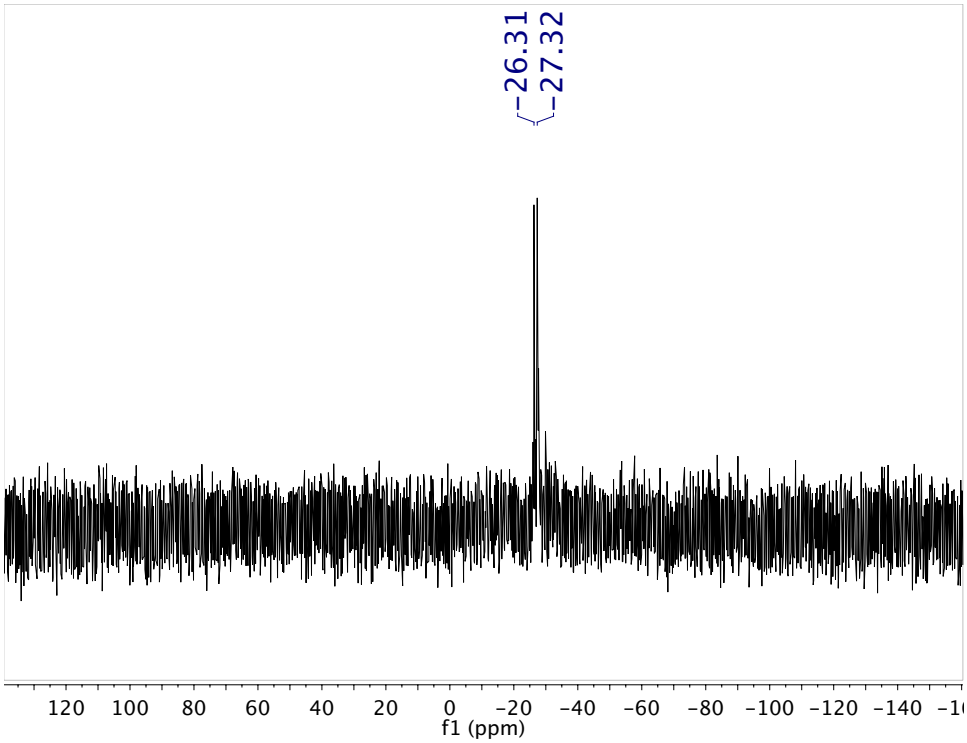

Figure C.1.15. $^{31}P\{^{1}H\}$ NMR spectrum of **6b**.

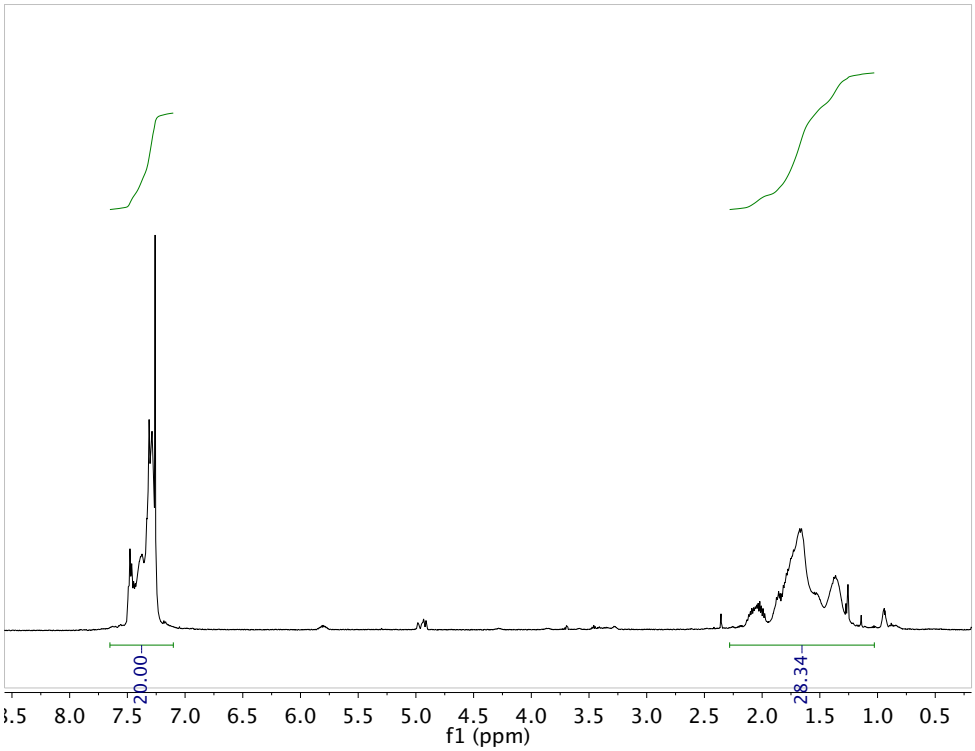

Figure C.1.16. ^{1}H NMR spectrum of **6b**.

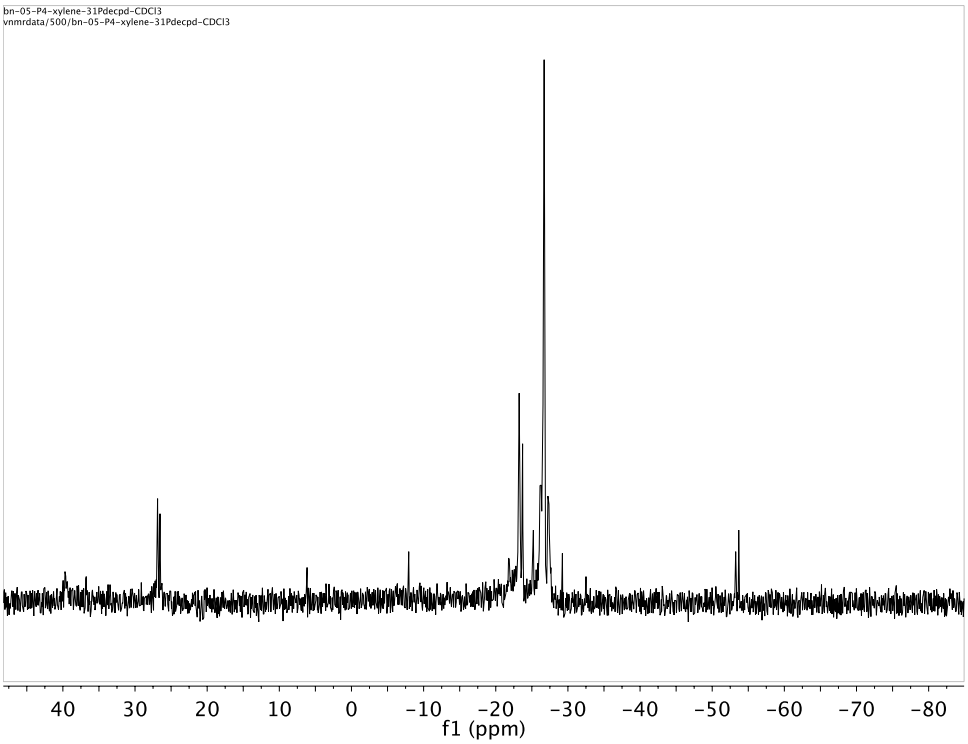

Figure C.1.17. $^{31}P\{^{1}H\}$ NMR spectrum of **6c**.

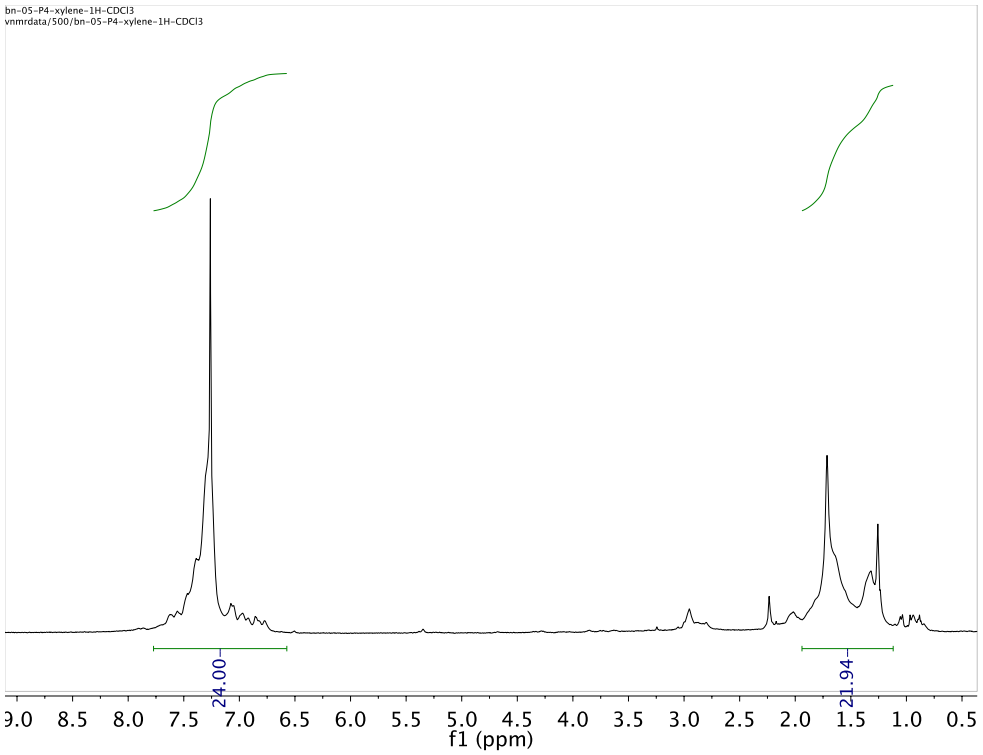

Figure C.1.18. ^{1}H NMR spectrum of **6c**.

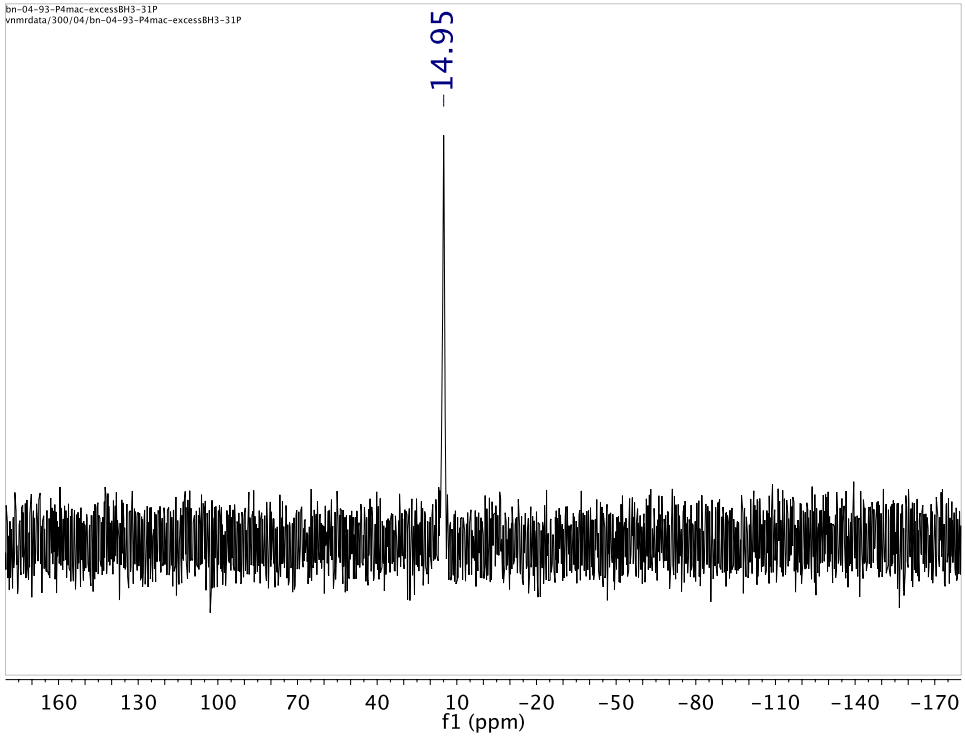

Figure C.1.19. $^{31}P\{^{1}H\}$ spectrum of 6b with excess BH_3·THF.

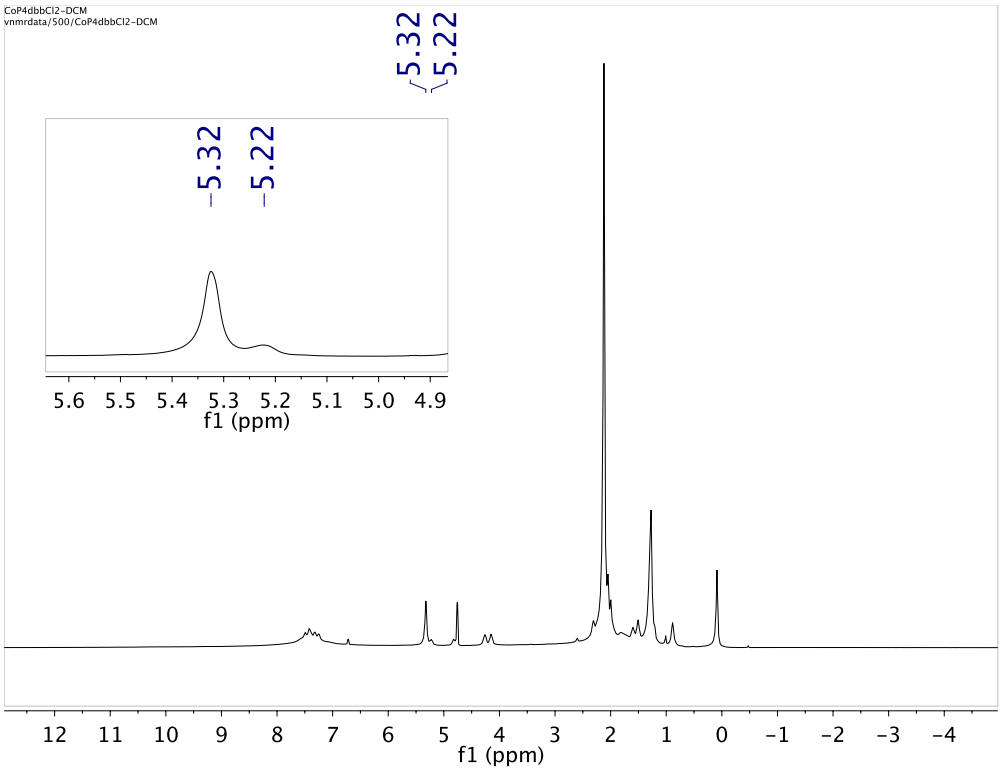

Figure C.1.19. ^{1}H NMR spectrum of Co(**6b**)Cl_2 for Evans' method.

C.2. Mass Spectra

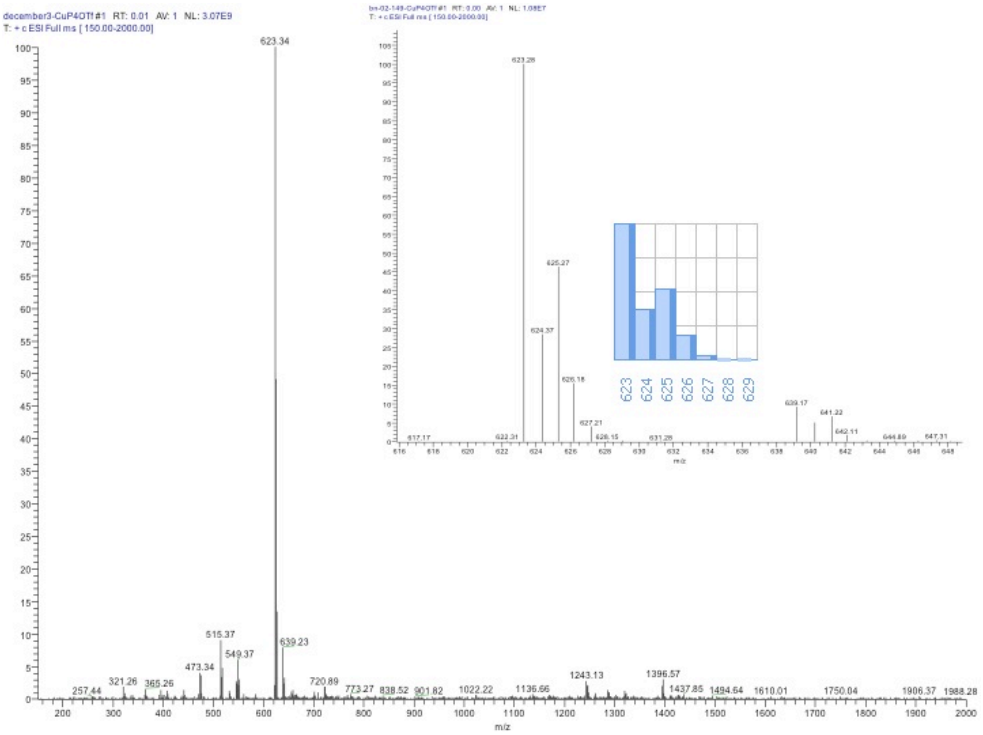

Figure C.2.1. ESI mass spectrum of **4.**

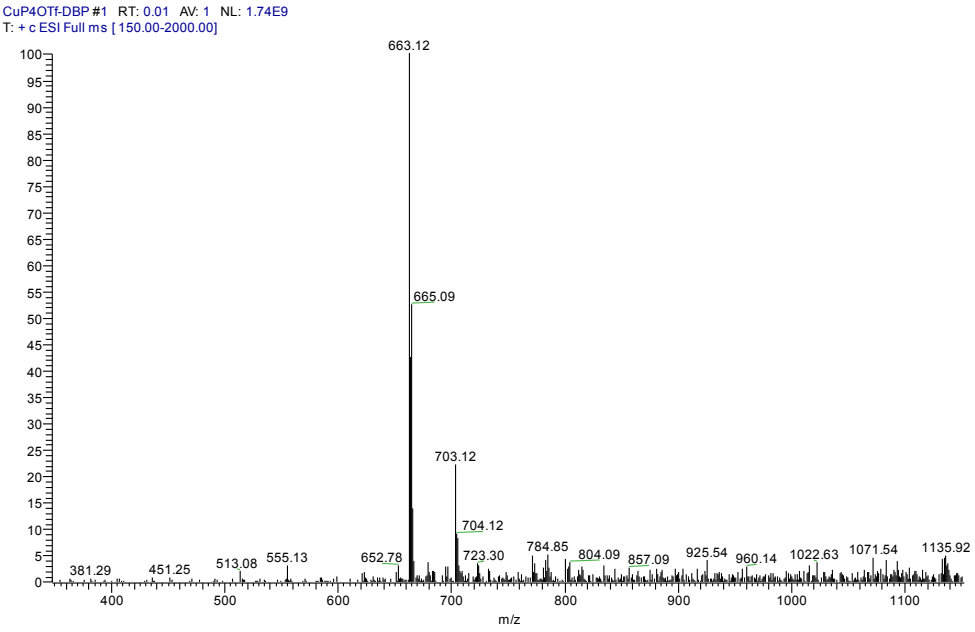

Figure C.2.2. ESI mass spectrum of **5a.**

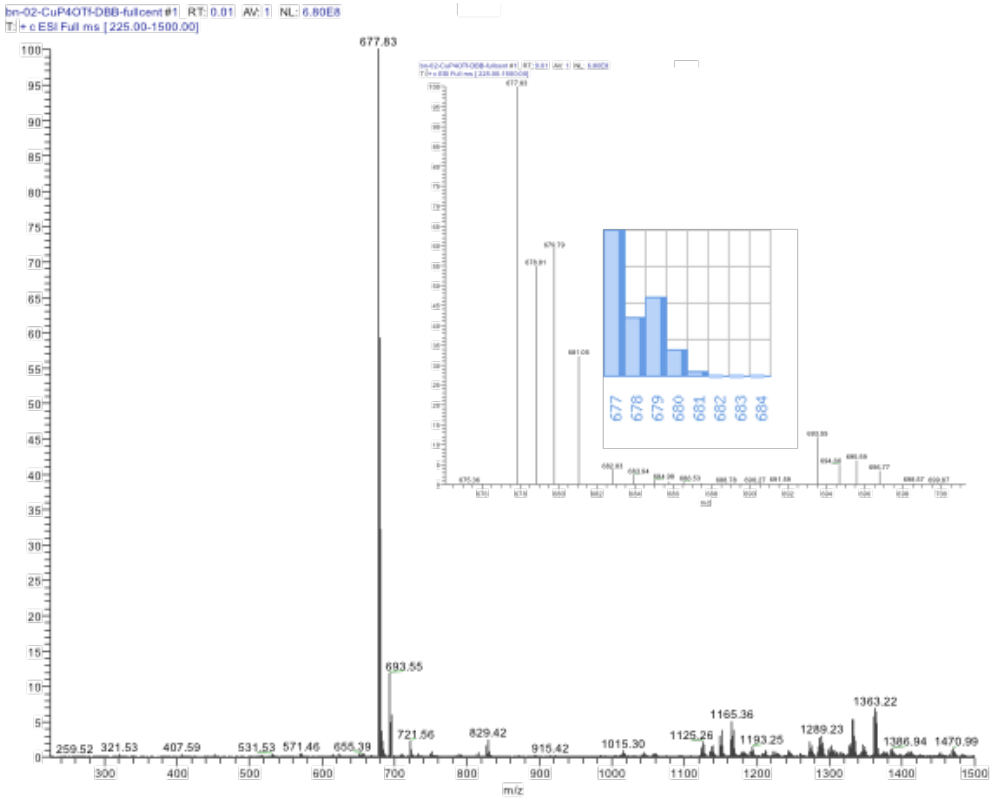

Figure C.2.3. ESI mass spectrum of **5b.**

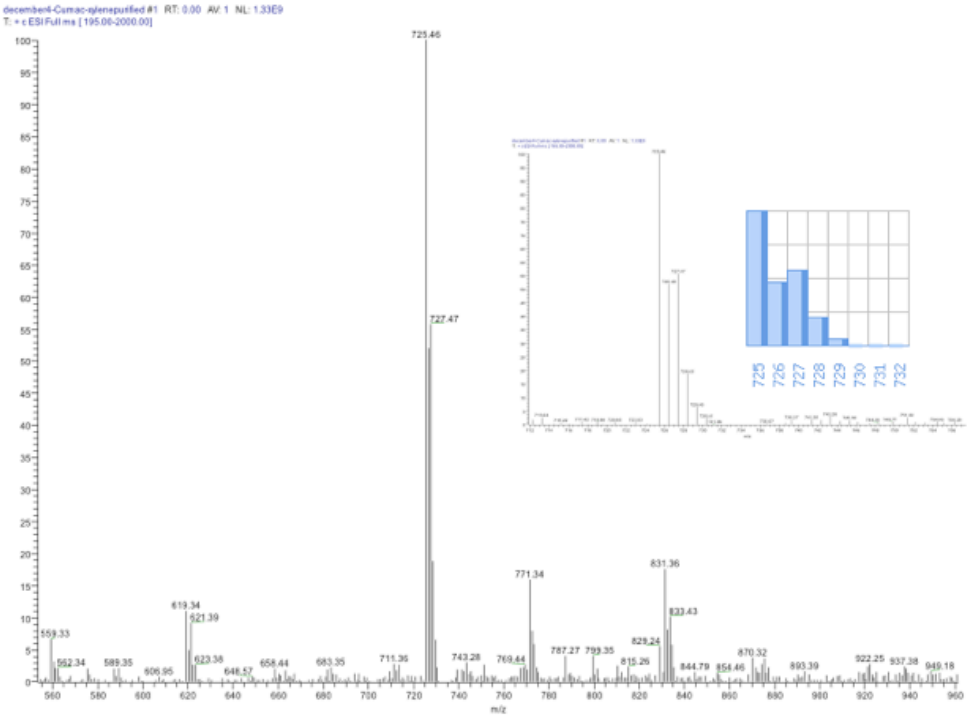

Figure C.2.4. ESI mass spectrum of **5c.**

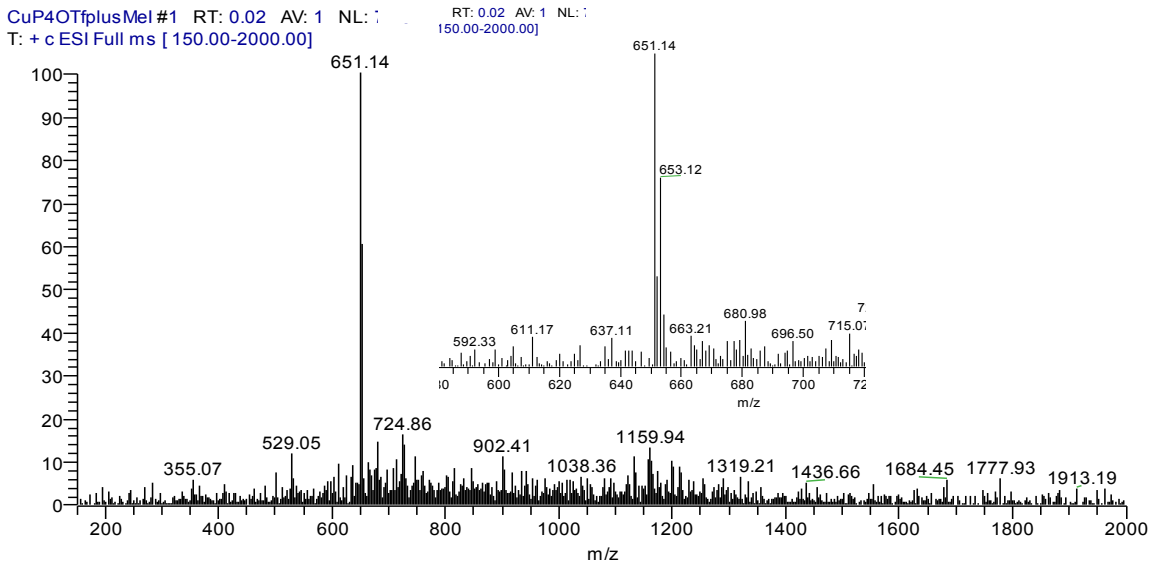

Figure C.2.5. ESI mass spectrum of **5d**.

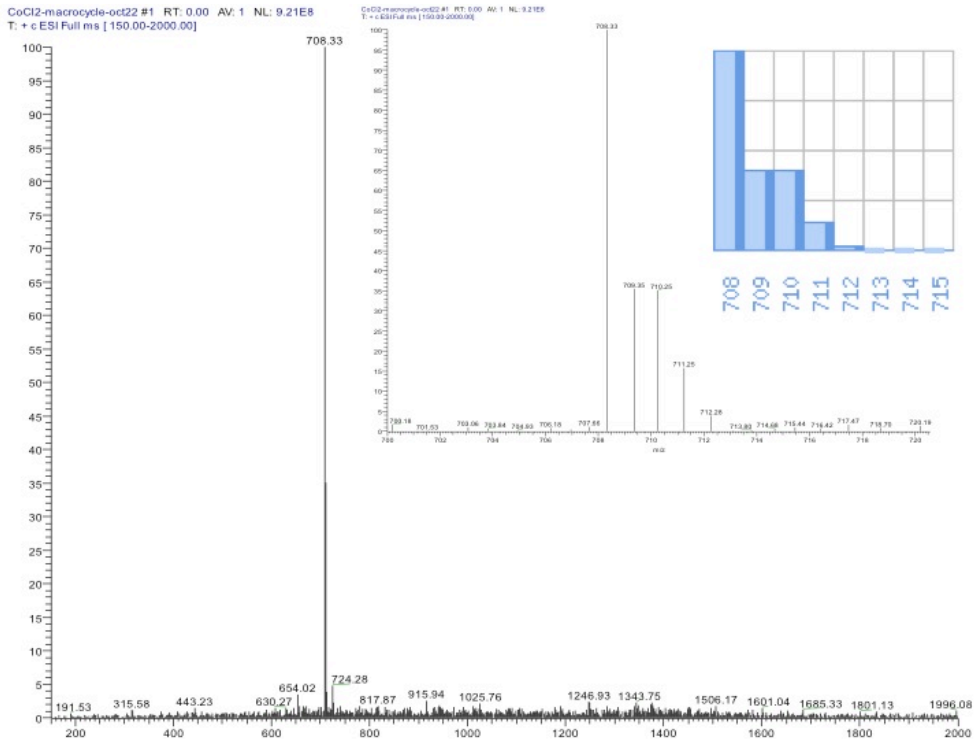

Figure C.2.5. ESI mass spectrum of Co(**6b**)Cl_2**.**

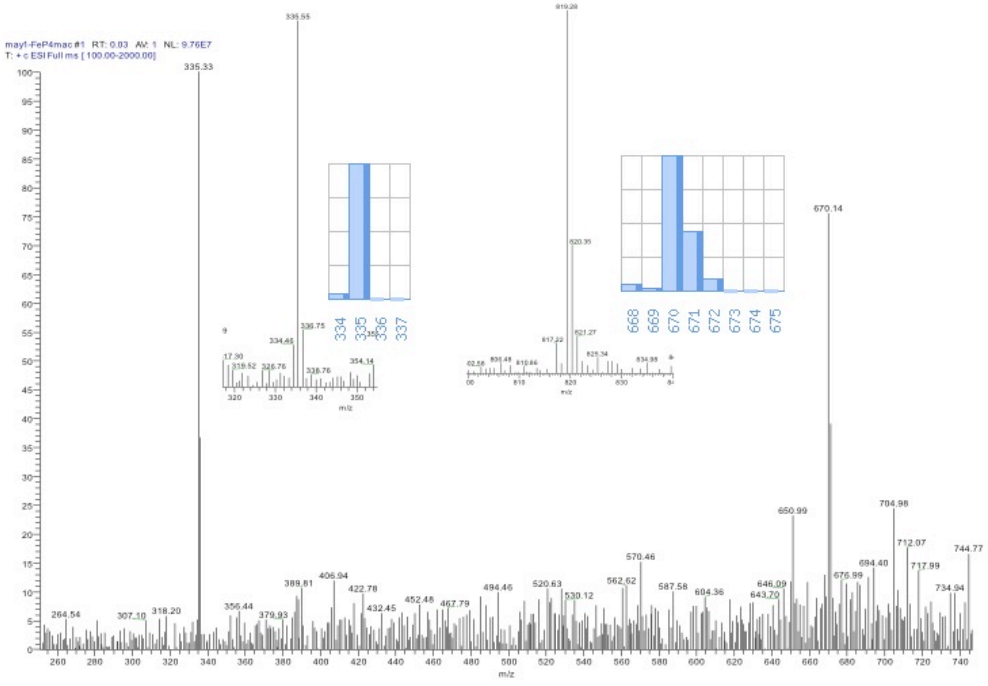

Figure C.2.6. ESI mass spectrum of [Fe(**6b**)$(CH_3CN)_2$]$(BPh_4)_2$**.**

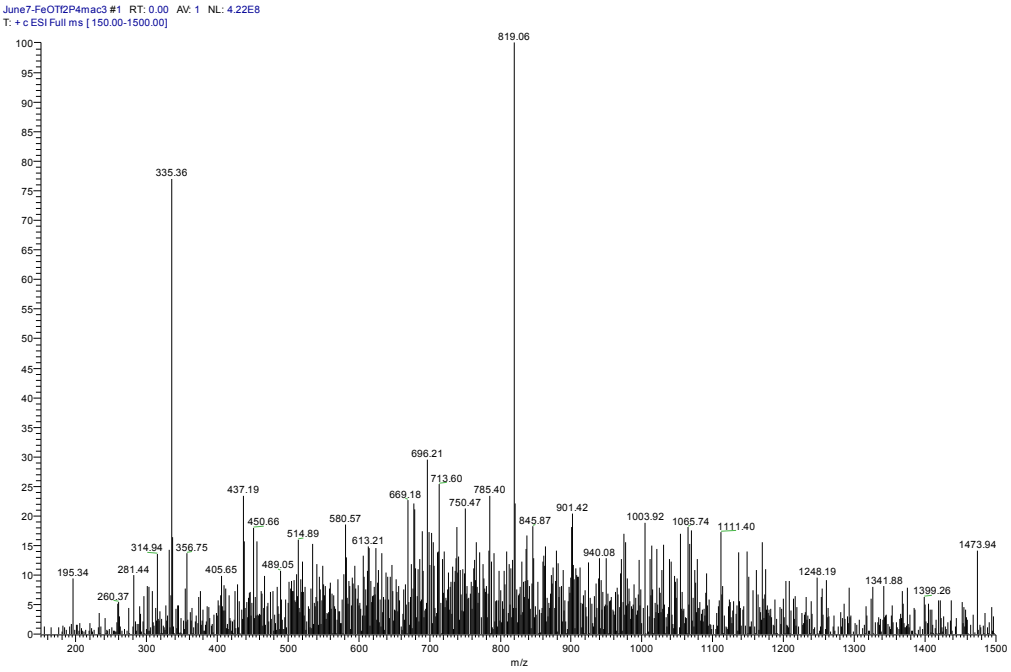

Figure C.2.7. ESI mass spectrum of [Fe(**6b**)(CH_3CN)$_2$](OTf)$_2$**.**

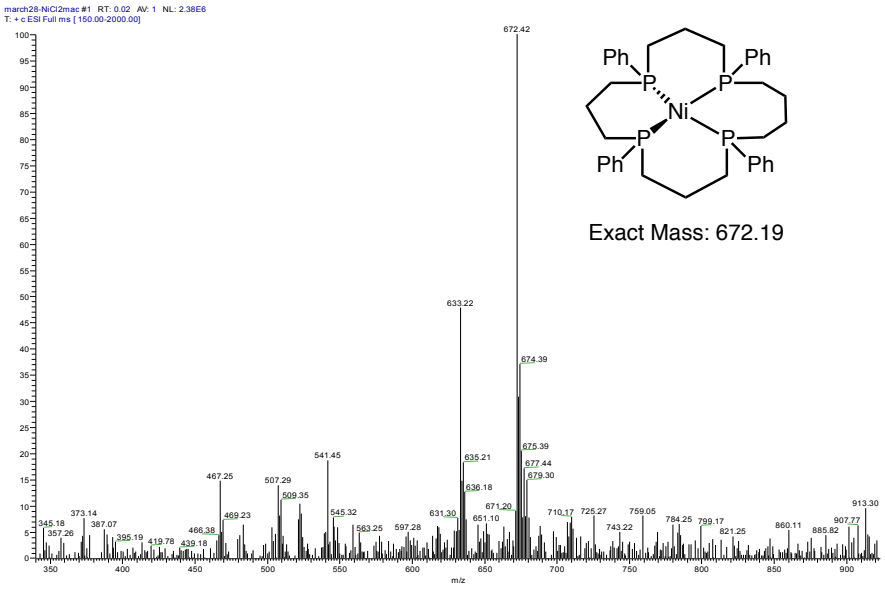

Figure C.2.7. ESI mass spectrum of [Ni(**6b**)]Cl_2.

C.3. Infrared Spectra

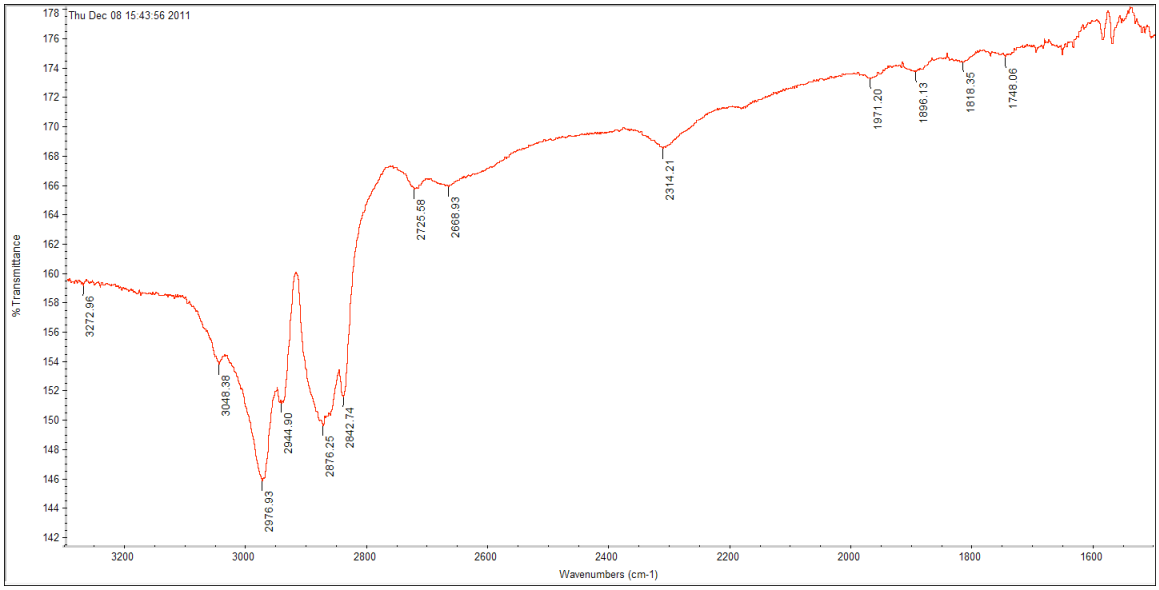

Figure C.3.1. Infrared spectrum of Cu(**3**)OTf, **4**.

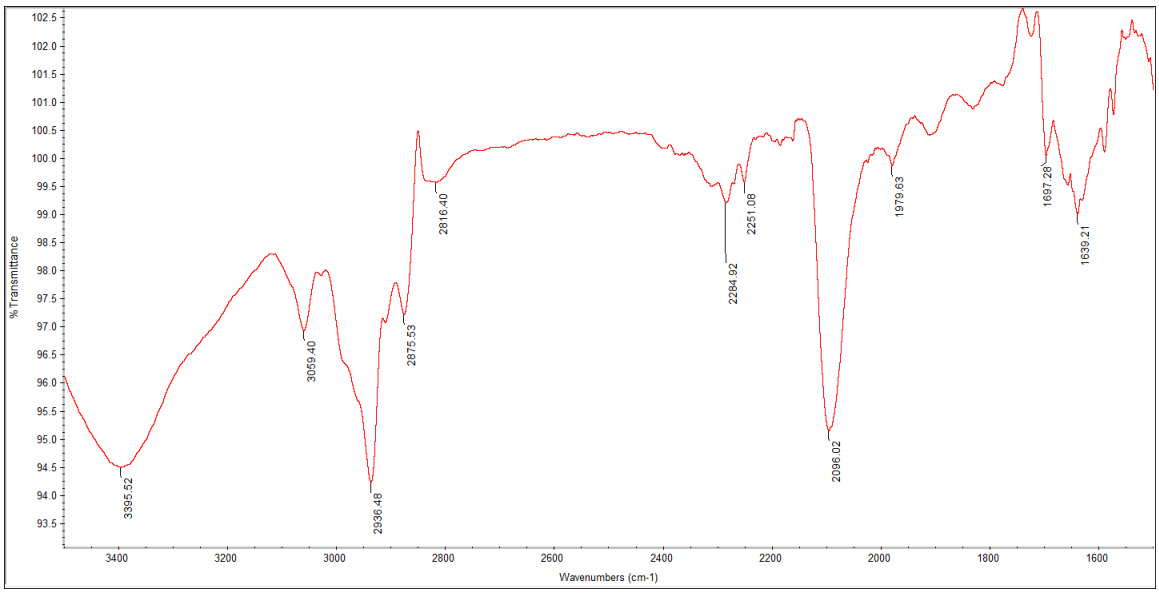

Figure C.3.2. Infrared spectrum of [Fe(**6b**)$(CH_3CN)_2$]$(OTf)_2$.

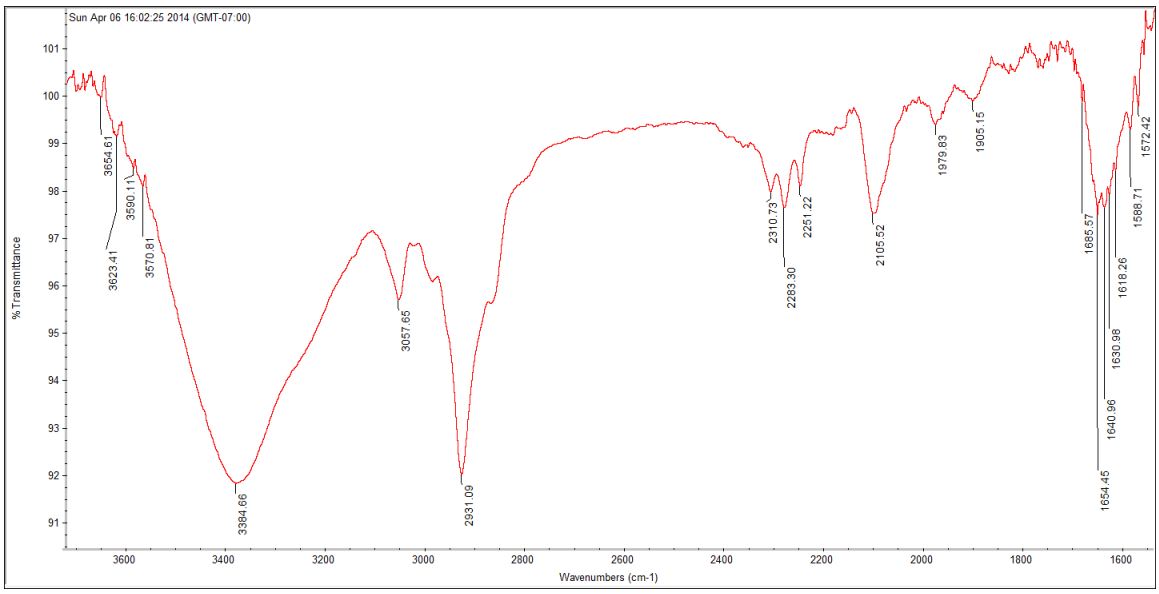

Figure C.3.3. Infrared spectrum of [Fe(**6b**)(CH_3CN)$_2$](OTf)$_2$ made in an Ar-filled glovebox.

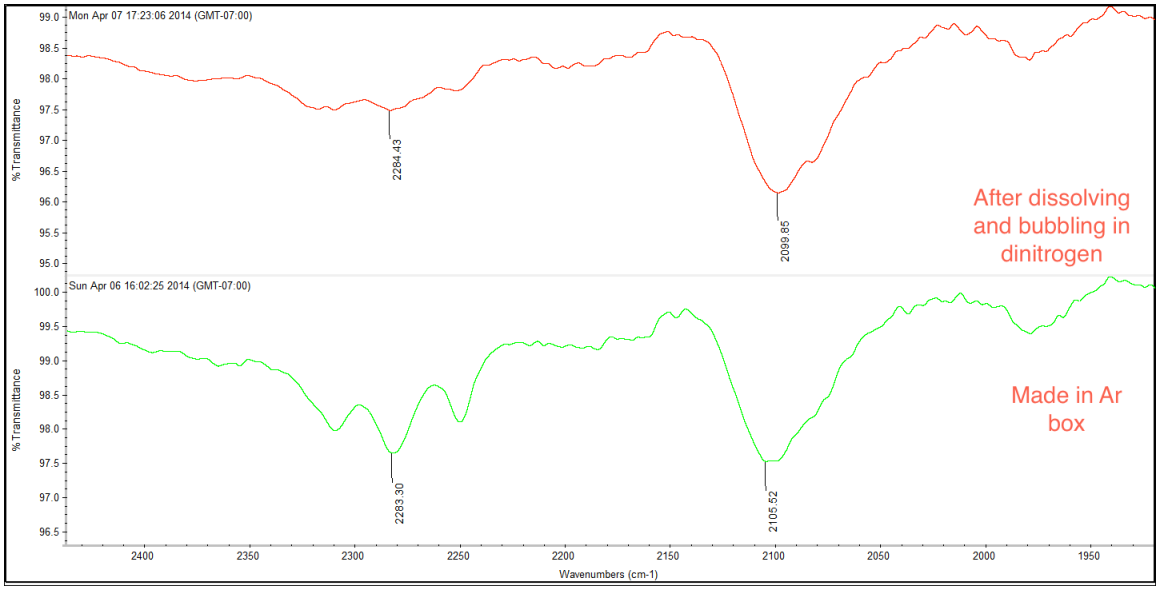

Figure C.3.3. Infrared spectrum of [Fe(**6b**)(CH_3CN)$_2$](OTf)$_2$ made in an Ar-filled glovebox, redissolved and and bubbled with N_2.

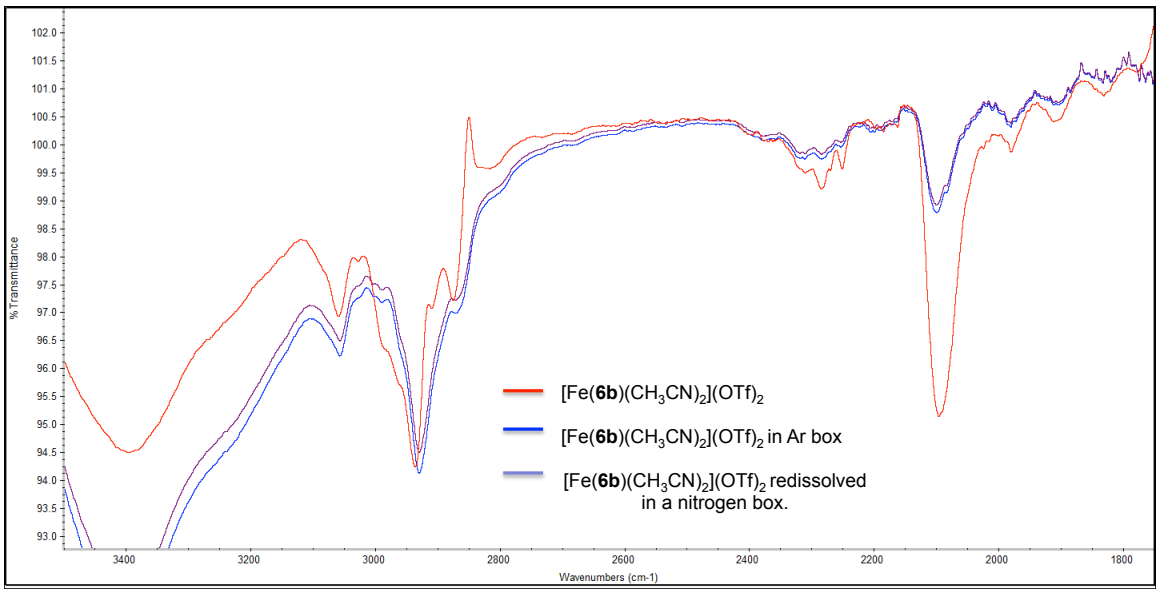

Figure C.3.4. Overlay of [Fe(**6b**)$(CH_3CN)_2$]$(OTf)_2$ made in an argon-filled glovebox vs. made in a nitrogen-filled glovebox.

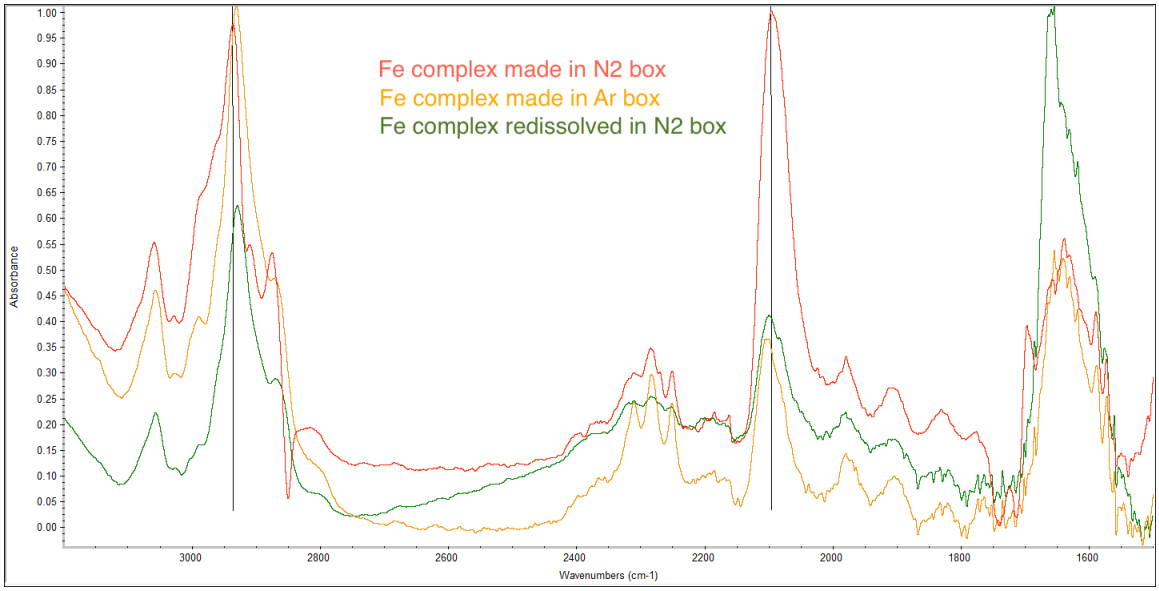

Figure C.3.5. Overlay of [Fe(**6b**)$(CH_3CN)_2$]$(OTf)_2$ made in an argon-filled glovebox vs. made in a nitrogen-filled glovebox (y-axis is absorbance).

C.4. UV-Vis Spectra

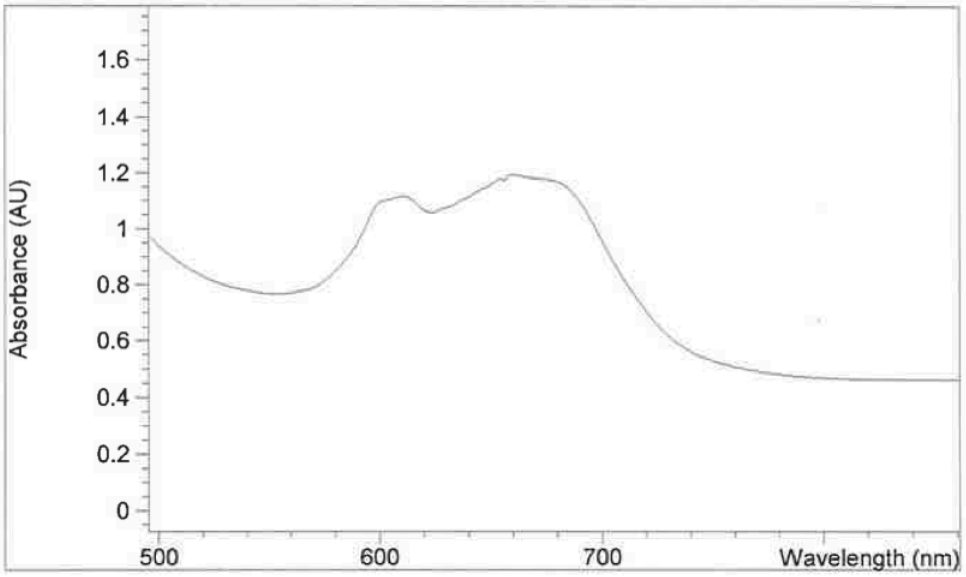

Figure C.4.1. UV-Vis spectrum of Co(**6b**)Cl_2 in dichloromethane.

C.5. Figures

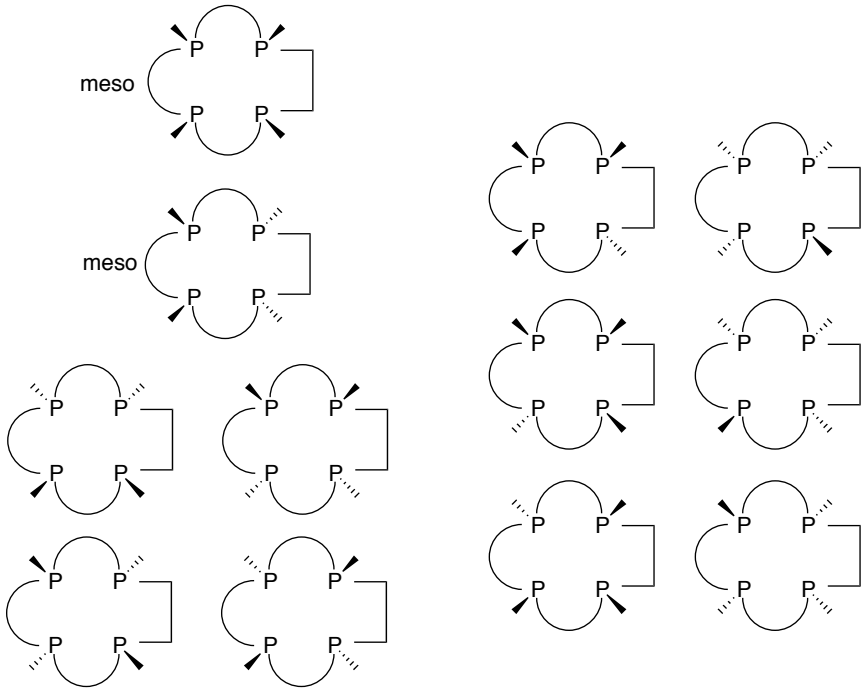

C.5.1. Possible stereoisomers of phosphine **6b** (arc = -C_3H_6-, box = -C_4H_8-).

APPENDIX D

SUPPORTING INFORMATION FOR CHAPTER V

D.1 NMR Spectra

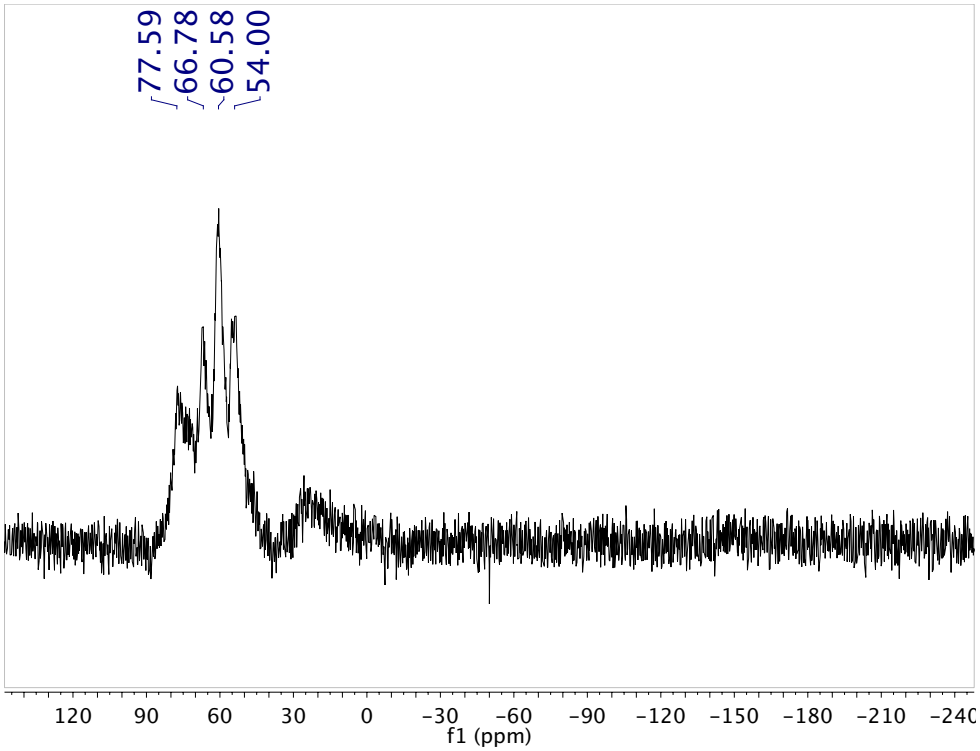

Figure D.1.1. $^{31}P\{^{1}H\}$ NMR Spectrum of **1** in $CDCl_3$.

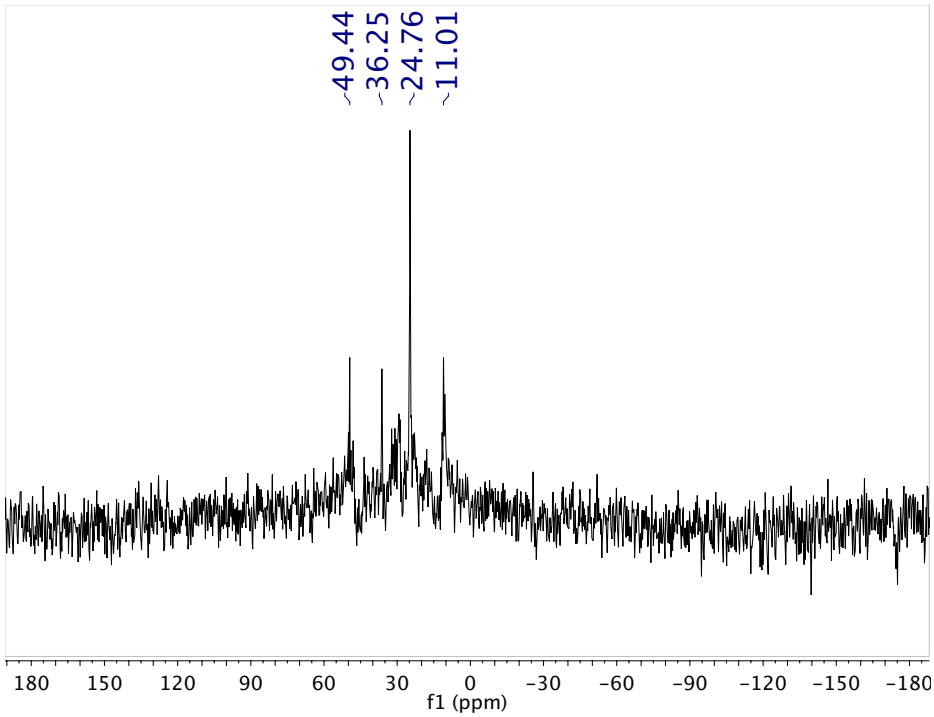

Figure D.1.2. $^{31}P\{^{1}H\}$ NMR Spectrum of **2** in $CDCl_3$.

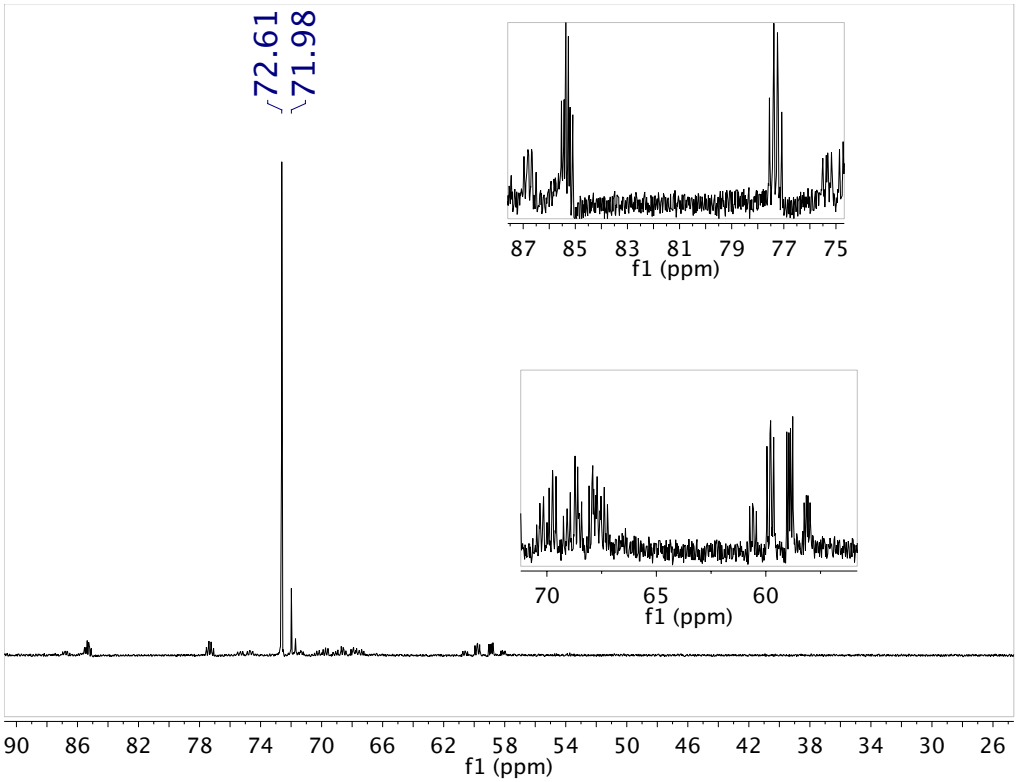

Figure D.1.3. $^{31}P\{^{1}H\}$ NMR Spectrum of **3** in $CDCl_3$.

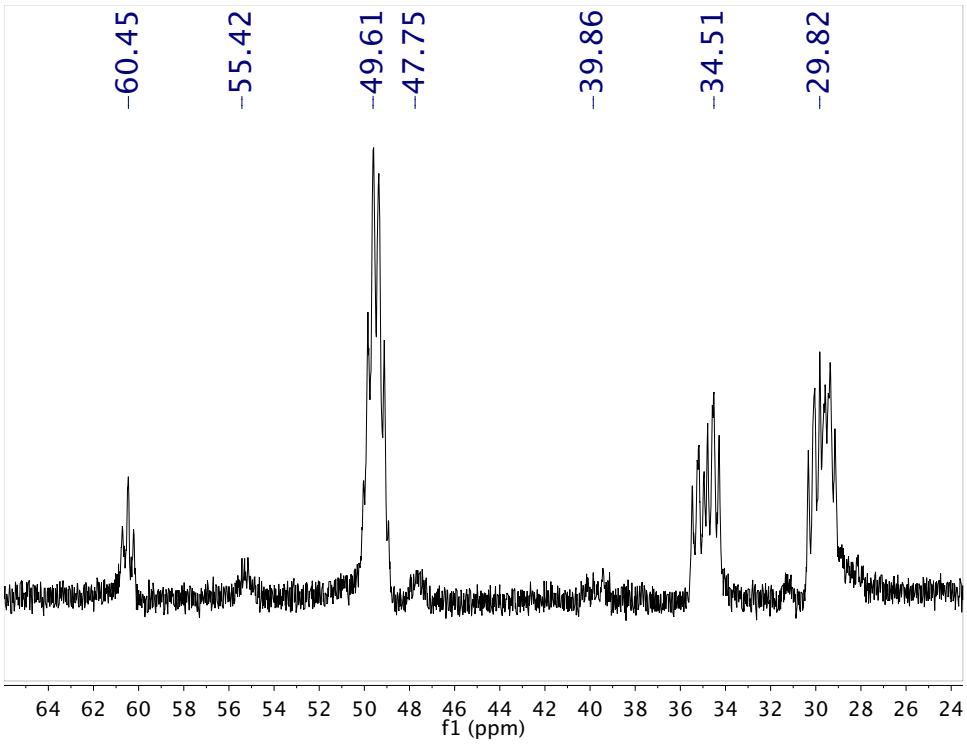

Figure D.1.4. $^{31}P\{^{1}H\}$ NMR Spectrum of **4** in $CDCl_3$.

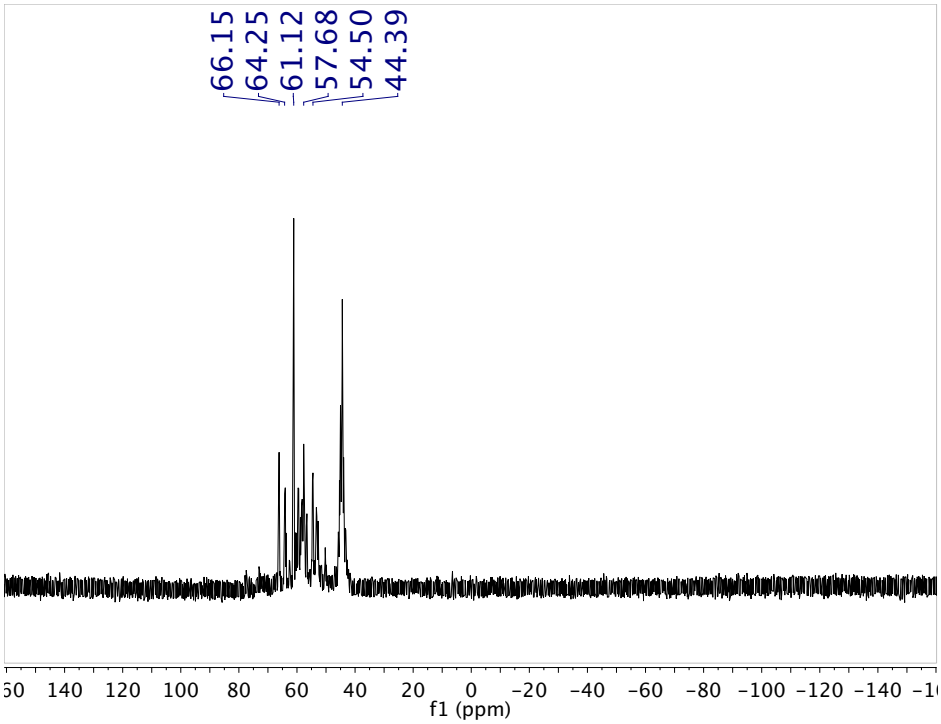

Figure D.1.5. $^{31}P\{^{1}H\}$ NMR Spectrum of **5** in $CDCl_3$.

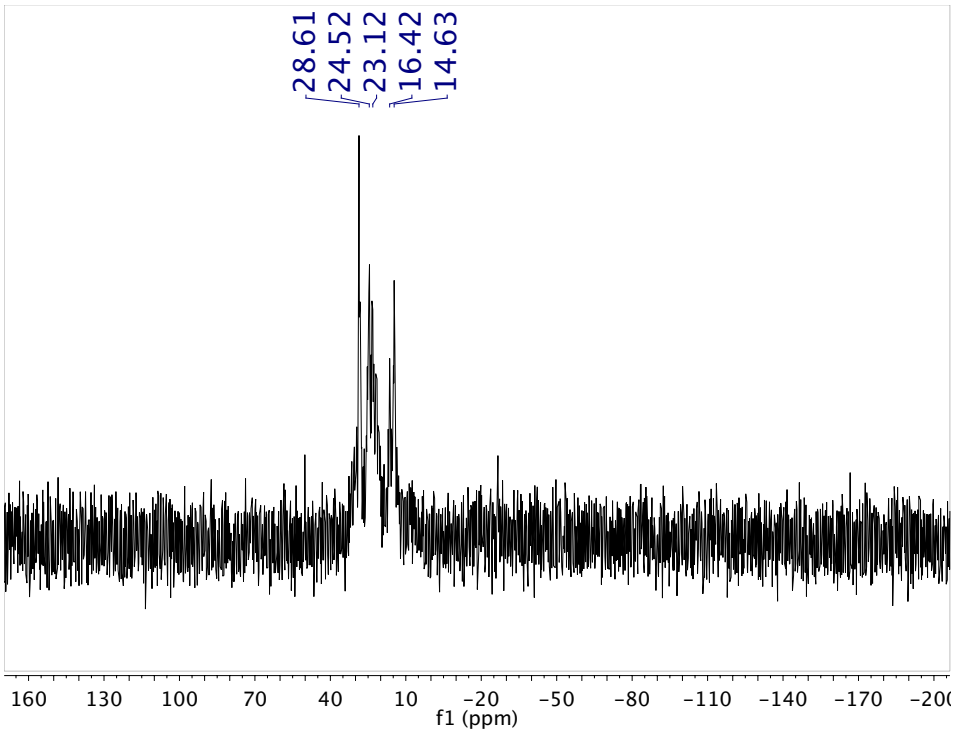

Figure D.1.6. $^{31}P\{^{1}H\}$ NMR Spectrum of **6** in $CDCl_3$.

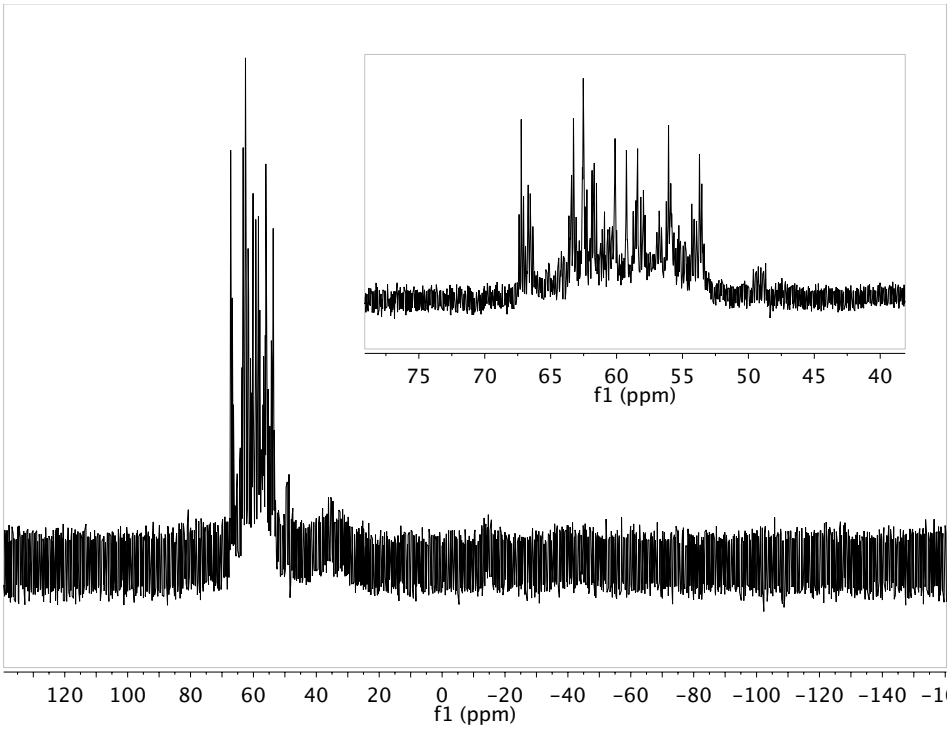

Figure D.1.7. $^{31}P\{^{1}H\}$ NMR Spectrum of **7** in $CDCl_3$.

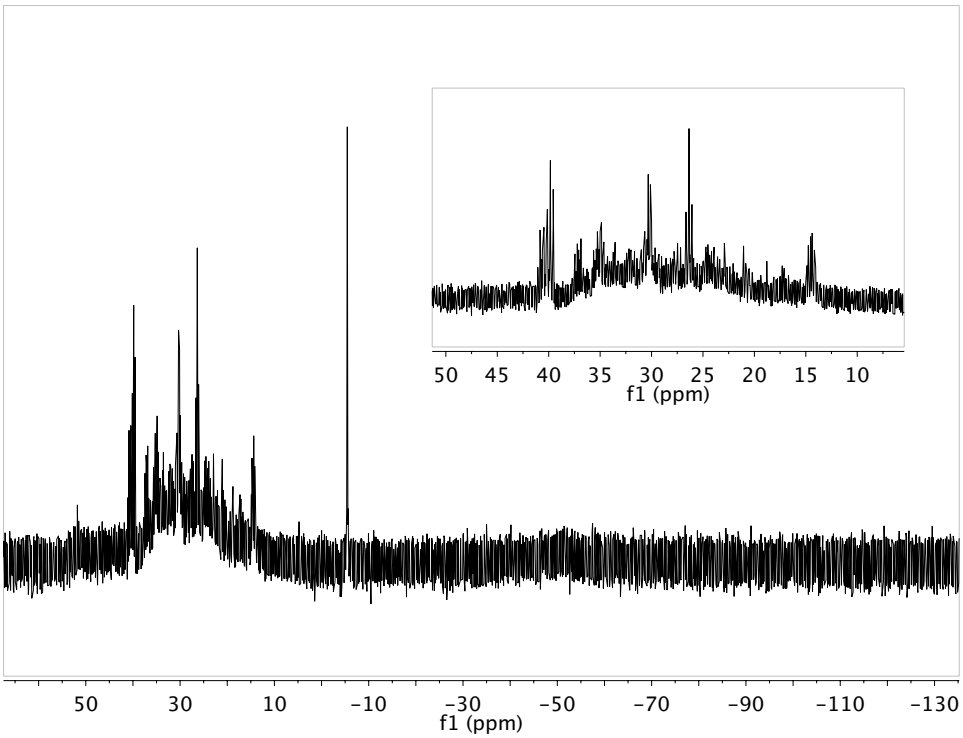

Figure D.1.8. $^{31}P\{^{1}H\}$ NMR Spectrum of **8** in $CDCl_3$.

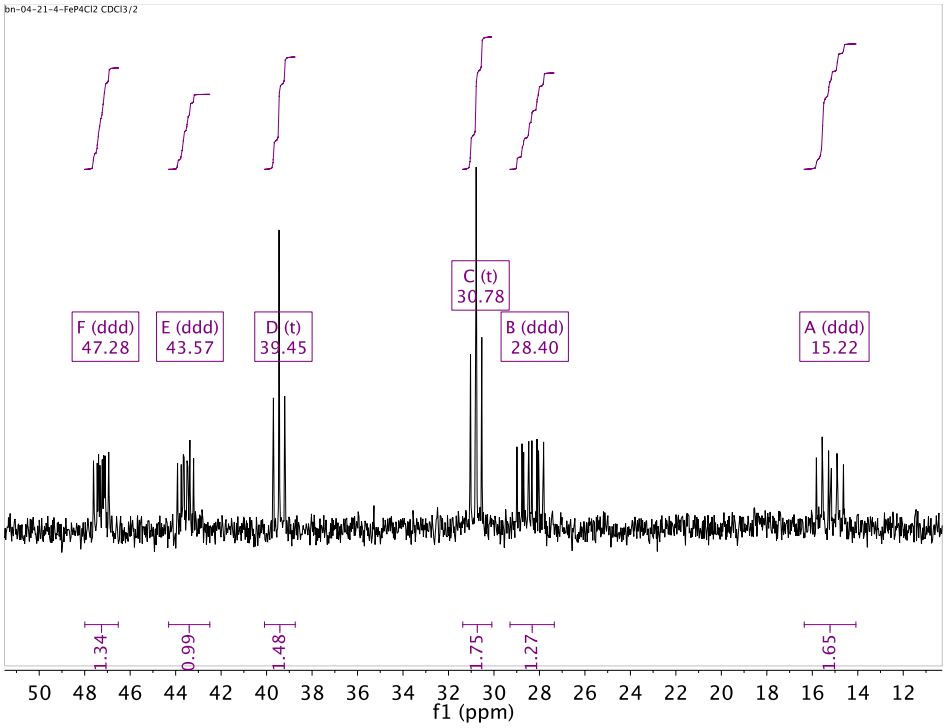

Figure D.1.9. $^{31}P\{^{1}H\}$ NMR Spectrum of **10a** in $CDCl_3$.

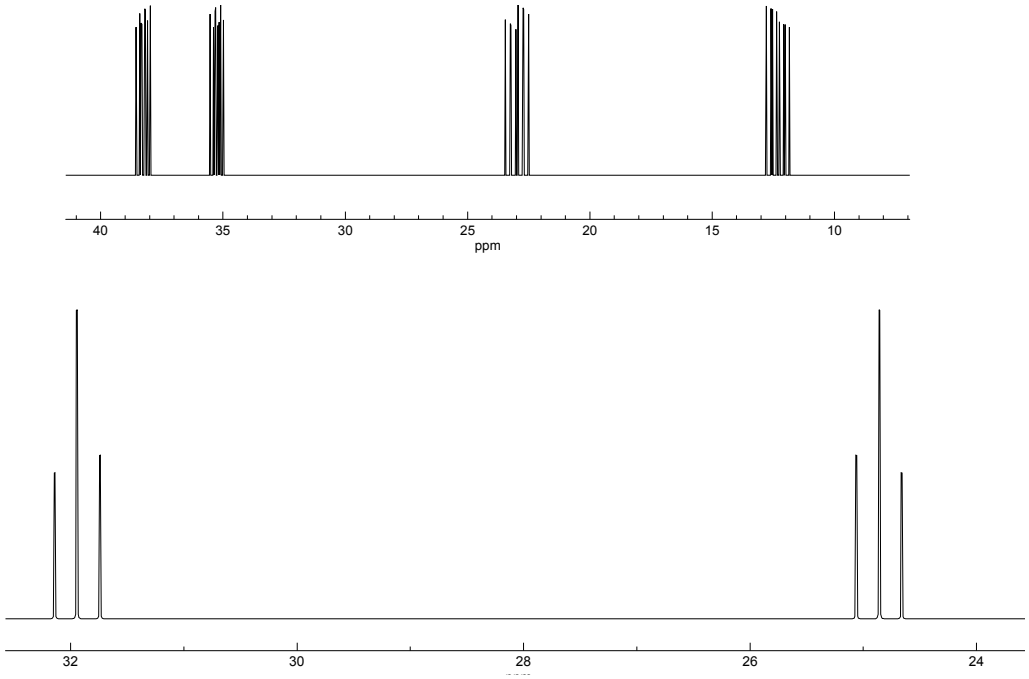

Figure D.1.10. Simulated $^{31}P\{^{1}H\}$ NMR Spectrum of **10a**.

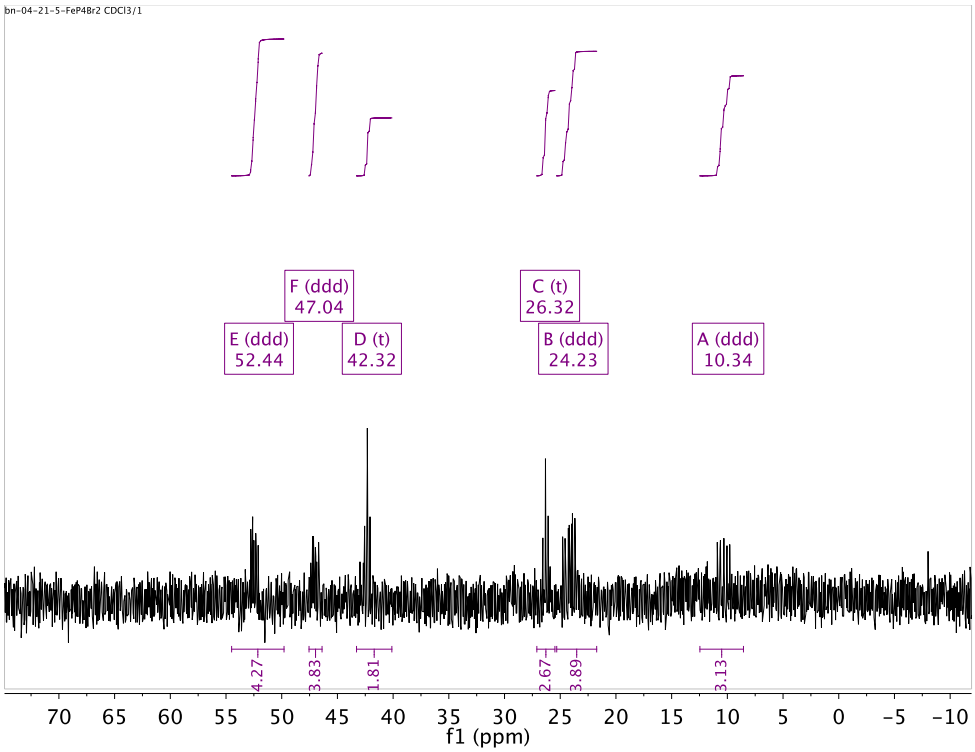

Figure D.1.11. $^{31}P\{^{1}H\}$ NMR Spectrum of **10b** in $CDCl_3$.

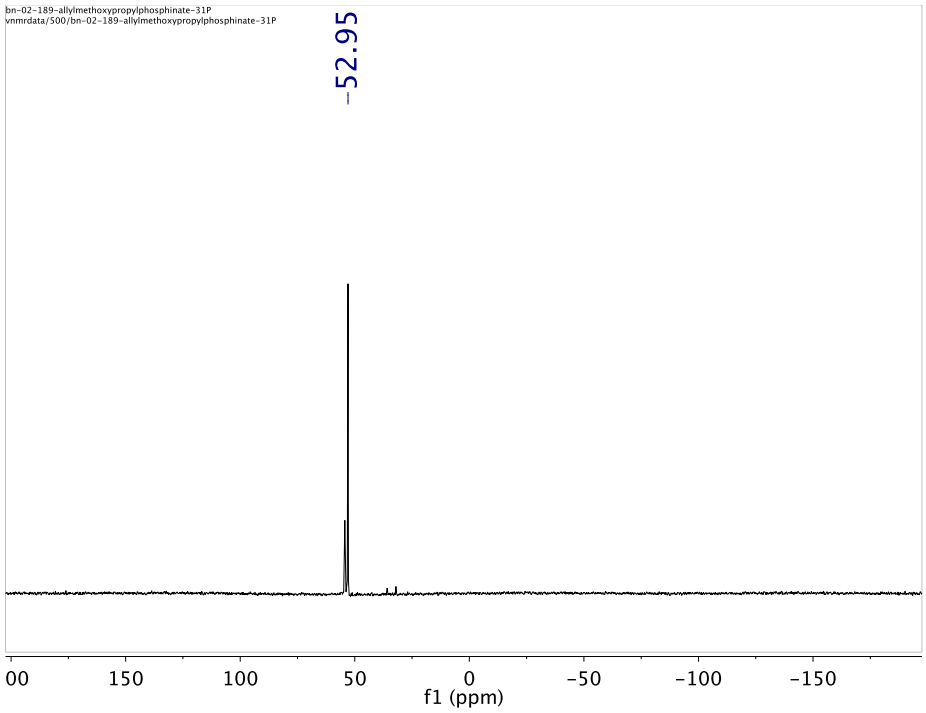

Figure D.1.12. $^{31}P\{^{1}H\}$ NMR Spectrum of **13a** in $CDCl_3$.

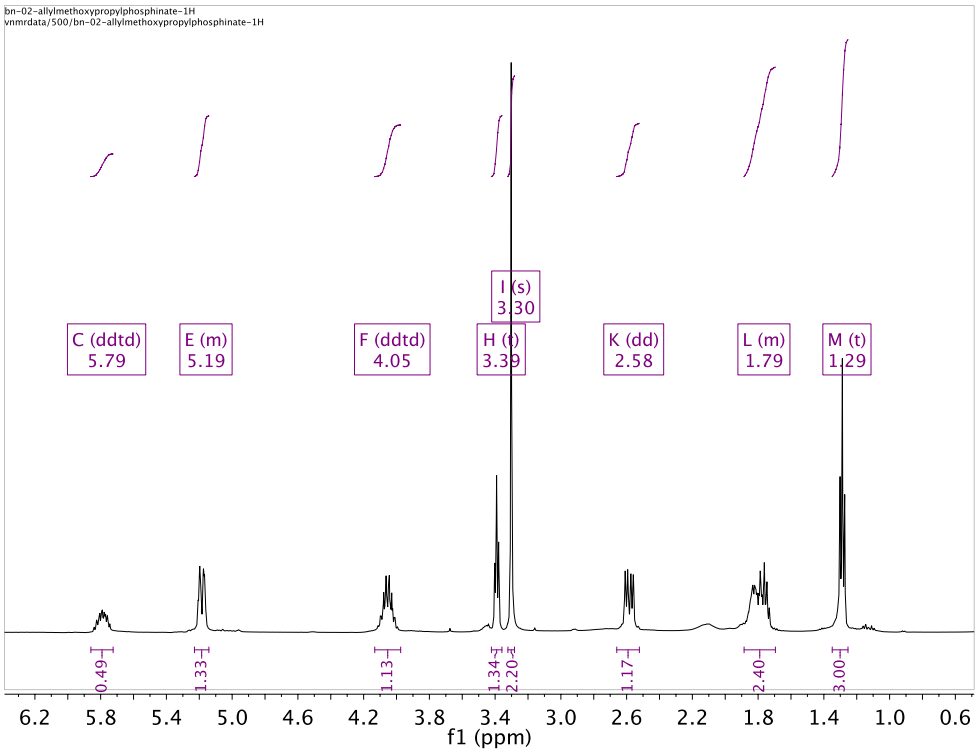

Figure D.1.13. ^{1}H NMR Spectrum of **13a** in $CDCl_3$.

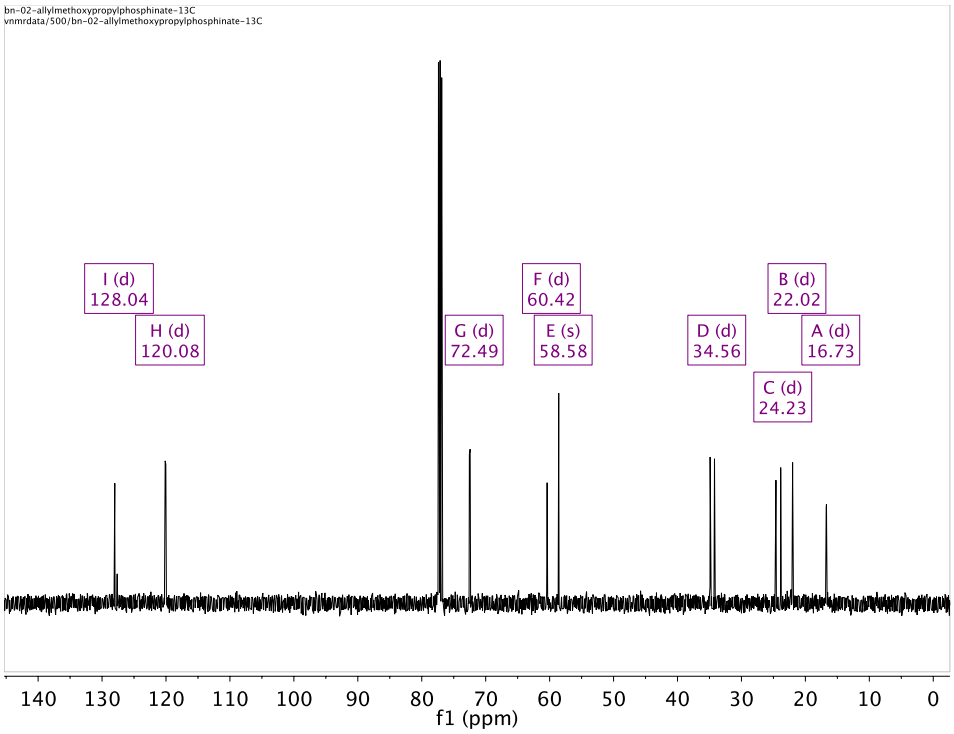

Figure D.1.14. ^{13}C NMR Spectrum of **13a** in $CDCl_3$.

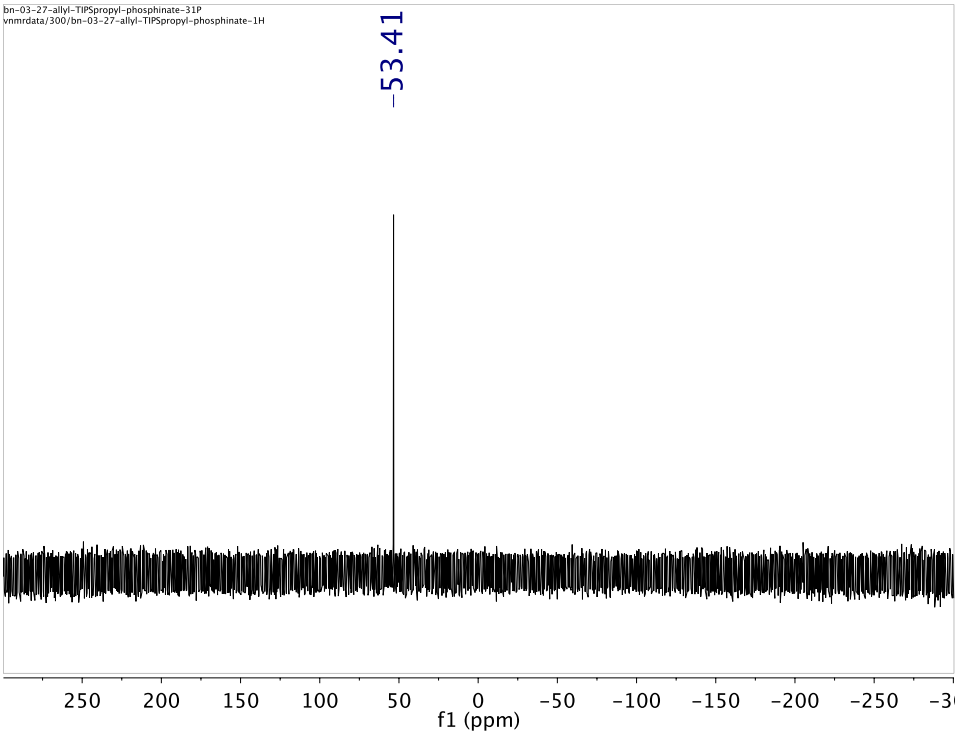

Figure D.1.15. $^{31}P\{^{1}H\}$ NMR Spectrum of **13b** in $CDCl_3$.

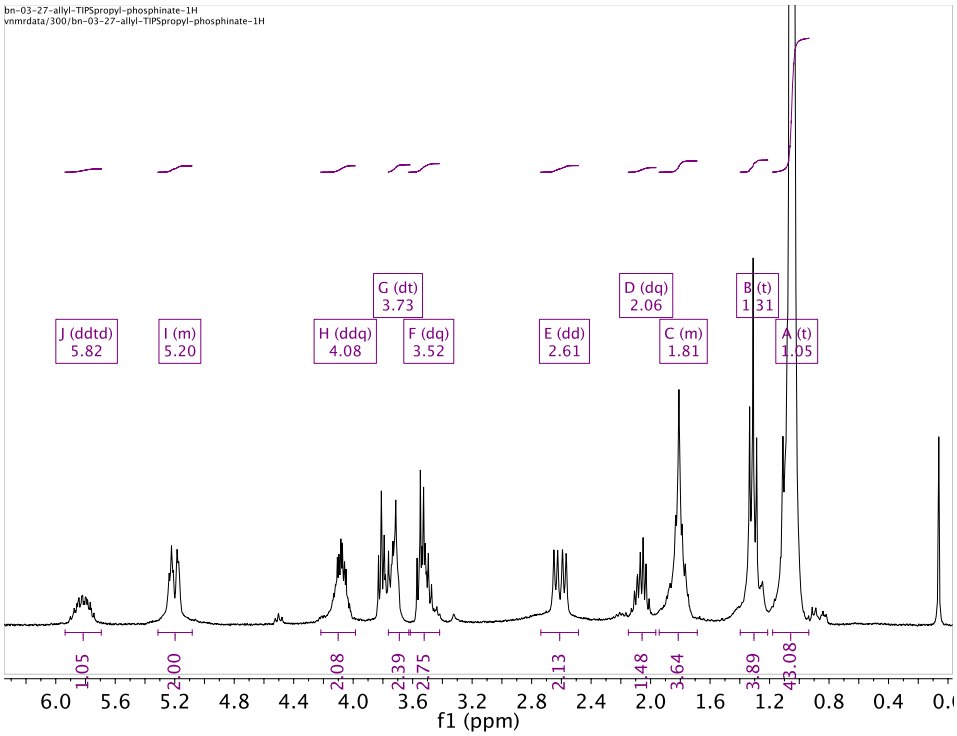

Figure D.1.16. ^{1}H NMR Spectrum of **13b** in $CDCl_3$.

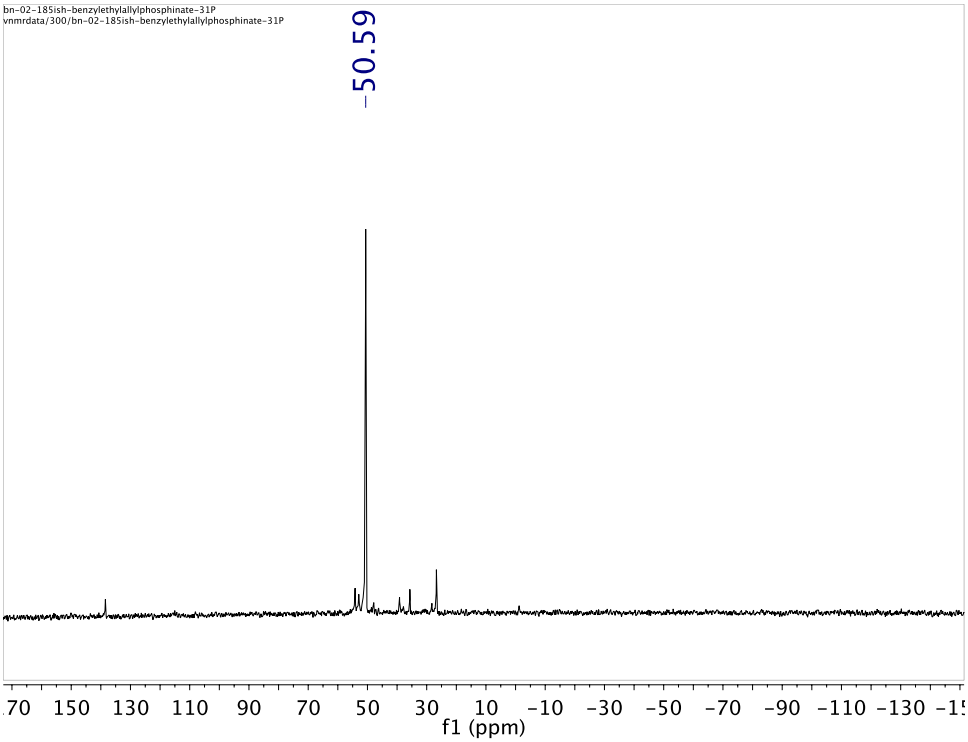

Figure D.1.17. $^{31}P\{^{1}H\}$ NMR Spectrum of **13c** in $CDCl_3$.

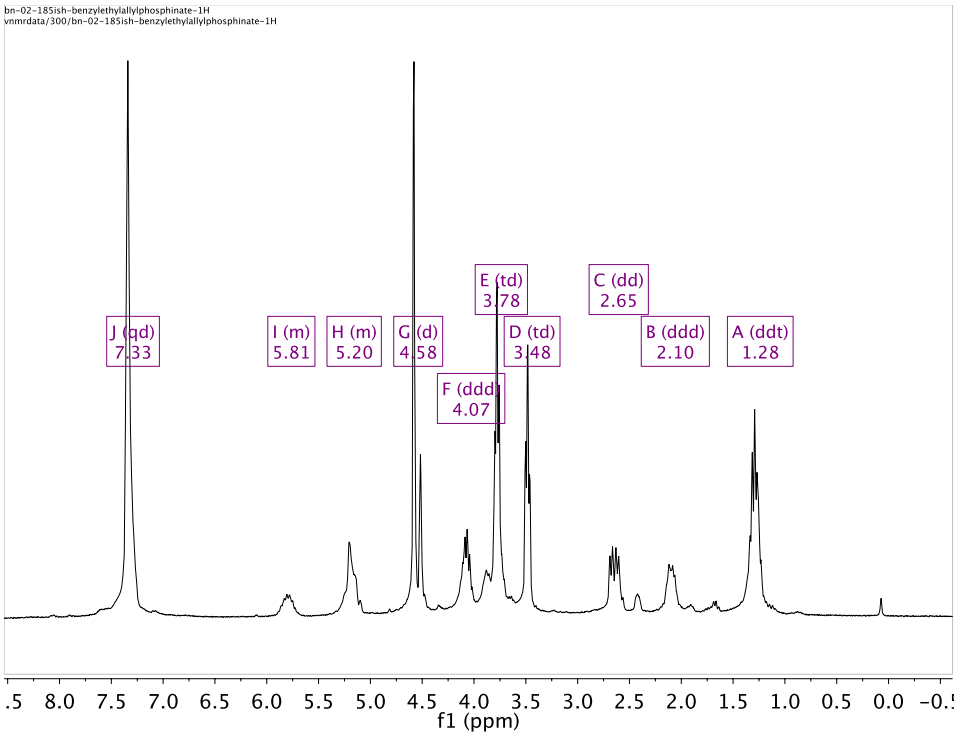

Figure D.1.18. ^{1}H NMR Spectrum of **13c** in $CDCl_3$.

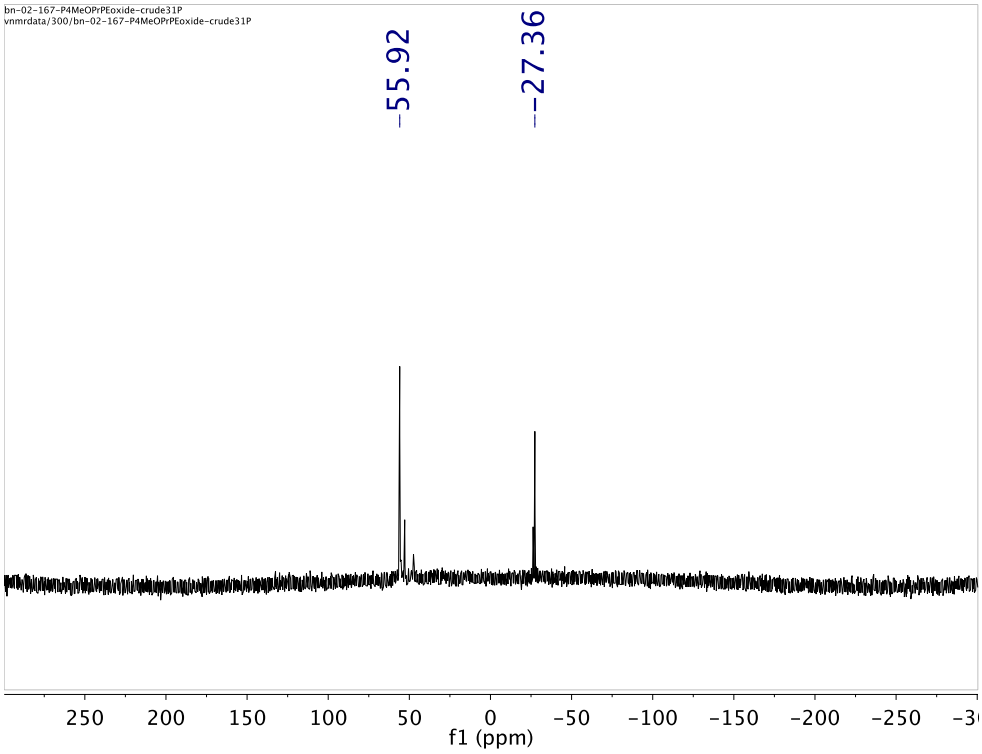

Figure D.1.19. $^{31}P\{^{1}H\}$ NMR Spectrum of **14** in $CDCl_3$.

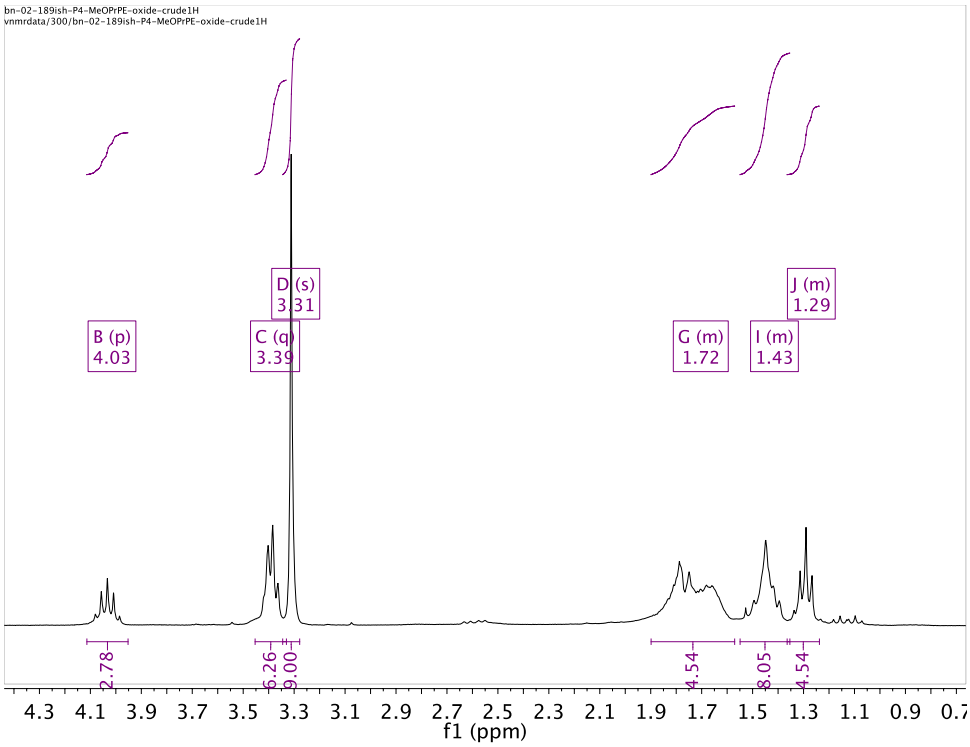

Figure D.1.20. ^{1}H NMR Spectrum of **14** in $CDCl_3$.

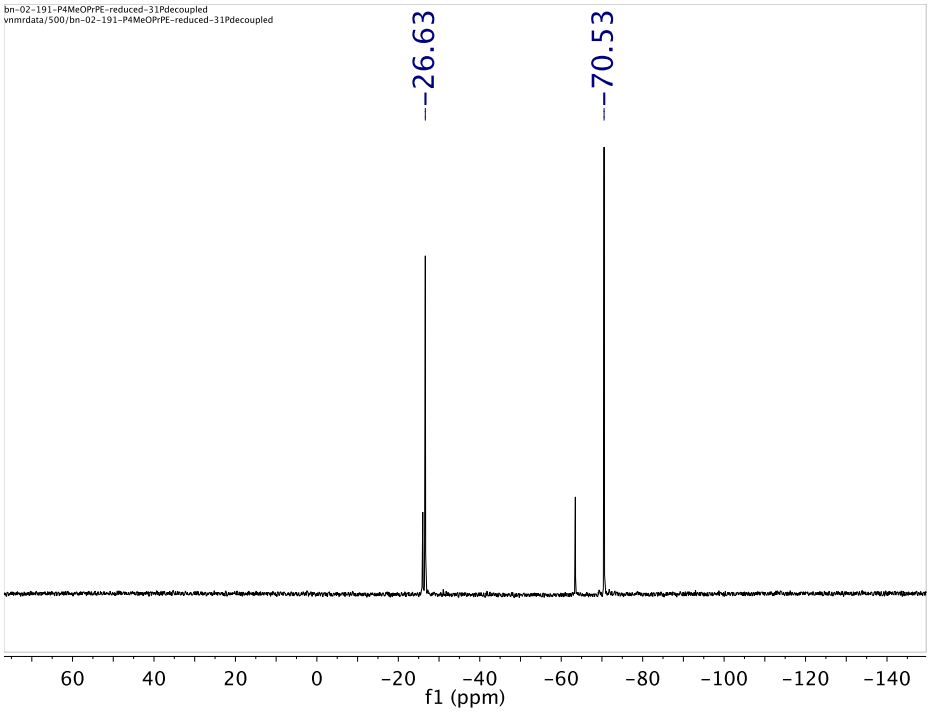

Figure D.1.21. $^{31}P\{^{1}H\}$ NMR Spectrum of **15** in $CDCl_3$.

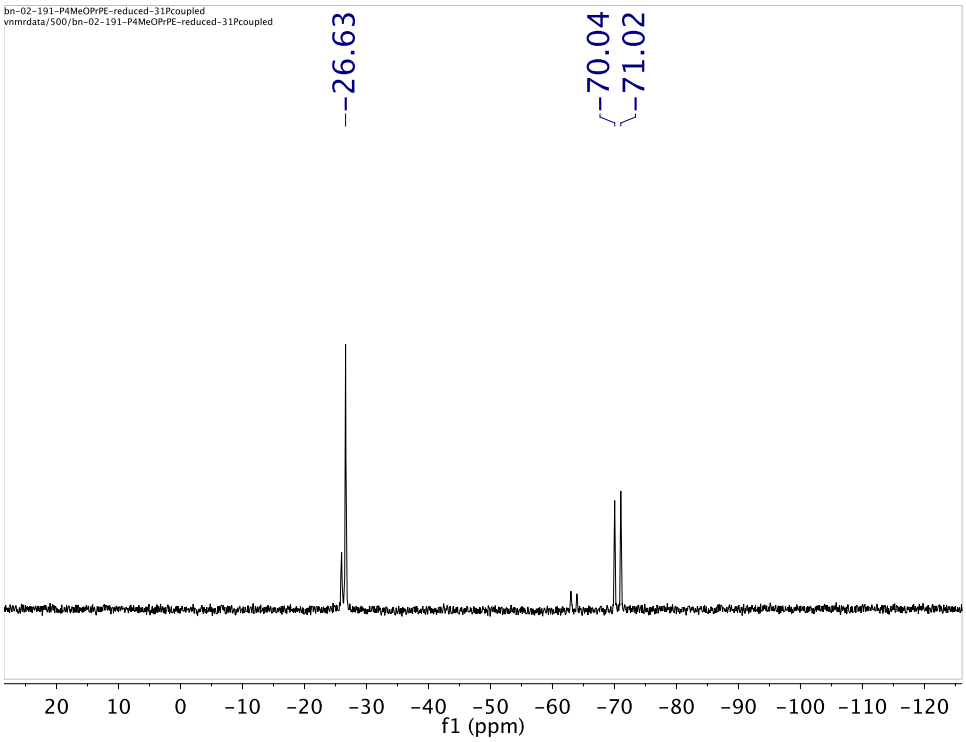

Figure D.1.22. ^{31}P NMR Spectrum of **15** in $CDCl_3$.

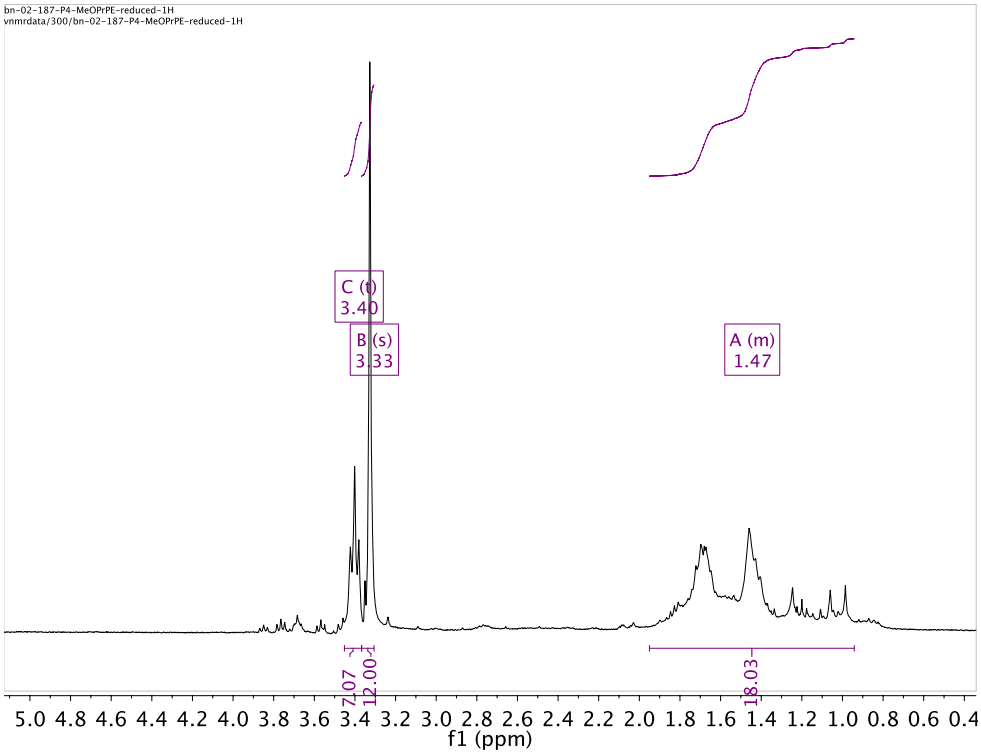

Figure D.1.23. ^{1}H NMR Spectrum of **15** in $CDCl_3$.

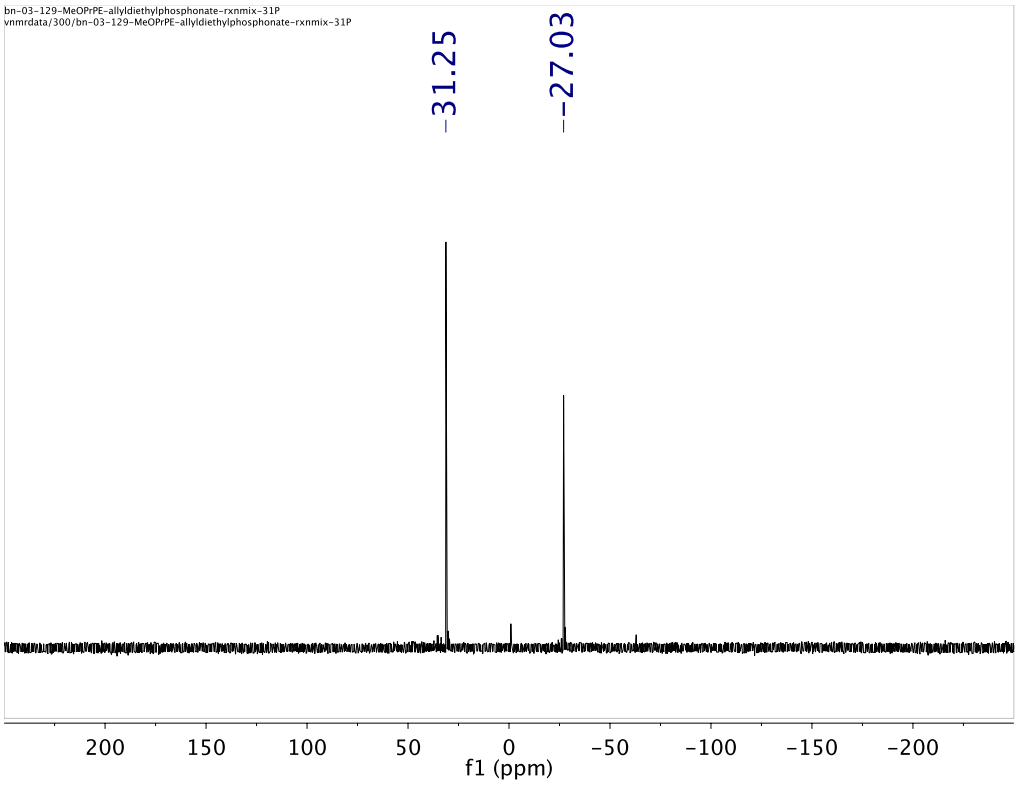

Figure D.1.24. $^{31}P\{^{1}H\}$ NMR Spectrum of **16** in $CDCl_3$.

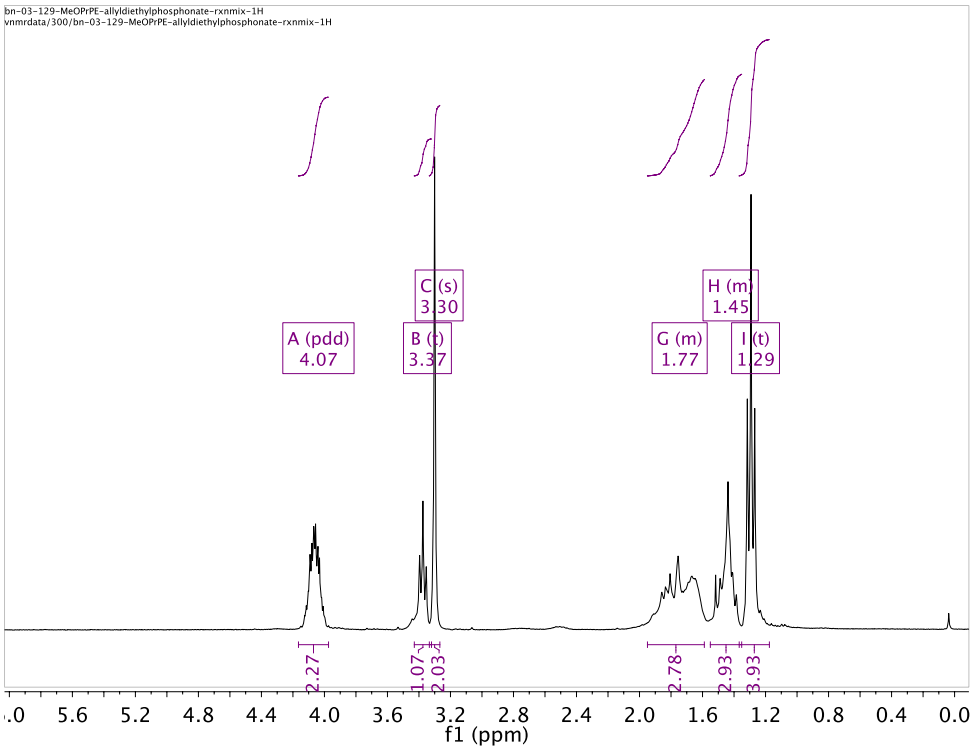

Figure D.1.25. ^{1}H NMR Spectrum of **16** in $CDCl_3$.

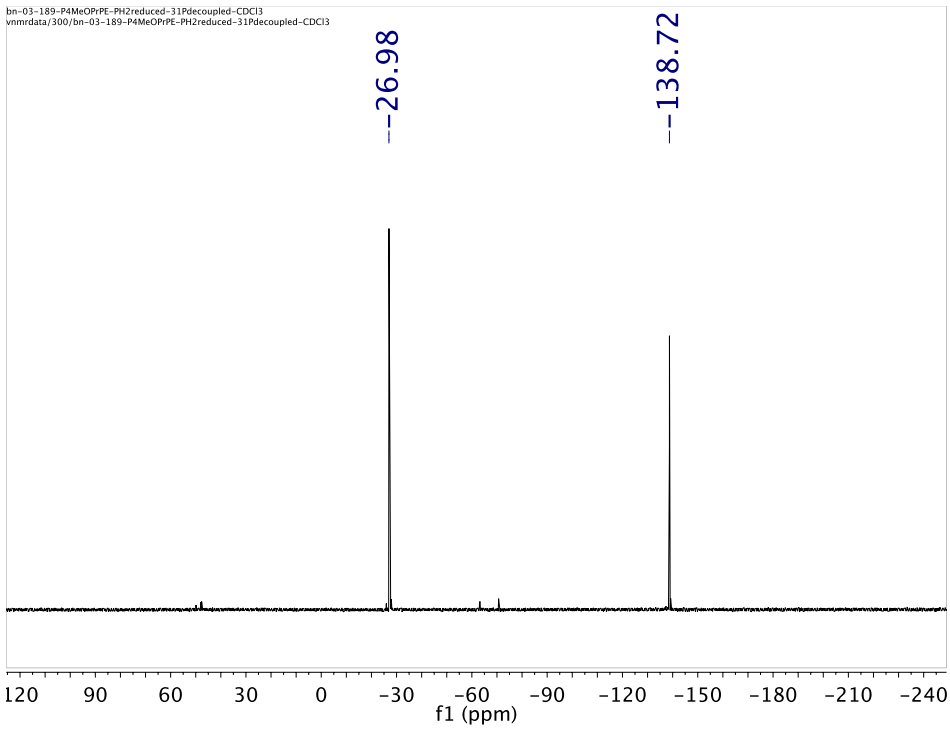

Figure D.1.26. $^{31}P\{^{1}H\}$ NMR Spectrum of **17** in $CDCl_3$.

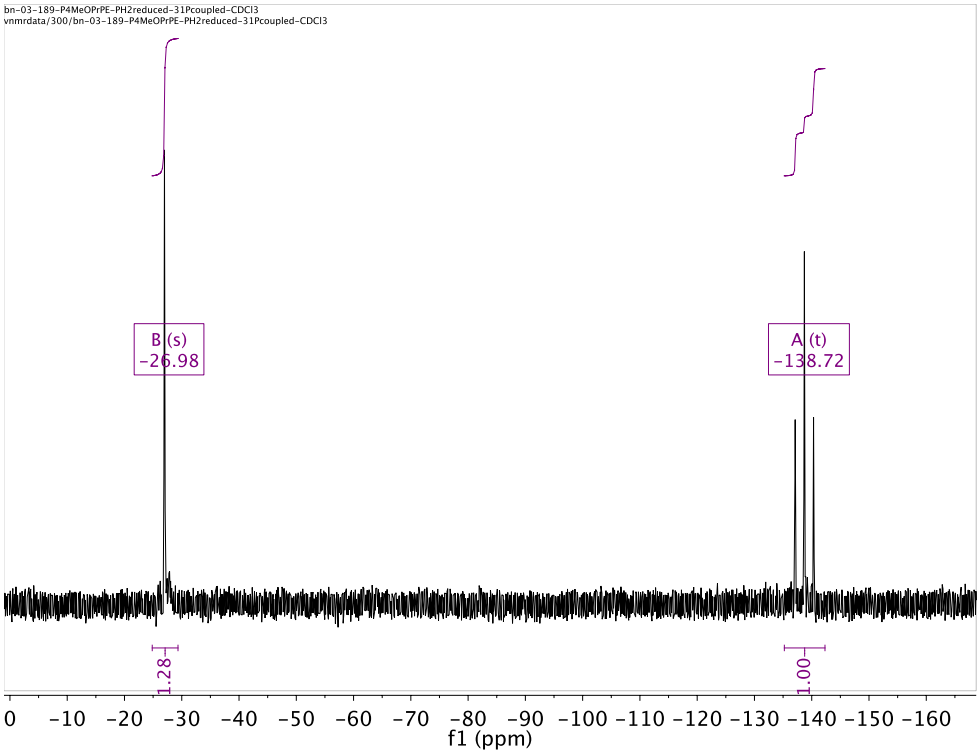

Figure D.1.27. ^{31}P NMR Spectrum of **17** in $CDCl_3$.

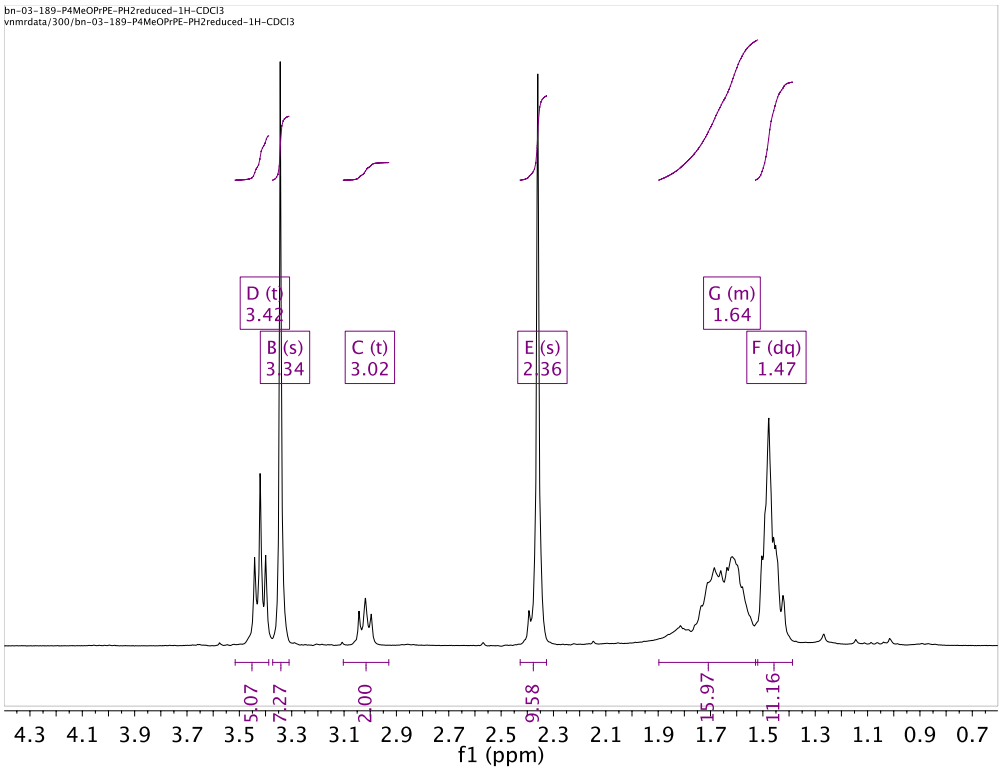

Figure D.1.28. ^{1}H NMR Spectrum of **17** in $CDCl_3$.

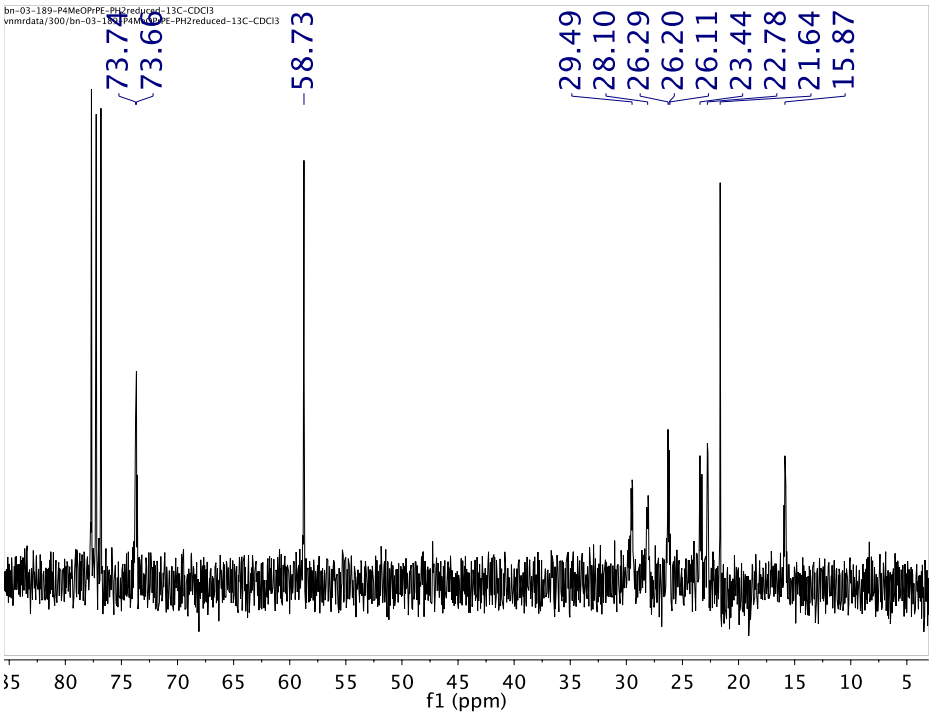

Figure D.1.29. ^{13}C NMR Spectrum of **17** in $CDCl_3$.

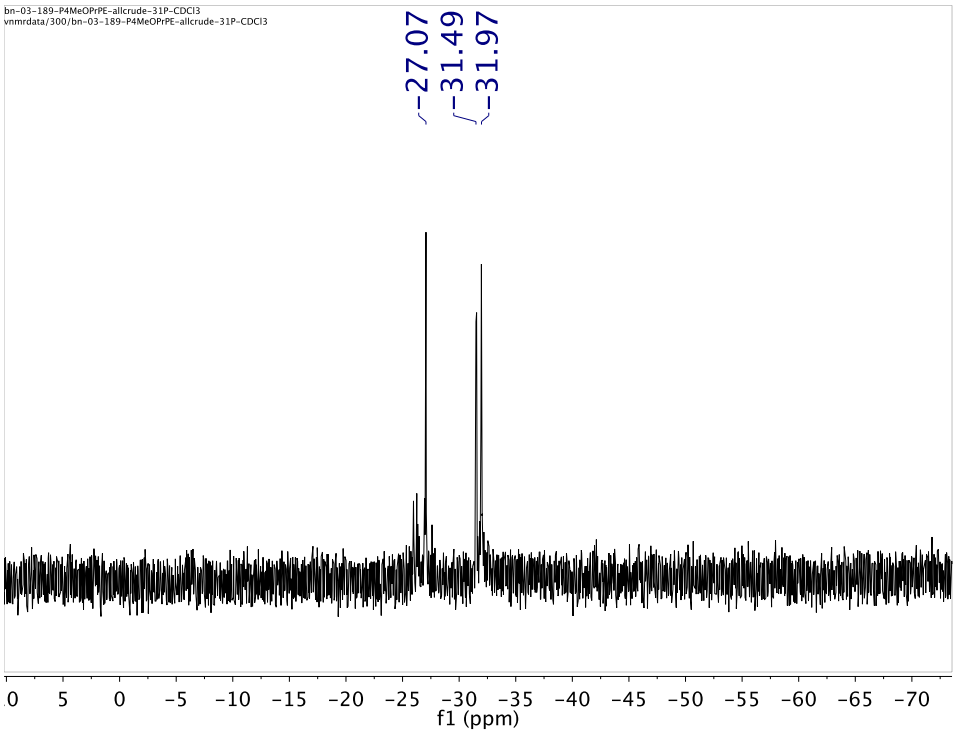

Figure D.1.30. $^{31}P\{^{1}H\}$ NMR Spectrum of **18** in $CDCl_3$.

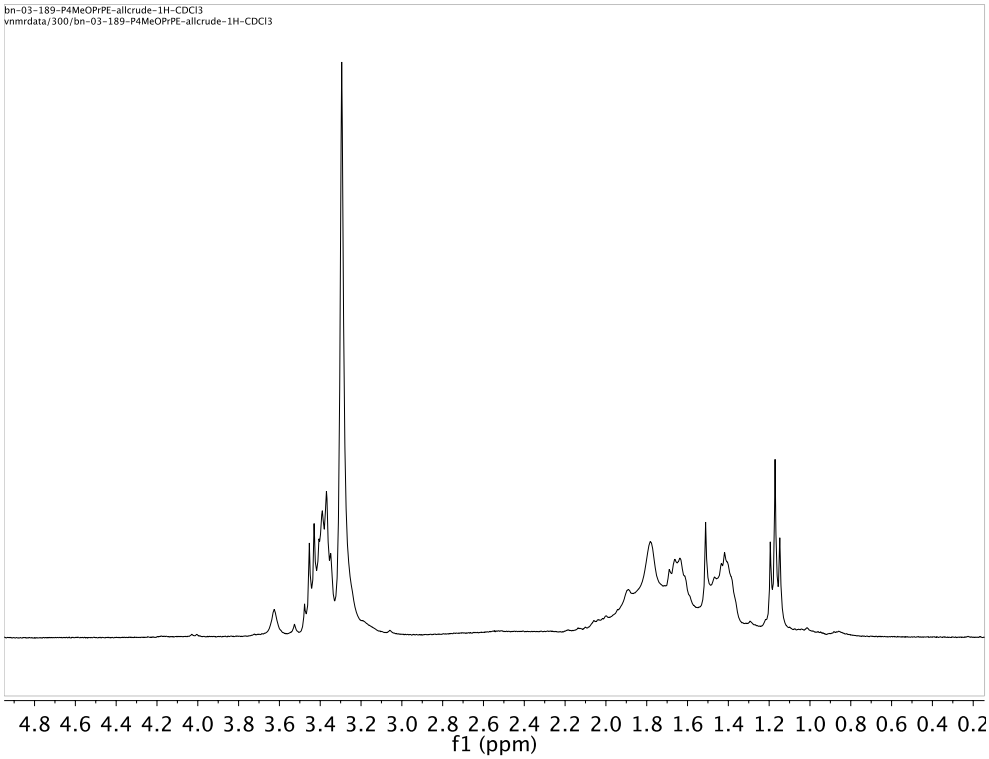

Figure D.1.31. ^{1}H NMR Spectrum of **18** in $CDCl_3$.

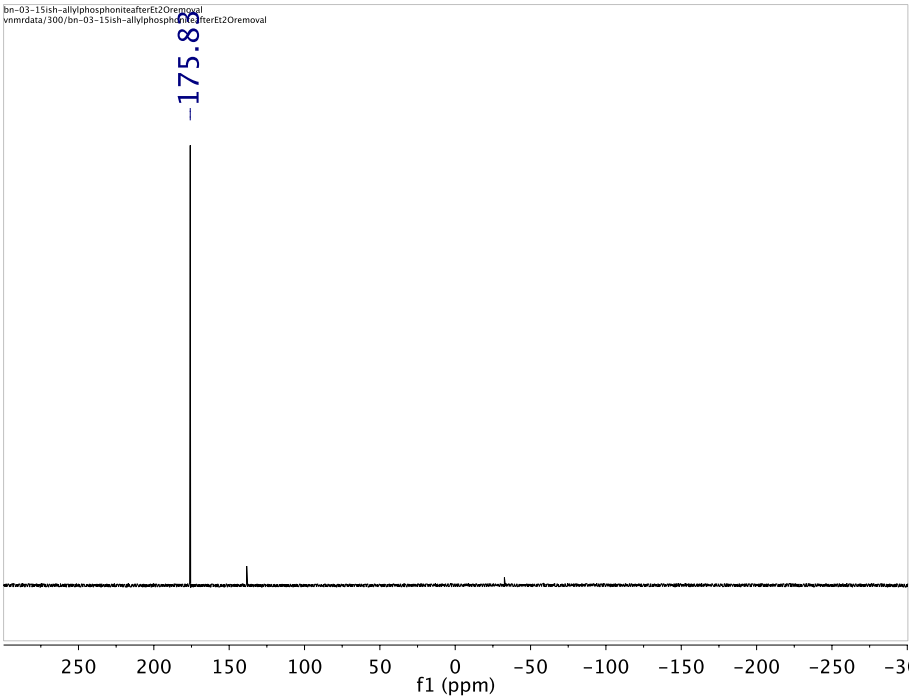

Figure D.1.32. $^{31}P\{^{1}H\}$ NMR Spectrum of **19** in $CDCl_3$.

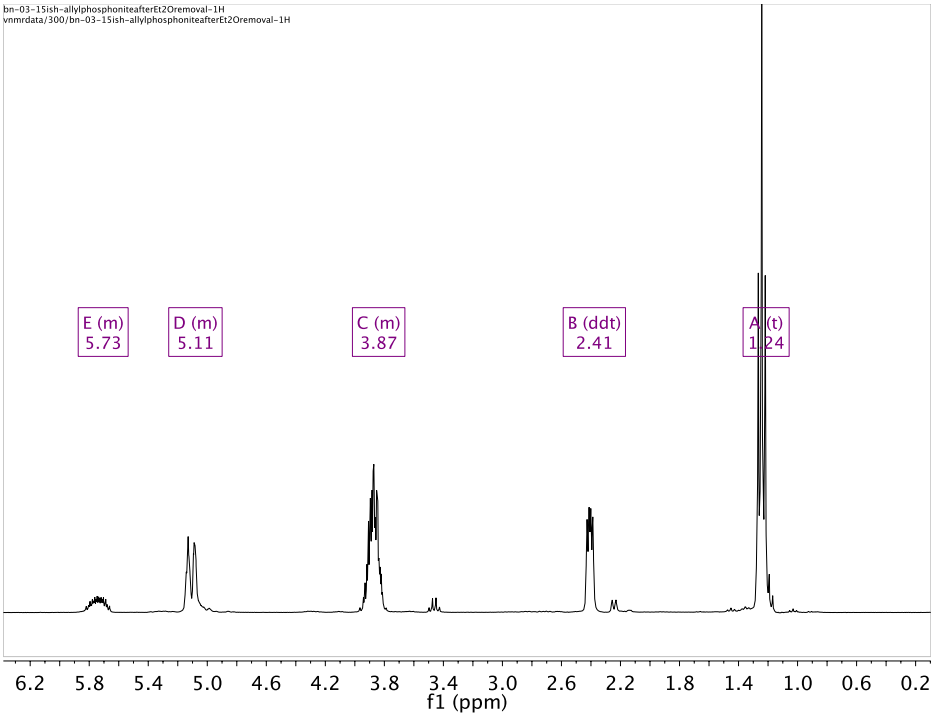

Figure D.1.33. ^{1}H NMR Spectrum of **19** in $CDCl_3$.

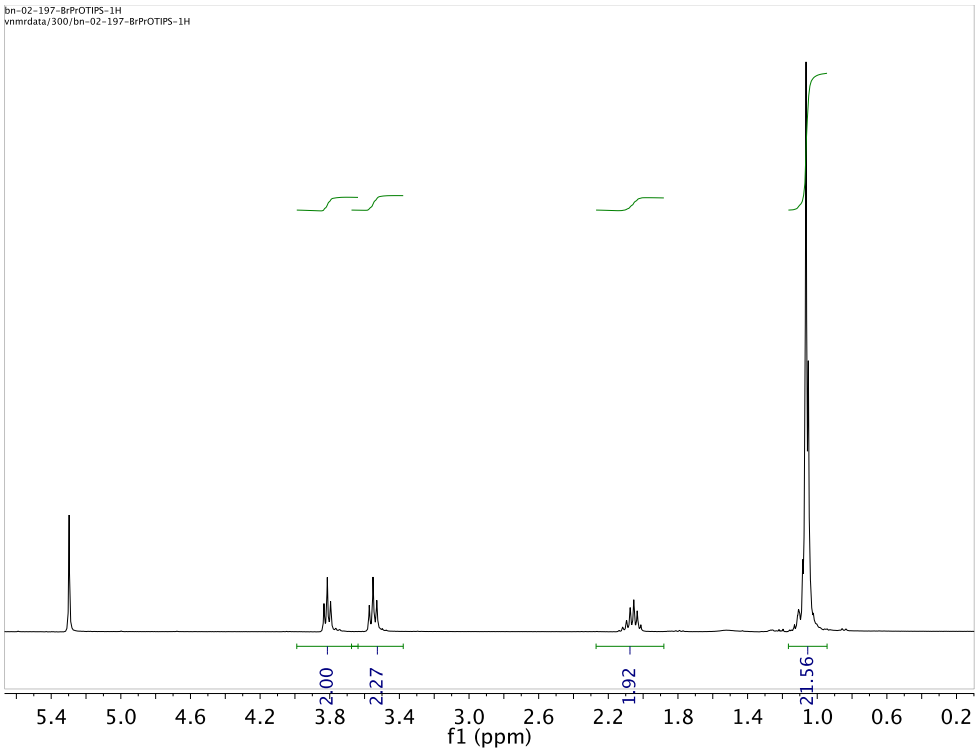

Figure D.1.34. ^{1}H NMR Spectrum of **20** in $CDCl_3$.

D.2. Mass Spectra

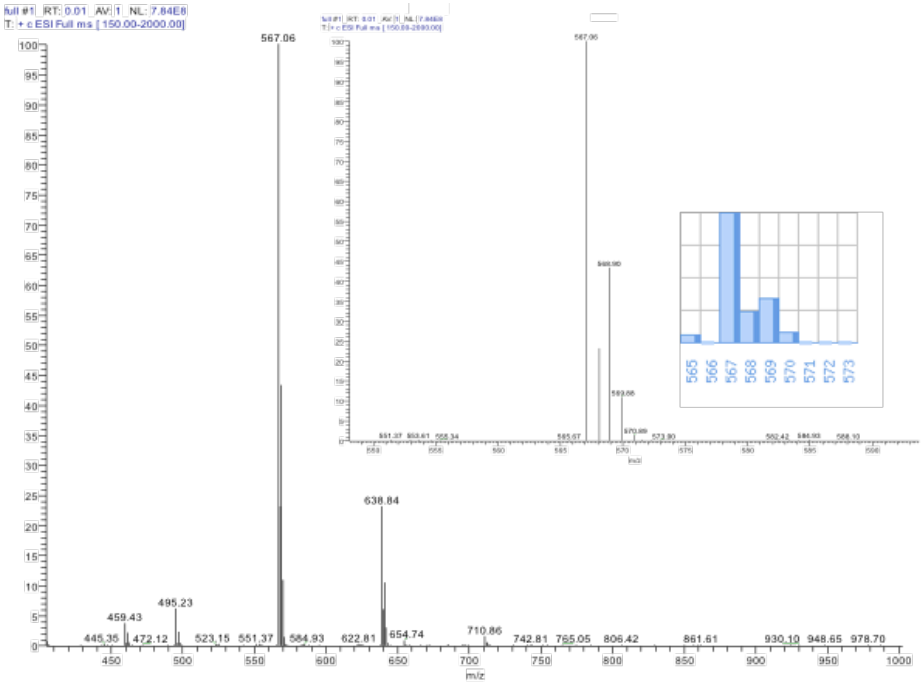

Figure D.2.1. ESI-MS of **1**.

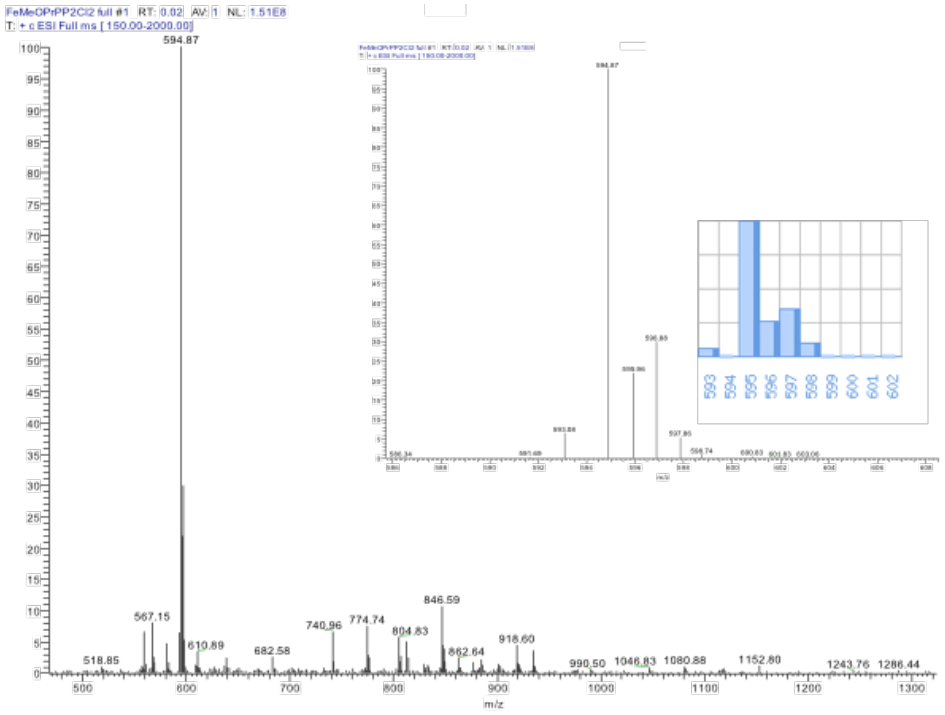

Figure D.2.2. ESI-MS of **2**.

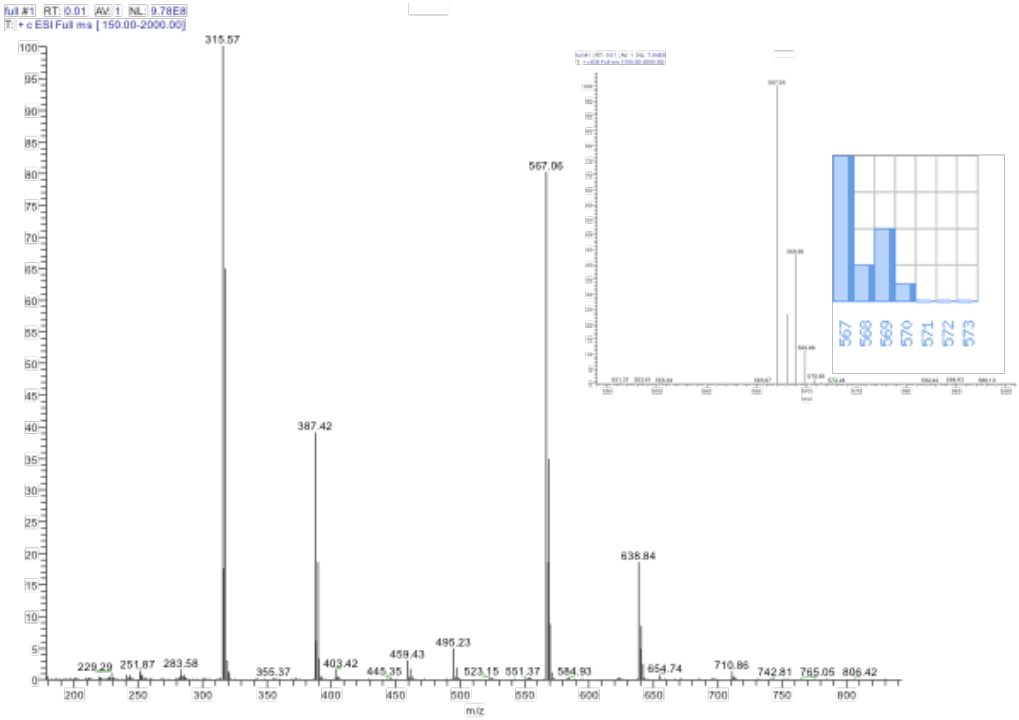

Figure D.2.3. ESI-MS of **3**.

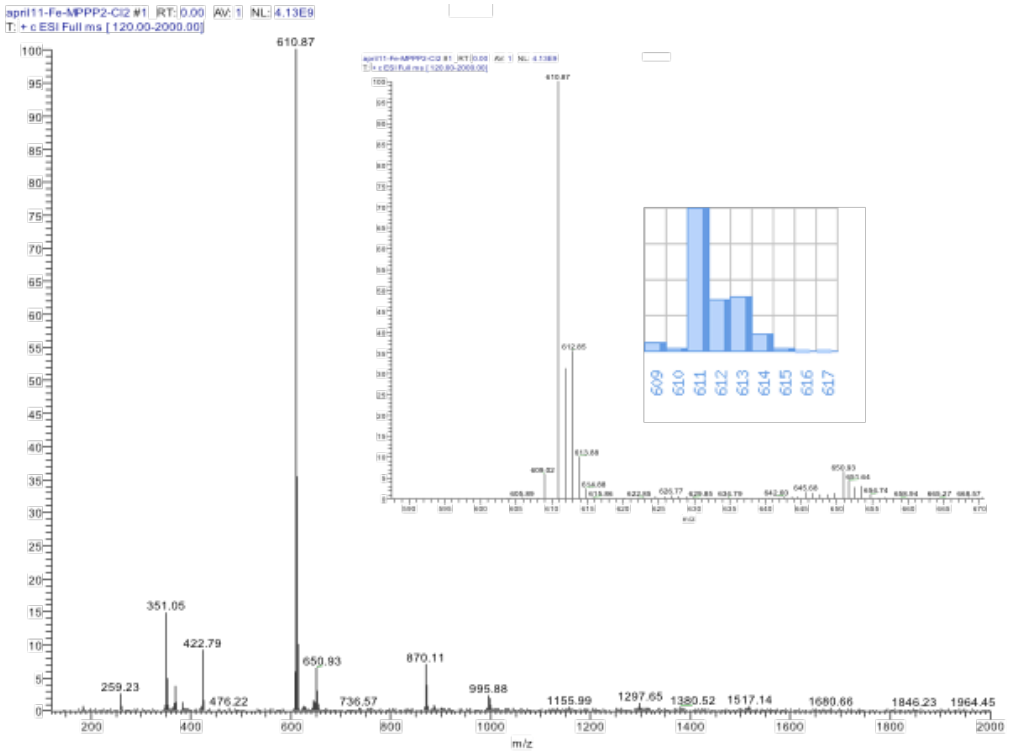

Figure D.2.4. ESI-MS of **4**.

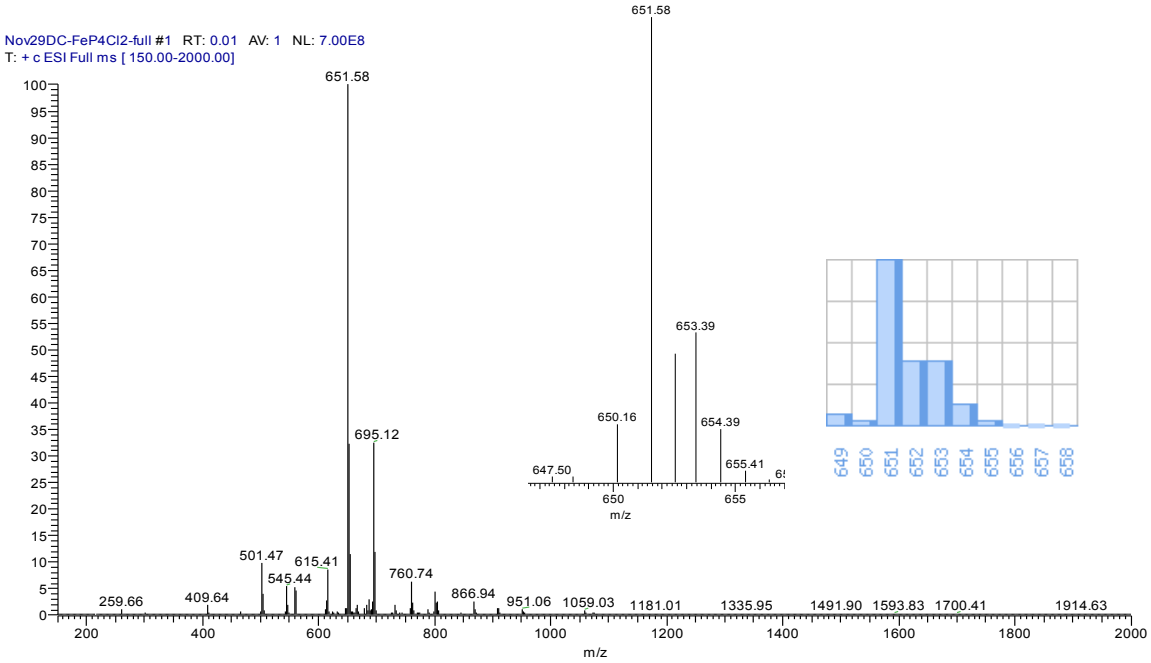

Figure D.2.5. ESI-MS of **10a**.

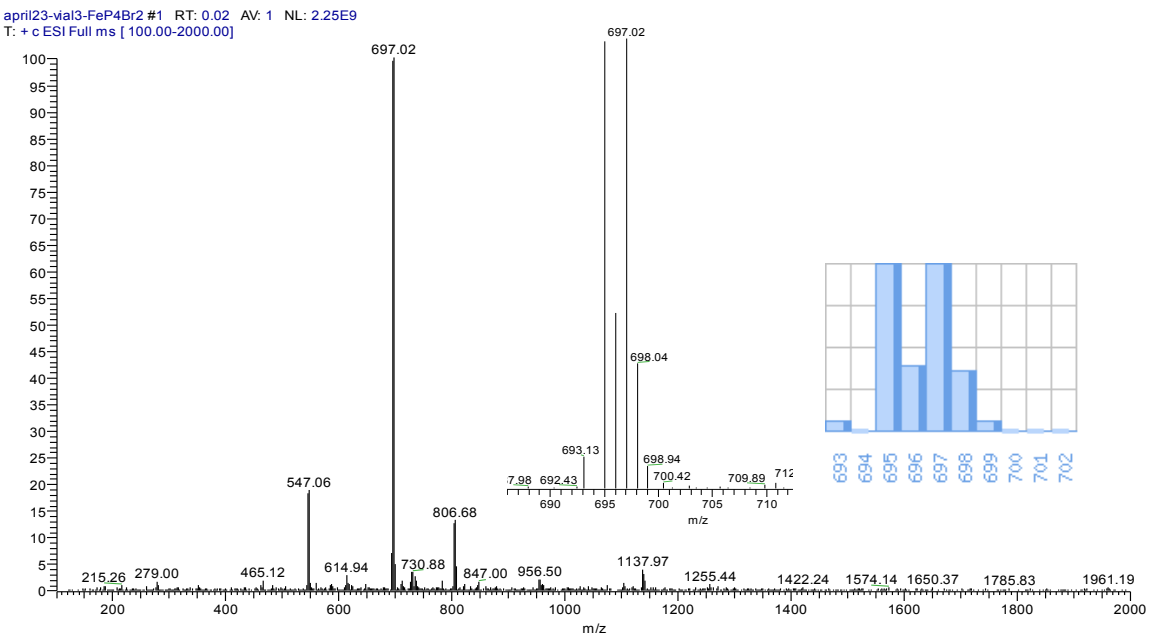

Figure D.2.6. ESI-MS of **10b**.

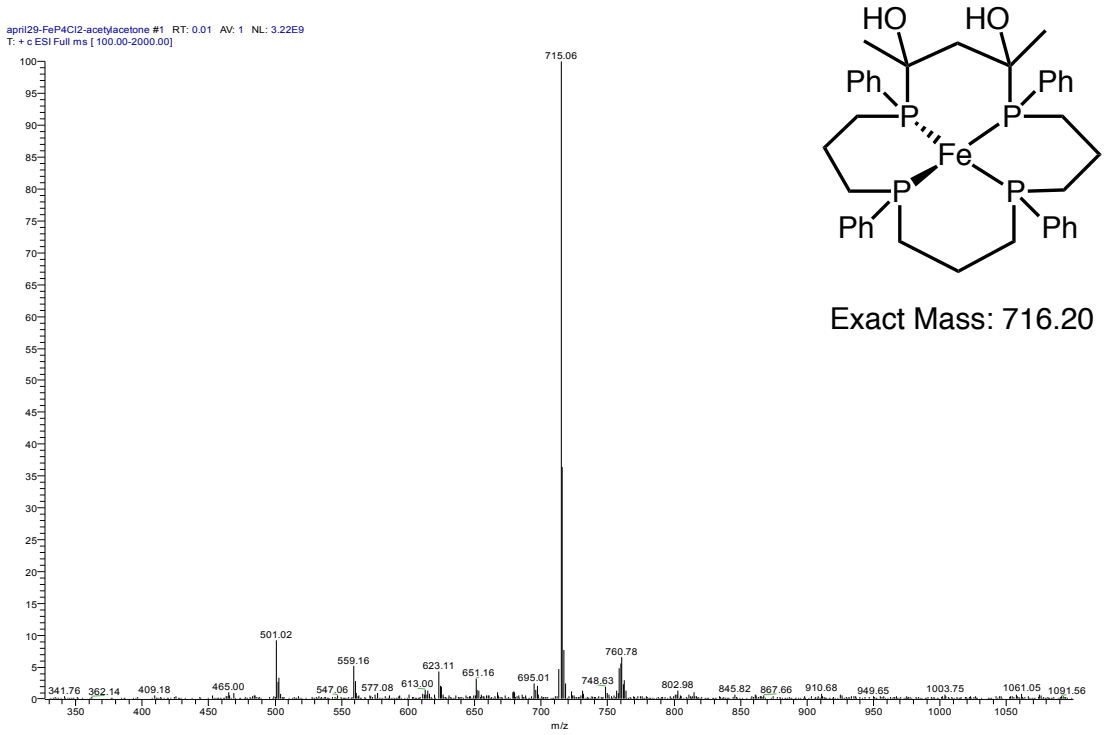

Figure D.2.7. ESI-MS of **12a**.

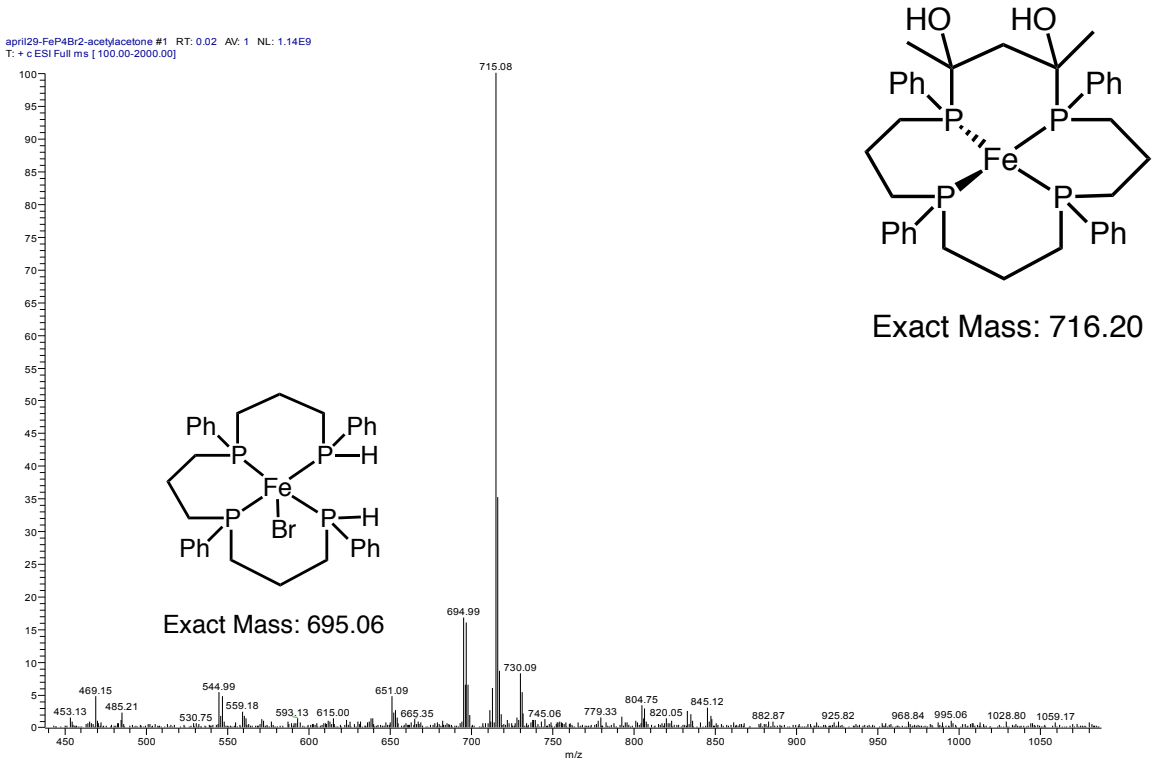

Figure D.2.7. ESI-MS of **12b**.

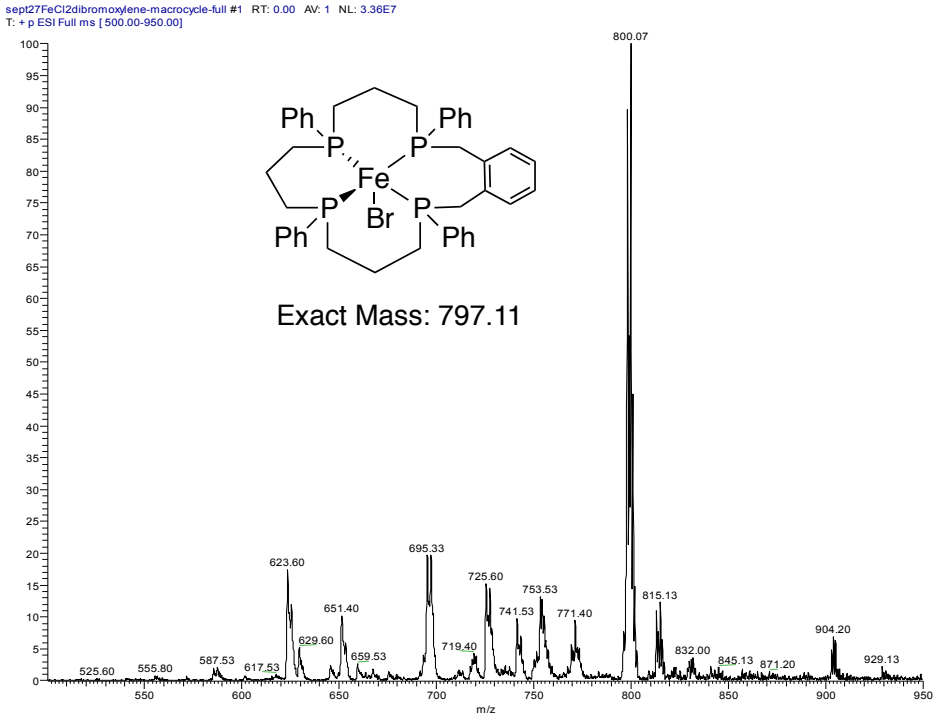

Figure D.2.8. ESI-MS of **10a** macrocyclized with *o*-dibromoxylene.

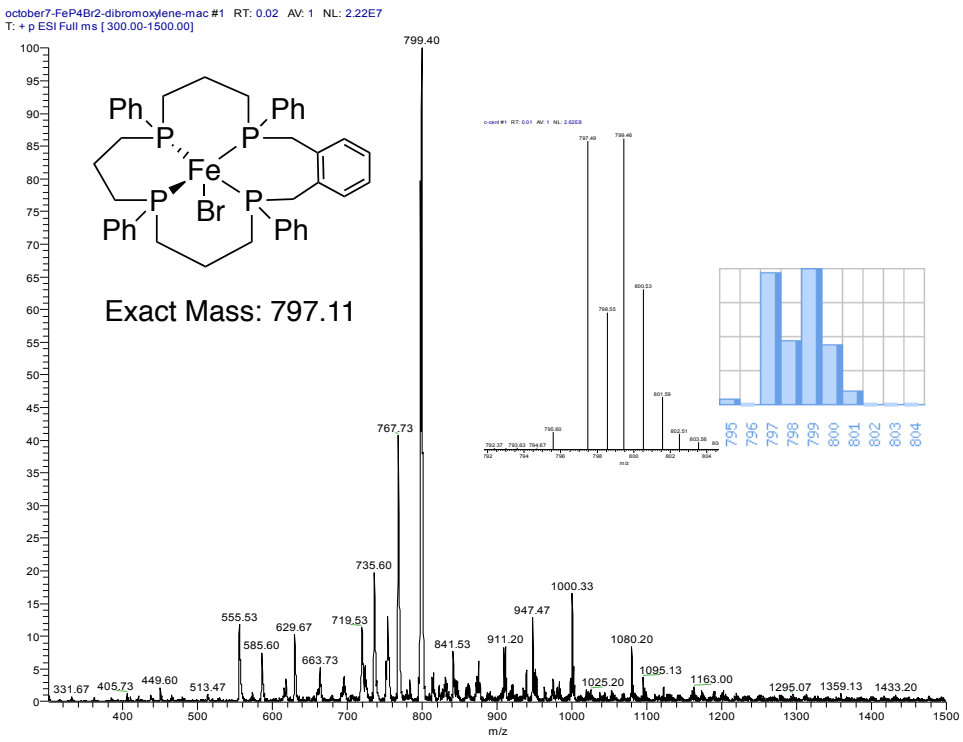

Figure D.2.9. ESI-MS of **10b** macrocyclized with *o*-dibromoxylene.

D.3. Infrared Spectra

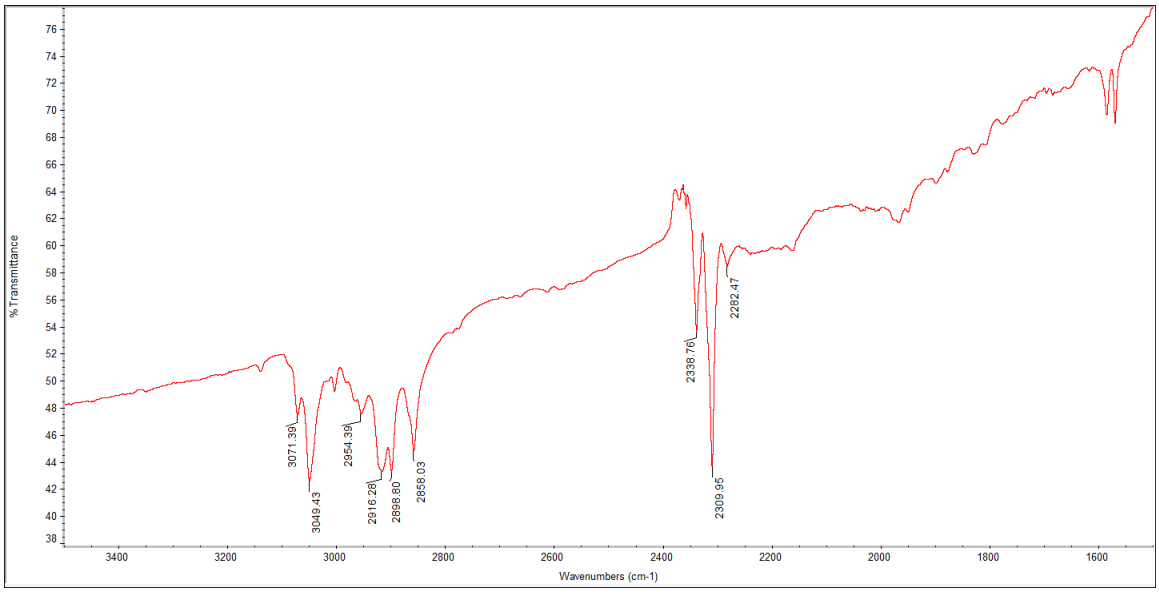

Figure D.3.2. IR Spectrum of **4**.

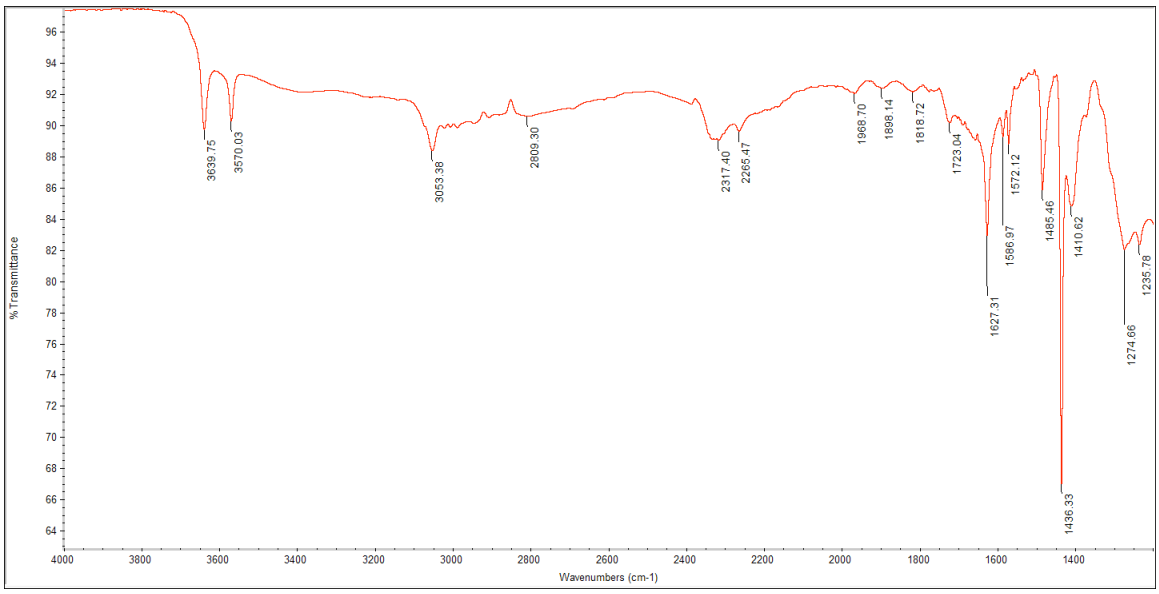

Figure D.3.3. IR Spectrum of $[Fe(MPPE)_2(CH_3CN)_2](OTf)_2$ (**7**).

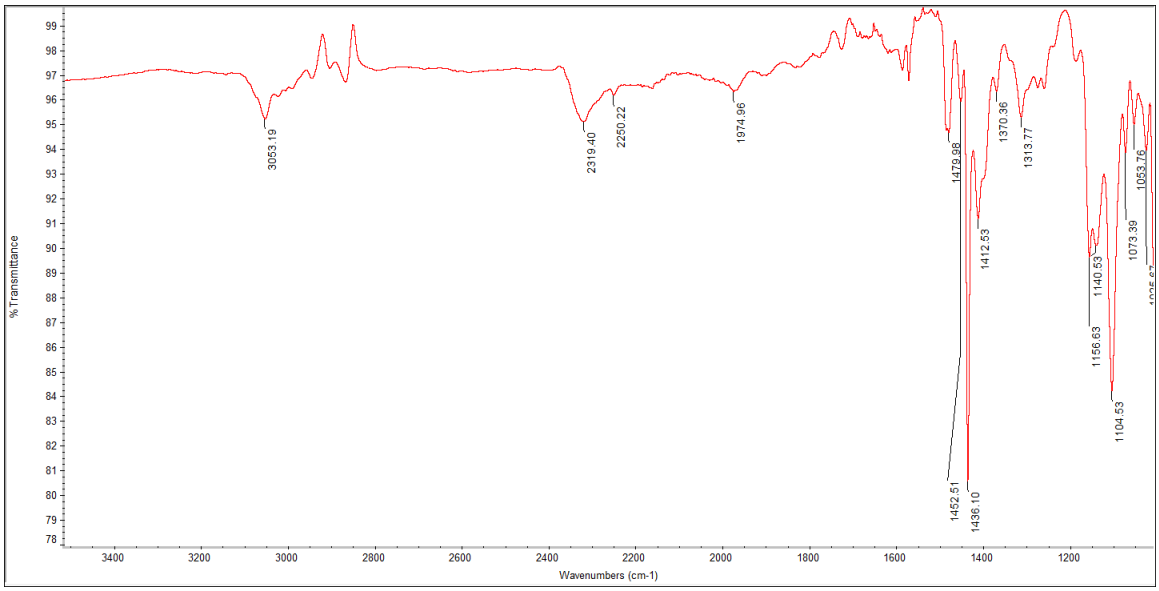

Figure D.3.4. IR Spectrum of **8**.

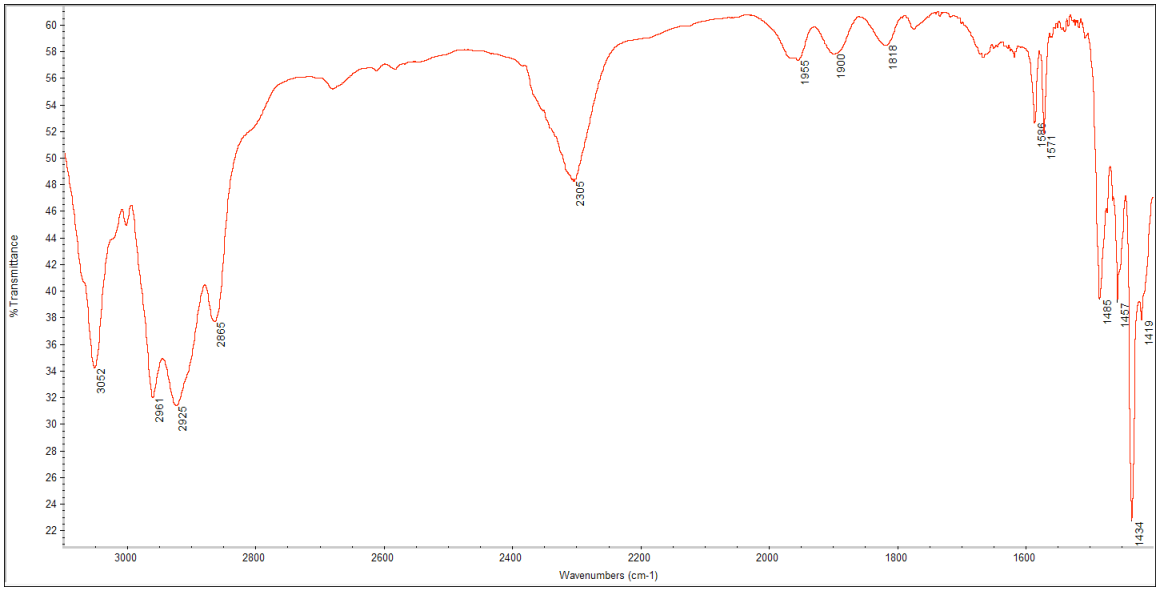

Figure D.3.5. IR Spectrum of **10a**.

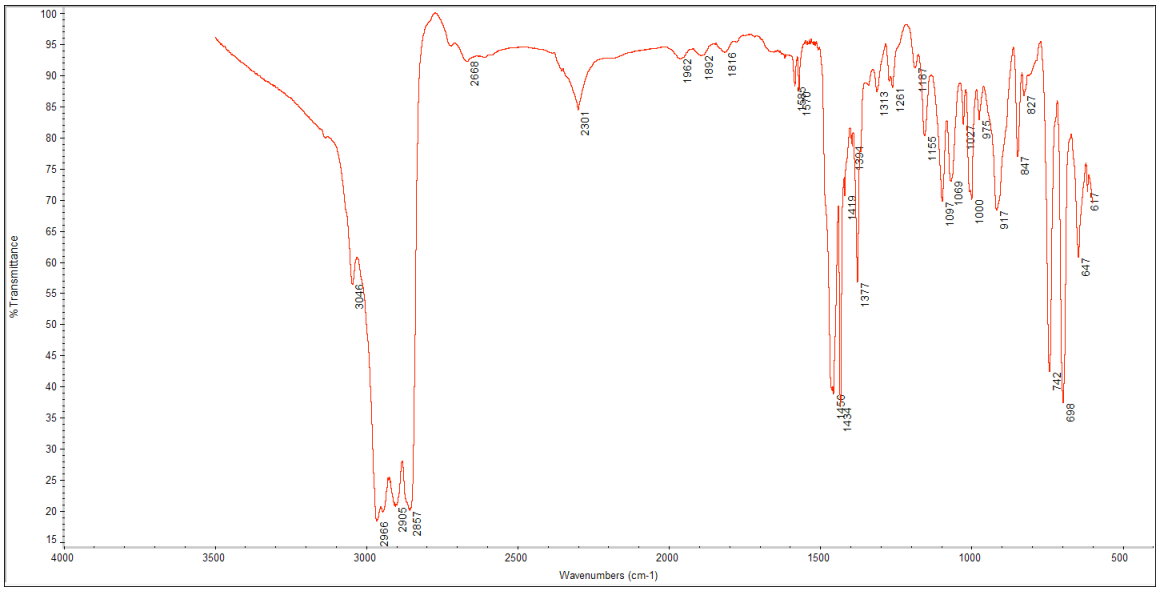

Figure D.3.5. IR Spectrum of **10b**.

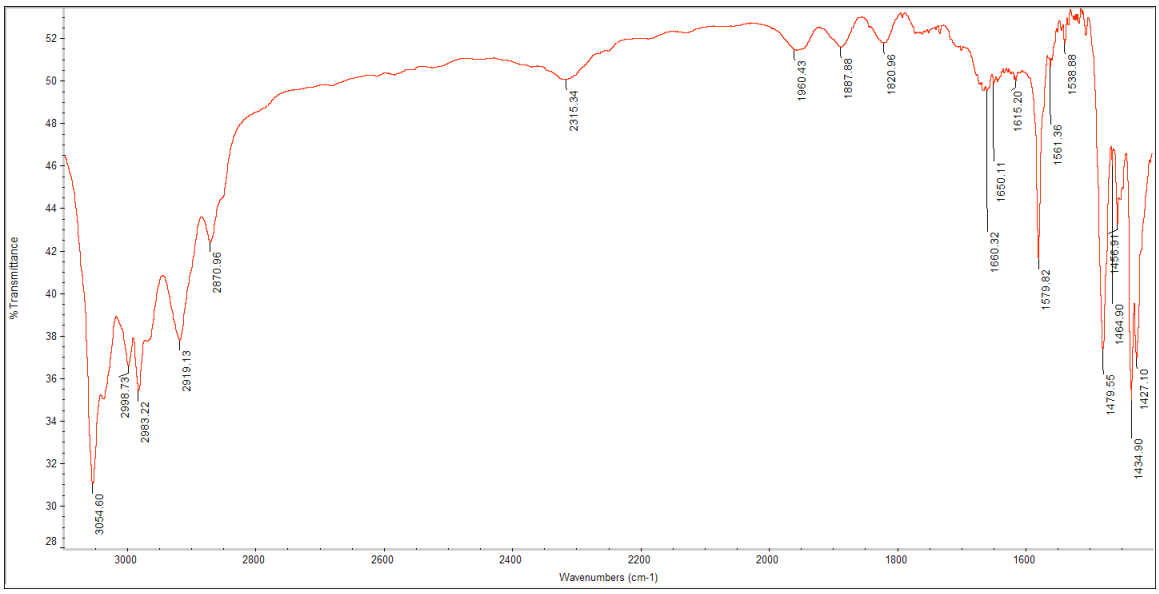

Figure D.3.6. IR Spectrum of **11**.

D.4. Crystal Data

Table D.4.1. Crystal data and structure refinement for *cis*-Fe(MPPP)$_2$Cl$_2$ (**4**).

Identification code	char1	
Empirical formula	C30 H36 Cl2 Fe P4	
Formula weight	647.22	
Temperature	173(2) K	
Wavelength	0.71073 Å	
Crystal system	Monoclinic	
Space group	P2(1)	
Unit cell dimensions	a = 9.194(2) Å	α = 90°.
	b = 16.406(4) Å	β = 111.439(4)°.
	c = 10.500(3) Å	γ = 90°.
Volume	1474.3(7) Å^3	
Z	2	
Density (calculated)	1.458 Mg/m^3	
Absorption coefficient	0.930 mm^{-1}	
F(000)	672	
Crystal size	0.20 x 0.10 x 0.04 mm^3	
	200	

Theta range for data collection	2.08 to 25.98°.
Index ranges	-11<=h<=11, -20<=k<=20, -12<=l<=12
Reflections collected	12433
Independent reflections	5700 [R(int) = 0.0412]
Completeness to theta = 25.98°	99.7 %
Absorption correction	Semi-empirical from equivalents
Max. and min. transmission	1.000 and 0.770
Refinement method	Full-matrix least-squares on F^2
Data / restraints / parameters	5700 / 1 / 350
Goodness-of-fit on F^2	1.038
Final R indices [I>2sigma(I)]	R1 = 0.0460, wR2 = 0.0918
R indices (all data)	R1 = 0.0578, wR2 = 0.0987
Absolute structure parameter	0.08(2)
Largest diff. peak and hole	0.752 and -0.388 e.$Å^{-3}$

Table D.4.2. Crystal data and structure refinement for *trans*-$[Fe(MPPP)_2(CH_3CN)_2](PF_6)_2$ (**8-PF$_6$**).

Identification code	char7	
Empirical formula	C36 H45 F12 Fe N3 P6	
Formula weight	989.42	
Temperature	173(2) K	
Wavelength	0.71073 Å	
Crystal system	Triclinic	
Space group	P-1	
Unit cell dimensions	a = 9.7075(8) Å	α = 96.9270(10)°.
	b = 10.7282(8) Å	β = 94.8200(10)°.
	c = 11.8667(9) Å	γ = 115.6710(10)°.
Volume	1092.83(15) $Å^3$	
Z	1	
Density (calculated)	1.503 Mg/m^3	
Absorption coefficient	0.647 mm^{-1}	
F(000)	506	
Crystal size	0.37 x 0.16 x 0.04 mm^3	
Theta range for data collection	1.75 to 27.00°.	

Index ranges	-12<=h<=12, -13<=k<=13, -15<=l<=15
Reflections collected	12344
Independent reflections	4732 [R(int) = 0.0161]
Completeness to theta = 25.98°	99.2 %
Absorption correction	Semi-empirical from equivalents
Max. and min. transmission	0.9746 and 0.7958
Refinement method	Full-matrix least-squares on F^2
Data / restraints / parameters	4732 / 0 / 358
Goodness-of-fit on F^2	1.064
Final R indices [I>2sigma(I)]	R1 = 0.0362, wR2 = 0.0969
R indices (all data)	R1 = 0.0400, wR2 = 0.1004
Largest diff. peak and hole	0.413 and -0.462 e.$Å^{-3}$

D.5. Figures

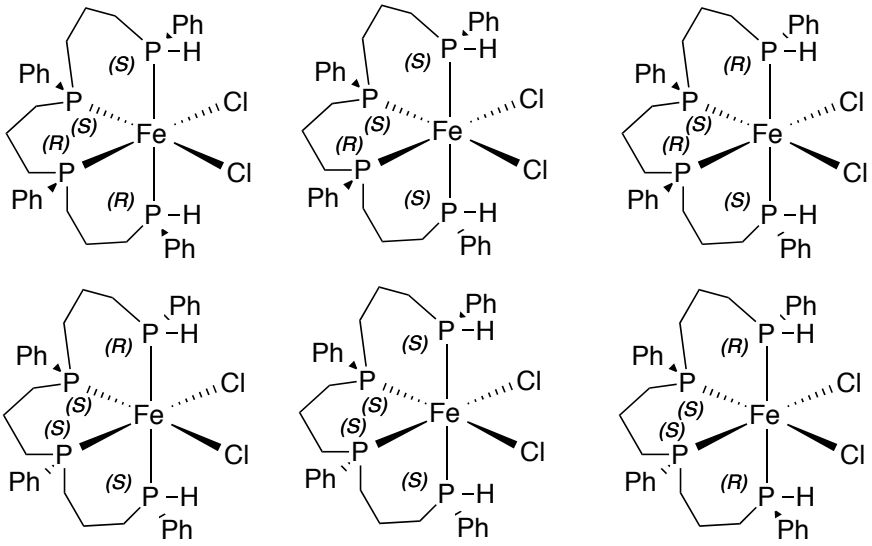

D.5.1. Possible isomers of *cis*-α-Fe(**10a**)Cl_2.

APPENDIX E

CRYSTAL STRUCTURE OF P,P'-DIPHENYLETHYLENEDIPHOSPHONIC ACID DIHYDRATE

This work was previously published: Swor, C. D.; Nell, B. P.; Zakharov, L. N.; Tyler, D. R. *Acta Cryst.* **2012**, o2456.

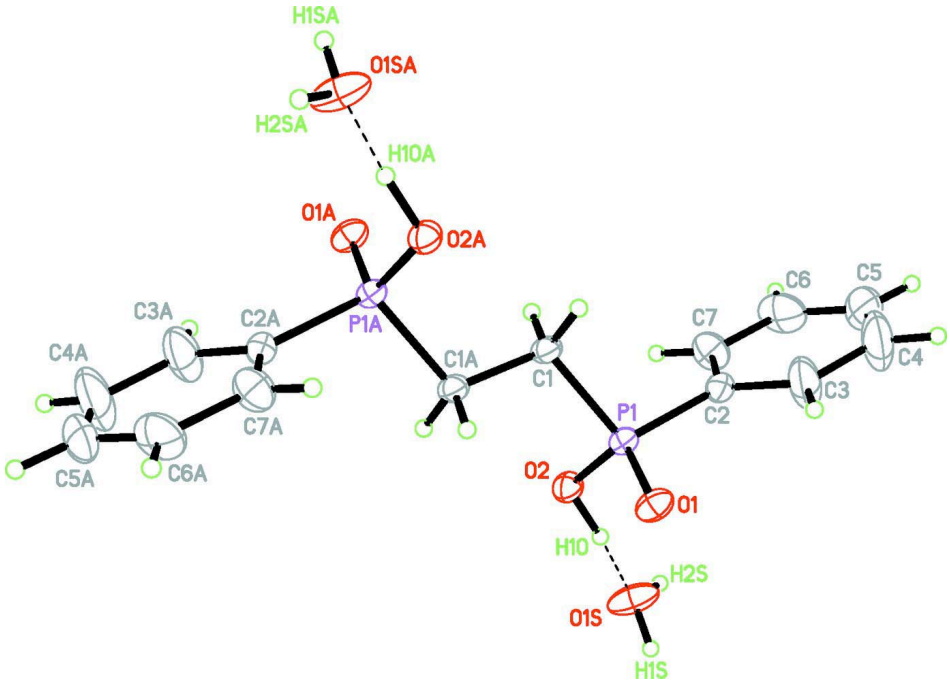

APPENDIX F

CRYSTAL STRUCTURE OF 1,2-BIS[(METHOXYPROPYL)PHOSPHINO]ETHANE TETRASULFIDE DISODIUM COORDINATION POLYMER

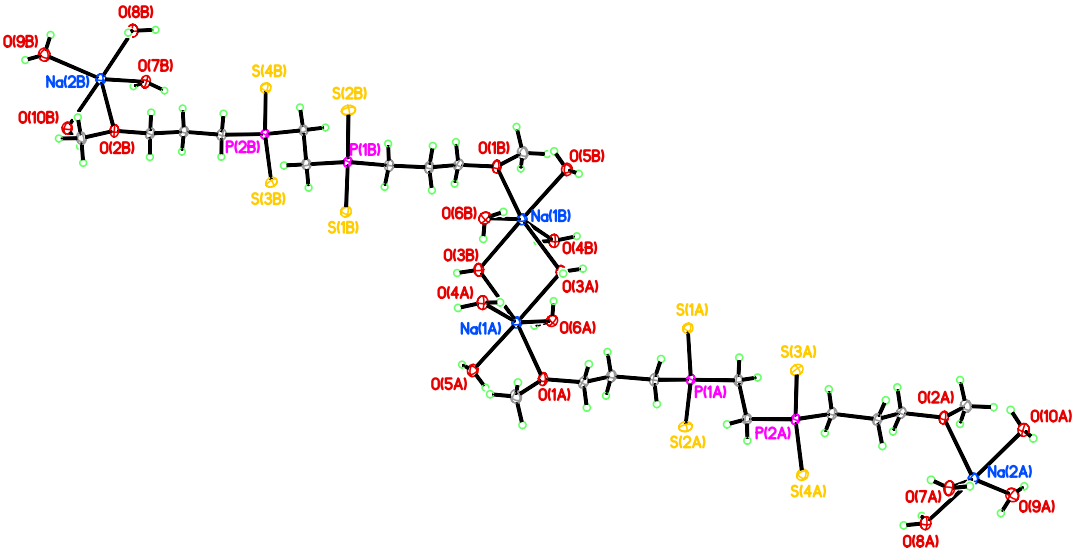

APPENDIX G

A STUDY OF THE FLUXIONAL BEHAVIOR OF *cis*-Fe(DMeOPrPE)$_2$(H)$_2$ (DMeOPrPE=1,2-[BIS(DIMETHOXYPROPYL)PHOSPHINO]ETHANE)

The experimental work in this appendix was performed by Susan R. Cooper during a rotation in the Tyler lab.

G.1. Abstract

The fluxional behavior of Fe(DMeOPrPE)$_2$(H)$_2$ has been studied using multinuclear variable temperature (VT) NMR studies. The hydrides in this complex are a *cis*- to each other in an octahedral geometry. Using VT NMR, a possible mechanism for this fluxional behavior has been proposed. The VT NMR results show that the complex has a coalescence temperature of 100 °C and the activation parameters of the fluxional process were calculated to be $\Delta H^{\ddagger}$ = 11.6 kcal/mol, $\Delta G^{\ddagger}$ = 14.3 kcal/mol and $\Delta S^{\ddagger}$ = -0.0092 kcal/mol.

G.2. Introduction

It has been long known that *cis*-dihydride iron phosphine complexes show non-rigid stereochemistry, which is observable on the NMR time scale.[1] Previous work has shown that iron complexes bearing 1,2-[bis(dimethoxypropyl)phosphino]ethane (DMeOPrPE) can be used to generate small amounts of ammonia.[2] One of the possible intermediates along the way to ammonia is the dihydride complex, Fe(DMeOPrPE)$_2$(H)$_2$

(Figure G.2.1). Recent work has shown that this complex exhibits fluxional behavior, but was not studied extensively.[3] In this note, we report the results of a multinuclear variable-temperature (VT) study examining the fluxional behavior of *cis*-$Fe(DMeOPrPE)_2(H)_2$. From an analysis of the spectra obtained, we were able to determine the activation parameters for the fluxional behavior of the complex. Additionally, the data obtained is compared to other *cis*-dihydride complexes to help lend insight into a mechanism for this fluxional behavior. Some of the most plausible options for a mechanism include: a Bailar twist mechanism, bond dissociation of an iron phosphorus bond, the two hydrides coming closer in a transition state to form an H_2 ligand and a mechanism where one hydrogen atom would move to an unoccupied face of a complex where the phosphorus ligands are arranged tetrahedrally and one hydrogen would remain in its original position.[4-6]

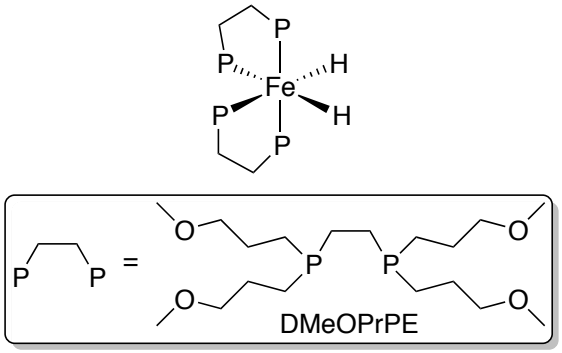

Figure G.2.1. *cis*-$Fe(DMeOPrPE)_2(H)_2$

G.3. Results and Discussion

Variable temperature (VT) NMR experiments were run to determine the activation parameters for the fluxional behavior of *cis*-Fe(DMeOPrPE)$_2$(H)$_2$. The coalescence point was 100 °C and the low temperature limit was -40 °C. Rate constants were determined (Figure G.3.1) and an Eyring plot was used to determined the activation parameters of the fluxional process to be $\Delta H^{\ddagger}$ = 11.6 kcal/mol, $\Delta G^{\ddagger}$ = 14.3 kcal/mol and $\Delta S^{\ddagger}$ = -0.009 kcal/mol. The activation parameters are similar to activation parameters for similar systems reported in the Table 1.[4,7]

There are four possible mechanisms suggested in the literature for H exchange in *cis*-Fe(P$_2$)$_2$(H)$_2$ similar systems, which show similar activation parameters to the parameters found in this study. One mechanism involves the Fe-P bond breaking and reforming in another place (Figure G.4.3). The bond dissociation energy of an iron phosphorus bond is 30-40 kcal/mol.[8,9] From the data observed for our system, this value is far too large for a bond dissociation mechanism to be the mechanism of this fluxional behavior. An Eyring plot was used to determine the activation parameters and compared to those for an intramolecular reaction of an H_2 ligand going to two terminal hydride ligands in an H_2-H complex (Figure G.3.2).[10] These activation parameters are also comparable and could suggest that an H_2 ligand formation and a subsequent 5-coordinate complex, which are known to have non-rigid stereochemistry, could be part of the mechanism for this fluxional behavior. Also, a mechanism where one hydrogen atom would move to an unoccupied face of a complex where the phosphorus ligands are arranged tetrahedrally and one hydrogen would remain in its original position could also

be possible due to the similarity of the activation parameters calculated for this mechanism.[4-6]

Table G.3.1. Comparison of Erying Plot Data with Selected References

	Eyring Plot data *cis*-$Fe(DMeOPrPE)_2(H)_2$ 298 K	Eyring Plot data *cis*-$Fe(P(OC_2H_5)_3)_4(H)_2$ 298 K	Eyring Plot data *trans*-$Fe(dppe)_2(H)(H_2)BF_4$ 300 K	Eyring Plot data *trans*-$Fe(depe)_2(H)(H_2)BPh_4$ 300 K
$\Delta G^{\ddagger}$ kcal/mol	14.3	13.7	14.0	13.0
$\Delta H^{\ddagger}$ kcal/mol	**11.6**	**11.1**	**11.0**	**12.2**
$\Delta S^{\ddagger}$ kcal/mol*K	-0.0092	-0.0088	-0.0010	-0.0025

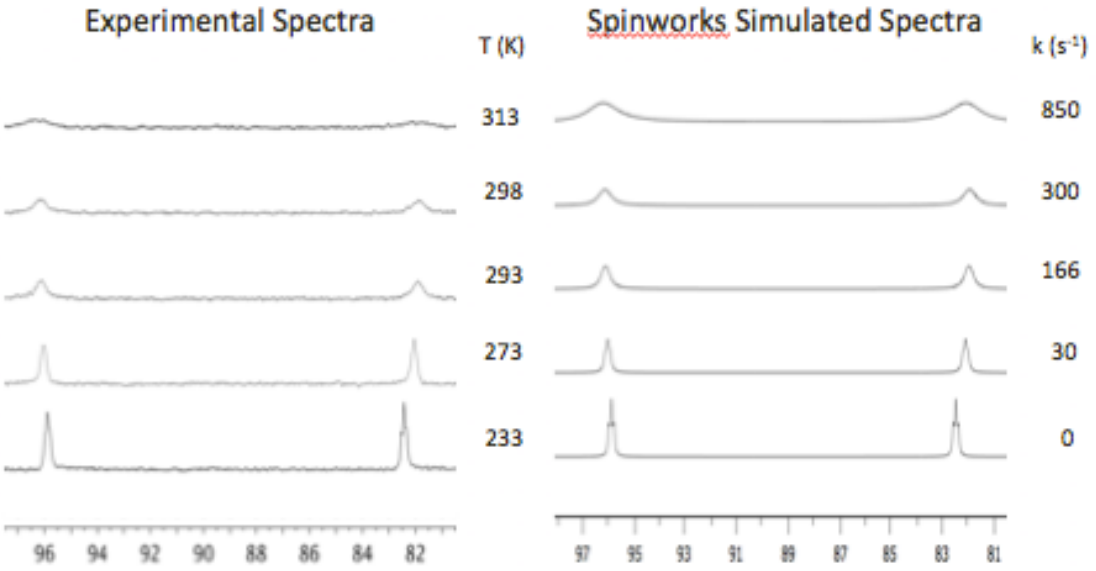

Figure G.3.1. $^{31}P\{^1H\}$ NMR Spectra for $Fe(DMeOPrPE)_2(H)_2$ at different temperatures. Experimental data is shown on the left and the simulated data with calculated rate constants are on the right.

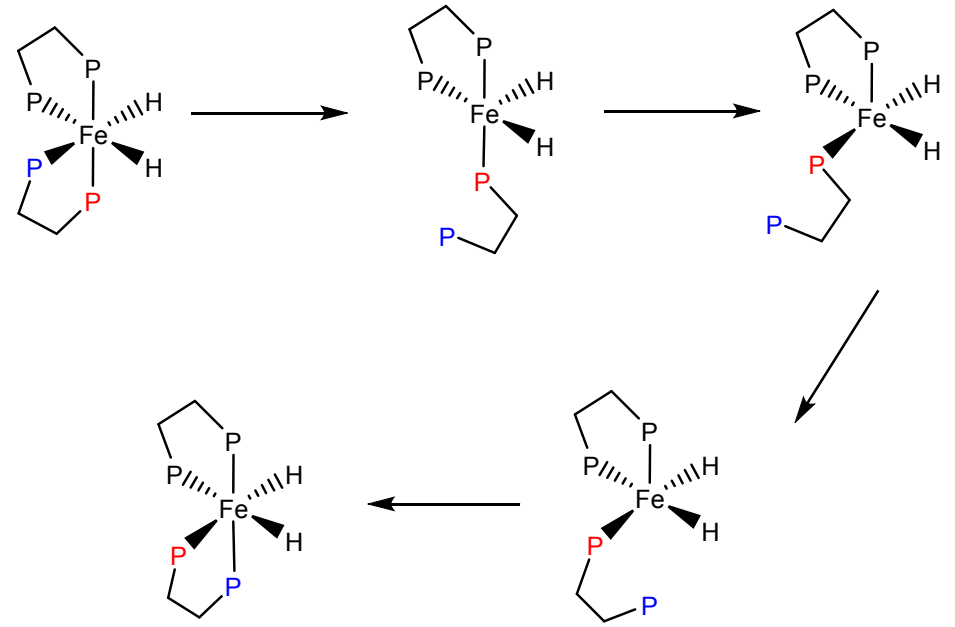

Figure G.3.2. Bond dissociation mechanism

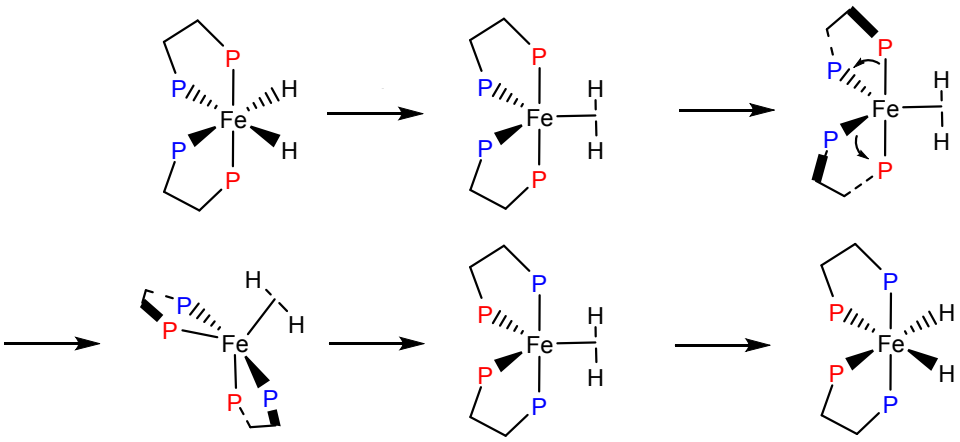

Figure G.3.3. Two hydrides coming closer in a transition state to form an H_2 ligand mechanism

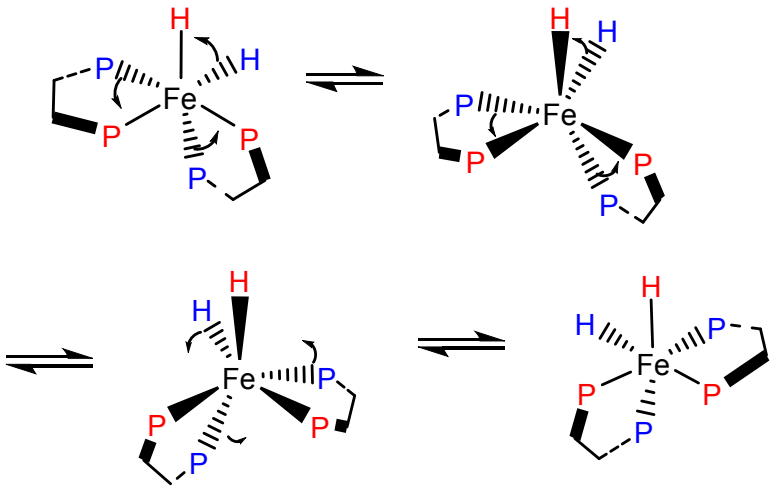

Figure G.3.4. Bailar twist mechanism

G.4. Conclusions

In this note, we report the activation parameters for the fluxional behavior of $Fe(DMeOPrPE)_2(H)_2$. The activation parameters obtained are similar to those obtained for other *cis*-dihydride systems, lending insight into the possible mechanism of fluxionality. From the data obtained, bond dissociation of an iron phosphorus bond is not likely the reason for fluxional behavior. Instead, the data correlates well with data seen for similar complexes where two hydrides form an H_2 ligand, rearrange, and reform the two hydrides.

G.5. Experimental Section

G.5.1. General Procedures. Unless otherwise noted, all experimental procedures were performed under an inert (Ar) atmosphere, using standard Schlenk and glovebox techniques. Commercially available reagents were used as received. HPLC-grade THF was dried and deoxygenated by passing through commercial columns of CuO, followed by alumina under an argon atmosphere. Deuterated solvents were obtained from

Cambridge Isotope Laboratories and degassed using three freeze-pump-thaw cycles. The synthesis of $Fe(DMeOPrPE)_2(H)_2$ has been previously reported.[3] Air-sensitive NMR samples were sealed in Ar-filled J-Young tubes. NMR spectra were obtained on a Varian Unity/Inova 500 spectrometer operating at a frequency of 500.62 MHz (^1H) or 202.45 MHz (^{31}P). The ^1H spectra were referenced to residual solvent peaks, and the ^{31}P NMR spectra were referenced to external 1% H_3PO_4 in D_2O.

For comparison, rate constants were determined by two different methods. One method used Equation 1, using the bandwidths determined by Mrestrenova software using a Lorentzian line shape.

$$k = (\Delta\nu_{1/2} - \Delta\nu_{1/2ref})\pi \tag{1}$$

The other method used Spinworks 4.0.0 Beta software and DNMR3 to determine rate constants. The activation parameters were determined using an Eyring plot and Equation 2. Both calculations results are shown in Table 2. In general, the two methods give comparable results.

$$k_r = \kappa \frac{(k_b T)}{h} \; e^{-\Delta G/RT} \tag{2}$$

Table G.5.1. Comparison of Simulation Data vs. Bandwidth Method.

	Eyring Plot Simulated 298 K	Eyring Plot Bandwidth 298 K
$\Delta G^{\ddagger}$ kcal/mol	14.3	14.3
$\Delta H^{\ddagger}$ kcal/mol	**11.6**	**9.8**
$\Delta S^{\ddagger}$ kcal/mol*K	-0.009	-0.015

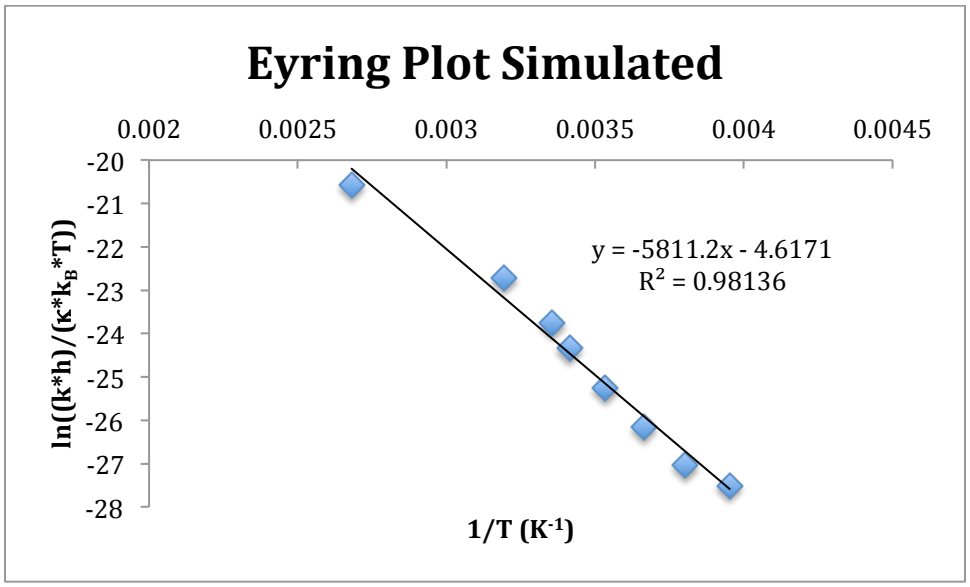

Figure G.5.1. Simulated data Eyring plot.

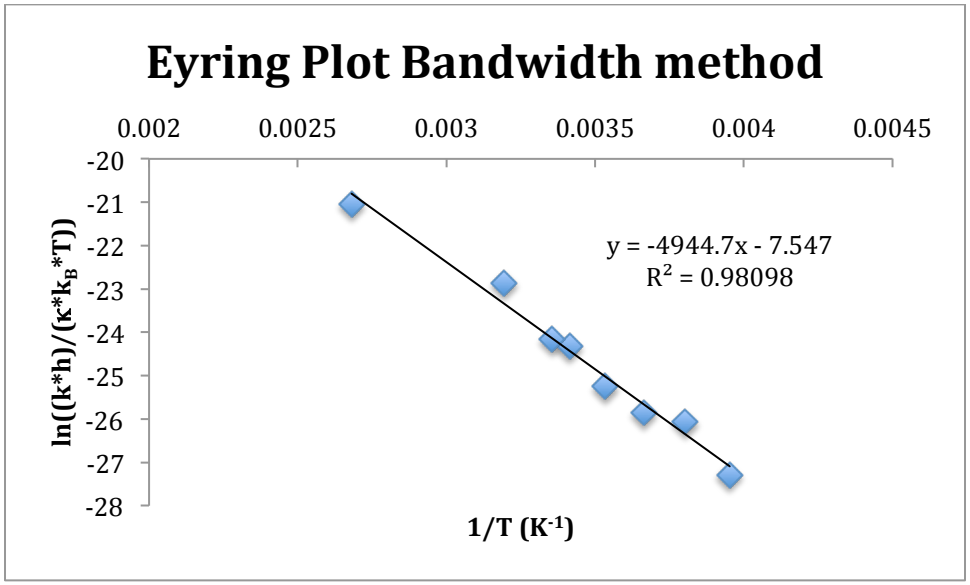

Figure G.5.2. Bandwidth method data Eyring plot.

G.6. References

(1) Meakin, P.; Muetterties, E. L.; Jesson, J. P. *J. Am. Chem. Soc.* **1973**, *95*, 75–88.
(2) Gilbertson, J. D.; Szymczak, N. K.; Tyler, D. R. *J. Am. Chem. Soc.* **2005**, *127*, 10184–10185.
(3) Balesdent, C. G.; Crossland, J. L.; Regan, D. T.; López, C. T.; Tyler, D. R. *Inorg. Chem.* **2013**, 14178–14187.
(4) Jesson, J. P.; Meakin, P.; Muetterties, E. L.; Tebbe, F. N. *J. Am. Chem. Soc.* **1971**, *93*, 4701–4709.
(5) Bailar, J. C., Jr. *Journal of Inorganic and Nuclear Chemistry* **1958**, *8*, 165–175.
(6) Gordon, J. G.; Holm, R. H. *J. Am. Chem. Soc.* **1970**, *92*, 5319–5332.
(7) Bautista, M. T.; Cappellani, E. P.; Drouin, S. D.; Morris, R. H.; Schweitzer, C. T.; Sella, A.; Zubkowski, J. *J. Am. Chem. Soc.* **1991**, *113*, 4876–4887.
(8) González-Blanco, Ò.; Branchadell, V. *Organometallics* **1997**, *16*, 5556–5562.
(9) Luo, L.; Nolan, S. P. *Inorg. Chem.* **1993**, *32*, 2410–2415.
(10) Bautista, M. T.; Earl, K. A.; Maltby, P. A.; Morris, R. H. *J. Am. Chem. Soc.* **1988**, *110*, 4056–4057.

REFERENCES CITED

CHAPTER I

(1) Atkins, P.; Overton, T.; Rourke, J.; Weller, M.; Armstrong, F.; Salvador, P.; Hagerman, M.; Spiro, T.; Stiefel, E. *Inorganic Chemistry*; 4 ed.; W. H. Freeman and Company: New York, 2006.

(2) Hartwig, J. *Organotransition Metal Chemistry: From Bonding to Catalysis*; University Science Books: Sausalito, California, 2010.

(3) Fey, N.; Orpen, A. G.; Harvey, J. N. *Coord. Chem. Rev.* **2009**, *253*, 704–722.

(4) van Leeuwen, P. W. *Homogeneous Catalysis: Understanding the Art*; Kluwer Academic Publishers: Dordrecht, 2004.

(5) Pignolet, L. *Homogeneous Catalysis with Metal Phosphine Complexes*; Plenum Press: New York, 1983.

(6) Tolman, W. *Activation of Small Molecules: Organometallic and Bioinorganic Perspectives*; Wiley-VCH: Weinheim, 2006.

(7) Gilbertson, J. D.; Szymczak, N. K.; Tyler, D. R. *J. Am. Chem. Soc.* **2005**, *127*, 10184–10185.

(8) Crossland, J. L.; Young, D. M.; Zakharov, L. N.; Tyler, D. R. *Dalton Trans.* **2009**, 9253.

(9) Crossland, J. L.; Balesdent, C. G.; Tyler, D. R. *Inorg. Chem.* **2011**, 439-445.

(10) Balesdent, C. G.; Crossland, J. L.; Regan, D. T.; López, C. T.; Tyler, D. R. *Inorg. Chem.* **2013**, 14178-14187.

(11) Chatt, J.; Pearman, A. J.; Richards, R. L. *Nature* **1976**, *259*, 204–204.

(12) George, T. A.; Kaul, B. B. *Inorg. Chem.* **1990**, *29*, 4969–4974.

(13) Leigh, G. J.; Jimenez-Tenorio, M. *J. Am. Chem. Soc.* **1991**, *113*, 5862–5863.

(14) Field, L. D.; Messerle, B. A.; Smernik, R. J. *Inorg. Chem.* **1997**, *36*, 5984–5990.

(15) Hirano, M.; Akita, M.; Morikita, T.; Kubo, H.; Fukuoka, A.; Komiya, S. *J. Chem. Soc., Dalton Trans.* **1997**, 3453–3458.

(16) Sellmann, D.; Hennige, A. *Angew. Chem. Int. Ed. Engl.* **1997**, *36*, 276–278.

(17) Fryzuk, M. D.; Johnson, S. A. *Coord. Chem. Rev.* **2000**, *200-202*, 379–409.

(18) Yandulov, D. V.; Schrock, R. R. *J. Am. Chem. Soc.* **2002**, *124*, 6252–6253.

(19) Betley, T. A.; Peters, J. C. *J. Am. Chem. Soc.* **2004**, *126*, 6252–6254.

(20) Pool, J. A.; Lobkovsky, E.; Chirik, P. J. *Nature* **2004**, *427*, 527–530.

(21) Evans, W. J.; Lee, D. S.; Rego, D. B.; Perotti, J. M.; Kozimor, S. A.; Moore, E. K.; Ziller, J. W. *J. Am. Chem. Soc.* **2004**, *126*, 14574–14582.

(22) Rodriguez, M. M.; Bill, E.; Brennessel, W. W.; Holland, P. L. *Science* **2011**, *334*, 780–783.

(23) Arashiba, K.; Miyake, Y.; Nishibayashi, Y. *Nature Chem* **2010**, *3*, 120–125.

(24) Maier, L. In *Organic Phosphorus Compounds*; John Wiley & Sons, Inc.: New York, 1972; Vol. 1.

(25) Quin, L. D. *A Guide to Organophosphorus Chemistry*; Wiley-Interscience, 2000.

(26) Pietrusiewicz, K. M.; Zablocka, M. *Chem. Rev.* **1994**, *94*, 1375–1411.

(27) Valentine, D., Jr. In *Asymmetric Synthesis*; Academic Press Inc.: New York, 1984.

(28) Imamoto, T.; Engle, R. Marcel Dekker: New York, 1992.

(29) Henderson, W. A., Jr.; Streuli, C. A. *J. Am. Chem. Soc.* **1960**, *82*, 5791–5794.

(30) Stewart, B.; Harriman, A.; Higham, L. J. *Organometallics* **2011**, *30*, 5338–5343.

(31) Honaker, M. T.; Hovland, J. M.; Nicholas Salvatore, R. *Current Organic Synthesis* **2007**, *4*, 31–45.

(32) Thenard, P. E. *C. R. Acad. Sci. Paris* **1847**, *25*, 892.

(33) Wagner, R. I.; Freeman, L. D.; Goldwhite, H.; Rowsell, D. G. *J. Am. Chem. Soc.* **1967**, *89*, 1102–1104.

(34) Staubitz, A.; Robertson, A. P. M.; Sloan, M. E.; Manners, I. *Chem. Rev.* **2010**, *110*, 4023–4078.

(35) Horner, L.; Hoffmann, H.; Beck, P. *Chem. Ber.* **1958**, *91*, 1583–1588.

(36) Kuchen, W.; Buchwald, H. *Chem. Ber.* **1958**, *91*, 2871–2877.

(37) Issleib, K.; Tzschach, A. *Chem. Ber.* **1959**, *92*, 704–711.

(38) Issleib, K.; Weichmann, H. *Chem. Ber.* **1968**, *101*, 2197–2202.

(39) Kuchen, W.; Buchwald, H. *Angew. Chem.* **1959**, *71*, 162–162.

(40) Fritzsche, H.; Hasserodt, U.; Korte, F. *Chem. Ber.* **1964**, *97*, 1988–1993.

(41) Marsi, K. L. *J. Org. Chem.* **1974**, *39*, 265–267.

(42) Li, Y.; Das, S.; Zhou, S.; Junge, K.; Beller, M. *J. Am. Chem. Soc.* **2012**, *134*, 9727–9732.

(43) Busacca, C. A.; Raju, R.; Grinberg, N.; Haddad, N.; James-Jones, P.; Lee, H.; Lorenz, J. C.; Saha, A.; Senanayake, C. H. *J. Org. Chem.* **2008**, *73*, 1524–1531.

(44) Busacca, C. A.; Lorenz, J. C.; Grinberg, N.; Haddad, N.; Hrapchak, M.; Latli, B.; Lee, H.; Sabila, P.; Saha, A.; Sarvestani, M.; Shen, S.; Varsolona, R.; Wei, X.; Senanayake, C. H. *Org. Lett.* **2005**, *7*, 4277–4280.

(45) Engel, R. *Handbook of organophosphorus chemistry*; Marcel Dekker, 1992.

(46) Dickson, R. S.; Elmes, P. S.; Jackson, W. R. *Organometallics* **1999**, *18*, 2912–2914.

(47) Chou, T.; Tsao, C.; Hung, S. C. *J. Org. Chem.* **1985**, *50*, 4329–4332.

(48) Dogan, J.; Schulte, J. B.; Swiegers, G. F.; Wild, S. B. *J. Org. Chem.* **2000**, *65*, 951–957.

(49) Rauhut, M. M.; Hechenbleikner, I.; Currier, H. A.; Schaefer, F. C.; Wystrach, V. P. *J. Am. Chem. Soc.* **1959**, *81*, 1103–1107.

(50) Glueck, D. S. *Dalton Trans.* **2008**, 5276–5286.

(51) Powell, J.; Sawyer, J. F.; Stainer, M. V. R. *Inorg. Chem.* **1989**, *28*, 4461–4470.

(52) Powell, J.; Gregg, M. R.; Sawyer, J. F. *Inorg. Chem.* **1989**, *28*, 4451–4460.

(53) Reger, D. L.; Belmore, K. A.; Mintz, E.; McElligott, P. J. *Organometallics* **1984**, *3*, 134–140.

(54) Dickson, R. S.; Paravagna, O. M. *Organometallics* **1992**, *11*, 3196–3201.

(55) Alonso, E.; Forniés, J.; Fortuño, C.; Martín, A.; Orpen, A. G. *Organometallics* **2001**, *20*, 850–859.

(56) Powell, J.; Fuchs, E.; Gregg, M. R.; Phillips, J.; Stainer, M. V. R. *Organometallics* **1990**, *9*, 387–393.

(57) Swor, C. D.; Tyler, D. R. *Coord. Chem. Rev.* **2011**, *255*, 2860–2881.

(58) Caminade, A-M..; Majoral, J. P. *Chem. Rev.* **1994**, *94*, 1183–1213.

(59) Ishiyama, T.; Nakazawa, H.; Miyoshi, K. *J. Organomet. Chem.* **2002**, *648*, 231–236.

(60) Diel, B. N.; Haltiwanger, R. C.; Norman, A. D. *J. Am. Chem. Soc.* **1982**, *104*, 4700–4701.

(61) Diel, B. N.; Brandt, P. F.; Haltiwanger, R. C.; Hackney, M. L. J.; Norman, A. D. *Inorg. Chem.* **1989**, *28*, 2811–2816.

(62) Edwards, P. G.; Fleming, J. S.; Liyanage, S. S.; Coles, S. J.; Hursthouse, M. B. *J. Chem. Soc., Dalton Trans.* **1996**, 1801.

(63) Coles, S. J.; Edwards, P. G.; Fleming, J. S.; Hursthouse, M. B. *J. Chem. Soc., Dalton Trans.* **1995**, 1139.

(64) Edwards, P. G.; Fleming, J. S.; Liyanage, S. S. *J. Chem. Soc., Dalton Trans.* **1997**, *0*, 193–198.

(65) Jones, D. J.; Edwards, P. G.; Tooze, R. P.; Albers, T. *J. Chem. Soc., Dalton Trans.* **1999**, 1045–1046.

(66) Adams, H.; Bailey, N. A.; Blenkiron, P.; Morris, M. J. *J. Chem. Soc., Dalton Trans.* **1997**, 3589–3598.

(67) Adams, H.; Bailey, N. A.; Blenkiron, P.; Morris, M. J. *J. Chem. Soc., Dalton Trans.* **2000**, 3074–3081.

(68) Adams, H.; Atkinson, M. T.; Morris, M. J. *J. Organomet. Chem.* **2001**, *633*, 125–130.

(69) Blake, A. J.; Champness, N. R.; Forder, R. J.; Frampton, C. S.; Frost, C. A.; Reid, G.; Simpson, R. H. *J. Chem. Soc., Dalton Trans.* **1994**, 3377.

(70) McAslan, E. B.; Blake, A. J.; Stephenson, T. A. *Acta Crystallogr. C.* **1989**, *C49*, 1811–1813.

(71) Price, A. J.; Edwards, P. G. *Chem. Commun.* **2000**.

(72) Edwards, P. G. P.; Malik, K. M. A. K.; Ooi, L.-L. L.; Price, A. J. A. *Dalton Trans.* **2006**, 433–441.

(73) Xie, J.; Huang, J.-S.; Zhu, N.; Zhou, Z.-Y.; Che, C.-M. *Chem. Eur. J.* **2005**, *11*, 2405–2416.

(74) Huang, J.-S.; Yu, G.-A.; Xie, J.; Wong, K.-M.; Zhu, N.; Che, C.-M. *Inorg. Chem.* **2008**, *47*, 9166–9181.

(75) Forder, R. J.; Reid, G. *Polyhedron* **1996**, *15*, 3249–3255.

(76) Crisp, G. T.; Salem, G.; Wild, S. B.; Stephens, F. S. *Organometallics* **1989**, *8*, 2360–2367.

(77) Buhro, W. E.; Gladysz, J. A. *Inorg. Chem.* **1985**, *24*, 3505–3507.

(78) Brunet, J.-J.; Chauvin, R.; Diallo, O.; Donnadieu, B.; Jaffart, J.; Neibecker, D. *J. Organomet. Chem.* **1998**, *570*, 195–200.

(79) Malisch, W.; Klüpfel, B.; Schumacher, D.; Nieger, M. *J. Organomet. Chem.* **2002**, *661*, 95–110.

(80) Chan, V. S.; Chiu, M.; Bergman, R. G.; Toste, F. D. *J. Am. Chem. Soc.* **2009**, *131*, 6021–6032.

(81) Chan, V. S.; Stewart, I. C.; Bergman, R. G.; Toste, F. D. *J. Am. Chem. Soc.* **2006**, *128*, 2786–2787.

(82) Gibson, G. L.; Morrow, K. M. E.; McDonald, R.; Rosenberg, L. *Inorg. Chem. Acta* **2011**, *369*, 133–139.

(83) van Lierop, B. J.; Fogg, D. E. *Organometallics* **2013**, *32*, 7245–7248.

(84) Paris, S. I. M.; Lemke, F. R.; Sommer, R.; Lönnecke, P.; Hey-Hawkins, E. *J. Organomet. Chem.* **2005**, *690*, 1807–1813.

(85) Paris, S. I. M.; Petersen, J. L.; Hey-Hawkins, E.; Jensen, M. P. *Inorg. Chem.* **2006**, *45*, 5561–5567.

(86) Acum, G. A.; Mays, M. J.; Raithby, P. R.; Powell, H. R.; Solan, G. A. *J. Chem. Soc., Dalton Trans.* **1997**, 3427–3434.

(87) Patel, B.; Pope, S. J.; Reid, G. *Polyhedron* **1998**, *17*, 2345–2351.

(88) Boettcher, H.-C.; Mereiter, K. *Inorg. Chem. Commun.* **2004**, *7*, 1225–1228.

(89) Hopewell, J.; Jankowski, P.; McMullin, C. L.; Orpen, A. G.; Pringle, P. G. *Chem. Commun.* **2010**, *46*, 100–102.

(90) Jankowski, P.; McMullin, C. L.; Gridnev, I. D.; Orpen, A. G.; Pringle, P. G. *Tetrahedron: Asymmetry* **2010**, *21*, 1206–1209.

(91) Issleib, K.; Weichmann, H. *Zeitschrift für anorganische und ...* **1968**.

(92) Hayter, R. G. *J. Am. Chem. Soc.* **1962**, *84*, 3046–3053.

(93) Hayter, R. G.; Humiec, F. S. *Inorg. Chem.* **1963**, *2*, 306–312.

(94) Hayter, R. G. *Inorg. Chem.* **1963**, *2*, 932–935.

(95) Hayter, R. G. *Inorg. Chem.* **1964**, *3*, 301–302.

(96) DelDonno, T. A.; Rosen, W. *J. Am. Chem. Soc.* **1977**, *99*, 8051–8052.

(97) DelDonno, T. A.; Rosen, W. *Inorg. Chem.* **1978**, *17*, 3714–3716.

(98) Brauer, D. J.; Gol, F.; Hietkamp, S.; Peters, H.; Sommer, H.; Stelzer, O.; Sheldrick, W. S. *Chem. Ber.* **1986**, *119*, 349–365.

(99) Bartsch, R.; Hietkamp, S.; Morton, S.; Stelzer, O. *Angew. Chem. Int. Ed. Engl.* **1982**, *21*, 375–376.

(100) Bartsch, R.; Hietkamp, S.; Morton, S.; Peters, H.; Stelzer, O. *Inorg. Chem.* **1983**, *22*, 3624–3632.

(101) Brauer, D. J.; Lebbe, T.; Stelzer, O. *Angew. Chem. Int. Ed. Engl.* **1988**, *27*, 438–439.

(102) Brauer, D. J.; Dörrenbach, F.; Lebbe, T.; Stelzer, O. *Chem. Ber.* **1992**, *125*, 1785–1794.

(103) Lebbe, T.; Machnitzki, P.; Stelzer, O.; Sheldrick, W. S. *Tetrahedron* **2000**, *56*, 157–164.

(104) Mizuta, T.; Okano, A.; Sasaki, T.; Nakazawa, H. *Inorg. Chem.* **1997**, *36*, 200–203.

(105) Leoni, P. *Organometallics* **1993**, *12*, 2432–2434.

(106) Leoni, P.; Chiaradonna, G.; Pasquali, M.; Marchetti, F.; Fortunelli, A.; Germano, G. *Inorg. Chem. Acta* **1997**, *264*, 185–191.

(107) Leoni, P.; Sommovigo, M.; Pasquali, M.; Sabatino, P.; Braga, D. *J. Organomet. Chem.* **1992**, *423*, 263–270.

(108) Albinati, A.; Lianza, F.; Pasquali, M.; Sommovigo, M.; Leoni, P.; Pregosin, P. S.; Ruegger, H. *Inorg. Chem.* **1991**, *30*, 4690–4692.

(109) Leoni, P.; Pasquali, M.; Sommovigo, M.; Albinati, A.; Lianza, F.; Pregosin, P. S.; Rüegger, H. *Organometallics* **1993**, *12*, 4503–4508.

(110) Leoni, P.; Pasquali, M.; Sommovigo, M.; Albinati, A.; Pregosin, P. S.; Rüegger, H. *Organometallics* **1996**, *15*, 2047–2052.

(111) Leoni, P.; Marchetti, F.; Paoletti, M. *Organometallics* **1997**, *16*, 2146–2151.

(112) Forder, R. J.; Mitchell, I. S.; Reid, G.; Simpson, R. H. *Polyhedron* **1994**, *13*, 2129–2133.

(113) Palmer, R. A.; Giles, H. F.; Whitcomb, D. R. *J. Chem. Soc., Dalton Trans.* **1978**, 1671–1677.

(114) Levason, W.; McAuliffe, C. A.; Riley, B. *Inorg Nucl Chem Lett* **1973**, *9*, 1201–1205.

(115) Brandon, J. B.; Dixon, K. R. *Can. J. Chem.* **1981**.

(116) Carty, A. J.; Hartstock, F.; Taylor, N. J. *Inorg. Chem.* **1982**, *21*, 1349–1354.

(117) Gebauer, T.; Frenzen, G.; Dehnicke, K. *Z. Naturforsch* **1992**, *47b*, 1505.

(118) Giannandrea, R.; Mastrorilli, P.; Nobile, C. F. *Inorg. Chem. Acta* **1999**, *284*, 116–118.

(119) Pelczar, E. M.; Nytko, E. A.; Zhuravel, M. A.; Smith, J. M.; Glueck, D. S.; Sommer, R.; Incarvito, C. D.; Rheingold, A. L. *Polyhedron* **2002**, *21*, 2409–2419.

(120) Leoni, P.; Pasquali, M.; Fortunelli, A.; Germano, G.; Albinati, A. *J. Am. Chem. Soc.* **1998**, *120*, 9564–9573.

(121) Leoni, P.; Pieri, G.; Pasquali, M. *J. Chem. Soc., Dalton Trans.* **1998**, 657–662.

(122) Leoni, P.; Manetti, S.; Pasquali, M.; Albinati, A. *Inorg. Chem.* **1996**, *35*, 6045–6052.

(123) Leoni, P.; Manetti, S.; Pasquali, M. *Inorg. Chem.* **1995**, *34*, 749–752.

(124) Leoni, P.; Pasquali, M.; Sommovigo, M.; Albinati, A.; Lianza, F.; Pregosin, P. S.; Rüegger, H. *Organometallics* **1994**, *13*, 4017–4025.

(125) Leoni, P.; Pasquali, M.; Sommovigo, M.; Laschi, F.; Zanello, P.; Albinati, A.; Lianza, F.; Pregosin, P. S.; Rueegger, H. *Organometallics* **1993**, *12*, 1702–1713.

(126) Leoni, P.; Pasquali, M.; Cittadini, V.; Fortunelli, A.; Selmi, M. *Inorg. Chem.* **1999**, *38*, 5257–5265.

(127) Leoni, P.; Chiaradonna, G.; Pasquali, M.; Marchetti, F. *Inorg. Chem.* **1999**, *38*, 253–259.

(128) Green, L. M.; Meek, D. W. *Polyhedron* **1990**, *9*, 35–45.

(129) Bader, A.; Nullmeyers, T.; Pabel, M.; Salem, G.; Willis, A. C.; Wild, S. B. *Inorg. Chem.* **1995**, *34*, 384–389.

(130) Albert, J.; Magali Cadena, J.; Granell, J.; Muller, G.; Panyella, D.; Sanudo, C. *Eur. J. Inorg. Chem.* **2000**, *2000*, 1283–1286.

(131) Albert, J.; Bosque, R.; Magali Cadena, J.; Delgado, S.; Granell, J. *J. Organomet. Chem.* **2001**, *634*, 83–89.

(132) Kakeya, M.; Tanabe, M.; Nakamura, Y.; Osakada, K. *J. Organomet. Chem.* **2009**, *694*, 2270–2278.

(133) Dyson, D. B.; Parish, R. V.; McAuliffe, C. A.; Pritchard, R. G.; Fields, R.; Beagley, B. *J. Chem. Soc., Dalton Trans.* **1989**, 907.

(134) Al-Sa'ady, A. K. H.; Moss, K.; McAuliffe, C. A.; Dick Parish, R. V. *J. Chem. Soc., Dalton Trans.* **1984**, 1609.

(135) Lane, E. M.; Chapp, T. W.; Hughes, R. P.; Glueck, D. S.; Feland, B. C.; Bernard, G. M.; Wasylishen, R. E.; Rheingold, A. L. *Inorg. Chem.* **2010**, *49*, 3950–3957.

(136) Blanco, M. C.; Fernández, E. J.; Jones, P. G.; Laguna, A.; López-de-Luzuriaga, J. M.; Olmos, M. E. *Angew. Chem. Int. Ed. Engl.* **1998**, *37*, 3042–3043.

(137) Lambert, B.; Desreux, J. F. *Synthesis* **2000**, *2000*, 1668–1670.

(138) Cain, M. F.; Hughes, R. P.; Glueck, D. S.; Golen, J. A.; Moore, C. E.; Rheingold, A. L. *Inorg. Chem.* **2010**, *49*, 7650–7662.

(139) Scriban, C.; Glueck, D. S. *J. Am. Chem. Soc.* **2006**, *128*, 2788–2789.

(140) Scriban, C.; Glueck, D. S.; Golen, J. A.; Rheingold, A. L. *Organometallics* **2007**, *26*, 1788–1800.

(141) Glueck, D. S. *Coord. Chem. Rev.* **2008**, *252*, 2171–2179.

(142) Anderson, B. J.; Glueck, D. S.; DiPasquale, A. G.; Rheingold, A. L. *Organometallics* **2008**, *27*, 4992–5001.

(143) Chapp, T. W.; Schoenfeld, A. J.; Glueck, D. S. *Organometallics* **2010**, *29*, 2465–2473.

(144) Chapp, T. W.; Glueck, D. S.; Golen, J. A.; Moore, C. E.; Rheingold, A. L. *Organometallics* **2010**, *29*, 378–388.

(145) Cain, M. F.; Reynolds, S. C.; Anderson, B. J.; Glueck, D. S.; Golen, J. A.; Moore, C. E.; Rheingold, A. L. *Inorg. Chem. Acta* **2011**, *369*, 55–61.

(146) Dakternieks, D.; Rolls, C. L. *Inorg. Chem. Acta* **1989**, *161*, 105–111.

CHAPTER II

(1) Finn, A. *Hydrocarbon Engineering* **2007**, *12*, 49–52.

(2) Mitariten, M. *Hydrocarbon Engineering* **2004**, *9*, 53–57.

(3) Kidnay, A. J.; Parrish, W. R. *Fundamentals of natural gas processing*; CRC Press: Boca Raton, 2010; pp. 1–31.

(4) Annual Energy Review - Energy Information Administration http://www.eia.gov/totalenergy/data/monthly/pdf/flow/primary_energy.pdf (accessed Apr 10, 2014).

(5) Miller, W. K.; Gilbertson, J. D.; Leiva-Paredes, C.; Bernatis, P. R.; Weakley, T. J. R.; Lyon, D. K.; Tyler, D. R. *Inorg. Chem.* **2002**, *41*, 5453–5465.

(6) Gilbertson, J. D.; Szymczak, N. K.; Crossland, J. L.; Miller, W. K.; Lyon, D. K.; Foxman, B. M.; Davis, J.; Tyler, D. R. *Inorg. Chem.* **2007**, *46*, 1205–1214.

(7) Melson, G. *Coordination chemistry of macrocyclic compounds*; Plenum Press: New York, 1979.

(8) Lambert, B.; Desreux, J. F. *Synthesis* **2000**, *2000*, 1668–1670.

(9) Hagen, K. S. *Inorg. Chem.* **2000**, *39*, 5867–5869.

(10) Kubas, G. J.; Monzyk, B.; Crumbliss, A. L. In *onlinelibrary.wiley.com*; Inorganic Syntheses; John Wiley & Sons, Inc.: Hoboken, NJ, USA, 1979; Vol. 19, pp. 90–92.

(11) Bacon, J.; Gillespie, R. J.; Quail, J. W. *Can. J. Chem.* **1963**, *41*, 3063–3069.

(12) Marker, A. *J. Magn. Reson.* **1982**, *47*, 118–132.

(13) Berners-Price, S. J.; Brevard, C.; Pagelot, A.; Sadler, P. J. *Inorg. Chem.* **1986**, *25*, 596–599.

(14) Berners-Price, S. J.; Johnson, R. K.; Mirabelli, C. K.; Faucette, L. F.; McCabe, F. L.; Sadler, P. J. *Inorg. Chem.* **1987**, *26*, 3383–3387.

(15) Mohr, B.; Brooks, E. E.; Rath, N.; Deutsch, E. *Inorg. Chem.* **1991**, *30*, 4541–4545.

(16) Mizuta, T.; Okano, A.; Sasaki, T.; Nakazawa, H. *Inorg. Chem.* **1997**, *36*, 200–203.

(17) Brauer, D. J.; Gol, F.; Hietkamp, S.; Peters, H.; Sommer, H.; Stelzer, O.; Sheldrick, W. S. *Chem. Ber.* **1986**, *119*, 349–365.

(18) Bartsch, R.; Hietkamp, S.; Morton, S.; Peters, H.; Stelzer, O. *Inorg. Chem.* **1983**, *22*, 3624–3632.

(19) Kang, Y. B.; Pabel, M.; Pathak, D. D.; Willis, A. C.; Wild, S. B. *Main Group Chemistry* **1995**, *1*, 89–98.

(20) Kagan, G.; Li, W.; Hopson, R.; Williard, P. G. *Org. Lett.* **2009**, *11*, 4818–4821.

(21) Li, W.; Kagan, G.; Yang, H.; Cai, C.; Hopson, R.; Dai, W.; Sweigart, D. A.; Williard, P. G. *Organometallics* **2010**, *29*, 1309–1311.

(22) Bertacco, A.; Mazzi, U.; Orio, A. A. *Inorg. Chem.* **1972**, *11*, 2547–2549.

(23) Kyba, E. P.; Alexander, D. C.; Hoehn, A. *Organometallics* **1982**, *1*, 1619–1623.

(24) Stalick, J. K.; Corfield, P. W. R.; Meek, D. W. *J. Am. Chem. Soc.* **1972**, *94*, 6194–6196.

(25) Bressan, M.; Rigo, P. *Inorg. Chem.* **1975**, *14*, 38–42.

(26) Bacci, M.; Midollini, S.; Stoppioni, P.; Sacconi, L. *Inorg. Chem.* **1973**, *12*, 1801–1805.

(27) Hartley, J. G.; Kerfoot, D. G. E.; Venanzi, L. M. *Inorg. Chem. Acta* **1967**, *1*, 145–148.

(28) Cloyd, J. C., Jr.; Meek, D. W. *Inorg. Chem. Acta* **1972**, *6*, 480–486.

(29) Horrocks, W. D., Jr.; Van Hecke, G. R.; Hall, D. D. *Inorg. Chem.* **1967**, *6*, 694–699.

CHAPTER III

(1) Berners-Price, S. J.; Johnson, R. K.; Mirabelli, C. K.; Faucette, L. F.; McCabe, F. L.; Sadler, P. J. *Inorg. Chem.* **1987**, *26*, 3383–3387.

(2) *Structure and Bonding*; Clarke, M. J.; Goodenough, J. B.; Ibers, J. A.; Jørgensen, C. K.; Mingos, D. M. P.; Neilands, J. B.; Palmer, G. A.; Reinen, D.; Sadler, P. J.; Weiss, R.; Williams, R. J. P., Eds.; Springer Berlin Heidelberg: Berlin, Heidelberg, 2005; Vol. 70, pp. 27–102.

(3) Lewis, J. S.; Zweit, J.; Blower, P. J. **1998**, *17*, 513–517.

(4) Marzano, C.; Pellei, M.; Colavito, D.; Alidori, S.; Lobbia, G. G.; Gandin, V.; Tisato, F.; Santini, C. *J. Med. Chem.* **2006**, *49*, 7317–7324.

(5) Marzano, C.; Gandin, V.; Pellei, M.; Colavito, D.; Papini, G.; Lobbia, G. G.; Del Giudice, E.; Porchia, M.; Tisato, F.; Santini, C. *J. Med. Chem.* **2008**, *51*, 798–808.

(6) Alidori, S.; Gioia Lobbia, G.; Papini, G.; Pellei, M.; Porchia, M.; Refosco, F.; Tisato, F.; Lewis, J. S.; Santini, C. *J Biol Inorg Chem* **2007**, *13*, 307–315.

(7) Lewis, J. S.; Zweit, J.; Dearling, J. L. J.; Rooney, B. C.; Blower, P. J. *Chem. Commun.* **1996**, 1093.

(8) Saito, K.; Saijo, S.; Kotera, K.; Date, T. *Chem. Pharm. Bull.* **1985**, *33*, 1342–1350.

(9) Lewis, J. S.; Heath, S. L.; Powell, A. K.; Zweit, J.; Blower, P. J. *J. Chem. Soc., Dalton Trans.* **1997**, 855–862.

(10) Blue, E. D.; Davis, A.; Conner, D.; Gunnoe, T. B.; Boyle, P. D.; White, P. S. *J. Am. Chem. Soc.* **2003**, *125*, 9435–9441.

(11) Townsend, J. M.; Blount, J. F.; Sun, R. C.; Zawoiski, S.; Valentine, D. *J. Org. Chem.* **1980**, *45*, 2995–2999.

(12) Nicola, C. D.; Effendy; Fazaroh, F.; Pettinari, C.; Skelton, B. W.; Somers, N.; White, A. H. *Inorg. Chem. Acta* **2005**, *358*, 720–734.

(13) Mao, Z.; Chao, H.; Hui, Z.; Che, C. M.; Fu, W.-F.; Cheung, K.-K.; Zhu, N. *Chem. Eur. J.* **2003**, *9*, 2885–2894.

(14) Nieckarz, G. F.; Weakley, T. J. R.; Miller, W. K.; Miller, B. E.; Lyon, D. K.; Tyler, D. R. *Inorg. Chem.* **1996**, *35*, 1721–1724.

(15) Saravana Bharathi, D.; Sridhar, M. A.; Shashidhara Prasad, J.; Samuelson, A. G. *Inorg. Chem. Commun.* **2001**, *4*, 490–492.

(16) Gschwind, R. M. *Chem. Rev.* **2008**, *108*, 3029–3053.

(17) Black, J. R.; Levason, W.; Spicer, M. D.; Webster, M. *J. Chem. Soc., Dalton Trans.* **1993**, 3129.

(18) Comba, P.; Katsichtis, C.; Nuber, B. *Eur. J. Inorg. Chem.* **1999**.

(19) Bacon, J.; Gillespie, R. J.; Quail, J. W. *Can. J. Chem.* **1963**, *41*, 3063–3069.

(20) Marker, A. *J. Magn. Reson.* **1982**, *47*, 118–132.

(21) Mohr, B.; Brooks, E. E.; Rath, N.; Deutsch, E. *Inorg. Chem.* **1991**, *30*, 4541–4545.

(22) Darensbourg, D. J.; Chao, C. S.; Reibenspies, J. H.; Bischoff, C. J. *Inorg. Chem.* **1990**, *29*, 2153–2157.

(23) Nadasdi, T. T.; Stephan, D. W. *Inorg. Chem.* **1994**, *33*, 1532–1538.

CHAPTER IV

(1) DelDonno, T. A.; Rosen, W. *J. Am. Chem. Soc.* **1977**, *99*, 8051–8052.

(2) DelDonno, T. A.; Rosen, W. *Inorg. Chem.* **1978**, *17*, 3714–3716.

(3) Lambert, B.; Desreux, J. F. *Synthesis* **2000**, *2000*, 1668–1670.

(4) Kang, Y. B.; Pabel, M.; Pathak, D. D.; Willis, A. C.; Wild, S. B. *Main Group Chemistry* **1995**, *1*, 89–98.

(5) Baacke, M.; Stelzer, O.; Wray, V. *Chem. Ber.* **1980**, *113*, 1356–1369.

(6) Kubas, G. J.; Monzyk, B.; Crumbliss, A. L. In *onlinelibrary.wiley.com*; Inorganic Syntheses; John Wiley & Sons, Inc.: Hoboken, NJ, USA, 1979; Vol. 19, pp. 90–92.

(7) Marker, A. *J. Magn. Reson.* **1982**, *47*, 118–132.

(8) Berners-Price, S. J.; Brevard, C.; Pagelot, A.; Sadler, P. J. *Inorg. Chem.* **1986**, *25*, 596–599.

(9) Berners-Price, S. J.; Johnson, R. K.; Mirabelli, C. K.; Faucette, L. F.; McCabe, F. L.; Sadler, P. J. *Inorg. Chem.* **1987**, *26*, 3383–3387.

(10) Kyba, E. P.; Davis, R. E.; Hudson, C. W.; John, A. M.; Brown, S. B.; McPhaul, M. J.; Liu, L.-K.; Glover, A. C. *J. Am. Chem. Soc.* **1981**, *103*, 3868–3875.

(11) Mizuta, T.; Okano, A.; Sasaki, T.; Nakazawa, H. *Inorg. Chem.* **1997**, *36*, 200–203.

(12) Brauer, D. J.; Gol, F.; Hietkamp, S.; Peters, H.; Sommer, H.; Stelzer, O.; Sheldrick, W. S. *Chem. Ber.* **1986**, *119*, 349–365.

(13) Crisp, G. T.; Salem, G.; Wild, S. B.; Stephens, F. S. *Organometallics* **1989**, *8*, 2360–2367.

(14) Buhro, W. E.; Gladysz, J. A. *Inorg. Chem.* **1985**, *24*, 3505–3507.

(15) Quin, L. D. *A Guide to Organophosphorus Chemistry*; Wiley-Interscience, 2000.

(16) Horrocks, W. D., Jr.; Van Hecke, G. R.; Hall, D. D. *Inorg. Chem.* **1967**, *6*, 694–699.

(17) Girolami, G. S.; Rauchfuss, T. B.; Angelici, R. J. **1999**.

(18) Bertacco, A.; Mazzi, U.; Orio, A. A. *Inorg. Chem.* **1972**, *11*, 2547–2549.

(19) Stalick, J. K.; Corfield, P. W. R.; Meek, D. W. *J. Am. Chem. Soc.* **1972**, *94*, 6194–6196.

(20) Bressan, M.; Rigo, P. *Inorg. Chem.* **1975**, *14*, 38–42.

(21) Bacci, M.; Midollini, S.; Stoppioni, P.; Sacconi, L. *Inorg. Chem.* **1973**, *12*, 1801–1805.

CHAPTER V

(1) Miller, W. K.; Gilbertson, J. D.; Leiva-Paredes, C.; Bernatis, P. R.; Weakley, T. J. R.; Lyon, D. K.; Tyler, D. R. *Inorg. Chem.* **2002**, *41*, 5453–5465.

(2) Gilbertson, J. D.; Szymczak, N. K.; Crossland, J. L.; Miller, W. K.; Lyon, D. K.; Foxman, B. M.; Davis, J.; Tyler, D. R. *Inorg. Chem.* **2007**, *46*, 1205–1214.

(3) Gilbertson, J. D.; Szymczak, N. K.; Tyler, D. R. *J. Am. Chem. Soc.* **2005**, *127*, 10184–10185.

(4) Crossland, J. L.; Balesdent, C. G.; Tyler, D. R. *Inorg. Chem.* **2011**, 439-445.

(5) Balesdent, C. G.; Crossland, J. L.; Regan, D. T.; López, C. T.; Tyler, D. R. *Inorg. Chem.* **2013**, 14178-14187.

(6) Crossland, J. L.; Young, D. M.; Zakharov, L. N.; Tyler, D. R. *Dalton Trans.* **2009**, 9253.

(7) Hagen, K. S. *Inorg. Chem.* **2000**, *39*, 5867–5869.

(8) Baacke, M.; Stelzer, O.; Wray, V. *Chem. Ber.* **1980**, *113*, 1356–1369.

(9) Mizuta, T.; Okano, A.; Sasaki, T.; Nakazawa, H. *Inorg. Chem.* **1997**, *36*, 200–203.

(10) Brauer, D. J.; Gol, F.; Hietkamp, S.; Peters, H.; Sommer, H.; Stelzer, O.; Sheldrick, W. S. *Chem. Ber.* **1986**, *119*, 349–365.

(11) Bartsch, R.; Hietkamp, S.; Morton, S.; Peters, H.; Stelzer, O. *Inorg. Chem.* **1983**, *22*, 3624–3632.

(12) DelDonno, T. A.; Rosen, W. *J. Am. Chem. Soc.* **1977**, *99*, 8051–8052.

(13) Bartsch, R.; Hietkamp, S.; Morton, S.; Stelzer, O. *Angew. Chem. Int. Ed. Engl.* **1982**, *21*, 375–376.

(14) Cecconi, F.; Di Vaira, M.; Midollini, S.; Orlandini, A.; Sacconi, L. *Inorg. Chem.* **1981**, *20*, 3423–3430.

(15) Chatt, J.; Hayter, R. G. *J. Chem. Soc.* **1961**, 5507.

(16) Girolami, G. S.; Wilkinson, G.; Galas, A. M. R.; Thornton-Pett, M.; Hursthouse, M. B. *J. Chem. Soc., Dalton Trans.* **1985**, 1339–1348.

(17) Bellerby, J. M.; Mays, M. J.; Sears, P. L. *J. Chem. Soc., Dalton Trans.* **1976**, 1232–1236.

(18) Baker, M. V.; Field, L. D.; Hambley, T. W. *Inorg. Chem.* **1988**, *27*, 2872–2876.

(19) Lewis, J.; Khan, M. S.; Kakkar, A. K.; Raithby, P. R.; Fuhrmann, K.; Friend, R. H. *J. Organomet. Chem.* **1992**, *433*, 135–139.

(20) Antberg, M.; Dahlenburg, L. *Inorg. Chem. Acta* **1985**, *104*, 51–54.

(21) Burrows, A. D.; Dodds, D.; Kirk, A. S.; Lowe, J. P.; Mahon, M. F.; Warren, J. E.; Whittlesey, M. K. *Dalton Trans.* **2007**, 570–580.

(22) Field, L. D.; Thomas, I. P.; Hambley, T. W.; Turner, P. *Inorg. Chem.* **1998**, *37*, 612–618.

(23) Jana, B.; Ellern, A.; Pestovsky, O.; Sadow, A.; Bakac, A. *Inorg. Chem.* **2011**, *50*, 3010–3016.

(24) Mays, M. J.; Prater, B. E.; Wonchoba, E. R.; Parshall, G. W. *Inorg. Synth.* **1974**, *15*.

(25) Swor, C. D.; Tyler, D. R. *Coord. Chem. Rev.* **2011**, *255*, 2860–2881.

(26) Glueck, D. S. *Dalton Trans.* **2008**, 5276–5286.

(27) *Simulated NMR Spectra with WINDNMR-Pro*; Reich, H. J., Ed.; Reich, H. J.

(28) Hazari, N. *Chemical Society Reviews* **2010**, *39*, 4044.

(29) Giannoccaro, P.; Rossi, M.; Sacco, A. *Coord. Chem. Rev.* **1972**, *8*, 77–79.

(30) Bressan, M.; Rigo, P. *Inorg. Chem. Acta* **1979**, *37*, 181–185.